African Journal of Biotechnology

Volume 15 Number 21, 25 May 2016

ISSN 1684-5315

Academic Journals

ABOUT AJB

The African Journal of Biotechnology (AJB) (ISSN 1684-5315) is published weekly (one volume per year) by Academic Journals.

African Journal of Biotechnology (AJB), a new broad-based journal, is an open access journal that was founded on two key tenets: To publish the most exciting research in all areas of applied biochemistry, industrial microbiology, molecular biology, genomics and proteomics, food and agricultural technologies, and metabolic engineering. Secondly, to provide the most rapid turn-around time possible for reviewing and publishing, and to disseminate the articles freely for teaching and reference purposes. All articles published in AJB are peer-reviewed.

Contact Us

Editorial Office: ajb@academicjournals.org

Help Desk: helpdesk@academicjournals.org

Website: http://www.academicjournals.org/journal/AJB

Submit manuscript online http://ms.academicjournals.me/

African Journal of Biotechnology

Table of Content: Volume 15 Number 21 25 May, 2016

ARTICLES

Effect of cadmium on the morphology and anatomy of *Salvinia auriculata* 891
Rodrigues, D. A., Vasconcelos Filho, S. C, Rodrigues, A. A., Rampazzo, D. F., Rodrigues, C. L., Vasconcelos, J. M. and Magalhães, P. A. N. R.

Surface composition and surface properties of water hyacinth (*Eichhornia crassipes*) root biomass: Effect of mineral acid and organic solvent treatment 897
Netai Mukaratirwa-Muchanyereyi, Jameson Kugara and Mark Fungayi Zaranyika

In-silico smart library design to engineer a xylose-tolerant hexokinase variant 910
Yasser Gaber

Morphological diversity in oleaginous watermelon (*Citrullus mucosospermus*) from the Nangui Abrogoua University germplasm collection 917
Ahou A. Gbotto, Kouamé K. Koffi, Nandy D. Fouha Bi, Serge T. Doubi Bi, Hippolyte H. Tro, Jean-Pierre Baudoin and Irié A. Zoro Bi

Impact of transgenic cotton expressing *cry1Ac* and *cry2Ab* genes on soil rhizosphere bacterial and fungal populations in soils of central Kenya 930
J. Swilla, C. N. Waturu and S. T. Rubindamayugi

Expression and purification of recombinant Shiga toxin 2B from *Escherichia coli* O157:H7 940
Marwa E. A. Aly, Amro S. Hanora, Tamer M. Essam and Magdy A. Amin

Genetic characterization by amplified fragment length polymorphism (AFLP) markers and morphochemical traits of *Carica papaya* L. genotypes 948
Mariela Vázquez Calderón, Javier O. Mijangos-Cortés, Manuel J. Zavala L., L. Felipe Sánchez Teyer, Adriana Quiroz M., Matilde Margarita Ortiz G., Fernando Amilcar Contreras M., Francisco Espadas G., Gabriela Fuentes Ortiz and Jorge M. Santamaría

Assessment of genetic diversity among sixty bread wheat (Triticum aestivum) cultivars using microsatellite markers 960
Vincent Mgoli Mwale, Xiuli Tang and Eric Chilembwe

Fermentative intensity of L-lactic acid production using self-immobilized pelletized Rhizopus oryzae 974
Shuizhong Luo, Xuefeng Wu, Yu Zhu, Xingjiang Li, Shaotong Jiang and Zhi Zheng

Effect of pH, various divalent metal ion and different substrates on glucoamylase activity obtained from Aspergillus niger using amylopectin from tiger nut starch as carbon source 980
Ezugwu A. L., Ottah, V. E., Eze, S. O. O. and Chilaka F. C.

Trials to improve the response of Orechromis niloticus to Aeromonas hydrophila vaccine using immunostimulants (garlic, Echinacea) and probiotics (Organic GreenTM and Vet-YeastTM) 989
Salah Mesalhy Aly, Mohamed A. Al Zohairy, Arshad H. Rahmani, Mohamed Fathi and Nashwa M. Abdel Atti

academicJournals

Vol. 15(21), pp. 891-896, 25 May, 2016
DOI: 10.5897/AJB2016.15317
Article Number: A26874658590
ISSN 1684-5315

http://www.academicjournals.org/AJB

African Journal of Biotechnology

Full Length Research Paper

Effect of cadmium on the morphology and anatomy of *Salvinia auriculata*

Rodrigues, D. A.[1*], Vasconcelos Filho, S. C[2], Rodrigues, A. A.[2,] Rampazzo, D. F.[2], Rodrigues, C. L.[2], Vasconcelos, J. M.[3] and Magalhães, P. A. N. R.[1]

[1]University of Rio Verde-Farm Sources of Knowledge, PO Box 104 CEP: 75901-970, Rio Verde, GO-Brazil.
[2]Federal Institute of Education and Technology Goiás, Rio Verde Campus. South highway Goiana Km 01, Zona Rural, Rio Verde - GO - CEP 75901-970. PO Box 66, Brazil.
[3]University of Brasilia, Campus Darcy Ribeiro, S / N - North Wing, CEP 70910-900, Brasília-Brazil.

Received 24 November, 2015; Accepted 28 April, 2016

This study aimed to evaluate the morphological and anatomical changes of *Salvinia auriculata* exposed to different concentrations 0, 2.5, 5, 7.5 and 10 µM of cadmium (Cd) and its effect on plant growth. The experiment was conducted in the laboratory of Plant Anatomy of the IF Goiano/Rio Verde Campus, Goiás. Cd free samples of *S. auriculata*, was obtained from the Aquários Plantados company, located in Belo Horizonte. The material was grown hydroponically for 20 days and after the experimental period, the leaf samples were fixed, including in historesin, cut to 5 µm thick thick, stained with toluidine blue and the images were obtained in an optical microscope. The toxic effects of Cd on *S. auriculata* was observed at lowest concentration with the appearance of chlorotic and necrotic spots. Microscopic analysis showed increased height and width of the aerenchyma gaps, mesophyll and a reduction in abaxial surface epidermal cells, due to increased doses of this metal. It was observed that *S. auriculata* is a plant sensitive to Cd, and thus indicated for environmental monitoring.

Key words: Ecological, aquatic species, pollution.

INTRODUCTION

The pollution of soil and water by heavy metals is due to industrial, agricultural activities and urbanization, and has become a serious problem with great environmental impacts (Carneiro et al., 2002). Contamination of water resources by heavy metals has been of concern to researchers and government agencies (Oliveira et al., 2001). Some of these metals, such as lead (Pb), zinc (Zn), arsenic (As) and cadmium (Cd), which in addition to being toxic in small quantities, are able to accumulate and interfere in the food web.

Cd is highly toxic, often disposed of improperly in the environment and may reach the soil, aquatic media or the air by the burning of municipal waste and fossil fuels, thus contaminating the environment and altering the ecosystem (Pino, 2005). The problems arising from this metal are not limited to the environmental area. Poisoning of living beings by this metal can bring specific problems according to the type of contamination, when

*Corresponding author. E-mail: douglasalmeida_rv13@hotmail.com.

poisoning occurs through the airways by inhalation of Cd dust, problems may occur in the respiratory tract and kidneys, which can lead to death; in the case of poisoning via oral ingestion of a significant amount of Cd, immediate poisoning and damage to the liver and kidneys may arise; poisoning through physical contact causes genetic changes (Brady and Humiston, 1986).

Worldwide, studies into the recovery of contaminated area by phytoremediation are being studied (Gardea-Torresdey et al., 2005; Vardanyan and Ingole, 2006). To evaluate the effectiveness of phytoremediation, it is necessary to expose the species in question to the contaminant, for a good phytoremediator, needs to accumulate relatively high concentrations of pollutants in its tissues without suffering toxic effects. However, if the plant is susceptible to the pollutant, presenting symptoms, it is considered an ecological pollution indicator.

According to Paiva et al. (2002), species, when exposed to heavy metal contaminated environments, respond in a very variable manner, it is necessary to test the behavior of each type of species, contamination period as well as evaluate the effect caused by the metal on morphology and growth, and resultant consequences to the macrophytes, confirming their use as bioindicadors. Due to lack of studies on the subject, this present study aims to evaluate the effects of Cd on the morphology and anatomy of *Salvinia* in order to contribute to information in environmental monitoring work.

MATERIALS AND METHODS

The experiment was conducted in plant anatomy laboratory at the Federal Institute of Education, Science and Technology Goiás (IFGoiano/Rio Verde Campus). Individuals of *S. auriculata* Aubl. (Salvinaceae) were purchased from the Aquários Plantados company, located in Belo Horizonte.

Plant growth

Adult *S. auriculata* individuals were disinfected using 1% sodium hypochlorite with immersion in this solution for 30 min. Plants were then washed with deionized water to remove excess hypochlorite. Subsequently, the plants were selected, to maintain homogeneity and placed in a 25 L capacity bowl containing Hoagland-Arnon nutrient solution modified with 1/5 ionic strength, pH 6.5 for 6 days for their adaptation.

After the adaptation period, plants were transferred to 1.2 L capacity pots with nutrient solution, maintaining the pH at 6.5 using 1 M HCl solution (hydrochloric acid) and 0.1 M NaOH (sodium hydroxide). To evaluate the effect of Cd, the following concentrations were adopted: 0 (T1), 2.5 (T2), 5 (T3), 7.5 (T4) and 10 µM (T5) in the form Cd $(NO_3)_2$. Morphological changes in the leaves were observed daily for 20 days. The solution was changed every three days and constantly aerated using a compressor.

Structural analysis

After 20 days of hydroponics 2 cm^2 leaf samples from leaf blade area were collected with the aid of forceps and cut with a disposable razor to one plant per pot, and fixed in Karnovsky solution (Karnovsky, 1965), for 24 h, dehydrated in increasing ethanol series, pre-infiltrated and infiltrated in historesin (Historesin, Leica) according to the manufacturer recommendations.

The material was sectioned to 5 µm thick, with a rotary microtome (RM 2155 model, Leica). The sections were stained with 0.05%, pH 4.0 toluidine blue (O'Brien et al., 1964) and mounted with Canada Balsam. The images were obtained in an Olympus BX61 microscope with a DP-72 camera.

The micro morphometric analyzes measurements were taken of the thicknesses of the epidermis (adaxial and abaxial faces), mesophyll and the aerenchyma gaps (height and width) of the leaves. All data were obtained with the aid of ImageJ - Image Processing and Analysis in Java software, Version 1.47, totaling 10 observations/ repetition for each structure evaluated.

The experimental design was completely randomized (CRD) with 4 replications and 5 treatments with each repetition consisting of 4 plants per pot. Data were subjected to analysis of variance (ANOVA) and regression using the statistical program Assistant.

RESULTS AND DISCUSSION

Plantlet growth

S. auriculata exposed to Cd show visible signs of toxicity, such as chlorosis and necrosis on the leaf surface with brown tint at the lowest dosage 2.5 µM (Figure 1B). With increasing doses of the metal added to the nutrient solution, the changes that the plant underwent were intensified (Figure 1C to F) compared to the control, free from the gradient (Figure 1A). This is a clear symptom observed in terrestrial plants, such as barley (Sridhar et al., 2007), as well as aquatic plants like *S. auriculata* (Siriwan et al., 2006) exposed to this metal.

According to Qian et al. (1999), the Cd^{2+} ions seem to be efficiently absorbed by the plant roots, their transport to other parts being very low, can be complexed and sequestered in cellular structures such as vacuoles, inhibiting its translocation to the shoot (Lasat, 2000). In addition, Cd can cause reduced growth, root development atrophy, leaf rolling and discoloration (Hutchinson and Czyrsk, 1975), necrotic tissue (Maine et al., 2000) and damage to metabolic systems or in protein synthesis (Oliveira et al., 2001).

At higher concentrations (10 and 20 µM of Cd) the toxicity symptoms most commonly observed by Oliveira and Mattiazzo (2001) working with water hyacinth was the presence of interveinal chlorosis in the leaves, which corroborates with the findings of the present study. Oliveira and Mattiazzo (2001) working with *Salvinia* observed reduction in plant survivability from Cd concentrations of 5 µM, and was not observed in this study.

Studies have shown that exposure of plants to high Cd concentrations causes growth inhibition and visible symptoms of chlorosis and necrosis in the leaves (Zhou et al., 2008; Clemens, 2006), caused by the photosynthetic decline and a decrease in the absorption and transport of nutrients (Larsson et al., 1998). When exposed to this gradient, plants are morphologically

Figure 1. *Salvinia auriculata* maintained for 20 days in nutrient solution with different concentrations of Cd. Control (A) and treated with 2.5, 5, 7.5 and 10 µM Cd (B, C, D, E, F) respectively. Dark spots were observed on the shoots (→).

damaged due to the substitution of Fe^{+2} by Cd^{+2} during physiological processes (Stohs and Bagchi, 1995). Yoshiara et al. (2006) working with *Nicotiana tabacum* observed that Cd causes Fe^{+2} deficiency.

Structural analyses

Compared to the control (Figure 2A), the leaf blade area showed alterations in the parenchymal architecture, with the increase in aerenchyma gaps of *S. auriculata* leaves (Figure 2B to F) evident. In aquatic plants, the aerenchyma developed mainly by the disintegration of cells, following several factors: oxygen deficiency promotes the production of ethylene by anaerobic stimulus, which causes an increase in the cellulase activity, which in turn leads to the cell disintegration and aerenchyma development (Fahn, 1982). In this case, the aerenchyma works as an alternative strategy for obtaining O_2 (Drew et al., 2000).

The same fact can be observed in the presence of Cd, as this metallic element stimulates ethylene production in plant species (Chen and Kao, 1995; Toppi et al., 1998). Although, the ethylene concentration in the different treatments was not evaluated in this present work, it is believed that the alterations observed in *S. auriculata* leaf aerenchyma may be related to changes in the concentrations of this hormone (Dantas et al., 2001).

In addition to alterations in epidermal cells, accumulation of content strongly stained was verified by toluidine blue (metachromasia) in the region beneath the adaxial epidermal (Figure 2B). Both at a Cd concentration of 7.5 µM as well as 10 µM, some points of the wall ruptured (Figure 2C, E and F).

The main changes caused by pollutants in plants are: increase or decrease in the production of some enzymes, genetic alterations and quantitative and qualitative alterations of metabolites (Pasqualini et al., 2003; Gerosa et al., 2003; Klumpp et al., 2006). As a result, symptoms arise such as chlorosis and necrosis in tissues and organs, leading to plant mortality, as are observed in this present study.

Increasing doses of Cd in the solution exerts adverse effect on plant growth. The plants were susceptible to this ion, since the lower dose of this element, besides causing visible symptoms on leaves, such as leaf tissue deterioration also caused a negative influence in plant growth during the twenty days of the experiment.

Sridhar et al. (2005) working with *Brassica juncea* (L) and *Palaquium ferrugineum* observed that the element Zn caused compression of the mesophyll and the reduction of intercellular spaces in the leaves. In *Elodea canadensis*, the mesophyll cells showed an increase in volume after Cd exposure, which led to a decline in the number of cells per area (Vecchia et al., 2005).

For the height of adaxial epidermis, it was observed

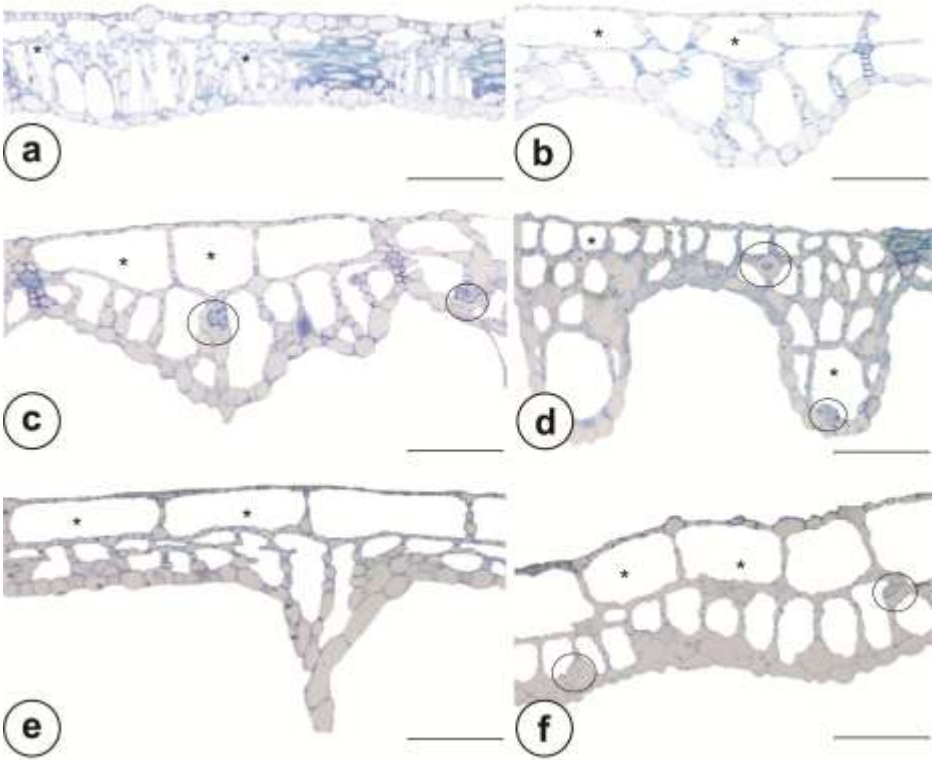

Figure 2. Leaf blade of *Salvinia auriculata* (cross sections stained with toluidine blue), after 20 days of experiment. A: control; B: 2.5 µM Cd; C: 5 µM Cd; D: 7.5 µM Cd; and E-F: 10 µM Cd. Disarrangement and increase of aerenchyma gaps (*). Accumulation of strongly stained contents (circle). Scale 200 µm.

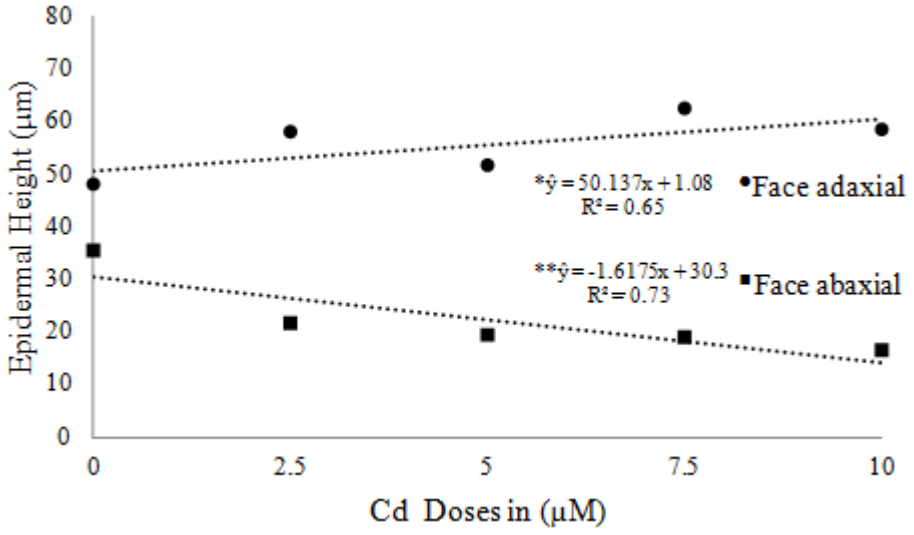

Figure 3. Regression analysis of the abaxial and adaxial face epidermis height of *Salvinia auriculata* leaves grown in Hoagland-Arnon solution, subjected to different concentrations of cadmium. *Significant at 5% probability. CV (%) = 13.56 (adaxial). **Significant at 1% level of probability. CV (%) = 26.29 (abaxial).

that from the 2.5 µM dose, the cells showed more elongation, resulting in increased thickness of this tissue with increased Cd concentrations (Figure 3). Plants grown without the presence of Cd showed larger abaxial epidermal cells, averaging 35.21 µm, while the lowest averages were observed in the treatments with 7.5 and

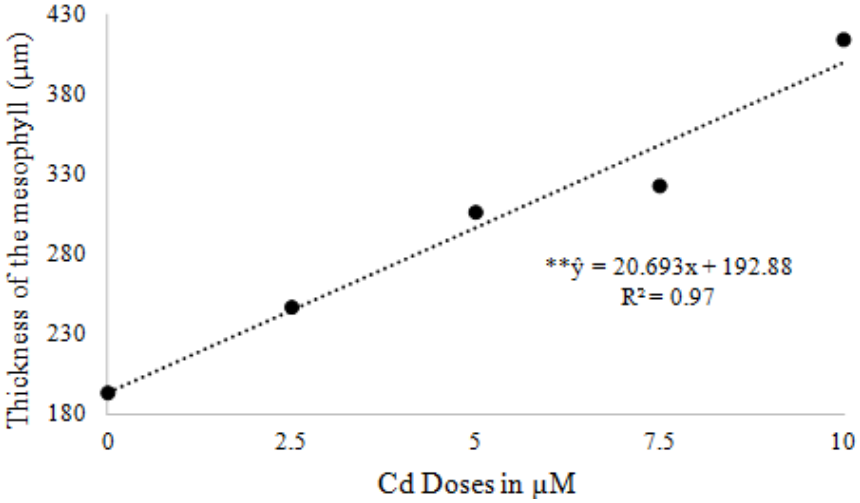

Figure 4. Regression analysis of the mesophyll thickness of the *Salvinia auriculata* leaves grown in Hoagland-Arnon solution, subjected to different concentrations of cadmium. **Significant at 1% level of probability. CV (%) = 7.43.

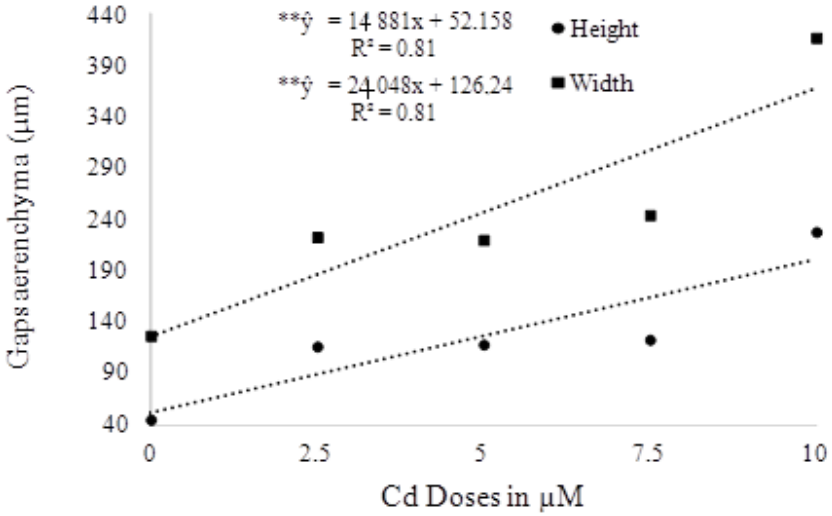

Figure 5. Regression analysis of *Salvinia auriculata* aerenchyma gap heights of leaves grown in Hoagland-Arnon solution, subjected to different concentrations of cadmium. **Significant at the 1% level of probability. CV (%) = 37.49 (gap height). **Significant at the 1% level of probability. CV (%) = 14:58 (gap width).

10 mM of Cd (Figure 3). In regression analysis, the model that best fit the data distribution was linear. Guglieri et al. (2007) working with *Platyhypnidium aquaticum* leaves observed reduction in the thickness of the leaf blade with the increase of Cd concentrations, not corroborating with results of the present work.

For the mesophyll thickness, the regression model that best fit the results was linear. The treatment with Cd at doses of 7.5 and 10 µM showed a mesophyll cell thickness increase (Figure 4). Alterations in the area and proportion of leaf tissue can be consequences of continuous exposure to heavy metals (Lux et al., 2011; Vaculik et al., 2012). Thus, the thickness increases in the mesophyll region at the higher Cd concentrations, which represents the larger diameter of the leaves.

Figure 5 presents the height of the aerenchyma gaps increased with higher doses of Cd compared to the control. The treatments influenced the aerenchyma elongation (Figure 5). The dose increases showed higher indices and it can be seen that treatment with 10 µM Cd presented a 426 µm thickness, differing from the other treatments (Figure 5). Pereira (2010) working with

Eichhornia crassipes submitted to Cd did not observe changes in the proportion of aerenchyma until it reaches the highest concentrations of this metal.

Conclusion

S. auriculata is a species sensitive to Cd, showing visible symptoms of toxicity, such as chlorosis and necrosis on the leaf surface from the lowest dose of that element, thus restricting its use in the decontamination of environments. On the other hand, it is indicated for environmental monitoring programs as an ecological indicator.

Conflict of interest

The author declares that there is no conflict of interest.

ACKNOWLEDGEMENT

The authors acknowledged Instituto Federal Goiano – Campus Rio Verde, Goiás.

REFERENCES

Brady JE, Humiston GE (1986). General Chemistry. Rio de Janeiro: Books Sci Tech, 1:2.

Carneiro MA, Siqueira JO, Moreira FMS de (2002). Behavior of herbaceous species in soil mixtures with different degrees of contamination with heavy metals. Braz. Agric. Res. 37(11):1629-1638.

Chen SL, Kao CH (1995). Prior temperature exposure affects subsequent Cd-induced ethylene production in rice leaves. Plant Sci. 104(2):135-138.

Clemens S (2006). Toxic metal accumulation, responses to exposure and mechanisms of tolerance in plants. Biochimie 88(11):1707-1719.

Dantas BF, Aragão CA, Alves JD (2001). Cálcio e o desenvolvimento de aerênquimas e atividade de celulase em plântulas de milho submetidas à hipoxia. Sci. Agric. 58(2):251-257.

Drew MC, He CJ, Morgan PW (2000). Programmed cell death and aerenchyma formation in roots. Trends Plant Sci. 5(3):123-127.

Fahn A (1982). Plant Anatomy, Oxford, Pergamon Press. 4:544.

Gardea-Torresdey JL, Peralta-Videa J, La Rosa G, Parson JG (2005). Phytoremediation of heavy metals and study of the metal coordination by X-ray absorption spectroscopy. Coord. Chem. Rev. 249(17):1797-1810.

Gerosa G, Marzuoli R, Bussotti F, Pancrazi M, Ballarin-Denti A (2003). Ozone sensitivity of Fagus sylvatica and Fraxinus excelsior young trees in relaton to leaf structure and foliar ozone uptake. Environ. Pollut. 125(1):91-98.

Guglieri A, Longhi-Wagner HM, Zuloaga FO (2007). Panicum Sect. Dichotomiflora (Hitchc. & Chase) Honda e P. sect. Virgata Hitchc. & Chase ex Pilg. (Poaceae: Panicoideae: Paniceae) no Brasil. Acta Bot. Bras. 21(4):785-805.

Hutchinson TC, Czyrsk AH (1975). Heavy metal toxicity and synergism to floating aquatic weeds. Verh. Int. Ver. Limnol. 19:2102-2111.

Karnovsky MJA (1965). Formaldehyde-glutaraldehyde fixative of high osmolarity for use in electron microscopy. J. Cell Biol. 27:137-138.

Klumpp A, Ansel W, klumpp G, Calatayud V, Carrec JP, He S, Peñuela J, Ribas A, Ro-Poulsen H, Rasmussen S, Sanz MJ, Ergne F (2006). Tradescantia micronucleus test Indicates genotoxic potential of traffic emissions in European cities. Environ. Pollut. 139(3):515-522.

Larsson EL, Bornman JF, Asp H (1998). Influence of UV-B radiation and Cd^{2+} on chlorophyll fluorescence, growth and nutrient content in Brassica napus. J. Exp. Bot. 49(323):1031-1039.

Lasat MM (2000. Phytoextraction of metals from contaminated soil: a review of plant/soil/metal interaction and assessment of pertinent agronomic issues. J. Hazard. Subst. Res. 2(5):1-25.

Lux, A, Martinka M, Vaculik M, White PJ (2011). Root responses to cadmium in the rhizosphere: a review. J. Exp. Bot. 62(1):21-37.

Maine MA, Duarte MV, Suné NL (2000). Cadmium Uptake by Floating Macrophytes. Water Res. 35(11):2629-2634.

O'brien TP, Feder N, Mccully ME (1964). Polychromatic staining of plant cell walls by toluidine blue O. Protoplasma 59(2):368-373.

Oliveira FC, Mattiazzo ME (2001). Mobility of heavy metals in a yellow Latosol treated with sewage sludge and cultivated with sugarcane. Rev. Sci. Agric. 58(4):807-812.

Oliveira JA, Cambraia J, Cano MAO, Jordão CP (2001). Absorption and accumulation of cadmium and its effects on the relative growth of water hyacinth plants and salvinia. Rev. Bras. Fisiol. Veg. 13(3):329-341.

Paiva HN, Carvalho JG, Siqueira JO (2002). Nutrient translocation index in cedar (Cedrela fissilis Vell.) and Ipe - Purple (Tabebuia impetiginosa (Mart.) Standl.) Subjected to increasing levels of cadmium , nickel and lead. Rev Árv. 26(4):467-473.

Pasqualini S, Piccioni C, Reale L, Ederli L, Torre GD, Ferranti F (2003). Ozone-induced cell death in tobaco cultivar Bel W3 plants. The role of programmed cell death in lesion formation. Plant Physiol. 133(3): 1122-1134.

Pereira FJ (2010). Anatomical and physiological characteristics of water hyacinth and phytoremediation rate of water lettuce grown in the presence of arsenic, cadmium and lead. Thesis (Doctorate in Plant Physiology) - Federal University of Lavras. 116.

Pino GAH (2005). Biosorption of heavy metals using coconut shell powder (Cocos nucifera). Dissertation (Masters in Metallurgical Engineering) - Pontifícia Universidade Católica do Rio de Janeiro, Rio de Janeiro 113 p.

Qian JH, Zayed A, Zhu YL, Yu M, Terry N (1999). Phytoaccumulation of trace elements by wetland plants: III. Uptake and accumulation of ten trace elements by twelve plant species. J. Environ. Qual. 28(5):1448-1456.

Siriwan P, Maleeya K, Prayad P, Suchart U (2006). Toxicity and bioaccumulation of cadmium and lead in Salvinia cucullata. J. Environ. Biol. 27(4):645-652.

Sridhar BBM, Diehl SV, Han FX, Monts DL, Su Y (2005). Anatomical changes due to uptake and accumulation of Zn and Cd in Indian mustard (Brassica juncea). Environ. Exp. Bot. 54(2):131-141.

Sridhar BBM, Han FX, Mont DL, Su Y (2007). Effects of Zn and Cd accumulation on structural and physiological characteristics of barley plants. Brazilian J. Plant Physiol. 19(1):15-22.

Stohs SJ, Bagchi D (1995). Oxidative mechanisms in the toxicity of metal ions. Free Radic. Biol. Med. 18(2):321-336.

Toppi LS, Lambardi M, Pazzagli L, Capuggi G, Durante M, Gabbrielli R (1998). Response to cadmium in carrot in vitro plants and cell suspension cultures. Plant Sci. 137(2):119-129.

Vaculik M, Konlechner C, Langer I, Adlassing W, Puschenreiter M, Lux A, Hauser MT (2012). Root anatomy and element distribution vary between two Salix caprea isolates with different Cd accumulation capacities. Environ. Pollut. 163:11-126.

Vardanyan LG, Ingole BS (2006). Studies on heavy metal accumulation in aquatic macrophytes from Sevan (Armenia) and Carambolin (India) lake systems. Environ. Int. 32(2):208-218.

Vecchia FD, La Rocca N, Moro I, De Faveri S, Andreoli C, Rascio N (2005). Morfhogenetic ultrastructural and physiological damages suffered by submerged leaves of Elodea canadensis exposed to cadmium. Plant Sci. 168(2):329-338.

Zhou QA, Zhang J, Fu J, Shi J, Jiang G (2008). Biomonitoring: an appeling tool for assessment of metal pollution in the aquatic ecosystem. Anal. Chim. Acta 606(2):35-150.

academicJournals

Vol. 15(21), pp. 897-909, 25 May, 2016
DOI: 10.5897/AJB2015.15068
Article Number: C5453DC58592
ISSN 1684-5315

http://www.academicjournals.org/AJB

African Journal of Biotechnology

Full Length Research Paper

Surface composition and surface properties of water hyacinth *(Eichhornia crassipes)* root biomass: Effect of mineral acid and organic solvent treatment

Netai Mukaratirwa-Muchanyereyi[1, 2], Jameson Kugara[1] and Mark Fungayi Zaranyika[1]*

[1]Chemistry Department, University of Zimbabwe, P. O. Box MP 167 Mount Pleasant, Harare, Zimbabwe.
[2]Bindura University of Science Education, Bindura, Zimbabwe.

Received 26 October, 2015; Accepted 11 March, 2016

The surface composition and surface properties of water hyacinth (*Eichhornia crassipes*) root biomass were studied before and after extraction with dilute nitric acid and toluene/ethanol (2/1, v/v) followed by ethanol, using Fourier Transform Infra-red (FT-IR) spectroscopy, thermogravimetric analysis, x-ray diffraction, scanning electron microscopy. FT-IR absorption bands were obtained at 3421, 2855, 1457 and 1035 cm^{-1} (O-H stretch, C-H vibration, C-H asymmetric deformation, and C-O stretch, respectively) and 1508, 1541 and 1559 cm^{-1} (all aromatic skeletal vibrations characteristic of lignin), as well as a C=O carboxylate stretch vibrational band at 1654 cm^{-1}. Scanning electron microscopy confirmed the root biomass to be amorphous and not to have a strongly structured surface. The dilute mineral acid and organic solvent treatment increased crystallinity. Thermogravimetric analysis Studies show that the treated biomass are more thermally stable than the untreated biomass. Data are presented showing that dilute mineral acid and organic solvent treatment resulted in a decrease in the amount of lignin in the biomass. The implications of the decrease in the percentage of lignin on the adsorption of volatile polar organic solvents and non-polar n-alkane hydrocarbons is discussed.

Key words: Water hyacinth, biomass, surface composition, Fourier Transform Infra-red (FT-IR) spectroscopy, scanning electron microscopy, x-ray diffraction spectroscopy, thermo gravimetric analysis.

INTRODUCTION

The use of lignocellulosic biomaterials as adsorbents for various types of inorganic and organic water pollutants has been reviewed by Gupta et al. (2009), Mahamadi (2011), Hubbe et al. (2014), Priya et al. (2014) and Tran et al. (2015). The interest in bio-sorbents derives from the fact that biomaterials are environment friendly and are readily available, and therefore qualify as low-cost adsorbents. Adsorbent properties of lignocellulosic materials depend on the plant type from which they are derived, the conditions under which the plant grew, the origin of the fibre (that is, whether root, rhizome, stem or leaf), particle size, surface composition, and any physical

*Corresponding author. E-mail: zaranyika@science.uz.ac.zw

or chemical pre-treatment the material is subjected to. Lignocellulosic biomaterials are composed of fibres that can be considered as naturally occurring composites, consisting mainly of helically wound cellulose microfibrils bound together by lignin and hemicelluloses. Cellulose is the most abundantly occurring natural polymer. Regardless of its source, cellulose is a polymer of β-D glucose units. The monomer units are linked together by □-(1-4)-glycosidic bonds forming straight chains. Each monomer has three hydroxyl groups. These chains are linked by hydrogen bonds as hydroxyl groups of the glucose units on one chain are able to form hydrogen bonds with an oxygen atom on the other chain. This enables the chains to be held together firmly to form microfibrils in which highly ordered (crystalline) regions exist with less ordered amorphous region (Celik and Demirbas, 2005).

Lignin is the second largest in abundance after cellulose. Unlike cellulose, lignin is a highly branched polyphenolic polymer that is three dimensional. It consists of three monomers namely p-coumary alcohol, coniferyl alcohol and sinapyl alcohols. These are found in lignin as phenylpropane units (Martone et al., 2009). Lignin is located in the spaces between cellulose and hemi-celluloses and pectin components in plant cell wall, and gives the plant cell wall mechanical strength. The percentage of lignin differs from one plant to another. In soft wood and hardwood, it forms 23 to 33% and 16 to 25% respectively of the total mass, whereas it forms 26 to 33% of the total mass in plant biomass (Miretzkya and Cirelli, 2010). Lignins differ in terms of the degree of carbon-carbon crosslinking between phenyl groups (Celik and Demirbas, 2005). In hardwood it is covalently linked with xylans whereas in softwood it's linked with galactogluconannans. The chemical composition and physical composition of lignin depends on the method of isolation employed to separate it from the polysaccharide moieties. The common functional groups in lignin include aliphatic and phenolic hydroxyl groups (9 to 11%), methoxy groups (13 to 26%), and carbonyl groups (Miretzkya and Cirelli, 2010).

Hemicelluloses are short chain polymers of about 200 monosaccharide units composed of glucose, xylose, mannose, galactose, rhannose, and arabinose. Hemi-celluloses and cellulose are bound to lignin by hydrogen bonds (Miretzkya and Cirelli, 2010). Lignocellulosic materials thus have carboxyl and hydroxyl functional groups that can be modified by chemical treatment to improve the selectivity of the adsorption (Bandosz, 2006). The available acidic and basic functional groups can be added or eliminated from the surface, thus governing the adsorption of either polar or non-polar species.

One plant that is receiving considerable attention as a potential low-cost bio-sorbent is water hyacinth *(Eichhornia crassipes)*. Water hyacinth is a floating aquatic weed belonging to the pickerel weed family, *Pontederiaceae.* It is one of the fastest growing plants, and can tolerate a considerable variation in nutrients, temperature and pH (Rezania et al., 2015). It has flourishing roots composed mainly of cellulose and lignin (Zheng et al., 2009). It has been investigated extensively for the removal of dyes from aqueous solution (Tarawou et al., 2007; Low et al., 1995; Rajamohan, 2009; Aboul-Fetoula et al., 2010; Saltabas et al., 2012; Khan et al., 2012; El-Khalary, 2007; Modenes et al., 2013; Mahamadi and Mawere, 2013; Uddin et al., 2013; Rajamohan et al., 2013; Kaur et al., 2013; Nath et al., 2014). Water hyacinth has also been investigated for the removal of phenols from polluted water by Woverton and McKown (1976). The adsorbent properties of water hyacinth biomass were recently reviewed by Priya et al. (2014) and Mahamadi (2011), who concluded that water hyacinth biomass showed excellent biosorbent properties, and that further investigations were required on the structural properties of the material before and after modification. The aim of the present study was to evaluate the effect of dilute mineral acid and organic solvent treatment on the surface chemistry and surface properties of water hyacinth root biomass. This was achieved by studying the surface composition and surface properties of the ground dried water hyacinth root biomass powder before and after extraction with dilute mineral acid (nitric acid) and an organic solvent mixture (toluene/ethanol, 2/1v/v, followed by ethanol), using Fourier Transform Infra-red (FT-IR) spectroscopy, thermo gravimetric analysis (TGA), x-ray diffraction (XRD), scanning electron microscopy (SEM) and atomic absorption spectrometry (for elemental composition), in addition to standard chemical and physical methods for moisture, mineral matter (or ash), organic matter, organic carbon and lignin content determination.

MATERIALS AND METHODS

Equipment

A DR-8001 Shimadzu FT-IR Spectrophotometer (Shimadzu Corporation, Japan) was used for infrared characterization of the water hyacinth root biomass. A Brucker D2 Phase diffractometer (Brucker (Pvt) Ltd, Karlsruhe, Germany) X-ray was used to record diffractograms (XRD) of ground dried water hyacinth roots. A Jeol 6510 (Jeol, USA) Scanning Electron Microscope was used to obtain the SEM micrograms. A 6200 flame atomic absorption spectrometer (Shimadzu Corporation, Japan) was used for measuring the elemental composition for the root biomass. Sieves, 150 and 212 μm (BS410/1986, Endecotss Ltd, London, England) were used to sieve the water hyacinth root biomass after grinding.

Water hyacinth root biomass

Water hyacinth plants were collected from Waerera river, Bindura, Zimbabwe, at Universal Transverse Mercator (UTM) coordinate of (318500; 8078400). At the laboratory, the plants were washed with tap water several times, and then washed with distilled water. The roots were separated from the tops, cut into pieces, and air dried for several days. The root samples were then ground using a mortar and pestle, and then sieved first through the 212 μm sieve, and

Table 1. Chemical composition of water hyacinth root biomass.

Variables	% MC[a]	%DM[b]	%MM[c]	%OM[d]	%OC[e]
Untreated	0.04±0.00	99.96±0.02	18.43±0.02	81.57±0.02	47.31±0.00
Nitric acid Treated	9.36±0.00	90.64±0.00	17.49±0.00	82.49±0.00	47.84±0.00
Organic solvent treated	0.057±0.00	99.94±0.03	17.41±0.03	82.59±0.03	47.90±0.00

[a]Moisture content; [B]dry matter; [C]mineral matter or ash content, [D]organic matter; [E]organic carbon.

Table 2. %Lignin in Water Hyacinth root biomass.

%Lignin			References
Untreated	Acid treated	Solvent treated	
23	20	17	This study
27.7			Girisuta et al., 2008
9.93			Poddar et al., 1991
9.27			Abdelhamid, 1991
26.36			Chanakya et al.,1996
3.5			Nigam, 2002
15.2			Mukherjee and Nandi, 2004
12.2			Ahn et al., 2012
5.3			Fileto-Perez et al., 2013

then the 150 μm sieve, retaining the 150 to 212 μm fraction. Potassium bromide (AR grade, Sigma -Aldrich, Germany) was used to prepare KBr pellets for FT-IR analysis.

Solvent extraction

Samples of dried water hyacinth root biomass, 150 to 212 μm particle size, were successively extracted for 24 h in a Soxhlet apparatus, with toluene/ethanol (2/1,v/v) followed by ethanol (Tshabalala and Han, 1999). Each sample was filtered under suction, rinsed with boiling water, and then transferred to an Erlenmeyer flask containing boiling water. The flask was placed in a hot water bath and left to boil for approximately 1 h. The extracted sample was filtered under suction and air dried for 48 h. The dry sample was stored in a sealed glass jar (Tshabalala and Han, 1999).

Acid treatment

The water hyacinth root biomass powder was acid washed by soaking in 0.1 M HNO_3 for 24 h, followed by washing with deionized water, and drying at 65°C for 24 h.

Mineral matter, organic matter and organic carbon determination

About 1.0 g of the oven-dried samples was ashed in a muffle furnace at 550°C for 8 h. The ash was weighed to determine the amount of ash or mineral matter in the sample. The percentage of organic matter and organic carbon was determined using the following equations.

$$\%MM = \left(\frac{AW}{DW}\right)100 \quad (1)$$

$$\%OM = \left(\frac{DW - AW}{DW}\right)100 \quad (2)$$

$$\%OC = (\%OM)/1.724 \quad (3)$$

Where, MM is mineral matter or ash, OM is organic matter, OC is organic carbon, AW is ash weight of the sample, DW is dry weight of the sample, and 1.724 is the van Bemmelen factor (that is, organic matter contains 58% OC) (Armecin and Gabon, 2008). The results obtained are shown in Table 1.

Lignin content determination

The amount of lignin in the untreated water hyacinth biomass and the treated water hyacinth root biomass was calculated from the remaining solid after the hydrolysis of the water hyacinth root biomass with 1.25% H_2SO_4 for 2 h followed by 72% H_2SO_4 for 4 h. The residues obtained were filtered and then washed with Distilled water in order to remove the sulphuric acid. The residues were then dried at 105°C to constant weight. The lignin in the samples was calculated using Equation 4 (Irfan et al., 2011).

$$Lignin\% = \frac{LigninWeight(g)\times 100}{BiomassWeight(g)} \quad (4)$$

The results obtained are shown in Table 2.

Elemental composition

Approximately 0.5 g of the ground water hyacinth root biomass were weighed into a 100 ml Teflon beaker and digested with a

Table 3. Elemental analysis of untreated and acid treated biomass.

Element	Analysis (μg/g)		% Removal
	Before acid washing	After acid washing	
Fe	2399.2±0.2	317.9±0.01	86.8
Ni	172.4±0.3	42.95±0.00	75.1
Cu	427.3±0.1	205.4±0.02	51.9
Pb	176.6±0.1	163.8±0.9	7.2
Cr	244.66±0.03	52.6±0.1	78.5
Zn	616.5±0.6	154.3±0.1	75.0

mixture of 1 ml of 65% perchloric acid, 5 ml of 55% nitric acid and 0.5 ml 98% sulphuric acid, all GR grade, Merck, Germany. Heating was continued until the volume was reduced to approximately 2 ml, before transferring to a 100 ml volumetric flask, and diluting to the mark with deionised water for analysis by flame atomic absorption spectrometry (Muramoto et al., 1989). The levels of Fe, Ni, Cu, Pb, Cr and Zn in the root biomass were determined before and after acid treatment. The results obtained are shown in Table 3.

FT-IR spectrophotometry

Transmission mode FT-IR spectra of the KBr pellets of ground water hyacinth root biomass were obtained within the 4000 to 400 cm^{-1} wave number range at 4 cm^{-1} resolution. 50 scans were run for each sample and averaged. Figure 4 shows the FT-IR spectra obtained.

Thermal gravimetric analysis (TGA)

Thermal characteristics of the natural and treated samples were studied using TGA (STA 6000, Perkin Elmer, Massachusetts, USA) at a range of 34 to 900°C in a nitrogen atmosphere at a heating rate of 20°C/min. The data for derivative of the thermogravimetric analysis were also obtained from the same instrument and was used to plot derivative thermogravimetric analysis curves (DTA) (Figures 2 and 3).

X-Ray diffraction (XRD) and scanning electron microscopy (SEM) analysis

X-ray diffractograms (XRD) of ground dried water hyacinth roots were recorded in a Brucker D2 Phase diffractometer (Brucker (Pvt) Ltd, Karlsruhe, Germany) using 30 kV, 10 mA and CuK α-radiation, a step size of 0.01°, and a step scan of 1.05 s were used for the entire reading range (10 to 65°). Figure 4 shows the XRD spectra obtained. The SEM micrograms were obtained using a Jeol 6510 (Jeol, USA) Scanning Electron Microscope. The samples were clamped in such a way that they were presented to the analysing beam. Figures 5 and 6 show the typical SEM microgram obtained.

RESULTS AND DISCUSSION

Effect of mineral acid and organic solvent treatment on the chemical composition of water hyacinth root biomass

Table 3 shows the elemental composition of the roots of water hyacinth from Waerera River, Bindura, Zimbabwe, before and after mineral acid treatment. Data for untreated water hyacinth root biomass was found to be 2399, 172, 427, 177, 245, and 617 μg/g for Fe, Ni, Cu, Pb, Cr and Zn, respectively. The data in Table 3 shows that up to 86.8, 78.5, 75.1, 75, 51.9 and 7% of Fe, Cr, Ni, Zn, Cu and Pb respectively can be removed by soaking the water hyacinth root powder in 0.1 M nitric acid for 24 h, followed by washing with deionized water, and oven drying at 65°C for 24 h. Thus, while acid washing does not remove any of the metals completely, Fe, Ni, Cu, Cr and Zn are removed to a greater extent than Pb, suggesting that the major portions of Fe, Ni, Cu, Cr and Zn are loosely bound in the root biomass while the greater portion of Pb is more strongly bound.

The ash content of untreated, mineral acid treated and organic acid treated water hyacinth root biomass was found to be 18.43, 17.49 and 17.41 respectively (Table 2). Abdelhamid and Gabr (1991) reported an ash content of 27.7, Poddar et al. (1991) reported 16.29% and Patel et al. (1993) 20.2% for water hyacinth. An ash content of 7.91% was reported by Carvalho et al. (2015) for straw. The reduction in the ash content for the mineral acid treated biomass is in agreement with elemental analysis data for the acid treated sample which show that heavy metal content decreased after acid treatment (Table 3). Organic solvent treatment also caused a 5.5% reduction in the mineral content, most probably as a result of removal of extractable metal organic complexes in the water hyacinth root biomass.

The lignin content for the untreated, acid treated and organic solvent treated root biomass was found to be 23, 20 and 17% respectively. These values are within the range of those reported in literature for water hyacinth (Table 2). The lignin content of water hyacinth has been found to vary from 3 to 28% (Ahn et al., 2012), while land plants can have 20 to 40% hemicelluloses, 30 to 50 cellulose and 15 to 30% lignin (Bhattacharya and Kumar, 2010). Table 2 shows that organic solvent and mineral acid treatment lead to a reduction in the lignin content of 26 and 13% respectively.

Table 4 summarizes the peaks observed in the FT-IR spectra of untreated water hyacinth root biomass. The bands at 3691.62 and 3400 cm^{-1} are attributed to O-H

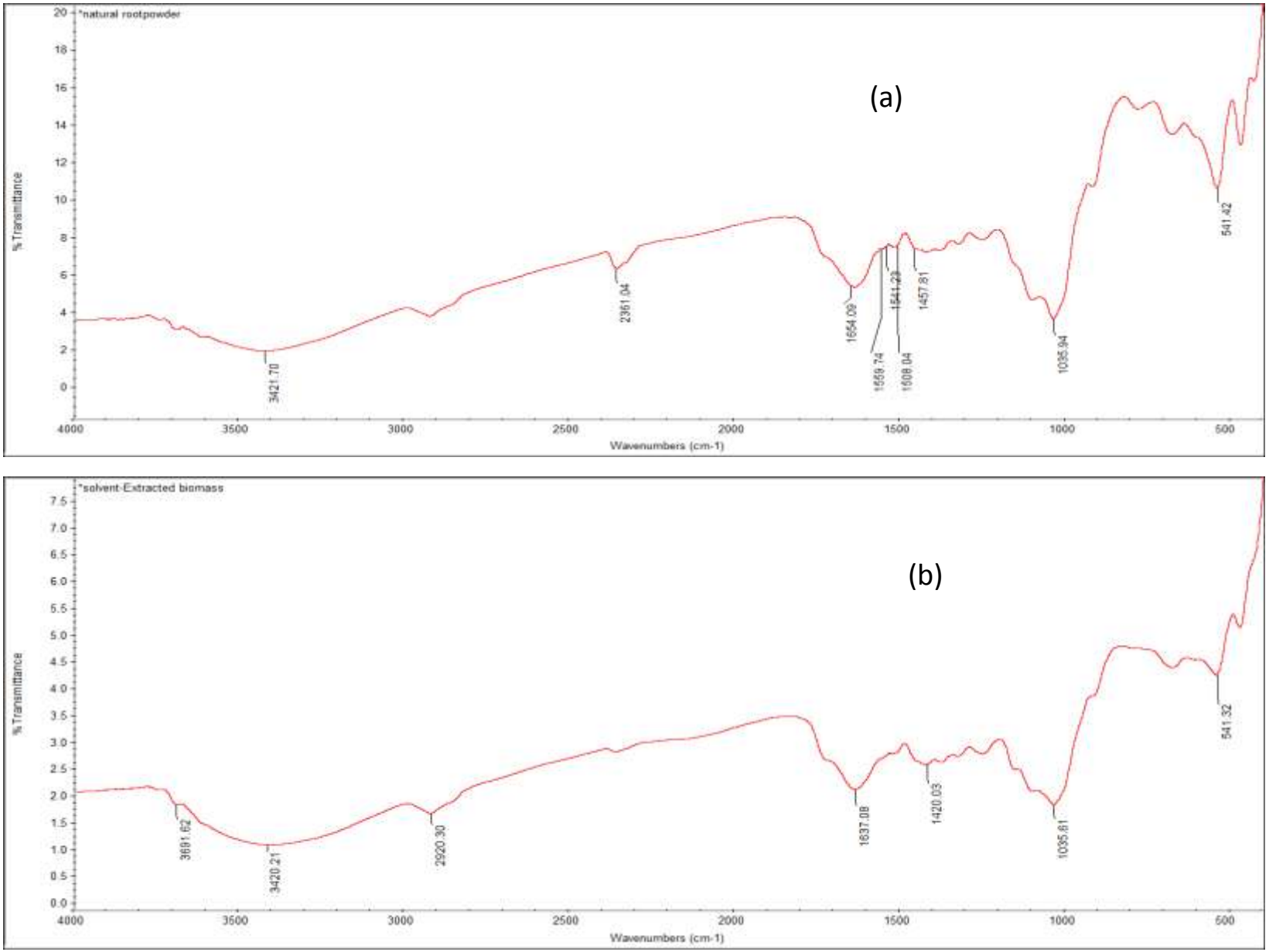

Figure 1. FTIR Spectra of (a) Natural, (b) solvent extracted, and (c) acid- treated water hyacinth biomass.

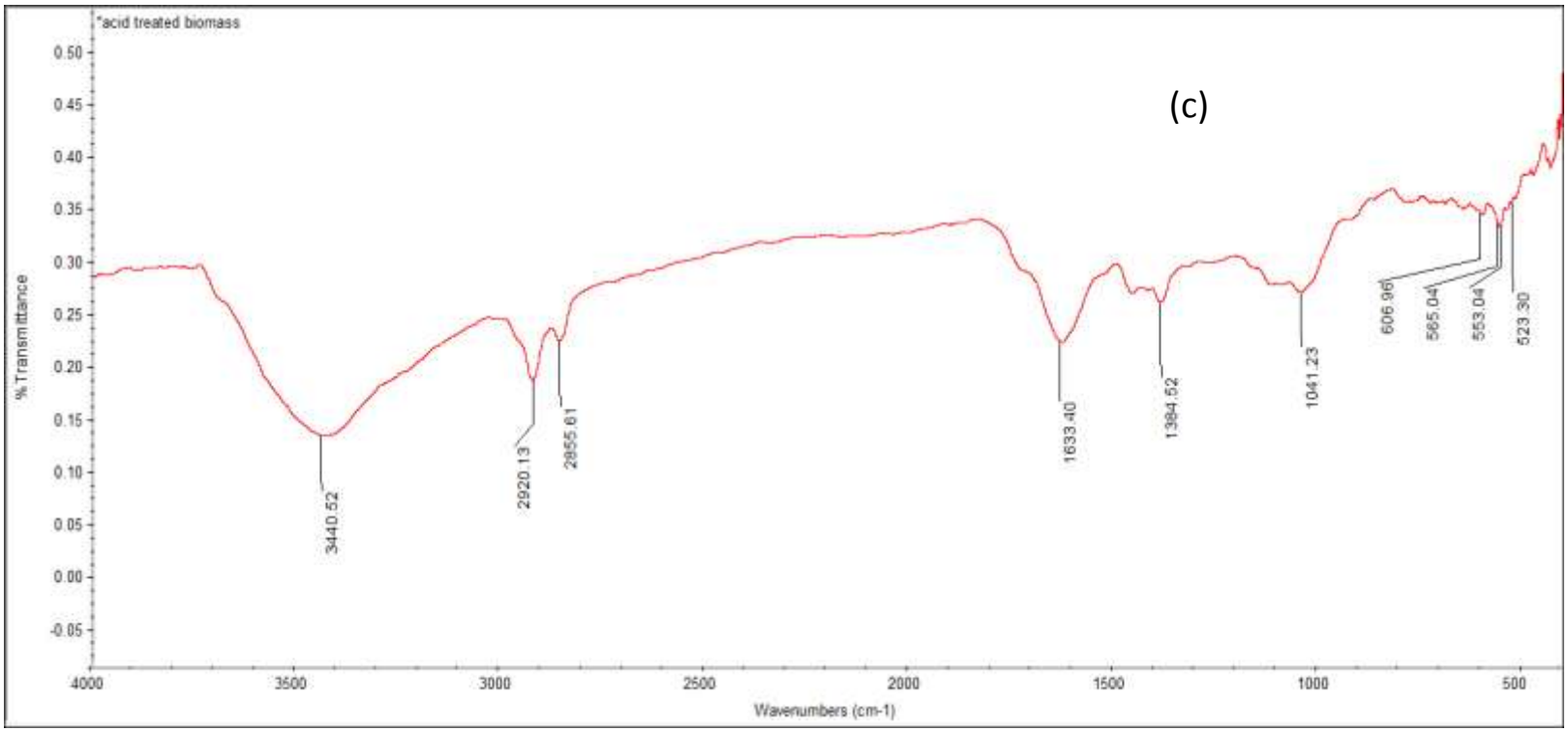

Figure 1. Contd.

stretch vibration (Sundari and Ramesh, 2012; Parikh, 1974). The band at 2920.30 cm^{-1} is attributed to C-H vibration for alkanes (Liu et al., 2006). The band at 2361.04 cm^{-1} was probably due to P-H or C=N (Parikh, 1974). The root biomass also shows a band at 1654.09 cm^{-1} attributed to C=O stretch vibration of carboxylate (Tshabalala et al., 2005; Liu et al., 2006; Southichak et al., 2006). Sundari and Ramesh (2012) reported a similar peak on water hyacinth nanofibers. The bands between 1500 cm^{-1} and 1600 cm^{-1} are attributed to the C=C aromatic skeletal vibration of lignin (Cordeiro et al., 2011a). The bands at 1457.81 and 1035.94 cm^{-1} are attributed to C-H deformation and C-O stretch respectively (Tshabalala et al., 2005). The presence of C-O stretch indicates the presence of alcoholic hydroxyl groups (Lim et al., 2008). FT-IR data thus suggest that the water hyacinth root biomass is mainly lignocellulosic in composition.

The FT-IR spectrum shows that untreated water hyacinth root biomass contains a greater percentage of cellulose than lignin or hemicelluloses. This is demonstrated by the fact that the most intense bands in the FT-IR of untreated water hyacinth root biomass are 3421.70, 2920 and 1035.94 cm^{-1} attributed to O-H and C-H stretch vibrations typical of cellulose (Cordeiro et al., 2011a).

FT-IR bands: Effect of acid washing and solvent extraction

The peak at 3691.62 cm^{-1}, O-H stretch, was present in the solvent extracted water hyacinth root biomass

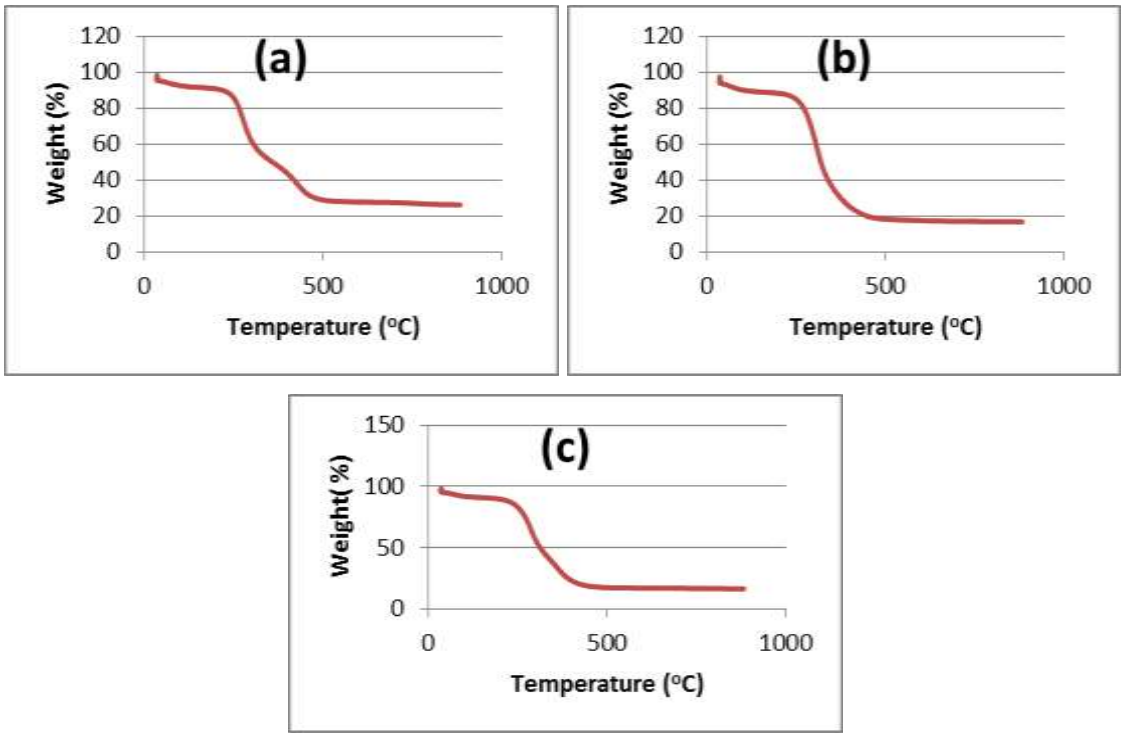

Figure 2. TGA thermogram of (a) untreated (b) solvent extracted, and (c) nitric acid treated water hyacinth (*Eichhornia crassipes*) root biomass.

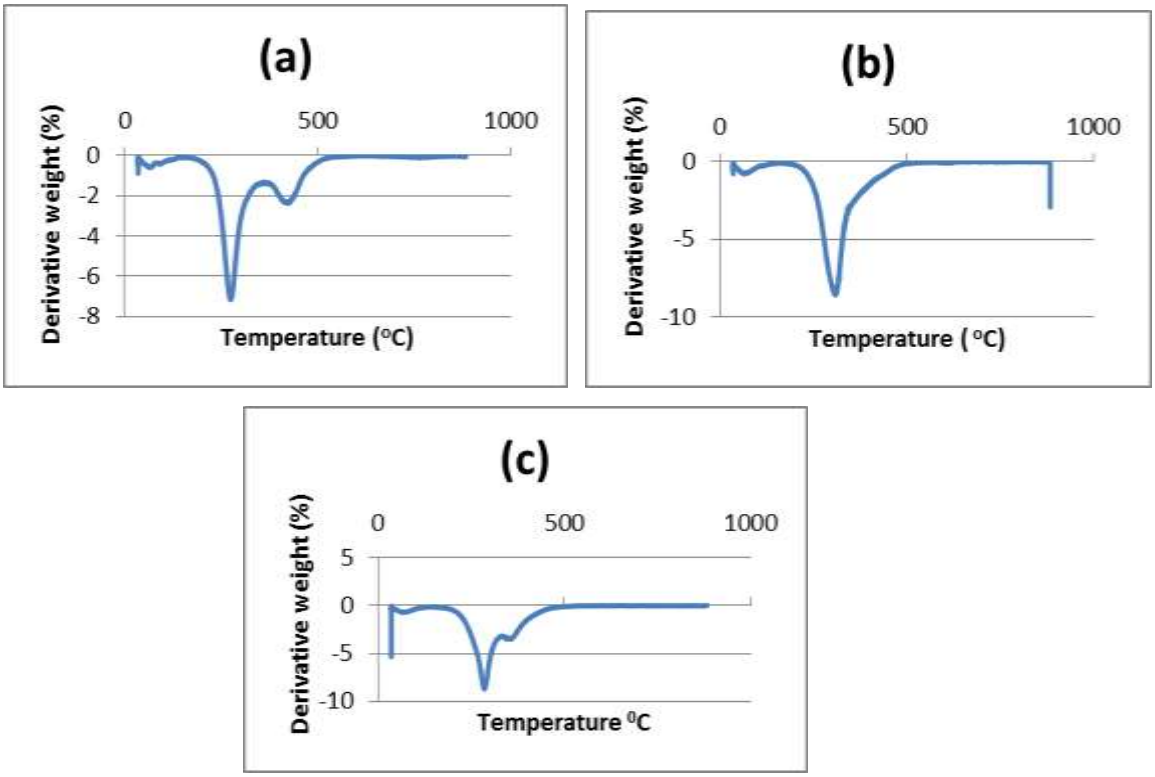

Figure 3. DTA curve for (a) untreated, (b) solvent treated, and (c) acid treated water hyacinth (*Eichhornia crassipes*) root biomass.

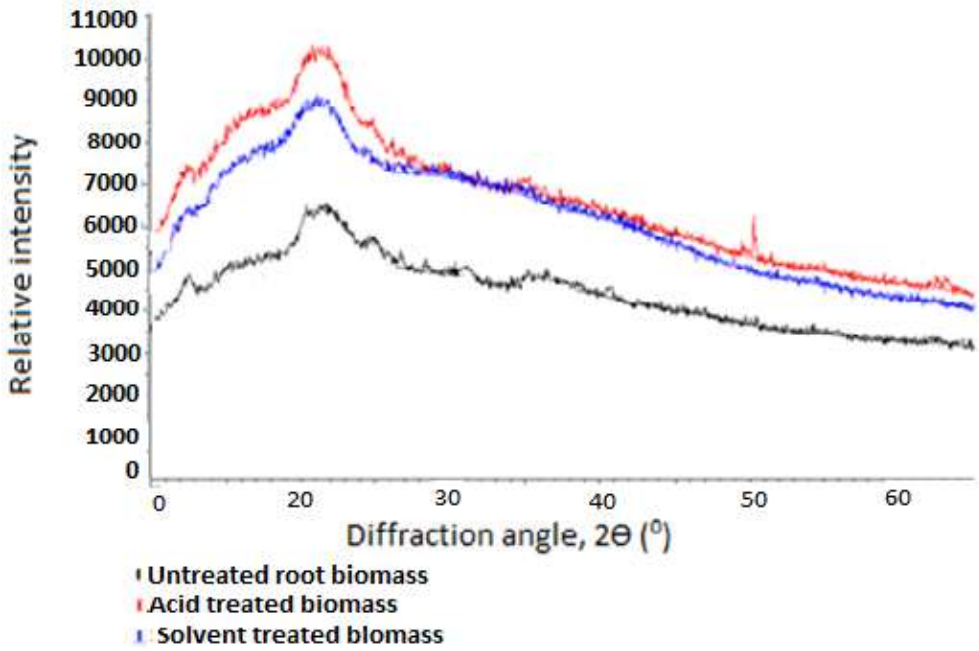

Figure 4. XRD diffractogram of ground dried water hyacinth (*Eicchornia crassipes*) untreated, acid treated and solvent extracted root biomass.

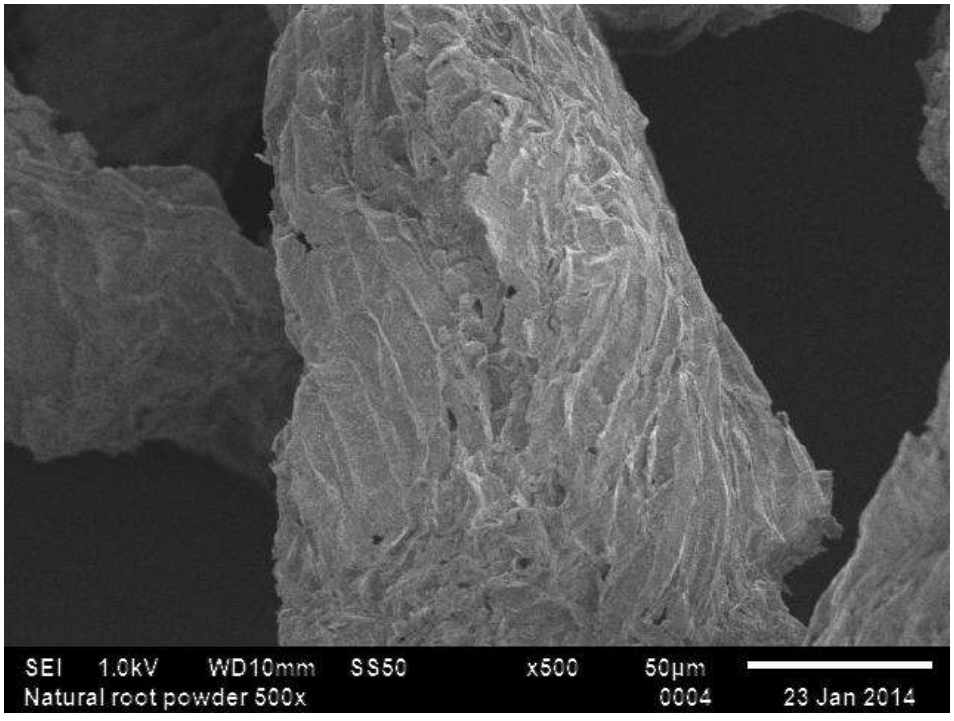

Figure 5. Scanning electron microscopy (SEM) micrograph of untreated ground dried water hyacinth (*Eicchornia crassipes*) root biomass.

sample, but was absent in the acid washed sample. Both solvent extracted and acid washed samples show the peak at 3420.70 cm^{-1}, O-H stretch vibration (bonded), although the peak for the solvent extracted sample is

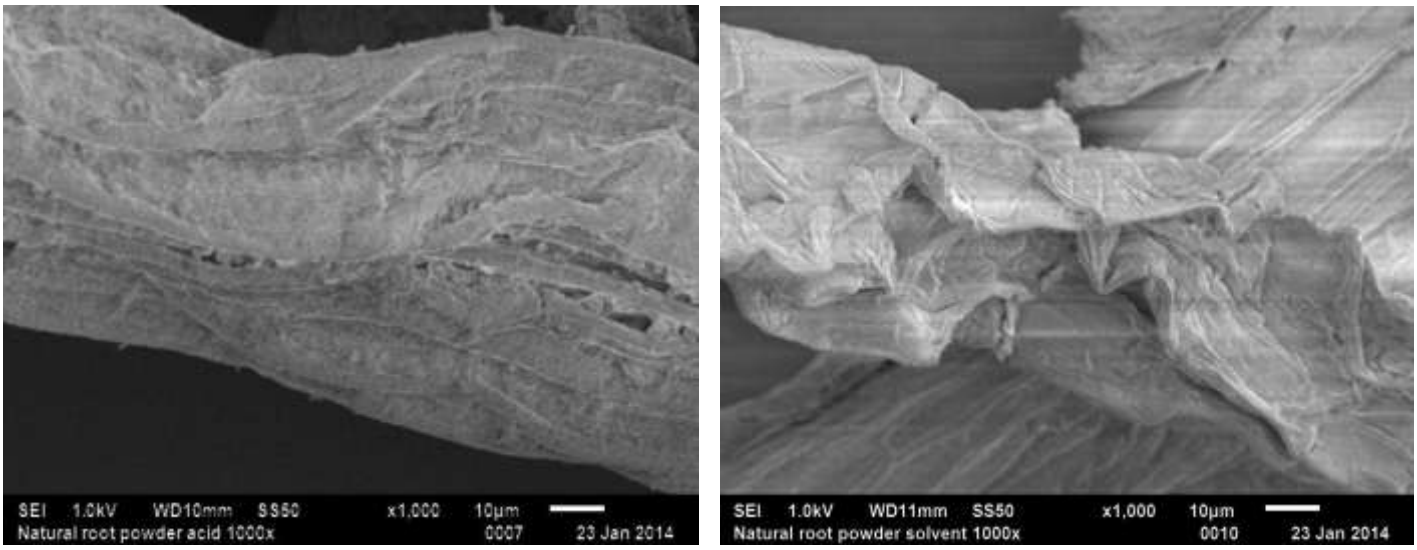

Figure 6. Scanning Electron Microscopy (SEM) microgram of ground dried water hyacinth (*Eicchornia crassipes*) root biomass: (a) acid treated; (b) solvent-extracted.

slightly shifted to higher energy at 3420.21 cm^{-1}, while that for acid washed sample is shifted downwards to 3440.52 cm^{-1}. The band at 2920.30 cm^{-1}, C-H vibration, is also present in both samples, but with a slight high energy shift to 2920.30 cm^{-1}. On the other hand, the band at 2361.04 cm^{-1}, was present in the solvent extracted sample, but absent in the acid washed sample. The loss of this peak in the acid washed sample was however accompanied by the appearance of a new peak at 2856.61 cm^{-1}. We attribute this new peak to C-H stretch (Parikh, 1974). The band at 1654.09 cm^{-1}, attributed to asymmetric and symmetric C-H stretch of the aliphatic groups (Parikh, 1974), is present in both mineral acid and organic solvent treated samples. The solvent extracted had a peak at 1637.08 cm^{-1} due to C=C and possibly adsorbed water. Peaks around that value are also due to C=O stretch vibration of carboxylate (Tshabalala et al, 2005; Liu et al., 2006; Southichak et al., 2006). The natural and the acid treated water hyacinth root biomass also showed the presence of the C=O stretch. Sundari and Ramesh (2012) reported a similar peak on the water hyacinth nanofibers (2012). Peaks between 1500 cm^{-1} and 1600 cm^{-1} are for the C=C aromatic skeletal vibration of lignin (Cordeiro et al., 2011a). These were observed in the natural biomass but not in the treated samples, suggesting that in the treated samples some lignin was removed by the treatment process. Peaks for C-H, as well as for C-O stretch, deformation was observed in all the samples (Tshabalala et al., 2005).The presence of C-O stretch indicates the presence of alcoholic hydroxyl groups (Lim et al., 2008). A summary of the peaks observed is shown in Table 4.

X-Ray diffraction and scanning electron microscopy analysis

In all the samples, Figure 4, there is a peak around the 22° reflection which corresponds to the (200) crystallographic plane (Tserki et al., 2005). A shoulder at around 16° is probably due to one of the 100 or ($\overline{100}$) planes (Thiebaud and Borredon, 1995). For materials that have high cellulose content like cotton, flax or other fibers, one may observe two peaks around 16°, but in cases where the content of amorphous materials such as lignin, hemicelluloses and amorphous cellulose is high, the two peaks are smeared and may appear as one shoulder. Thus the appearance of one peak at 16° in all the XRD diffractograms for the water hyacinth root biomass samples, suggests the presence of a high content of such amorphous materials in untreated, mineral acid treated and organic acid treated water hyacinth root biomass. The relative intensities of the peaks for the treated samples are higher than for the untreated sample suggesting the treatment procedures increased the crystallinity of the biomass. This could be as a result of removal of some amorphous constituents of the root biomass during treatment. Zafeiropoulos et al. (2002) reported a similar increase in crystallinity after acetylation of flax fiber. Similarly, Cordeiro et al. (2011b) reported an increase in crystallinity for sisal fiber after alkaline treatment.

The SEM microgram, Figure 5, shows that the root powder does not have a thick epiticuticular wax layer and it does not have a strongly structured surface, in agreement with the XRD results. The organic solvent and

Table 4. Summary of FT-IR bands in untreated water hyacinth root biomass.

Band (cm^{-1})	Assignment	References
3691.62	O-H stretch, alcohols	Parikh, 1974
3421.70	O-H stretch, alcohols	Tshabalala et al., 2005
2920.30	C-H vibration; alkanes.	Liu et al., 2006; Tahir and Alam, 2014.
2361.04	KBr	Tahir and Alam, 2014
1654.09	C=O stretch, carboxylate; KBr	Southichak et al., 2006
1559.74	C=O carbonyl	Parikh, 1974
	C=C aromatic skeletal vibration of lignin	Cordeiro et al. 2011a
1541.23	C=N stretchning.	Parikh, 1974; Gouveia et al., 2009
	C=C Aromatic skeletal vibration of lignin	Cordeiro et al., 2011a
1508.04	C=N; C-N amides; C=C Aromatic skeletal vibration of lignin; lignin ester	Parikh, 1974; Cordeiro et al 2011a; Southchak et al., 2006.
1457.81	C-H deformation assymetric	Cordeiro et al., 2011a
1035.94	C-O Stretch	Lim et al., 2008

mineral acid treatment caused partial disintegration of the surface probably due to removal of part of hemicelluloses and lignin that interconnects the cellulose fibrils (Figures 5 and 6).

Thermogravimetric analysis

The initial loss in mass in the TGA curves (Figure 2, 50 to 200°C) is due to loss of adsorbed moisture in the water hyacinth root biomass. The residues that remain in untreated and treated biomass after 500°C constitute carbonaceous materials. The treatment increased the stability of the biomass. From the DTA curves (Figure 3), the main decomposition temperatures for the untreated, acid treated and organic solvent treated were found to be 270, 282.96 and 301.14°C respectively. The lower decomposition temperature for the untreated biomass probably is due to the presence of higher content of pectin, lignin and hemicelluloses which have lower decomposition temperature (Chen et al., 2011). The decomposition of the polymer structure of lignin start at low temperature of 200 to 600°C (Brebu and Vasile, 2010; Kubo and Kadla, 2008).

Effect of surface composition on adsorbent properties

Recently, Mukaratirwa-Muchanyereyi et al. (2015) reported that the enthalpy of adsorption of volatile n-alkane hydrocarbons (n-hexane to n-decane) by water hyacinth root biomass increases following dilute mineral acid or organic solvent treatment, whereas that for volatile polar organic solvents (diethyl ether, dichloro-methane, acetone, ethyl acetate) increases after similar treatment. Figure 7 shows the correlation of enthalpy for the adsorption of the volatile polar solvents on water hyacinth root biomass and % lignin of the root biomass. All the plots show negative slope suggesting there is a positive correlation between enthalpy of adsorption and % lignin in the root biomass. Mukaratirwa-Muchanyereyi et al. (2015) attributed the decrease in the enthalpy of adsorption following mineral acid and organic solvent treatment to the removal of lignin and hemicelluloses on treatment. This interpretation is consistent with the trend in Figure 7. On the basis of these results we conclude that the adsorption of polar solvents by water hyacinth root biomass occurs mainly on lignin functional groups. For the adsorption of non-polar n-alkanes n-hexane, n-heptane and n-octane (Figure 8), the opposite trend is observed, suggesting negative correlation between enthalpy of adsorption and % lignin. The regression curves for n-hexane, n-heptane and n-octane show high linearity, with R^2 values of 0.8368, 0.8331 and 0.956 respectively. The increase in the enthalpy of following mineral acid and organic solvent treatment, suggests that the adsorption of the three n-alkanes by water hyacinth root biomass occurs mainly on cellulose chains. N-nonane shows a very low negative correlation coefficient (R^2 = 0.0286), suggesting little or no correlation between enthalpy of adsorption and % lignin for n-nonane.

Conclusions

From the foregoing discussion we conclude that the surface of the water hyacinth root biomass is composed of several different functional groups which include aliphatic groups, carboxylates, aromatic and alcoholic moities. Dilute mineral acid and organic solvent treatment lead to, not only changes in the surface compsition, but also a reduction in the level of lignin in the biomass, with the concequential increase in crystallity and thermal stability of the biomass.

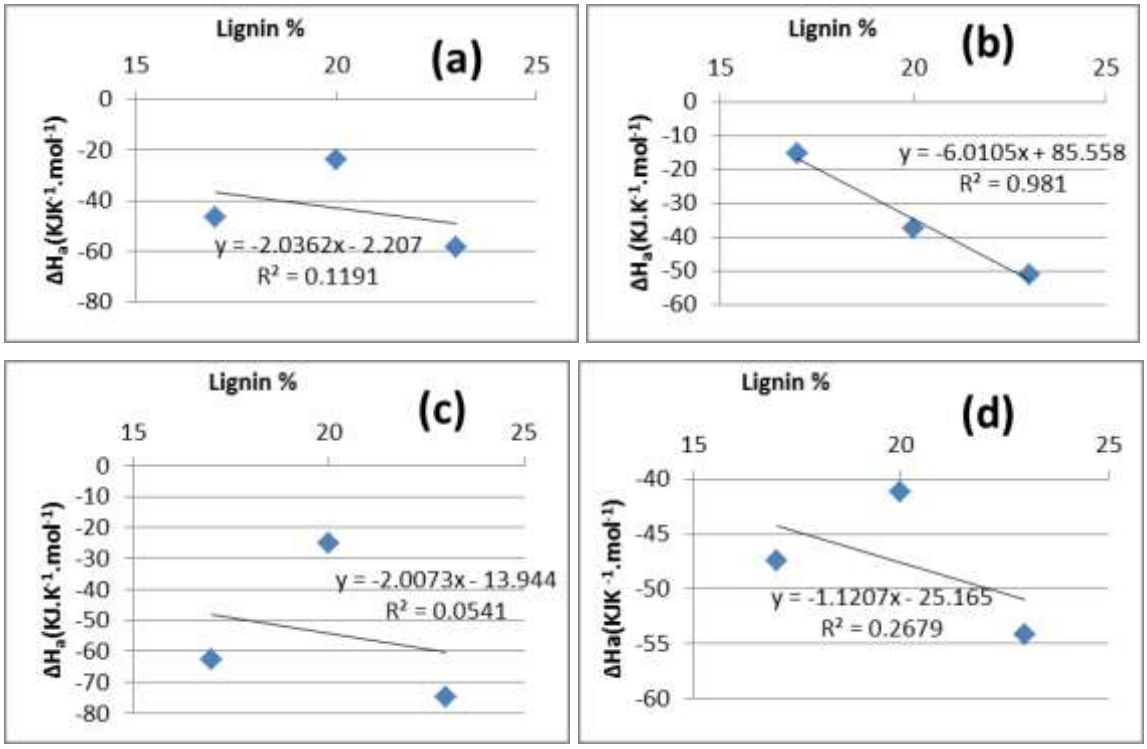

Figure 7. Plot of ΔHa versus % lignin in water hyacinth root biomass: (a) Diethyl ether, (b) acetone, (C) dichloromethane and (d) ethyl acetate.

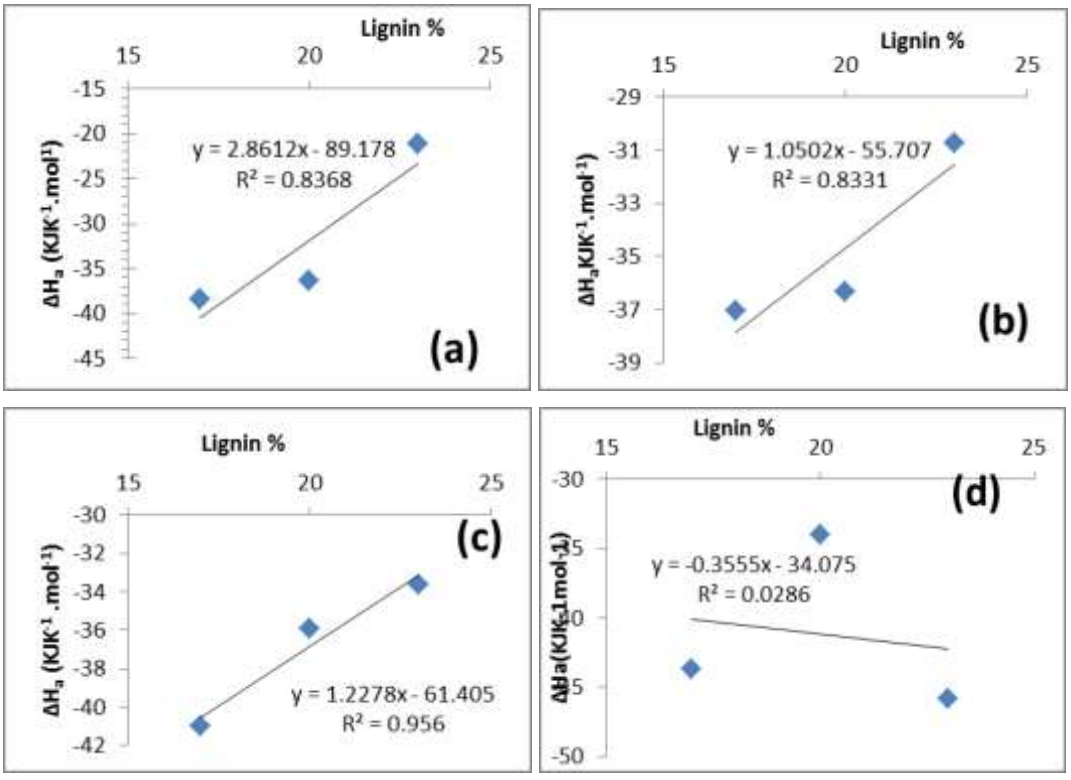

Figure 8. Plot of ΔHa versus lignin percentage in the biomass a) Hexane b) Heptane c) Octane, d) Nonane.

Conflict of Interests

The authors have not declared any conflict of interests.

REFERENCES

Aboul-Fetouh MS, Elmorsi TM, El-Kady JM, El-Adawi HA (2010). Water hyacinth stems: a potential natural adsorbent for the adsorption of acid green 20 dye. Environ. Sci. 5:257-266.

Ahn DJ, Kim SE, Yan HS (2012). Optimization of pretreatment and Saccharification for production of bioethanol from WHC by *Saccharomyces cerevisiae*, Bioprocess. Biosyst. 35:35-41.

Armecin RB, Gabon FM (2008). Biomass, organic carbon and mineral matter contents of abaca (*Musa textilis Nee*) at different stages of growth. Ind. Crop Prod. 28:340-345.

Bandosz TJ (2006). Activated carbon surfaces in environmental remediation. Academic Press.

Bhattacharya A, Kumar P (2010). Water hyacinth as a potential biofuel crop. Electron. J. Environ. Agric. Food Chem. 9(1):112-122.

Brebu M, Vasile C (2010). Thermal degradation of lignin: A review. Cellulose Chem. Technol. 44(9):353-363.

Celik A, Demirbas A (2005) Removal of heavy metal ions from aqueous solutions via adsorption onto modified lignin from pulping wastes. Energy Sources 27(12): 1167-1177. DOI: 10.1080/00908310490479583.

Chanakya HN, Borgaonkar S, Meena G, Jagadish KS (1996). Solid phase biogas production with garbage or water hyacinth. Bioresour. Technol. 46:227-231.

Chen W, Yu H, Liu Y, HaiY, Zhang M, Chen P (2011). Isolation and characterization of cellulose nanofibers from four plant cellulose fibers using a chemical-ultrasonic process. Cellulose 10:433-442.

Cordeiro N, Gouveia C, Jacob JM (2011a). Investigation of surface properties of physico-chemically modified natural fibers using inverse gas chromatography. Ind. Crop Prod. 33:108-115.

Cordeiro N, Gouveia C, Moraes AGO, Amico SC (2011b). Natural fibers characterization by inverse gas chromatography. Carbohydr. Polym. 84:110-117.

El-Khalary MI (2007). Kinetics and mechanism of adsorption of methylene blue from aqueous solution by nitric acid treated water hyacinth. J. Hazard. Mater. 147(1-2):28-36.

Fileto-Perez HA, Rutiaga-Quinones JG, Gonzalez-Aguila CN, Paez JB, Lopez J, Rutiaga-Quinones OM (2013). Evaluation of *Eichhornia crassipes* as an alternative raw material for reducing sugars production. Bioresources 8:5340-5348.

Girisuta B, Danon B, Manurung R, Janssen L, Heeres H (2008). Experimental and kinetic modeling studies on the acid-catalysed hydrolysis of the water hyacinth plant to levulinic acid. Bioresour. Technol. 99:8367-8375.

Gouveia FL, Oliveira RMB, Oliveira TB, Silva IM, Nanscimento SC, Sena KXFR, Albuquetque JFC (2009). Synthesis, antimicrobial and Cytotoxic activities of some 5- arylidene-4-thioxo-thiazohdine-2-ones. Eur. J. Med. Chem. 44:2038-2043.

Gupta VK, Carrott PJM, Ribeiron MMLR, Suhas (2009) Low-cost adsorbents: Growing approach to Wastewater Treatment-A review. Critic. Rev. Environ. Sci. Technol. 39:783-842.

Hubbe MA, Park J, Park S (2014). Cellulosic substrates for removal of pollutants from aqueous systems. A review. Part4. Dissolved petrochemical compounds. Bioresources 9:7782-7925.

Irfan M, Syed Q, Abbas S, Sher MG, Baig S, Nadeem M (2011). FTIR and SEM analysis of thermo-chemical fractionated sugarcane bagasse. Turk. J. Biochem. 36:322-328.

Kaur S, Rani S, Mahajan S, Kumar R (2013). Adsorption kinetics for removal of hazardous dye Congo red by biowaste materials as adsorbents. J. Chem. Volume 2013, Article ID 628582,12 pages.

Khan MR, Mozumder SI, Islam A, Prasad DMR, Alam MM (2012). Methylene Blue Adsorption onto Water Hyacinth: Batch and Column Study. Water Air Soil Pollut. 223:2943-2953.

Kubo S, Kadla JF (2008). Thermal decomposition study of isolated lignin using temperature modulated TGA. J. Wood Chem. Technol. 28:106-121.

Lim SF, Zheng YM, Zou SW, Chen JP (2008). Characterization of copper adsorption onto an alginate encapsulated magnetic sorbent by a combined FT-IR, XPS and mathematical modeling study. Environ. Sci. Technol. 42:2551-2556.

Liu CC, Wang MK, Chiou CS, Li YS, Lin YA, Huang SS (2006). Chromium removal and sorption mechanism from aqueous solutions by wine processing waste sludge. Ind. Eng. Chem. Res. 45:889-8899.

Low KS, Lee CK, Tan KK (1995). Biosorption of basic dyes by water hyacinth roots. Bioresource Technology 52(1): 79-83. DOI: 10.1016/0960-8524(95)00007-2.

Mahamadi C (2011). Water hyacinth as a biosorbent: A review. Afr. J. Environ. Sci. Technol. 5(13):1137-1145.

Mahamadi C, Mawere E (2013). Kinetic modelling of methylene blue and crystal violet dyes adsorption on alginate-fixed water hyacinth in single and binary systems. Am. J. Anal. Chem. 4:17-24.

Martone PT, Estevez JM, Lu F, Ruel K, Denny MW, Somerville C, Ralph J (2009). Discovery of lignin in seaweed reveals convergent evolution of cell-wall architecture. Curr. Biol. 19:169-175.

Miretzkya P, Cirelli AF (2010). Cr (VI) and Cr (III) removal from aqueous solution by raw and modified lignocellulosic materials: A review. J. Hazard. Mater. 180:1-19.

Modenes AN, Ross AA, Souza BV, Dotto J, Geraldi CQ, Espinoza-Quinones FR, Kroumov AD (2013). Biosorption of BF-4B reactive red dye by using leaves of macrophytes *Eicchornia crassipes*. Int. J. Bioautomation 17(1):33-44.

Mukaratirwa-Muchanyereyi N, Kugara J, Zaranyika MF (2015a). Thermodynamic parameters for the adsorption of volatile n-alkane hydrocarbons on water hyacinth (*Eichhornia Crassipes*) root biomass: Effect of organic solvent and mineral acid treatment. Afr. J. Environ. Sci. Technol. 9:282-291.

Mukherjee R, Nandi B (2004). Improvement of *in vitro* digestibility through biological treatment of water hyacinth biomass by two Pleurotus species. Int. Biodeterior. Biodegradation 53:7-12.

Muramoto S, Oki Y, Nishizaki H, Aoyama I (1989). Variation in some element contents of water hyacinth due to cadmium or nickel treatment with or without surface active agents. J. Environ. Sci. Health A24:925-934.

Nath A, Sudip C, Chiranji B (2014). Bioadsorption of industrial dyes from aqueous solution onto water hyacinth (*Eichhornia crassipes*): Equilibrium, kinetic and sorption mechanism study. Desalination Water Treat. 52(7-9):1484-1494.

Nigam J (2002). Bioconversion of water hyacinth (*Eichhornia crassipes*) hemicelluloses acid hydrosylate to motor fuel ethanol by xylose-fermenting yeast. J. Biotechnol. 97:107-116.

Parikh VM (1974). Absorption spectroscopy of organic molecules, Addison-Wesley, Reading, Massachusetts.

Poddar K, Mandal L, Banerjee GC (1991). Studies on water hyacinth (*Eichhornia crassipes*) - Chemical composition of the plant and water from different habitats. Indian Vet. J. 68:833-837.

Priya ES, Selvan PS (2014). Water hyacinth (Eichhornia crassipes) – An efficient and economic adsorbent for textile effluent treatment – A review. Arabian J. Chem. in Press.

Rajamohan N (2009). Equilibrium studies on sorption of an anionic dye onto acid activated water hyacinth roots. Afr. J. Environ. Sci. Technol. 3:399-404.

Rajamohan N, Rajasimman M, Rajeshkannan R, Sivaprakash B (2013). Kinetic modeling and isotherm studies on a batch removal of acid red 114 by an activated plant biomass. J. Eng. Sci. Technol. 8(6):778-792.

Rezania S, Ponraj M, Din MFM, Songip AR, Sairan FM, Chelliapan S (2015).The diverse applications of water hyacinth with main focus on sustainable energy and production for new era: An overview. Renew. Sustain. Energy Rev. 41:943-954.

Saltabas O, Teker M, Konuk Z (2012). Biosorption of cationic dyes from aqueous solution by water hyacinth roots. Glob. Nest. J. 14(1):24-31.

Southichak B, Nakano K, Nomura M, Chiba N, Nishimura O (2006). *Phragmites australis*: A novel biosorbent for the removal of heavy metals from aqueous solution. Water Res. 40:2295-2302.

Sundari MT, Ramesh A (2012). Isolation and characterization of cellulose nanofibers from the aquatic weed water hyacinth - *Eichhornia crassipes*. Carbohydr. Polym. 87(2):1701-1705.

Tahir H, Alam U (2014). Lignocellulosic non-conventional low cost biosorbent for elution of comassie brilliant blue (R-250). Int. J. Chem. 6:56-72.

Tarawou T, Horsfall Jr M, Vicente JL (2005). Adsorption of Methyl red by water hyacinth (*Eichhornia crassipes*). Biomass. Chem. Biodivers. 4:2236-2245.

Thiebaud S, Borredon ME (1995). Solvent-free wood esterification with fatty acid chlorides. Bioresour. Technol. 52:169-173.

Tran VS, Ngo HH, Guo W, Zhang J, Liang S, That CT, Zhang X (2015). Typical low cost biosorbents for adsorptive removal of specific organic pollutants from water. Bioresour. Technol. 182:353-363.

Tserki V, Matzinos P, Kokkou S, Panayiotou C (2005). Novel biodegradable composites bases on treated lignocellulosic waste flour as filler. Part I. Surface chemical modification and characterization of waste flour. Compos. Part A Appl. Sci. Manuf. 36(7):965-974.

Tshabalala MA, Han JS (1999). Effect of solvent extraction on surface energy of kenaf powder. In: Sellers T, Reichert NA (eds), Kenaf Properties, Processing and Products, Mississippi State University, Mississippi, pp. 121-131.

Tshabalala MA, Jakes J, Vanlandingham MR,Wang S, Peltonen J (2005). Surface characterization. In Rowell, R.M.(ed), Handbook of Wood Chemistry and Wood Composite. CRC Press, Boca Raton, pp. 217-247.

Uddin MD, Islam MT, Chakrabarti MH, Islam MS (2013). Adsorptive removal of methylene blue from aqueous solutions by means of HCl treated water hyacinth: isotherms and performance studies. J. Purity Utility React. Environ. 2(3):63-84.

Woverton BC, McKown MM (1976). Water hyacinth for removal of phenols from polluted water. Aquat. Bot. 2:191-201.

Zafeiropoulos NE, Williams DR, Baillie CA, Matthews FL (2002). Engineering and characterisation of the interface in flax fibre/polypropylene composite materials. Part I: Development and investigation of surface treatments. Compos. Part A Appl. Sci. Manuf. 33(8):1083-1093.

Zheng JC, Feng HM, Lama MH, Lama PK, Ding YW, Yua HQ (2009). Removal of Cu (II) in aqueous media by biosorption using water hyacinth roots as a biosorbent material. J. Hazard. Mater. 171:780-785.

academicJournals

Vol. 15(21), pp. 910-916, 25 May, 2016
DOI: 10.5897/AJB2015.15143
Article Number: A8A27B158594
ISSN 1684-5315

http://www.academicjournals.org/AJB

African Journal of Biotechnology

Full Length Research Paper

In-silico smart library design to engineer a xylose-tolerant hexokinase variant

Yasser Gaber

Microbiology Department, Faculty of Pharmacy, Beni-Suef University, Beni-Suef, 62511, Egypt.

Received 2 December, 2015; Accepted 19 April, 2016

Saccharomyces cerevisiae **has two hexokinases *Sc*Hxk1 and *Sc*Hxk2 that catalyze ATP-dependent phosphorylation of glucose and other hexoses. *Sc*Hxk2 plays an important role in glucose metabolism and the process of bioethanol production. The presence of xylose in the fermentation medium was found to inhibit *Sc*Hxk2. Therefore development of *Sc*Hxk2 variants that are resistant to the action of xylose is needed. In the current study, in-silico investigation was done aiming to select the amino acids in *Sc*Hxk2 that can be targeted in an engineering experiment. Using Autodock Vina, xylose binding to *Sc*Hxk2 structure (PDB 1IG8) was predicted. The information available about hexokinase family in the publicly available hexokinase 3DM database were investigated and the conservancy patterns for potential residues in the xylose-binding site were extracted. The study eventually presented 54 suggested mutants that might lead to a xylose-tolerant hexokinase. Top correlated positions in the hexokinase superfamily indicated 6 proposed double-mutants that are worth to be included in the proposed smart library.**

Key words: Library design, hexokinase, 3DM, database, protein engineering, xylose.

INTRODUCTION

Saccharomyces cerevisiae hexokinase 2 (*Sc*Hxk2) catalyzes the phosphorylation of glucose to glucose 6-phosphate via transfer of an ATP phosphate group to the 6-position on the glucose. In addition to this catalytic activity, *Sc*Hxk2 is involved in the regulation of other genes using glucose catabolite repression mechanism (Moreno and Herrero, 2002). *Sc*Hxk2 is found to be irreversibly inhibited by xylose. Xylose has similar structure to glucose and has the ability to bind to the glucose binding site in *Sc*Hxk2 structure. In the presence of ATP, xylose was found to induce autophosphorylation of the *Sc*Hxk2 at Ser158 position (Heidrich et al., 1997). Therefore *S. cerevisiae* cannot efficiently utilize glucose in the presence of xylose. Xylose is an abundant hydrolytic product obtained from the pre-treatment of the lignocellulosic material used as feedstock for bioethanol production. Therefore, development of *Sc*Hxk2 variants able to efficiently utilize glucose in the presence of high concentration of xylose is required.

The directed evolution approach to engineer enzyme

E-mail: Yasser.Gaber@pharm.bsu.edu.eg.

Table 1. Docking results of xylose into *Saccharomyces cerevisiae* hexokinase 2 (PDB: 1IG8).

Binding site	Residues	Occurrence [%]	Binding affinity Kcal/mol
A	Ser158, Asn210, Asp211, Thr212, Ile231, Phe232, Gly233, Gly235, Val236, Asn237, Asn267, Glu269, Gly271, Glu302	**77.7**	**- 5.1**
B	Ile66, Pro67, Gly68, Phe157, Ser158, Phe159, Pro160, Ala161, Ser162, Gln163, Leu208, Ile209, Asn210, Thr213, Asn267, Glu269	**11.1**	**- 4.9**
C	Arg93, Gln109, Thr156, Asp211, Thr212, Thr215, Ile231, Asp417, Gly418, sp458, Gly459, Ser460, Gly461	**11.1**	**- 4.7**

variants with new properties has provided many successes over the last two decades (Wang et al., 2012). This approach necessitates the creation of a library of thousands of mutants followed by use of a good screening system to select for the desired variants. For efficient directed evolution experiment, the library size should be reduced to ease the screening effort. With the aid of advanced computer programs, the design of the library for directed evolution experiment becomes smarter and the library size becomes smaller (Nobili et al., 2013; Wijma and Janssen, 2013).

The 3DM database systems are high quality structural alignments of related protein structures (Joosten, 2007; Kuipers et al., 2010b). For each group of related protein structures, a superfamily is built and a consensus core is assigned. The consensus facilitates a unified numbering scheme for all the sequences in the superfamily that is, the 3DM-numbering scheme. This 3DM numbering allows knowledge transfer between similar residues that occupy the same spatial position in homologous protein structures. The 3DM also collects mutation information found in literature and link them to the 3DM numbers (Kuipers et al., 2010a). The successful application of 3DM for enzyme engineering, either for improving thermostability or catalytic property such as enantioselectivity has been described in Cerdobbel et al. (2011); Jochens et al. (2010) and Nobili et al. 2013).

In the current report, investigation of the *Sc*Hxk2 structure within the light of 3DM information was done. Selected positions in the active site were evaluated and suggested mutations were given that might increase the enzyme resistance to the inhibitory effect of xylose.

MATERIALS AND METHODS

Structure analysis of ScHxk2 was based on the protein structure deposited in the protein data bank PDB 1IG8 (Kuser et al. 2000), using YASARA Structure software (Krieger et al. 2002). The docking experiment of xylose was done using AutoDock Vina integrated in YASARA Structure software (ver. 13.9.8). Xylose coordinates, were extracted from the PDB: 2E2Q and energy was minimized using YASARA Structure and AMBER99 force field (Trott and Olson, 2010). The analysis of contacts between xylose and the surrounding residues in 1IG8 after the docking experiment was done using the Analysis/Contact function in YASARA Structure.

The amino acid sequence of *Sc*Hxk2 [UniProt accession no. P04807] was searched in the 3DM hexokinase database and was found under the identifier name: HXKB_YEAST. *Sc*Hxk2 belongs to the subfamily 1IG8A that includes 97 aligned sequences, and the consensus core contains 19 variable regions. The 3DM hexokinase database is built based on 20 structures, 547 aligned sequence and includes information from 2177 mutations. The superfamily has a consensus core of 214 residues. The superfamily is divided into 5 subfamilies based on five prototype protein data bank (PDB) structures namely: 1BDGA, 1IG8A, 1SZ2B, 2DGKN and 3CZAN. Each of these subfamilies has subfamily consensus which has some minor differences compared to the superfamily consensus. 3DM conservancy pattern for residues identified as targets for mutations were extracted, and the library designed considered the highest five alternatives for each target residues with a threshold of selection ≥ 0.4%.

RESULTS AND DISCUSSION

S. cerevisiae has two isoenzymes of hexokinase that catalyse phosphorylation of glucose in addition to other hexoses e.g. fructose and mannose. *Sc*Hxk2 structure has been determined using X-ray diffraction at a resolution of 2.2Å (Kuser et al., 2000). The structure has been determined without co-crystalized substrates or inhibitors. 1IG8 is composed of two domains that show significant movement upon glucose binding. Therefore, 1IG8 has two conformations referred to as either open or closed conformation. The docking experiment performed in the current report using AutoDock Vina, showed that xylose could probably occupy three main different binding sites inside 1IG8 structure (Table 1). The binding site A showed higher occurrence rate (77.7%) and slightly better binding affinity (-5.1 kcal/mol) compared to the other sites B and C

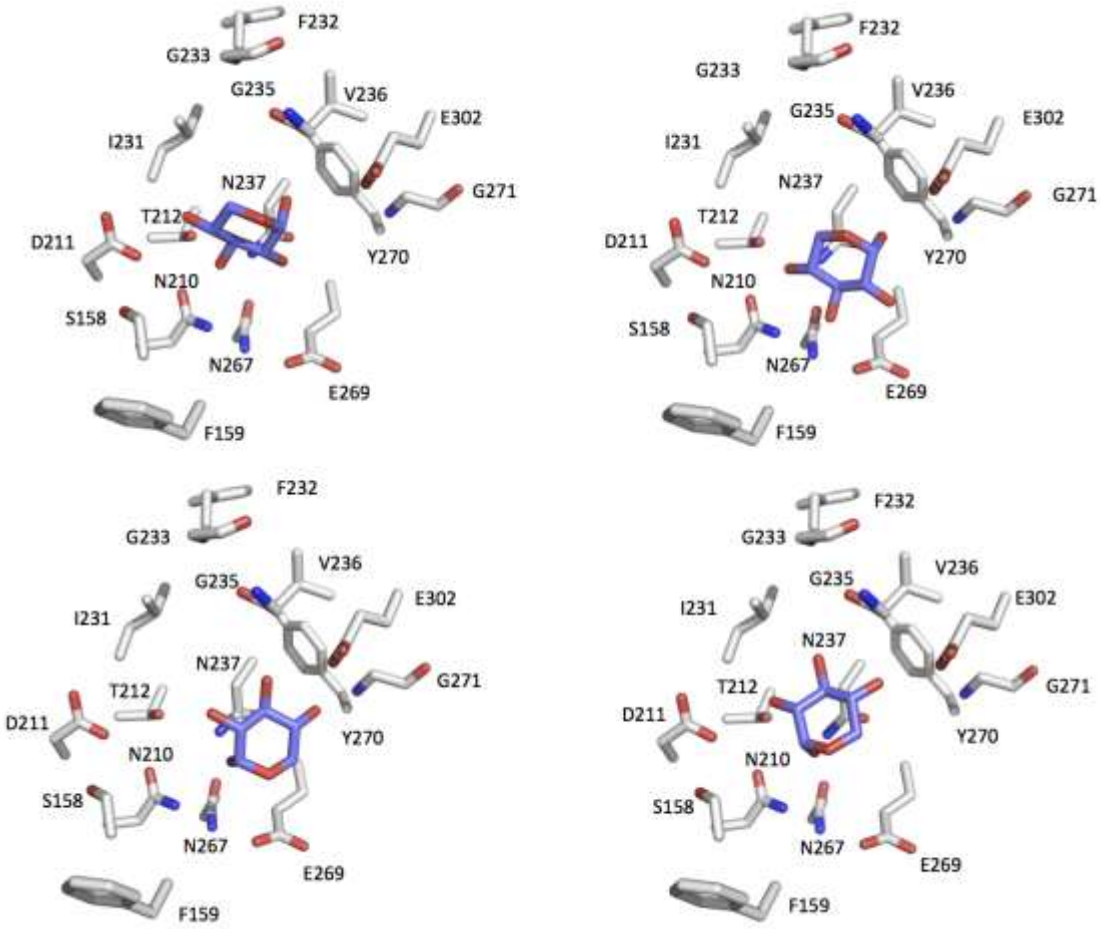

Figure 1. Docking of xylose into PDB 1IG8 showing different poses inside the binding site A (Table 1). The binding site is composed of: Ser158, Asn210, Asp211, Thr212, Ile231, Phe232, Gly233, Gly235, Val236, Asn237, Asn267, Glu269, Gly271 and Glu302. The figure is created using PyMol software.

(Table 1). Kuser et al. (2000) defined the glucose binding site based on the obtained X-ray crystallographic and modeling data. They found glucose to be coordinated by extensive hydrogen bonding with the surrounding polar residues. Figure 1 shows different poses of xylose docked into the binding site A. The highly conserved residues: Asp211, Glu302, and Asn237 are within 5-Å distances to xylose (Figure 1). Xylose was X-ray determined in a hexokinase derived from the hyperthermophilic archaeon *Sulfolobus tokodaii* at 2.0Å resolution (PDB: 2E2Q) (Nishimasu et al., 2007). Xylose was found coordinated by three acidic residues: Asp140, Asp95 and Asp71 in 2E2Q active site. These acidic residues are the equivalent to the residues Glu203 and Asp211 found in binding site A in 1IG8 (Figure 1).

The basic idea in 3DM database is the numbering scheme that allows identification of equivalent amino acid residues in the space for a certain family of proteins. Figure 2 shows screenshots of hexokinase 3DM database interface. Figure 2A shows *Sc*Hxk2 sequence with two numbering schemes: the original sequence numbering and 3DM numbering. The green parts of the sequence belong to consensus core of the superfamily and the white parts belong to variable regions. Figure 2B shows the top correlated positions in the hexokinase superfamily and Figure 2C shows the detailed correlation score given by the 3DM to the correlated positions no. 46 and 52. Table 2 shows the residues of *Sc*Hxk2 selected as potential targets for mutations. The residues are based on the docking results of xylose and information in literature regarding the glucose binding inside related hexokinases. One aspect of smart library design is to exclude whatever mutations might be deleterious to the protein proper folding. The 3DM was consulted regarding the selected targeted mutation residues (Table 2). The conservancy pattern for each of targeted residues was

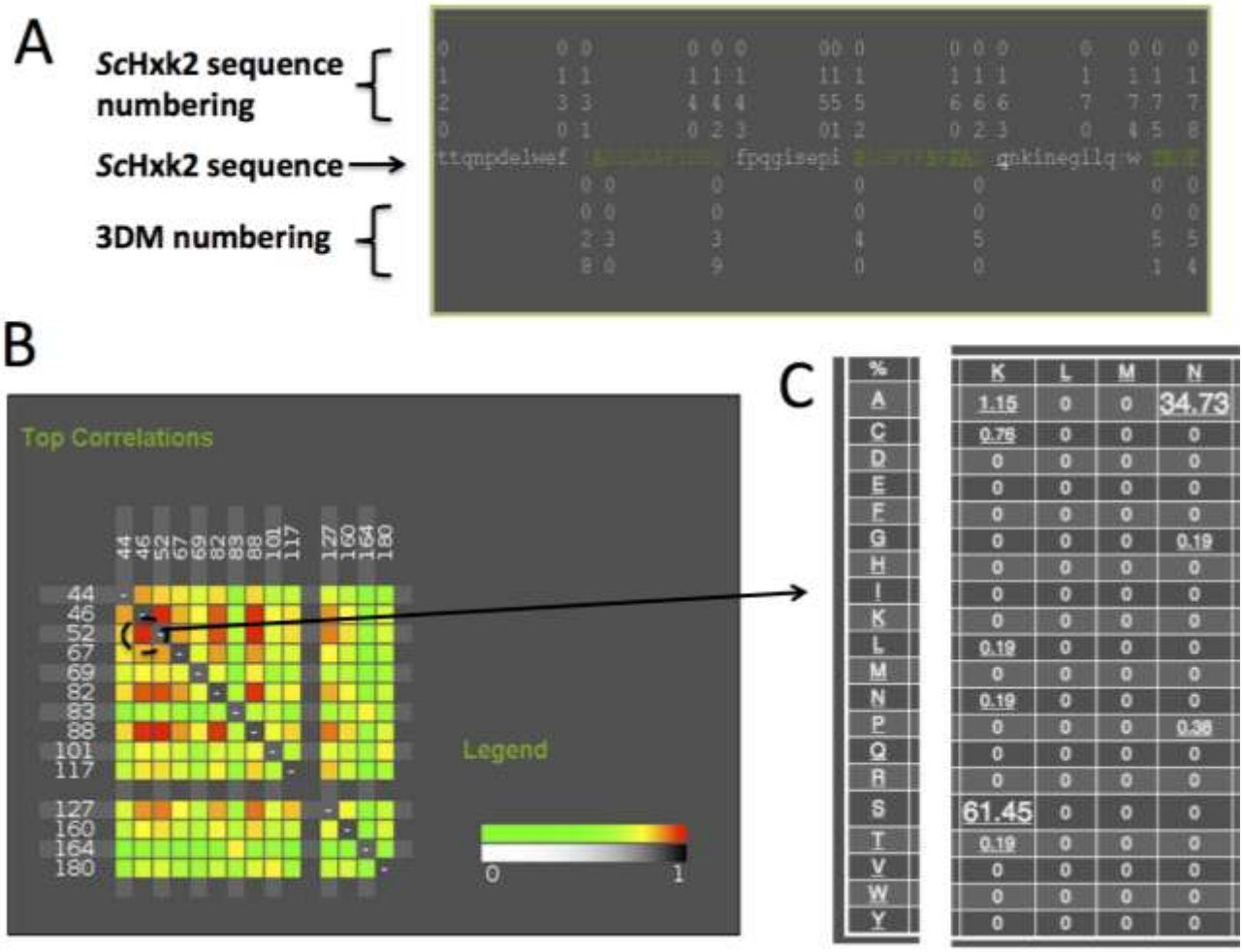

Figure 2. Screenshots of 3DM database interface. A, Hexokinase 3DM database showing part of *Sc*Hxk2p with its numbering and the equivalent 3DM numbers. Green parts of the sequence correspond to the consensus for the family designated by the 3DM system which means *Sc*Hxk2 position number 131 is equivalent to position number 28 in the 3DM numbering. White parts of the sequence are variable regions (for example Arg173 is equivalent to the 3DM number e13). B, Top correlated positions in the Hexokinase superfamily. The numbers shown are the 3DM numbers. The 3DM no. 46 and 52 are equivalent to the residues Ser158 and Lys176 respectively in *Sc*Hxk2. The correlation heat-map was generated by 3DM Hexokinase database (www.bio-prodict.nl). The red color indicates high correlation and the green color indicates low correlation. C, detailed correlation of the positions 46 and 52; Ser158 and Lys176 are highly correlated to each other (3DM correlation score 61.450. Also, Ala158 and Asn176 are highly correlated to each other (3DM correlation score 34.73).

extracted from the 3DM and presented as percentages in Table 2. It was observed that some target residues were highly conserved such as Asn210 that has been found to have 99.27% predominance in the hexokinase super-family. Such a high percentage does not recommend mutation of such position and therefore was excluded from the proposed library (Table 3). Bergdahl et al. (2013) engineered *Sc*Hxk2 targeting selected residues in the glucose binding site. Comparing our library (Tables 3) to the results obtained by Bergdahl *et al*., showed interesting observations. First, there is an agreement of the successful mutation described by the Bergdahl et al. (2013) to the 3DM conservancy pattern that is, Phe159Tyr. Phe159Tyr corresponds to the 3DM number 47 and Tyr is found in 9% of the total sequences of the superfamily (Table 2), which is a relatively high percentage. More interestingly, when the conservancy is calculated based on the subfamily 1IG8A, Tyr is found in 47% of all the sequences at this position (3DM no 47). This mutation specifically agrees with the 3DM suggestion. In another example that shows that statistical data might give suggestions that do not match with conventional mutation strategies, 3DM has not suggested to replace the basic residue Lys176 (3DM number 52)

Table 2. The Hexokinase 3DM database conservancy pattern (%) for residues located in xylose binding site in *Sc*Hxk2. Dark red shaded cells indicate high conservancy.

Target residues	3DM No.	3DM conservancy pattern (%)																			
		A	V	I	L	F	W	Y	C	M	S	T	G	P	H	N	Q	D	E	K	R
S158*	46	35.1			0.2				0.7		62.9	0.2	0.4	0.4		0.2					
F159	47		0.9	0.2		55.5		9	7.7		0.7	1.1	19.9	0	0.4	4.2		0.2			0.2
R173	e13[a]	1							1		1	4.2			2.1	1	2.1			5.2	82.3
K176*	52	0.2		0.2										0.2	0.2	34.6				64.7	
N210	65															99.27					
D211	66		0.9										0.2		0.2	0.6		98			0.2
T212	67	2.9	0.2		1.5	31.4		1.5			2.8	58.6	1.1								
I231*	82	1.3	1.7	62.8		0.2					0.4	0.2	33.4			0.2					
F232	83	13.03	21.28	10.64	13.67	15.6		0.18	0.55	1.1	0.37	0.18		23.12	0.18						
G233	84	0.6		0.2							0.9		98.2			0.2					
T234	85	1.3			0.2	0.2		0.2		0.2	1.5	96.3				0.2					
G235	86			0.9									98.9			0.2					
V236	87	1.83	4.01	0.37	32.48	2.94			12.66	0.73	14.5	30.09			0.37						
N237*	88												34.31			65.5					
N267	96	8.23	1.1								4.57	0.37	2.74	15.72	0.18	63.44		0.73	2.38	0.55	
E269	98												0.2		0.2			0.9	98.5	0.2	
G271	100	1.5			0.2				0.4		3.5	2.6	91.6					0.2	0.2		
E302	120					0.2												0.6	99.1		0.2

* Top correlated positions.

with its related residue Arg at any instance (Table 2), instead Asn was found to be the strong candidate for a mutation (34 %). Similarly, the residue Asp211 (3DM no. 66) has never been found to be replaced by Glu residue. Intriguingly, Arg was found at this site in a small percentage (0.2 %) of sequences. The Gly271 residue (3DM no. 100) was found to be replaced by Ser, Thr and Ala residues at probabilities 3.5, 2.6 and 1.5% respectively, which are much higher than the Cys residue (0.4%) chosen by Bergdahl et al. (2013) in their engineering experiments. Similarly, the strong candidate to replace the position Thr212 (3DM no. 67) is Phe (31.4%) and not Ser (Bergdahl et al., 2013).

A very important feature that is provided by the 3DM database is the identification of the correlated positions. Correlated positions within a superfamily mean that a residue is found in nature to mutate simultaneously in correlation with another residue. This kind of correlated mutations might be of importance for correct protein folding or certain catalytic function. The correlated positions, however, are almost impossible to using the computational design protocols. Figures 1B and 1C show the top correlated positions in the hexokinase superfamily. The correlation analysis of the superfamily show that there are strong correlations between the positions 46 and 52 which are equivalent to the *Sc*Hxk2 positions Ser158 and Lys176 respectively. Ser158 has been defined as the site of phosphorylation upon xylose binding in the presence of ATP resulting in inactive hexokinase. Mutation of this residue to Ala, Cys, Gly, or Pro residues will lead to proper folded proteins according to the 3DM information (Table 2). However, this position is annotated as highly correlated to other positions in the hexokinase superfamily namely the 3DM positions 52, 82 and 88. Therefore, we suggested mutating this position to be in accordance with the correlation data provided by 3DM (Table 3). If the

Table 3. The proposed smart library designed to engineer hexokinase 2 into a xylose-tolerant hexokinase variant, totally 54 mutants including 6 double-mutants are suggested. The highest 5 alternatives suggested by the conservancy pattern by Hexokinase 3DM database was used with a threshold of selection ≥ 0.4%.

Target residue(s)	3DM No.	Suggested mutations					Number
S158*	46	A	C	G	P	-	4
F159	47	Y	C	T	G	N	5
R173	e13[a]	K	T	H	Q	-	4
K176*	52	N	-	-	-	-	1
N210	65	-	-	-	-	-	0
D211	66	V	N	-	-	-	2
T212	67	A	F	S	-	-	3
I231*	82	A	V	G	-	-	3
F232	83	A	V	I	L	P	5
G233	84	A	S	-	-	-	2
T234	85	A	S	-	-	-	2
G235	86	I	-	-	-	-	1
V236	87	L	F	C	S	T	5
N237*	88	G	-	-	-	-	1
N267	96	A	S	G	P	E	5
E269	98	D	-	-	-	-	1
G271	100	A	S	T	-	-	3
E302	120	D	-	-	-	-	1
Top correlated positions							
S158K176		A158N176					1
S158I231		A158G231					1
S158N237		A158G237					1
K176I231		N176G231					1
K176N237		N176G237					1
I231N237		G231G237					1
Total mutants							54

*Top correlated positions.

3DM position 46 (*Sc*Hxk2 Ser158) is mutated to Ala the 3DM position 52 (*Sc*Hxk2 Lys176) is mutated to Asn (3DM correlation score 34.37). This correlation was observed in 184 sequences all of which are under the subfamily 1SZ2B. Heidrich et al. (1997) mutated Ser158 to Ala and the activity was dramatically decreased compared to the wild type. The correlation of these two positions might interpret the recorded decreased enzymatic activity. Lys176 and Asn176 are found to interact by hydrogen bonding to the glucose in the active site as determined by X-ray experiments in the PDB entries: 1SZ2 and 1BDG. Therefore, the pairs Ser158Lys176 or Ala158Asn176 contribute to proper binding of glucose in the active site and have strong influence on the enzymatic activity.

It can be concluded from the present investigation that statistical information available for the hexokinase 3DM superfamily can be efficiently exploited to engineer the yeast hexokinase 2. A library of a very small size is prepared that can be easily implemented in the laboratory. Table 3 shows a list of positions in *Sc*Hxk2 active site and the most probable point mutations that can be experimentally done according to 3DM consensus. We envisage that the application of the proposed mutations can lead to deeper understanding of the structure-function relationship of *Sc*Hxk2 and identification of new enzyme variants that might resist the inhibitory action of xylose.

Conflict of Interests

The authors have not declared any conflict of interests.

REFERENCES

Bergdahl B, Sandström AG, Borgström C, Boonyawan T, van Niel EWJ, Gorwa-Grauslund MF (2013). Engineering yeast hexokinase 2 for

improved tolerance toward xylose-induced inactivation. PloS one 8(9):e75055-e75055.
Cerdobbel A, De Winter K, Aerts D, Kuipers R, Joosten HJ, Soetaert W, Desmet T (2011). Increasing the thermo stability of sucrose phosphorylase by a combination of sequence-and structure-based mutagenesis. Protein Eng. Des. Sel. 24(11):829-834
Heidrich K, Otto A, Behlke J, Rush J, Wenzel KW, Kriegel T (1997). Autophosphorylation-inactivation site of hexokinase 2 in *Saccharomyces cerevisiae.* Biochem. 36(8):1960-1964
Jochens H, Aerts D, Bornscheuer UT (2010). Thermostabilization of an esterase by alignment-guided focussed directed evolution. Protein Eng. Des. Sel. 23(12):903-909.
Joosten HJ (2007). 3DM: from data to medicine. PhD Thesis, University of Wageningen, Wageningen, The Netherlands.
Krieger E, Koraimann G, Vriend G (2002). Increasing the precision of comparative models with Yasara NOVA-a self-parameterizing force field. Proteins: Struct. Funct. Genet. 47:393-402.
Kuipers R, van den Bergh T, Joosten H-J, Lekanne dit Deprez RH, Mannens MM, Schaap PJ (2010a). Novel tools for extraction and validation of disease-related mutations applied to fabry disease. Hum. Mutat. 31(9):1026-1032,
Kuipers RK, Joosten HÄ, van Berkel WJ, Leferink NG, Rooijen E, Ittmann E, van Zimmeren F, Jochens H, Bornscheuer U, Vriend G (2010b). 3DM: systematic analysis of heterogeneous superfamily data to discover protein functionalities. Proteins: Structure, Function, and Bioinformatics 78(9):2101-2113.
Kuser PR, Krauchenco S, Antunes OAC, Polikarpov I (2000). The High Resolution Crystal Structure of Yeast Hexokinase PII with the Correct Primary Sequence Provides New Insights into Its Mechanism of Action. J. Biol. Chem. 275(27):20814-20821.
Moreno F, Herrero P (2002). The hexokinase 2-dependent glucose signal transduction pathway of *Saccharomyces cerevisiae*. FEMS Microbiol. Rev. 26(1):83-90
Nishimasu H, Fushinobu S, Shoun H, Wakagi T (2007). Crystal Structures of an ATP-dependent Hexokinase with Broad Substrate Specificity from the Hyperthermophilic Archaeon *Sulfolobus tokodaii*. J. Biol. Chem. 282(13):9923-9931.
Nobili A, Gall MG, Pavlidis IV, Thompson ML, Schmidt M, Bornscheuer UT (2013). Use of 'a small but smart' libraries to enhance the enantioselectivity of an esterase from *Bacillus stearothermophilus* towards tetrahydrofuran-3-yl acetate. FEBS J. 280(13):3084-3093.
Trott O, Olson AJ (2010). Auto Dock Vina: Improving the speed and accuracy of docking with a new scoring function, efficient optimization, and multithreading. J. Comput. Chem. 31(2):455-461.
Wang M, Si T, Zhao H (2012). Biocatalyst development by directed evolution. Bioresour. Technol. 115:117-125.
Wijma HJ, Janssen DB (2013). Computational design gains momentum in enzyme catalysis engineering. FEBS J. 280(13):2948-2960.

academicJournals

Vol. 15(21), pp. 917-929, 25 May, 2016
DOI: 10.5897/AJB2015.14701
Article Number: 221607E58596
ISSN 1684-5315

http://www.academicjournals.org/AJB

African Journal of Biotechnology

Full Length Research Paper

Morphological diversity in oleaginous watermelon (*Citrullus mucosospermus*) from the Nangui Abrogoua University germplasm collection

Ahou A. Gbotto[1]*, Kouamé K. Koffi[1], Nandy D. Fouha Bi[1], Serge T. Doubi Bi[1], Hippolyte H. Tro[1], Jean-Pierre Baudoin[2] and Irié A. Zoro Bi[1]

[1]Université Nangui Abrogoua, UFR des Sciences de la Nature, 02 BP 801 Abidjan 02, Côte d'Ivoire.
[2]Unité de Phytotechnie Tropicale et d'Horticulture, Faculté universitaire des Sciences agronomiques de Gembloux, Passage des Déportés 2, B-5030 Gembloux, Belgium.

Received 6 May, 2016; Accepted 11 April, 2016

A hundred and seventy-one oleaginous watermelon accessions either collected from different countries or obtained from gene banks were evaluated and compared based on 11 quantitative morphological traits. Principal component analysis on 11 traits revealed 81.19% of the total variability and pointed out variations among accessions, mainly on the basis of fruit size and weight. The dendrogram and factorial discriminant analysis clustered the accessions in four groups. The multivariate analysis of variance showed a significant difference between the four groups and accessions of the group 2 had higher agronomic performances. The confusion matrix gave the details about accessions assignment and pointed out that breeders must have recourse to several multivariate analyses to have better agromorphological classification of accessions. The traits related to fruit size and weight were the most accession distinctive. Consequently, fruit morphological traits could be used for accession identification during collecting missions.

Key words: *Citrullus mucosospermus*, morphological characterization, multivariate analysis, oleaginous cucurbit.

INTRODUCTION

Cucurbits are present in both the New and Old World and are among the most important plant families that supply human with edible products and useful fibers. Cucurbits are divided into five sub-families: Fevilleae, Melothrieae, Cucurbitaceae, Sicyoideae, and Cyclanthereae.The genus *Citrullus* Schrad. ex Eckl et Zeyh placed closest to a clade formed by *Peponium* and *Lagenaria*, the latter including the bottle gourd (*Lagenaria siceraria*), confirming previous findings(Schaefer and Renner, 2011). *Citrullus*, member of the cucurbit family, includes seven species: (1) *Citrullus lanatus* (Thunb.) Matsum. et Nakai (2n = 22), found in tropical and subtropical climates

*Corresponding author. Email: gizachew.gh@gmail.com.

worldwide; (2) *Citrullus amarus* Schrad. 1836 syn. *C. caffer* Schrad. 1838, also known as *C*. *lanatus* var. *caffrorum* (Alef.) Fosb. or *C. lanatus* var. *citroides* (L.H. Bailey) Mansf.; it is the preserving melon grown in Southern Africa and called tsamma melon (Whitaker and Bemis, 1976) is used to make jams since at least the fifteenth century (Bailey, 1930); (3) *Citrullus mucosospermus* Fursa, the so-called egusi melon, largely referred to as a subspecies of *C. lanatus* by many authors (including recently(Hammer and Gladis, 2014)), but which was earlier raised at specific rank(Fursa, 1972, 1981, 1983); (4) *Citrullus colocynthis* (L.) Schrad. (2n = 22), a perennial species growing in sandy areas throughout Northern Africa and adjacent Asia; (5) *Citrullus ecirrhosus* Cogn., another perennial wild species (Meeuse, 1962); (6) *Citrullus rehmii* De Winter, an annual wild species (de Winter, 1990), and (7) *Citrullus naudinianus* (Sond.) Hook.f., from the Namib-Kalahari region.

Watermelon (*Citrullus vulgaris*) (Cucurbitaceae) includes several other economically important species such as cucumber (*Cucumis sativus*), melon (*Cucumis melo* L), squash (*Cucurbita pepo*), calabash (*L. siceraria*), and pumpkin (*Citrullus maxima*). *C. lanatus* is an annual species, which has wild, cultivated, and feral forms.

In the finding that the watermelon and its sister species are West African plants suggests that the natural range of watermelon may have extended into Libya or into Egypt during more humid periods of the Pleistocene and Holocene(Schulz, 1987, 1991). Alternatively, watermelon seeds may have been traded from West Africa to Northern Africa. The illustrations found in Egyptian tombs of watermelon served on a tray suggest that these fruits were eaten raw, perhaps as a dessert. Seeds found in ancient Egyptian tombs, including that of Thutankhamun (Hepper, 1990) should ideally be studied using ancient DNA approaches.

Genetically, the cultivated watermelon is closest to plants from West Africa that represents the gene pool from which watermelon was domesticated (Chomicki and Renner, 2014). The sister species of watermelon is *C. mucosospermus*, the egusi melon from Nigeria to Senegal and described by Fursa (1983), Che et al. (2003), and Dane and Liu (2007). In consideration of the findings by Fursa (1983)and Chomicki and Renner (2014), the egusi-type watermelon is recognized as *C. mucosospermus* throughout this paper.

The "egusi" watermelon of West Africa is cultivated for its oleaginous and nutritious seeds that are important in the social and cultural live of several peoples (Burkill, 1985; Oyulu, 1977; van der Vossen et al., 2004; Achigan-Dako et al., 2008). For example, dried slightly toasted and ground seeds are used as soup thickener. The "egusi" seeds are reported to be rich in nutrients ~60% lipids and ~30% proteins (Loukou et al., 2007). Edible oil can also be extracted from the seeds. Commonly found in many traditional cropping systems, the plant is well adapted to extremely divergent agro-ecosystems and various cropping systems characterized by minimal inputs. *C. lanatus* thus represents an excellent plant model for which improved cropping systems implementation can insure the economic prosperity of rural women that are the main producers in tropical Africa. The west African watermelon is generally considered as allogamous, monoecious, entomophilous, and protandrous(Gusmini and Wehner, 2003). This species is named as *C. lanatus* var. *lanatus* or as *C. lanatus* subsp. *Mucosospermus* (Fursa, 1972) or *C. colocynthis*(Hutchinson and Dalziel, 1954).

Particularly, in Côte d'Ivoire, indigenous and minor crops for local consumption have almost disappeared in favor of exotic species. Some farmers still continue to produce these crops not far from their home or on small plots cleared after harvest of the main annual crops (yams, corn, peanut, etc.) (Zoro Bi et al., 2003). Thus, some of them such as oleaginous cucurbits are still found in the market. According to Zoro Bi et al. (2003) and Djè et al. (2006), *C. mucosospermus* (but identified as *C. lanatus* by these authors in Côte d'Ivoire) is the species most widely distributed and most commercialized in Côte d'Ivoire. This plant is mainly grown in savanna areas in the North, in the pre-forest areas in Central, East, and South(Djè et al., 2006). Two distinct cultigroups have been described on the basis of the morphology of seeds. The first one (wlèwlè) is characterized by glossy seeds with a tapered proximal extremity. This morphotype is subdivided into three cultivars according to the size of the seeds(Djè et al., 2006). Fruit color of this cultigroup, is almost uniform, greenish or whitish. The second (bebu), with one cultivar has green fruit also, but with dark longitudinal bands. The seeds are heavier and have a flat ovoid shape with rugged and thick ends (Zoro Bi et al., 2003).Although the oleaginous type of *Citrullus* is an economical important crop in west Africa. Few studies were conducted on genetic resources of this plant (Ndabalishye, 1995; Djè et al., 2006) previously reported to be morphological differentiated especially in terms of fruit and seed characters.

The objectives of the present study were to survey and analyze variations in plant, fruit and seed morphology in *C. lanatus* oleaginous type collection from Côte d'Ivoire. This represents the first study on collection and characterization of *C. lanatus* oleaginous type germplasm in Nangui Abrogoua University.

MATERIALS AND METHODS

Plant and collection sites

In this study, 171 accessions of *C. lanatus* oleaginous type were used. They were provided from seven countries: Benin, Côte d'Ivoire, France, Ghana, Nigeria, Togo, and Turkey (Table 1). The samples were collected from farmers' stock, genebank or purchased from local seed markets. The selected accessions were divided into four cultivars defined on the basis of seed size and

Table 1 Passport data of accessions used for morphological analysis of Citrullus mucosospermus.*mucosospermus*.

Identification number	Country	Collection site	Cultivar	Rind feature	Seed color
CL-001	CI	Agbaou	B	UMG	Br
CL-002	CI	Agbaou	B	UMG	Br
CL-004	CI	Agbaou	B	UMG	Br
CL-005	CI	Agbaou	B	DGS	Ye
CL-006	CI	Agbaou	B	MGS	Br
CL-007	CI	Agbaou	B	MGS	Br
CL-008	CI	Agbaou	B	MGS	Br
CL-009	CI	Agbaou	B	MGS	Br
CL-010	CI	Agbaou	B	MGS	Br
CL-011	CI	Grand Alépé	B	MGS	Br
CL-012	CI	Grand Alépé	B	DGS	Ye
CL-013	CI	Assié Koumassi	B	DGS	Br
CL-014	CI	Assié Koumassi	WSS	UMG	Br
CL-015	CI	Bongouanou	WSS	MGS	Br
CL-016	CI	Bongouanou	WSS	DGS	Br
CL-017	CI	Bongouanou	WMS	DGS	Br
CL-019	CI	Assié Koyekro	WMS	DGS	Br
CL-020	CI	Assié Koumassi	WSS	MGS	Br
CL-021	CI	Assié Koyekro	WMS	UMG	Br
CL-023	CI	Danguira	B	MGIS	Br
CL-024	CI	Danguira	B	MGS	Br
CL-025	CI	Ananda	WMS	MGS	Br
CL-027	CI	Assabrikobenankro	WSS	MGS	Br
CL-029	CI	M'Bahiakro	WMS	ULG	Or
CL-030	CI	Fleguessanga	B	DGS	Ye
CL-031	CI	Fleguessanga	B	UMG	Br
CL-032	CI	Pohokaha	B	DGS	Ye
CL-033	CI	Pohokaha	B	MGS	Br
CL-034	CI	Pohokaha	B	MGS	Br
CL-035	CI	Gohitafla	WMS	MGS	Br
CL-036	CI	Manfla	WMS	MGIS	Br
CL-037	CI	Manfla	WMS	MGIS	Br
CL-040	CI	Manfla	WMS	MGIS	Br
CL-041	CI	Manfla	WMS	MGIS	Br
CL-043	CI	Manfla	WMS	MGIS	Br
CL-046	CI	Manfla	WMS	MGIS	Br
CL-047	CI	Manfla	WMS	MGIS	Br
CL-049	CI	Tibéita	WMS	UMG	Br
CL-050	CI	Tibéita	WMS	DGS	Br
CL-051	CI	Tibéita	WMS	DGS	Br
CL-052	CI	Badiéfla	WMS	DGS	Br
CL-053	CI	Badiéfla	WMS	DGS	Br
CL-054	CI	Bibikorefla	WMS	DGS	Br
CL-055	CI	Gouenfla	WMS	DGS	Br
CL-056	CI	Drikoifla 1	WMS	DGS	Br
CL-058	CI	Zambléfla	WMS	DGS	Br
CL-059	CI	Bibikorefla	WMS	DGS	Br
CL-060	CI	Botiéfla	WMS	MGIS	Br
CL-063	CI	Bohikouifla	WMS	UMG	Br
CL-064	CI	Gouafla	WMS	UMG	Br
CL-065	CI	Zraluo	WMS	UMG	Br

Table 1. Contd.

CL-066	CI	Gohitafla	WMS	UMG	Br
CL-068	CI	Gohitafla	WMS	UMG	Br
CL-069	CI	Gohitafla	WMS	LGS	Br
CL-070	CI	Gohitafla	WMS	MGIS	Br
CL-071	CI	Bonoua	B	DGS	Ye
CL-072	CI	Agbaou	B	MGIS	Br
CL-073	CI	Agbaou	B	MGIS	Br
CL-074	CI	Ahoutoué	B	DGS	Br
CL-076	CI	Grand Alépé	B	UMG	Br
CL-077	CI	M'Bahiakro	WMS	UMG	Br
CL-079	CI	Korhogo	WBS	ULG	Or
CL-081	CI	Ananda	WMS	MGIS	Br
CL-082	CI	Dikodougou	B	MGIS	Br
CL-083	CI	Pleuro	B	MGIS	Br
CL-084	CI	Guiembé	B	MGIS	Br
CL-085	CI	Koumbala	B	MGIS	Br
CL-086	CI	Koumbala	B	MGIS	Br
CL-087	CI	Koumbala	B	DGS	Br
CL-088	CI	Koumbala	WMS	DGS	Br
CL-089	CI	Koumbala	B	DGS	Br
CL-090	CI	Ferkessedougou	B	DGS	Br
CL-091	CI	Ferkessedougou	B	ULG	Br
CL-092	CI	Katiola	B	ULG	Br
CL-093	CI	Dikodougou	B	ULG	Br
CL-094	CI	Assalékro	WMS	ULG	Br
CL-095	CI	Assalékro	WMS	ULG	Br
CL-096	CI	Assalékro	WMS	ULG	Br
CL-097	CI	Assalékro	WMS	ULG	Br
CL-098	CI	Assalékro	WMS	ULG	Br
CL-099	CI	M'Bato	WMS	ULG	Br
CL-101	CI	M'Bato	WMS	DGS	Br
CL-102	CI	Koffiagrokro	WMS	DGS	Br
CL-103	CI	Koffiagrokro	WMS	DGS	Br
CL-104	CI	Grogro	WMS	DGS	Br
CL-107	CI	Grogro	WMS	DGS	Br
CL-108	CI	Grogro	WMS	DGS	Br
CL-112	CI	N'Denou	WMS	DGS	Br
CL-113	CI	N'Denou	WMS	DGS	Br
CL-115	CI	Dossakassou	WMS	DGS	Br
CL-118	CI	Dossakassou	WMS	UMG	Br
CL-121	CI	Bediala	WMS	UMG	Br
CL-122	CI	Bediala	WMS	UMG	Br
CL-124	CI	Daloa	WMS	UDG	Br
CL-126	CI	Bediala	WMS	UDG	Br
CL-127	CI	Bediala	WMS	UDG	Br
CL-130	CI	Nanoufla	WMS	UDG	Br
CL-131	CI	Bediala	WMS	UDG	Br
CL-136	CI	Nanoufla	WMS	UDG	Br
CL-137	CI	Assie-Assasso	WMS	UDG	Br
CL-138	CI	Assie-Assasso	WSS	UDG	Br
CL-139	CI	Yoboué Blessou	WMS	UDG	Br
CL-140	CI	Abokouman	WMS	UDG	Br

Table 1. Contd.

CL-141	CI	Abokouman	WMS	UMG	Or
CL-142	CI	Abokouman	WMS	MGIS	Br
CL-146	CI	Yanvo	WMS	MGIS	Br
CL-148	CI	Iguela	B	MGIS	Br
CL-149	CI	Iguela	B	MGIS	Br
CL-150	CI	Iguela	B	MGIS	Br
CL-151	CI	Iguela	B	MGIS	Br
CL-153	CI	Korobo	WMS	MGIS	Br
CL-154	CI	Korobo	WMS	UMG	Br
CL-155	CI	N'Golokaha	B	UMG	Br
CL-156	CI	N'Golokaha	B	UMG	Br
CL-157	CI	N'Golokaha	B	UMG	Br
CL-163	CI	N'Golokaha	B	UMG	Br
CL-164	CI	N'Golokaha	B	UMG	Br
CL-167	CI	Baifla	WMS	UMG	Br
CL-168	CI	Tranhonfla	WMS	UMG	Br
CL-171	CI	Tranhonfla	WMS	UMG	Br
CL-172	CI	Tranhonfla	WMS	UMG	Br
CL-173	CI	Baifla	WMS	DGS	Br
CL-174	CI	Oufouediékro	WMS	MGIS	Br
CL-175	CI	Sakassou	WMS	DGS	Br
CL-176	CI	Yablassou	WMS	DGS	Br
CL-178	CI	Sandôh	WMS	DGS	Br
CL-179	CI	Maounou N'Zuessi	WMS	MGIS	Br
CL-181	CI	M'Bahiakro	WBS	UDG	Br
CL-182	CI	Yaouloukro	WMS	UDG	Br
CL-183	CI	Djakro	WSS	UDG	Br
CL-184	CI	Attiegouakro	WMS	UDG	Br
CL-185	CI	Yoboué Blessou	WMS	UDG	Br
CL-188	CI	Ahoulikro	WMS	MGIS	Br
CL-189	CI	Bodokro	WMS	UDG	Br
CL-190	CI	Bodokro	WMS	UDG	Br
CL-192	CI	Ouellé	WMS	UDG	Br
CL-193	CI	Bodokro	WMS	DGS	Br
CL-194	CI	Bodokro	WMS	DGS	Br
CL-195	CI	Bodokro	WMS	DGS	Br
CL-198	CI	Attiégouakro	WMS	DGS	Br
CL-199	CI	Attiégouakro	WMS	DGS	Br
CL-202	CI	N'Golokaha	B	DGS	Br
CL-203	CI	N'Golokaha	B	DGS	Br
CL-204	CI	N'Golokaha	B	DGS	Br
CL-205	CI	N'Golokaha	WMS	UDG	Br
CL-207	CI	N'Golokaha	B	UDG	Br
CL-208	CI	N'Golokaha	B	UDG	Br
CL-209	T	Kara	B	DGS	Br
CL-210	Bn	Ketou	B	MGIS	Br
CL-211	France	-	Wat	MGIS	Bl
CL-212	France	-	Wat	MGIS	Wh
CL-217	CI	Manfla	WMS	MGIS	Br
CL-218	CI	Manfla	WMS	DGS	Br
CL-219	Bn	Savin	B	DGS	Br
CL-221	Bn	Ketou	B	DGS	Br

Table 1. Contd.

CL-223	N	Oyo	B	UMG	Br
CL-226	N	Ogun	B	UDG	Br
CL-234	Turquie	-	WMS	UDG	Br
CL-236	CI	Katiola	WMS	UDG	Br
CL-237	CI	Katiola	WMS	UDG	Br
CL-238	CI	Petionara	WMS	UDG	Br
CL-239	CI	Katiola	WMS	UDG	Br
CL-242	Ghana	Makola City	WSS	LGS	Br
CL-244	Ghana	Makola City	WSS	UDG	Br
CL-245	Ghana	Kaneshie	WSS	MGS	Br
CL-246	CI	Petionara	WMS	MGS	Br
CL-247	CI	Doubasso	WMS	MGS	Br
CL-248	CI	Doubasso	WMS	MGS	Br

Bl: Black; Bn: Benin; Br: brown; CL: *Citrullus mucosospermus*; G: Ghana; CI: Côte d'Ivoire; N: Nigeria; T: Togo; B: bebu; WBS: wlèwlè big seed; WMS: wlèwlè medium seed; WSS: wlèwlè small seed; DGS: dark green with strips; LG: light green; LGS: Light Green with strips; MGS: medium green with strips; MGIS: medium green with intermittent strips; UDG: uniformly dark green; ULG: uniformly light green; UMG: uniformly medium green; Or: orange; Wh: white; Ye: yellowish.

Table 2. Origins and size of *Citrullus mucosospermus* samples used for morphological traits analysis.

Cultigroup	Cultivar	Sample size per country							
		Côte d'Ivoire	Benin	Ghana	Nigeria	Togo	France	Turkey	Total
Wlèwlè	Big seeds	2	-	-	-	-	-	-	2
	Medium seeds	101	-	-	-	-	-	-	101
	Small seeds	7	-	3	-	-	-	-	10
Bebu	Bebu	49	3		2	1	-	-	55
Watermelon	Watermelon	-	-	-	-	-	2	1	3
Total		159	3	3	2	1	2	1	171

designated small-, medium-, big-seeded, and thickened margin seeds. Thickened margin seeds size varies between 153 and 205 mm², big seeds from 125 to 151 mm², medium seeds from 86 to 110 mm², and small seeds from 41 to 52 mm²(Djè et al., 2006). Accessions (2 to 101) were sampled per cultivar, according to seeds availability (Table 2).

Study site

The trials were regularly monitored throughout the growing season in 2011 and 2012 (May to November). Farm experiment was conducted in the village of Manfla, located in the centre (6°49′34.38″N, 5°43′47.68″W) 400 km North Abidjan (Côte d'Ivoire). Annual rainfall varies from 800 to 1400 mm with a long-term mean of 1200 mm, and the annual mean temperature is 27°C. A complete description of study site was done by Kouassi and Zoro Bi (2010).

Experimental design

Planting was done according to a completely randomized block design, with seven replications. Each replicate consisted of a 24×27 m containing 70 holes at a depth of 3 cm, resulting in 7 holes per accession. The planting distance was 3 m between and within rows with 1.5 m of edges. A manual weeding was carried out during plant development to prevent weed invasion. Disease and pest control was carried out using a carbamate-based insecticide applied when necessary.

Traits measurement

Accessions were examined using 11 quantitative traits subdivided into four vegetative and seven yield characters selected from standard descriptors for cucurbits(Maggs-Kölling et al., 2000; Marr et al., 2007; Morimoto et al., 2005; Koffi et al., 2008). Data were measured in five plants and five fruits per accession.

Vegetative traits measured were limb length (LL), limb width (LWI), plant length (PL), and number of branches from the central taproot (BN) for each plant. Yield characters measured were weight (FWE), length (FL), width (FWI), seeds cavity diameter (SCD), seeds number (SN), and seeds weight (SW). Seed traits analyzed included 100-seeds weight (100-SWE). Measurements on 100-seeds weight were scored using five individuals randomly selected on each plant (Table 3).

Data analysis

Statistical analyses were carried out with STATISTICA software

Table 3. List of descriptors used for characterization of *Citrullus lanatus* samples used for morphological traits analysis.

Character	Codes	Type and period of observation
Vegetative character		
Limb length (cm)[a]	(LL)	Measured after formation of the first fruit
Limb width (cm)[a]	(LWI)	Measured after formation of the first fruit
Plant length (m)[b]	(PL)	Measured 120 days after planting
Number of branches[b]	(BN)	Total number of branches per plant at 120 days after planting
Yield character		
Fruit weight (g)[a]	(FWE)	Weight of the mature fruits
Fruit length (cm)[a]	(FL)	Measured on the mature fruits
Fruit diameter (cm)[a]	(FD)	Measured on the mature fruits
Seed cavity diameter (cm)[a]	(SCD)	Measured on the mature fruits
Number of seeds per fruit[a]	(NS)	Total number of seeds per fruit
Seeds weight per fruit[a]	(SW)	Weight of all seeds taken for a given individual after drying
100-seeds weight per fruit (g)	(100-SWE)	Weight of 100 seeds taken for a given individual after drying

A measurement on five organs per plant; b measurement on each plant per accession.

package version 7.1(StatSoft, 2005). Principal Component Analysis (PCA) was applied to identify most discriminant parameters followed by hierarchical cluster analysis using unweighted pair-group method using arithmetic average (UPGMA) method. Multivariate analysis of variance (MANOVA) and a factorial discriminant analysis (FDA) were performed to check difference between the variable means for each group obtained with the clustering analysis. A confusion matrix was constructed, to check the reliability of groups as defined by the hierarchical clustering.

RESULTS

Descriptors variation

The relative discriminating capacity of the PCA is shown by their Eigenvalues. The result of the PCA (Table 4) showed that five Principal Component axes (PC) had Eigenvalues greater than 1 all together accounted for over 80% of the total variability. The first five principal components accounted for 81.19% of the total variability. The first principal component (PC1) accounted for 23.85%, while the second principal component (PC2) accounted for 17.32%. The PC1 is loaded with fruit length (0.824), fruit diameter (0.919), and seed cavity diameter (0.890). These results indicated that this component was determined by individuals with big fruit. The PC2 was loaded with limb length (0.966), and the limb width (0.947). This component was determined by individuals with broad leaves. PC3, PC4, and PC5 accounted for 14.19, 13.54, and 12.29%. They were correlated to number of branches, and plant length for PC3, number of seeds per fruit and 100-seeds weight per fruit (100-SWE) for PC4 and seeds weight per fruit for PC5. These results indicated that PC3 was determined by individuals of large size plant. PC4 and PC5 were determined by most productive individuals.

Accessions structuration

The unweighted pair group method arithmetic (UPGMA) using a Euclidian distances matrix, subdivided the accessions analyzed into four major groups. These groups differ in the distance by 30 (Figure 1). All groups are mixture of accession of various origin, cultivar or cultigroup.

The highest number of accessions was located in cluster III with 53 accessions, followed by clusters II and I with 48 and 46 accessions, respectively. Cluster IV had 24 accessions. Comparison of groups using the MANOVA showed significant differences between the four groups (F= 19.91; P<0.001). This is due to all the 11 characters measured. The ANOVA showed significant difference among groups (Table 5). All parameters revealed a partial distinction of groups.

Discriminant functions resulting from variables to classify the units formed on the four groups are shown in Table 6. The two first canonical variables which had an Eigenvalue higher than 1 were retained to describe the total variability of the accessions. The two factors selected together, explained 87.54% of the total variation. The first canonical variable, *FDA1,* described 58.33% of the total variation. This component was positively correlated with the number of branches and was negatively correlated with limb width, number of seed per fruit, and 100-seeds weight. The second canonical variable, *FDA2,* explained 29.21% of the total variation and was mostly and positively constructed from fruit diameter. Figure 2 shows the position of the accessions in relation with the first two discriminant factors. Based on these analyses, accessions of group 2 were noted to have the biggest leaves. The smallest leaves were observed in accession of group 1. The most number of

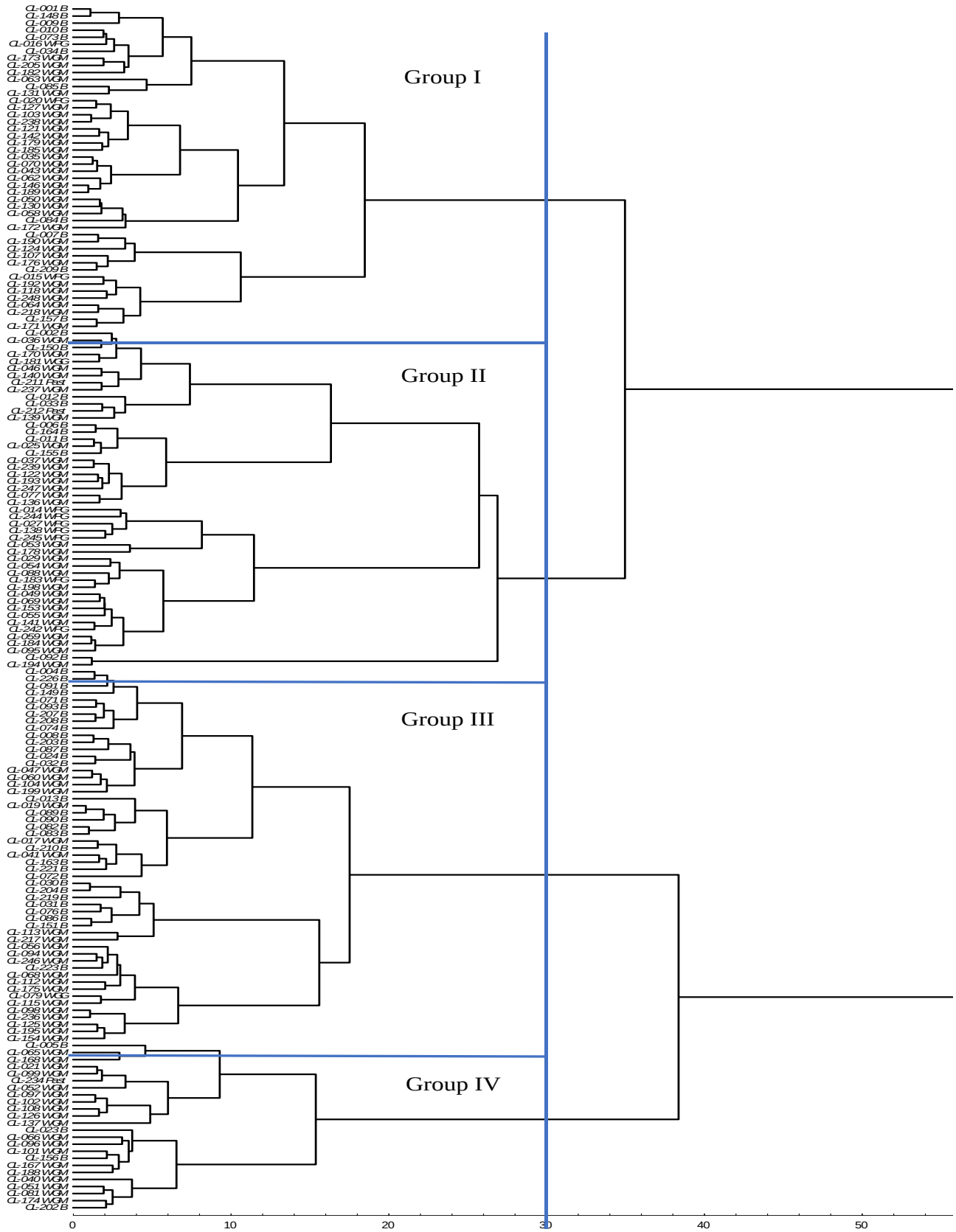

Figure 1. Dendrogram of *Citrullus lanatus* oleaginous type accessions in four group generated by using 11 quantitative morphological characters. CL: *Citrullus lanatus*; W: 'Wlèwlè '; B: 'Bebu'; PG: small seeds; GM: medium seeds; GG: big seeds; Past Watermelon; Group I (46 accessions), Group II (48 accessions), Group III (53 accessions), and Group IV (24 accessions).

Table 4. Correlation coefficients explained by the first five principal components (PCs) for 11 traits analysed in 171 accessions of *Citrullus mucosospermus*.

Eigenvector	PC 1	PC 2	PC 3	PC 4	PC 5
Eigenvalues	2.623	1.905	1.562	1.490	1.352
% of variance explained	23.846	17.319	14.197	13.543	12.294
Cumulative contribution (%)	23.846	41.165	55.362	68.905	81.199
LL	0.051	0.966*	-0.041	0.015	0.016
LWI	0.056	0.947*	-0.137	-0.039	0.033
BN	-0.013	-0.171	0.843*	0.015	-0.119
PL	-0.044	-0.002	0.885*	-0.021	0.102
FWE	0.409	0.141	-0.129	0.080	-0.469
FL	0.824*	0.061	0.102	-0.018	-0.112
FD	0.919*	0.026	-0.077	0.017	0.163
SCD	0.890*	0.015	-0.088	-0.046	0.194
NS	0.206	0.078	-0.004	-0.785*	0.467
SW	0.274	0.125	-0.088	0.080	0.861*
100-SWE	0.118	0.030	-0.010	0.925*	0.265

*****Significant correlation values. LL: Limb length; LWI: limb width; PL: plant length; BN: number of branches; FWE: fruit weight; FL: fruit length; FD: fruit diameter; SCD: seed cavity diameter; NS: number of seeds per fruit; SW: seeds weight per fruit; 100-SWE: 100-seeds weight per fruit.

Table 5. Agro-morphological characteristic of 11 traits analyzed in the four groups provided by the dendrogram with UPGMA methods.

Variable	G1 (N=46)	G2 (N=48)	G3 (N=53)	G4 (N=24)	*F*	*P*
LL	10.95±1.02^{b}	13.00±1.31^{a}	12.5±1.26^{a}	11.17±1.02^{b}	30.27	<0.001
LWI	9.19±0.95^{c}	11.53±1.32^{a}	10.67±1.24^{b}	9.17±0.99^{c}	41.04	<0.001
BN	3.95±1.58^{b}	3.28±0.91^{b}	3.41±1.2^{b}	8.39±3.45^{a}	55.04	<0.001
PL	1.97±0.69^{b}	1.90±0.70^{b}	2.04±0.6^{b}	3.26±0.68^{a}	25.91	<0.001
FWE	0.66±0.13^{ab}	0.74±0.59^{a}	0.51±0.12^{b}	0.54±0.12^{b}	4.83	0.003
FL	10.01±1.3^{a}	9.92±0.82^{a}	9.01±0.86^{b}	9.38±1.34^{b}	9.59	<0.001
FD	10.28±0.63^{a}	10.14±0.54^{a}	9.25±0.48^{b}	9.36±1.84^{b}	34.00	<0.001
SCD	8.22±0.54^{a}	8.11±0.49^{a}	7.27±0.45^{b}	7.36±0.75^{b}	36.32	<0.001
NS	159.91±45.87^{b}	212.12±68.12^{a}	129.56±30.40^{c}	145.58±30.93^{bc}	26.57	<0.001
SW	10.35±2.71^{b}	12.25±3.34^{a}	10.01±2.68^{b}	8.58±1.71^{c}	10.66	<0.001
100-SWE	7.79±2.52^{ab}	6.98±2.42^{b}	8.86±2.70^{a}	6.52±1.75^{b}	7.12	<0.001

LL: Limb length; LWI: limb width; PL: plant length; BN: number of branches; few: fruit weight; FL: fruit length; FD: fruit diameter; SCD: seed cavity diameter; NS: number of seeds per fruit; SW: seeds weight per fruit; 100-SWE: 100-seeds weight per fruit; G1: group 1; G2: group 2; G3: group 3; G4: group 4.

the longest plants were observed in group 4. Groups 1 and 2 have the larger and heavier fruit. The best seed yield is obtained with accessions of group 2, but 100 seed-weight was higher in groups 1 and 3.

According to confusion matrix, the composition of groups as defined by the hierarchical clustering is different. Group 1 contains 41 accessions instead of 46. Accessions CL-146 and CL-172 have been reclassified in group 2. Similarly, accessions CL-142 and CL-085 have been reclassified in group 3 and accession CL-131 has been reclassified in group 4. Group 2 consists of 44 instead of 48 accessions. An enrollment of 50 accessions belongs to group 3 instead of 53. Group 4 includes 23 accessions instead of 24 (Table 7).

DISCUSSION

To maintain, evaluate and utilize germplasm efficiently, it is important to investigate the extent of genetic diversity available. Morphological characterization is an important step in the description and classification of crop germplasm, because a breeding program mainly depends upon the magnitude of morpho-phenological variability (Smith

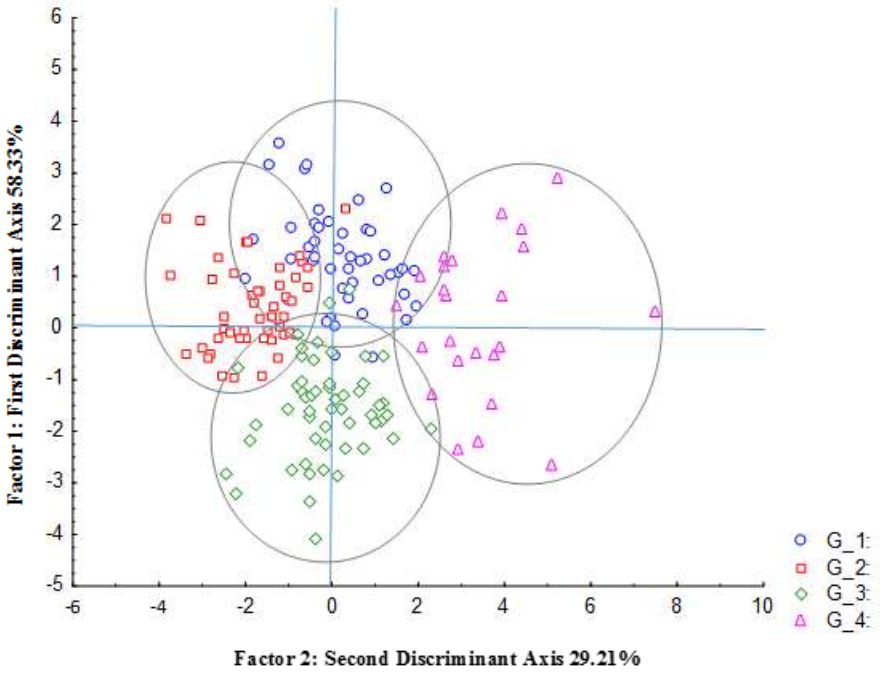

Figure 2. Representation on the discriminant plane of accessions in relation with the two discriminant factors, 1 and 2. G_1: group 1; G_2: group 2; G_3: group 3, G_4: group 4.

Table 6. Eigenvectors, eigenvalues, and inertia percentage explained by the two first canonical variables for 11 traits analysed in 171 accessions of *Citrullus mucosospermus*.

Eigenvector	F1	F2
Eigenvalue	2.67	1.33
Inertia percentage	58.33	29.21
Cumulative inertia percentage	58.33	87.54
Vegetative character		
LL	-0.03	-0.40
LWI	-0.51*	-0.19
BN	0.63*	0.16
PL	0.47	-0.07
Yield character		
FWE	-0.14	0.3
FL	-0.01	-0.05
FD	0.17	0.62*
SCD	-0.26	0.35
NS	-0.77*	0.15
SW	0.05	0.03
100-SWE	-0.54*	-0.47

***Significant correlation higher than 0.5. LL: Limb length; LWI: limb width; PL: plant length; BN: number of branches; few: fruit weight; FL: fruit length; FD: fruit diameter; SCD: seed cavity diameter; NS: number of seeds per fruit; SW: seeds weight per fruit; 100-SWE: 100-seeds weight per fruit; F1: discriminant factor 1; F2: discriminant factor 2.

Table 7. Classification matrix based on the groups obtained by agromorphological characters.

Group	Classification(%)	G 1	G 2	G 3	G 4
G 1	89.13	41	2	2	1
G 2	91.66	3	44	1	0
G 3	94.33	2	1	50	0
G 4	95.83	1	0	0	23
Total	92.39	47	47	53	24

G1: Group 1; G2: group 2; G3: group 3; G4: group 4.

et al., 1991).

In this study, 171 accessions of *Citrullus* of Nangui University collection were characterized based on morphological traits. In the analysis made to estimate the relative contributions of the different traits studied towards the overall phenotypic variation among the 171 accessions, a total of five principal components (PCs), explained 81.2% of variability. Fruit-related parameters were the most discriminant. In fact, fruit length, fruit diameter, and seed cavity diameter were parameters which contributed more to the first principal component (24%), implying that 24% of the variability was explained by these parameters. These results suggest that fruit size is a useful criterion for separating *Citrullus* accessions. In the cucurbit family, the significant contribution of the fruit traits to morphological variability has been reported for watermelon (Gusmini and Wehner, 2003; Maggs-Kölling et al., 2000). According to Achigan-Dako (2015) diagnostic morphological markers among species include fruit such as fruit size.

The least discriminant parameters were numbers of seeds and seeds weight. This finding is due to the fact that medium-sized seeds represented 60% of sample analyzed. Contrary to these results, Achigan-Dako et al. (2015) demonstrated that other major differentiation traits is related to seed.

Although our accessions originated from seven different countries, they did not cluster according to geographical distribution. This may be suggestive of the single ancestry of the analyzed plants (Dane and Liu, 2007). This may be because genetically, the cultivated watermelon is closest to plants from West Africa that represents the gene pool from which watermelon was domesticated (Chomicki and Renner, 2014). The sister species of watermelon is *C. mucosospermus*, the egusi melon, ranging from Nigeria to Senegal (Renner et al., 2014). Plants from Benin closely resemble the collection type of the name *C. mucosospermus* (which is from Ghana). In order to explain the low genetic diversity of *C. mucosospermus* (but identified as *C. lanatus*), Dane and Liu (2007) demonstrated that the watermelon varieties have diverged into small populations. Moreover, the domestication and the resulting selection may have reduced the genetic diversity from the original watermelon crops. Levi et al. (2001) also revealed that cultivated watermelon exhibited narrow genetic base as a results of many years cultivation and selection for specific qualities.

Morphological and genetic characterization of Hungarian and Turkish accessions of watermelon (including *C. lanatus* and *C. colocynthis*) revealed that germplasm resources present a wide range of diversity (Sari et al., 2005; Solmaz and Sari, 2009; Solmaz et al., 2010). However, accessions of the two countries show many similarities and therefore cannot be separated clearly (Szamosi et al., 2009). In the present study, comparison of the four groups using a MANOVA combined with factorial discriminant analysis, allowed the classification of accessions according to agro-morphological characters. Accessions of group 2 had the biggest leaves. The smallest leaves were observed in accession of group 1. The largest number of ramification and longest plants were observed in group 4.

Groups 1 and 2 have the largest and heaviest fruits. The best seed yield is obtained with accessions of group 2, but 100 seed-weight was higher in groups 1 and 3 than in the two other groups. Morphological variation analysis in landraces of *C. mucosospermus* (but identified as *C. lanatus* by authors in Côte d'Ivoire) also allowed to classify accessions based on fruit and seed traits (Adjoumani et al., 2012).

Although, the Hierarchical Cluster Analysis gave a clear separation of accessions in distinct groups, the confusion matrix displayed a reclassification of some accessions. Accessions CL-146 and CL-172 has been reclassified in group 2. Accessions CL-142 and CL-085 has been reclassified in group 3 and accession CL-131 has been reclassified in group 4.

Traditionally, watermelon breeders focus on fruit quality traits. These traits include sugar content, flesh color, fruit size, and rind patterns (Hashizume et al., 2003). Investigations of the inheritance of fruit morphology and quality traits date back as far at the 1930's (Porter, 1933, 1937). Since then, many efforts have been made to better understand traits associated with watermelon fruit quality and morphology. Many genes have been described that control the internal fruit quality and morphology in watermelon (Guner and Wehner, 2004). An internal fruit characteristic that has received attention is the Brix value.

A linkage map was developed and a QTL that accounts for 19% of the variation in Brix was mapped on linkage group (LG) 8 (Prothro, 2010). Fruit shape and weight are important external characteristics that breeders must consider when developing watermelon cultivars.

Watermelon shape can be classified as being either round, oval, blocky or elongate (Wehner et al., 2001). The only gene described that controls fruit shape is the elongate fruit gene (O). Fruit weight has recently become an important consideration for breeders due to increased

consumer preference for smaller sized watermelons (Gusmini and Wehner, 2007). Watermelons have traditionally been classified into five categories based on fruit weight. These are icebox (less than 5.5 kg), small (5.5 to 8.0 kg), medium (8.1 to 11.0 kg), large (11.1 to 14.5 kg), giant (greater than 14.5 kg), and recently mini fruit size (1.5 to 4.0 kg) was added (Gusmini and Wehner, 2007; Maynard, 2001). No genes have been identified that are responsible for fruit weight inwatermelon (Gusmini and Wehner, 2007; Maynard, 2001). Fruit quality and morphological traits, such as the ones described earlier, gain the most attention from watermelon breeders. There are many other important traits in watermelon that receive little to no attention. The egusi seed trait is one of these traits. The egusi seed trait has been shown to be inherited as a single gene (Gusmini et al., 2004).

A single QTL was identified for rind thickness (Prothro, 2010). The objective when breeding for this trait should be to have a rind thickness that is a small percentage of the fruit diameter. Three QTL were identified for fruit length and two QTL were identified for fruit width, in the same region on LG5. Another QTL for fruit length was identified on LG3. But it is not known if they are associated with the elongate fruit gene. Kumar et al. (2009) produced a population segregating for fruit shape and found that his data did not fit the single gene theory for fruit shape inheritance. Watermelons varieties that produce fruit that fit into the weight category most preferred by consumers must be available for growers(Gusmini and Wehner, 2007). The QTL identified for fruit length and fruit width should be useful for fruit weight selection in a breeding program. Two QTL were identified for this trait on LG2. Another QTL was identified for seed oil percentage. This QTL falls between the locations of the two QTL identified for the egusi seed trait on LG2 (Prothro et al., 2012).

Conclusion

A great deal of diversity morphological traits has been observed in *C. mucosospermus* oleaginous type accessions from the Nangui Abrogoua University collection. From the present investigation, it was concluded that the indigenous oleaginous cucurbit *C. mucosospermus* displayed a wide range of diversity for most of the morphological traits studied. Traits related to fruit size and weight were the most accession distinctive. Consequently, fruit morphological traits could be used for accession identification during collecting missions. Accessions had been divided into four groups in which group 2 had the highest seed yield. Therefore, accessions of this group must be used to enhance yield. These findings are important to plan future germplasm sampling and evaluation studies.

Conflict of Interests

The authors have not declared any conflict of interests.

REFERENCES

Achigan-Dako EG, Avohou ES, Linsoussi C, Ahanchede A, Vodouhe RS, Blattner FR (2015). Phenetic characterization of *Citrullus spp*. (Cucurbitaceae) and differentiation of egusi-type (*C. mucosospermus*). Genet. Resour. Crop. Evol. 62(8):1159-1179.

Achigan Dako EG, Fagbemissi R, Avohou HT, Vodouhe RS, Coulibaly O, Ahanchede A (2008). Importance and practices of egusi crops (*Citrullus lanatus* (Thunb.) Matsum. & Nakai, *Cucumeropsis mannii* Naudin and *Lagenaria siceraria* (Molina) Standl. cv.'Aklamkpa') in sociolinguistic areas in Benin. Biotechnol. Agron. Soc. Environ. 12(4):393-403.

Adjoumani K, Kouonon LC, Akaffou DS, Dje Y (2012). Diversité variétale chez l'espèce *Citrullus lanatus* (Matsumura et Nakai) et opportunités d'amélioration génétique des cultivars. Eur. J. Sci. Res. 67(4):564-579.

Bailey LH (1930). Three discussions in Cucurbitaceae. Gentes Herb. 2:175-186.

Burkill HM (1985). The useful plants of West Tropical Africa. Richmond, Surrey, UK: Royal Botanic Gardens, Kew.

Che K-p, Liang C-y, Wang Y-g, Jin D-m, Wang B (2003). Genetic assessment of watermelon germplasm using the AFLP technique. HortScience 38(1):81-84.

Chomicki G, Renner SS (2014). Watermelon origin solved with molecular phylogenetics including Linnaean material: another example of museomics. New Phytol. 205: 526-532.

Dane F, Liu J (2007). Diversity and origin of cultivated and citron type watermelon (*Citrullus lanatus*). Genet. Resour. Crop. Evol. 54:1255-1265.

Djè Y, Kouonon CL, Zoro Bi IA, Gnamien YG, Baudoin JP (2006). Etude des caractéristiques botaniques, agronomiques et de la biologie florale du melon africain (*Cucumis melo* L. var. agrestis Naudin, *Cucurbitaceae*). Biotechnol. Agron. Soc. Environ. 10(2):109-119.

Fursa TB (1972). On the taxonomy of the genus *Citrullus* Schad. Bot. Zh. 57:31-34.

Fursa TB (1981). Intraspecific classification of watermelon under cultivation. Kulturpflanze 29: 297-300.

Fursa TB (1983). Novyi vid arbuza *Citrullus* mucosospermus (Fursa) Fursa (A new species of watermelon *Citrullus mucosospermus* (Fursa) Fursa.) Trudy Prikl. Bot. Genet. Selek. 81:108-112.

Guner N, Wehner TC (2004). The genes of watermelon. HortScience 39:1175-1182.

Gusmini G, Wehner TC (2003). Polygenic inheritance of some vine traits in two segregating watermelon families. Cucurbit Genet. Coop. Rep. 26:32-35.

Gusmini G, Wehner TC (2007). Heritability and genetic variance estimates for fruit weight in watermelon. HortScience 42:1332-1336.

Gusmini G, Wehner TC, Jarret RL (2004). Inheritance of Egusi Seed Type in Watermelon. Journal of Heredity 95(3):268-270.

Hammer K, Gladis T (2014). Notes on infraspecific nomenclature and classifications of cultivated plants in Compositae, Cruciferae, Cucurbitaceae, Gramineae (with a remark on *Triticum dicoccon* Schrank) and Leguminosae. Genet. Resour. Crop. Evol. 61:1555-1567.

Hashizume T, Shimamoto I, Hirai M (2003). Construction of a linkage map and QTL analysis of horticultural traits for watermelon [*Citrullus lanatus* (THUNB.) MATSUM & NAKAI] using RAPD, RFLP and ISSR markers. Theor. Appl. Genet. 106:779-785.

Hepper FN (1990). Pharaoh's flowers: the botanical treasures of Tutankhamun. Chicago, IL, USA & London, UK: HMSO.

Hutchinson J, Dalziel JM (1954). Flora of West Tropical Africa: the British West African Territories, Liberia, the French and Portugese territories south of latitude 18o N to Lake Chad, and Fernado Po. London.

Koffi KK, Gbotto AA, Malice M, Djè Y, Bertin P, Baudoin JP, Zoro Bi IA

(2008). Morphological and allozyme variation in a collection of *Cucumeropsis mannii* Naudin (Cucurbitaceae) from Côte d'Ivoire. Biochem. Syst. Ecol. 36: 777-789.
Kouassi NJ, Zoro Bi IA (2010). Effect of sowing density and seedbed type on yield and yield components in Bambara Groundnut (*Vigna subterranea*) in woodland savannas of Côte d'Ivoire. Exp. Agric. 46:99-110.
Kumar RS, Parthiban KT, Rao GM (2009). Molecular characterization of Jatropha genetic resources through inter-simple sequence repeat (ISSR) markers. Mol. Biol. Rep. 36:1951-1956.
Levi A, Thomas CE, Wehner TC, Zhang X (2001). Low genetic diversity indicates the need to broaden the genetic base of cultivated watermelon. HortScience 36(6):1096-1101.
Loukou AL, Gnakri D, Djè Y, Kippré AV, Malice M, Baudoin JP, Zoro Bi IA (2007). Macronutrient composition of three cucurbit species cultivated for seed consumption in Côte d'Ivoire. Afr. J. Biotechnol. 6(5):529-533.
Maggs-Kölling GL, Madsen S, Christiansen JL (2000). A phenetic analysis of morphological variation in *Citrullus lanatus* in Namibia. Genet. Resour. Crop. Evol. 47:385-393.
Marr KL, Xia Y-M, Bhattarai NK (2007). Allozymic, morphological, phenological, linguistic, plant use, and nutritional data of *Benincasa hispida* (Cucurbitaceae). Econ. Bot. 61:44-59.
Maynard DN (2001). An introduction to the watermelon. Alexandria, VA, USA: ASHS Press.
Meeuse AD (1962). The Cucurbitaceae of Southern Africa. Bothalia 8: 1-111.
Morimoto Y, Maundu P, Fujimaki H, Morishima H (2005). Diversity of landraces of the white-flowered gourd (*Lagenaria siceraria*) and its wild relatives in Kenya: fruit and seed morphology. Genet. Resour. Crop. Evol. 52:737-747.
Ndabalishye I (1995). Agriculture vivrière Ouestafricaine à travers le cas de la Côte d'Ivoire: monographie. IDESSA, Bouaké, Côte d'Ivoire.
Oyulu C (1977). A quantitative and qualitative study of seed types in egusi (*Citrullus colocynthis* L). Trop. Sci. 19:55-62.
Porter DR (1933). Watermelon breeding. Hilgardia 7: 533-552.
Porter DR (1937). Inheritance of certain fruit and seed characters in watermelons. Hilgardia, pp. 489-509.
Prothro J, Sandlin K, Abdel-Haleem H, Bachlava E, White V, Knapp S, McGregor C (2012). Main and epistatic quantitative trait loci associated with seed size in watermelon. J. Am. Soc. Hortic. Sci. 137(6): 452-457.
Prothro JM (2010). Genetic mapping of phenotypic and quantitatibe trait loci underlyinf horticulturaly important traits in watermelon, The University of Georgia, Athens, Georgia.
Renner SS, Chomicki G, Greuter W (2014). (2313) Proposal to conserve the name Momordica lanata (*Citrullus lanatus*) (watermelon, Cucurbitaceae), with a conserved type, against *Citrullus battich*. Taxon 63(4):941-942.
Sari N, Solmaz I, Yetisir H, Unlu H (2005). Watermelon genetic resources in Turkey and their characteristics. III International symposium on cucurbits 731:433-438.
Schaefer H, Renner SS (2011). Phylogenetic relationships in the order Cucurbitales and a new classification of the gourd family (Cucurbitaceae). Taxon 60:122-138.
Schulz E (1987). Die Holozäne Vegetation der Zentralen Sahara (N-Mali, N-Niger, SW-Libyen). In Palaeoecology of Africa and the surrounding Islands, 18:143-161.
Schulz E (1991). Holocene environments in the central Sahara. Hydrobiologia 214:359-365.
Smith SE, Doss AA, Warburton M (1991). Morphological and agronomic variation in North African and Arabian alfalfas. Crop Sci. 31:1159-1163.
Solmaz I, Sari N (2009). Characterization of watermelon (*Citrullus lanatus*) accessions collected from Turkey for morphological traits. Genet. Resour. Crop. Evol. 56:173-188.
Solmaz I, Sari N, Aka-Kacar Y, Yalcin-Mendi YN (2010). The genetic characterization of Turkish watermelon (*Citrullus lanatus*) accessions using RAPD markers. Genet. Resour. Crop. Evol. 57:763-771.
StatSoft (2005).STATISTICA, logiciel d'analyse de données. www.statsoft.fr.
Szamosi C, Solmaz I, Sari N, Bársony C (2009). Morphological characterization of Hungarian and Turkish watermelon (*Citrullus lanatus* (Thunb.) Matsum. et Nakai) genetic resources. Genet. Resour. Crop. Evol. 56:1091-1105.
van der Vossen HAM, Denton OA, El Tahir IM (2004).*Citrullus lanatus* (Thunb.) Matsum. & Nakai. In PROTA (Plant Resources of Tropical Africa / Ressources végétales de l'Afrique tropicale) (Eds Grubben GJH and Denton OA). Wageningen, Netherlands. http://database.prota.org/search.htm: Protabase.
Wehner TC, Shetty, N.V., Elmstron GW (2001). Breeding and seed production. In Watermelons: Characteristics, production, and marketing, 27-73 (Ed Maynard DN). Alexandria, VA: ASHS Press.
Whitaker TW, Bemis WB (1976). Cucurbits. In Evolution of crop plants, pp. 64-69.
Zoro Bi IA, Koffi KK, Djè Y (2003). Caractérisation botanique et agronomique de trois espèces de cucurbites consommées en sauce en Afrique de l'Ouest: *Citrullus* sp.,*Cucumeropsis mannii* Naudin et *Lagenaria siceraria* (Molina) Standl. Biotechnol. Agron. Soc. Environ. 7(3-4):189-199.

academicJournals

Vol. 15(21), pp. 930-939, 25 May, 2016
DOI: 10.5897/AJB2013.13125
Article Number: 2FEAE7558598
ISSN 1684-5315

http://www.academicjournals.org/AJB

African Journal of Biotechnology

Full Length Research Paper

Impact of transgenic cotton expressing *cry1Ac* and *cry2Ab* genes on soil rhizosphere bacterial and fungal populations in soils of central Kenya

J. Swilla[1]*, C. N. Waturu[2] and S. T. Rubindamayugi[1]

[1]Department of Molecular Biology and Biotechnology, University of Dar es Salaam, P. O. Box 35179, Dar es Salaam, Tanzania.
[2]Kenya Agricultural Research -Thika, Kenya.

Received 6 August, 2013; Accepted 2 December, 2015

The impact of 9 months cultivation of transgenic *Bacillus thuringiensis (Bt)* cotton on selected culturable bacterial and fungal populations in rhizosphere soil was investigated. The transgenic *Bt* cotton line (06Z604M), isoline (99M03) and a non-*Bt* cotton line (HART 89M) were planted in confined field site in Samuru-Thika where non-*Bt* cotton had been continuously cultivated for the past 2 years. Rhizosphere soil samples were collected at planting, maturity, flower and boll, and boll-opening stages and harvesting stages of cotton. Numbers of culturable soil microbial groups (bacteria, actinomycetes and fungi) involved in decomposition and nutrients recycling were measured at CFU and population levels. The proteins did not show effects on bacterial, actinomycetes and fungal counts and populations possibly as a result of adsorption of the proteins on soil particles, which could have rendered the proteins inaccessible for microbial utilization. Culturable microbial population and colony counts arranged in decreasing order were 06Z604D>99M03>HART89M, similar to the amounts of MBC and clay in the soils. Moreover, bacteria and fungi counts were higher at 110 DAS in 06Z604D than in 99M03 and HART89M plot soils. Our observations suggest that insecticidal proteins (*Cry1Ac* and *Cry2Ab2*) produced by Bollgard II *Bt* cotton could persist in tropical soils as a result of adsorption on soil clays but that there were no observable effect on the studied culturable microbial groups.The data presented here showed no consistent statistically significant differences ($p<0.005$) in the numbers of different groups of culturable bacteria, actinomycetes and fungi between rhizosphere soil of *Bt*, isoline and Hart 89M cotton lines in the same field, and no obvious trends in the numbers of the culturable bacteria and fungi with the increasing growth duration. Moreover, the studied culturable bacterial and fungal groups were positively correlated ($p>0.001$) with soil respiration and microbial biomass, which exhibited uneven trend with the treatments. Generally Soil from 06Z604D showed the slight higher microbial populations and CFU count, whilst HART 89M showed slight lower microbial count. This depicts the fact that slight variability in the treatments, quality and content of the root exudates might have a temporal or permanent shift in micro biota populations of a variety of crop studied.This study therefore suggests that a single-year cultivation of transgenic *Bt* cotton may not affect the functional bacterial and fungi populations in rhizosphere soil.

Key words: *Bacillus thuringiensis*, bacteria, population, colony forming units, fungi, *Bt* cotton.

INTRODUCTION

There is growing debate about the potential value of modern biotechnology, and in particular of transgenics, in helping to achieve Africa's development and food security goals. The challenge facing policymakers is not only to understand what the technology can do, or has done elsewhere, but also to establish what opportunities it presents to Africa. Currently, Africa's area under transgenic crop cultivation has witnessed a steady growth from 1.4 million hectares in 2006 (South Africa alone) to more than 3.5 million hectares in 2013 (South Africa, Egypt, Sudan and Burkina Faso) (Clive, 2014).

Transgenic crop plants modified to confer resistance against pests represent a potential environmentally safe tool to decrease the amount of chemical pesticides used in agriculture. Both field and laboratory studies showed that transgenic plants expressing *Bacillus thuringiensis* (Bt) cry proteins afford effective resistance to the larvae of a number of Lepidoptera species (Mapuranga et al., 2015). For example, *Bt* cotton plants are protected against the cotton bollworm, Helicoverpa armigera thus reducing the requirement for multiple insecticide treatments and the risk of pollution from chemical insecticide applications (Gutierrez et al., 2015). However, the release of genetically modified plants into the environment has become a public concern due to their potential environmental risks.

Environment risk assessment of transgenic plants has been mainly focused on (a) transfer of genes from the crops to wild relatives and related species (Snow and Palma, 1997; Hails, 2000), (b) resistance evolution to herbicide-tolerant crops, virus-resistant crops and insect-resistant crops and (c) impacts on non-target organisms and ecosystems (Schwember, 2008). The concerns of the impacts of transgenic plants on soil ecosystems were particularly over soil microorganism species, populations, and biodiversity (US EPA 2000; Kostov et al., 2014).

Inevitably, *Bt* toxin is introduced to soil primarily through the degradation of plant biomass remnants (Zhang et al., 2014), root exudates, through pollen deposition during tasseling, e.g., maize and by incorporation of plant residues after harvest (Zhang et al., 2015). There is no consensus about the persistence of the Cry proteins in soils. Some studies have shown that repeated and large scale use of transgenic *Bt* crops could lead to the accumulation and persistence of Bt proteins in soil (Saxena et al., 2010; Bakhsh et al., 2015). Bt toxin can quickly bind to clay minerals (Marutescu, 2012; Valldor et al., 2015) and humic acids in soil. The binding of *Bt* toxin onto soil particles reduces its bioavailability to microbes and consequently reduces its microbial degradation, but does not eliminate its insecticidal activity. Therefore, *Bt* toxin can be accumulated and kept toxic for over 234 days in soil (Marutescu, 2012).

Bt toxin produced by *Bt* corn had been reported to have no long-term effects on total numbers of culturable bacteria, fungi, protozoa and nematodes (Saxena and Stotzky, 2001; Yang et al., 2014). In China, two of the three studied transgenic *Bt* cottons (Line 247 and Line 249) were reported to cause a transient increase in total bacterial and fungal population levels, but neither the third *Bt* (Line 81) cotton nor the purified *Bt* toxins had any significant effect on the total numbers of bacteria and fungi (Zhang et al., 2014). *Bt* tobacco gave a significant rise in the number of nematodes (Yang et al., 2014). It was reported that the rate of degradation of *Bt* toxin and its impacts on soil ecosystems were related to the types and concentrations of *Bt* toxin, *Bt* crop varieties, constitution of soil microbes, soil types as well as soil chemical and physical characteristics (Stotzky, 2010). Genetic manipulation of the plants produces a change in plant characteristics, aside from Bt toxin production, that could influence the growth and species composition of soil microorganisms (Tarafdar et al., 2012). A plant can modify its rhizosphere through ion uptake, root exudates, rhizo-deposition (carbon loss from roots) and changes in the acidity and alkalinity of the rhizosphere (Day et al., 2010). Therefore, studying the fate of *Bt* toxin in the rhizosphere and its impacts on soil culturable bacteria is an important aspect of the risk assessment of Bt toxin produced by Bt cotton to the tropical soil ecosystems of central Kenya.

MATERIALS AND METHODS

Experimental site

This experiment was conducted during both short (November-December) and long rain seasons (March-June) in a confined field site at the Kenya Agricultural Research Institute (KARI), Thika, (01° 01'S and 37° 06' E) at about 1000 m above sea level. The climate of Thika is semi-arid and subtropical and characterized by hot dry seasons and cold rainy seasons. The total precipitation during the study period was 431 mm, and average daily air temperatures ranged from 14.9 to 25.5°C. The soil (0 to 15 cm depth) was used in this experiment was collected from the rhizosphere of the three cultivars of the KARI research site. The soil reaction (pH) was acidic for crop growth with low organic matter content. The confined field trial (CFT) experiment duration was between November 2009 and July 2010.

Transgenic plant lines

The transgenic cotton cultivar 06Z604D (Bollgard II) carrying both

*Corresponding author. E-mail: aicha.mechakra@umc.edu.dz. Tel: +213 554045501.

cry1Ac and *cry2Ab2* genes developed by the Monsanto Ag Products LLC, 800 N Lindberg Blvd St. Louis Missouri, 63167, USA was used. Bollgard II cotton event 15985 was developed by Monsanto Company to produce the *Cry2Ab2* insect control protein, which provides effective season-long control of key lepidopteran insect pests. This product was produced by re-transformation of Bollgard® cotton event 531, which produces the Cry1Ac insect-control protein. Its Isoline (99M03) was obtained from the same source. The commercial cotton cultivar (HART 89M) originally used in Central Kenya was used as the conventional cotton. Seeds of all cotton cultivars were provided through the Kenya Agricultural Research Institute, KARI- Thika.

Treatments

This study included three treatments: *Bt* cotton (06Z6O4D), isoline (99M03) and conventional (HART 89M), with three blocks and completely randomized 18 plots. The plants were grown in a confined experimental site (25x25 m) in (5x25 m) blocks and in (3x5 m) blocks. The path width between plots was 0.5 m apart and the buffer zone/crop was 3 m around the experimental site. No chemical or organic manure was applied during the entire growing period. In each plot plants were maintained to maturity. Irrigation was applied during long droughts especially during early growth times. Insecticide sprays (Descis and Booster) were done equally/evenly in all plots. Since both the 99M03 and the HART 89M contained no *Bt* gene, it was assumed that any change in soil ecological functions were due to the result of the *Bt* gene/ protein/toxin.

Field design and sampling

Experiments were performed between December 2009 and July 2010 at Kari-Thika Samuru field trial site central province, in Central Kenya. The trial site had been cultivated with conventional cotton (HART 89M). Seeds of both the transgenic cotton (06Z604D), isoline (99M03) and the conventional cotton (HART 89M) were sown in a randomized block design in three blocks each on 18 plots with 3x5 m for each cultivar/treatment. Each time, rhizosphere soil of all the plots were sampled during the growing duration, and the plant were left undisturbed. Soil samples were collected at the planting, flowering, maturity, boll and boll-opening stages and harvesting (0, 64, 88, 120, 154 and 175 days) of cotton development. Soil samples were collected by digging out soil around the rhizosphere area (up to 20 cm from the plant). For each sampling, rhizosphere soil from 4 randomly selected plants per plot was mixed and used as a composite rhizosphere soil sample. The soil samples were analyzed at KARI NARL and KARI-Muguga of the Kenya Agricultural Research Institute in Nairobi and Muguga.

Sample collection processing and analyses

Soil samples were collected on six sample dates: 15 December 2009 (sample day 0); 17 February 2010 (sample day 64); 25 March 2010 (sample day 90); 14 April 2010 (sample day 110); 27 May 2010 (sample day 154); and 18 June 2010 (sample day 175). Soil samples (approx. 100-200 g) were collected with a 3 cm diameter soil coring device to a depth of 15 cm. For each sample date, four samples per plot within each treatment row was sampled. The 4 soil cores per plot were pooled into one bag. A total of 72 (4 cores per plot x 18 plots) pooled soil samples were collected at each sample day. A clean soil coring device was used for collecting soil cores from each sample plot. Collected samples were immediately transferred in cool box to KARI Muguga and NARL for laboratory analysis the very and the next day. Analyses used for the soil samples, and the sample days on which they were performed and are given in Table 1.

Serial dilutions of soil suspension from the different cotton rhizospheric soils from the 18 plots were prepared. The inoculum from each dilution was deposited as a drop onto the surface of a solid growth medium from a calibrated dropping pipette. Each 20 µl drop was allowed to fall from the 2.5 cm height onto the surface of the well dried medium, where it spreads over 1.5 to 2 cm. Each of the (6) 18 plates received a single drop of the same dilution. Colony counts were made in the drop areas showing the largest numbers of discrete colonies. The mean counts of the (6) plates gives the viable counts per 20 µl of dilution and from this the viable count in the original sample was calculated (Miles and Misra drop plate method, 1985)

Soil samples from each plot were collected at 0, 64, 88, 110, 154, 175 days after sowing (DAS), and were used for microbial cultures, counts and evaluation of soil moisture content. Ten grams of freshly collected soil from each plot were thoroughly mixed for 5 min (tray shaker) with 90 ml of sterile water, and then diluted 10 fold to 10^{-6}. For fungi, dilutions 10^{-2}-10^{-3} were used and for bacteria 10^{-5}-10^{-6}. The resulting suspensions were then spiral plated (Spiral System) in the appropriate culture media. The selective medium used to isolate fungi from soil was MEA (Malt extract agar, Difco Co., amended with 100 mg L^{-1} tetracycline hydrochloride; 50 mg L^{-1} rose Bengal). Isolations of bacteria were done in 5% TSA (Tryptic soy agar Difco Co., amended with 50 mg L^{-1} benomyl). Number of colonies per plate was determined directly two and five days after inoculation for bacteria and fungi, respectively.

Twenty bacterial isolates from each replication were randomly picked with sterile tooth picks, grown in TSA, and maintained in small tubes (1.2 ml) with 1.0 ml of sterile water. Identification of bacterial isolates was based on analysis of fatty acid methyl-esters profiles (Stead, 1988). Bacterial samples were prepared as described by Kloepper et al. (1992), analyzed with a Hewlett-Packard Gas Chromatography (5890 II), and identified according to Sherlock Microbial Identification System software. Twenty fungal isolates from each replication were randomly picked and maintained in tubes with MEA. Identification of fungi was based on morphology and growth on MEA, PDA and Czapek Dox Agar (Difco Co.), and consulting appropriate literature (Domsch et al., 1980).

Laboratory incubation for numeration of culturable bacteria

A drop plate method was used to determine the numbers of the colony-forming units (c.f.u.) of culturable bacteria. To enumerate the three culturable microbial groups, rhizospheric soil from three plants (of a particular treatment) was sampled in triplicate in each plot on a monthly basis during growth stages and after harvest. The same sampling batches were used to determine the bacterial colonies. Cottons were last harvested on July 2010 and the plants were left in the field for post harvest studies. The rhizospheric soil samples collected within the same plot were then mixed thoroughly. An amount of about 10 g of the mixed soil sample was added into 100 ml of sterile water, shaken for 20 min, and then diluted to $10^{-5.}$ An amount of 0.1 ml of the suspension was evenly spread onto agar plate in triplicate, and they were then incubated at 30°C for 3 days for enumeration. The colonies were visually counted.

Determination of total bacterial and fungal population

To determine the total bacterial and fungal populations, rhizosphere soil were homogenized in a pestle to break the clods. Samples were prepared in sterile distilled water by suspending 1 g soil in 100 ml water and shaking the sample vigorously for 20 min on an orbital shaker at 250 rpm. The primary soil suspensions were serially

Table 1. Bacterial populations in soil rhizosphere of 06Z604D expressing both *cry1Ac* and *cry2Ac* genes at five different crop growth stages at Thika CFT site.

Treatment	Mean rhizosphere culturable bacterial population (Cells/g dry Soil)				
	Sampling time (DAS)				
	0	64	110	154	175
06Z604D	$1.85x10^5$	$3.32x10^5$	$4.32x10^5$	$5.74x10^5$	$5.46x10^5$
99M03	$1.97x10^5$	$2.92x10^6$	$8.12x10^4$	$9.58x10^5$	$1.06x10^6$
HART89M	$1.78x10^5$	$3.56x10^5$	$8.91x10^4$	$5.21x10^5$	$6.23x10^5$

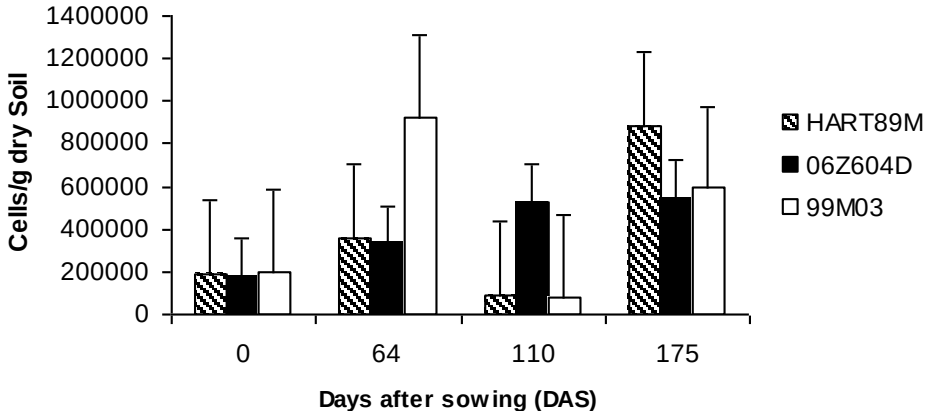

Figure 1. Bacteria populations in the three crop lines with growth time.

diluted further and 10^{-4} dilutions were plated on nutrient agar (NA) and Rose-Bengal supplemented potato dextrose agar (PDA) media in Petri plates to determine populations of bacterial and fungal populations respectively. The plates were incubated at 27 to 30°C for 3 and 7 days for bacteria and fungi respectively and observed for the appearance of colonies. The population count of the organisms was recorded after the stipulated incubation periods. The differences in the total bacterial and fungal populations in 06Z604D, 99M03 and HART 89M rhizosphere were determined using SAS package with analysis of variance (ANOVA).

Statistical analysis of data

The experiment encompassed triplicate experimental units and all data obtained were analyzed in respect of the statistical significance of the differences observed within treatments and between treatments. Response variables such as microbial populations and CFU numbers were analyzed using two-way analysis of variance (ANOVA) and principal components analysis (PCA). For ANOVA, the data were considered to be significantly different using the 5% P-value ($P<0.05$) as the criterion.

RESULTS

Physio-chemical parameters

Variations of rainfall, soil temperature (at 0 to 20 cm depth) and percentage moisture content are presented in Figure 1. The highest rainfall was 209 mm in March 2010 while in December 2010 there was no rain at all. The total rainfall between December 2009 and July 2010 was 810 mm. The normal rain seasons in East Africa occur in Nov-Dec (short rains) and March to May (long rains). However, during the study period, the rains started in late February 2010 and continued through March to late July 2010. Soil temperature and the percentage moisture content ranged from 20 to 34.5°C and 15.8 to 33.3% respectively. Soil temperatures were higher during hot dry seasons and lower during the rain season while the percentage moisture contents were higher during cool rainy season and lower during hot dry season. However, the variations in values of both soil temperature and percentage moisture content depended on the time and weather the measurement was taken. The lowest soil temperature was recorded in April 2010 and the highest in December 2009. The lowest percentage moisture content was recorded in December 2009 and the highest was in February 2010.

Bacterial populations

Comparison between plots

The results of the bacterial population study are

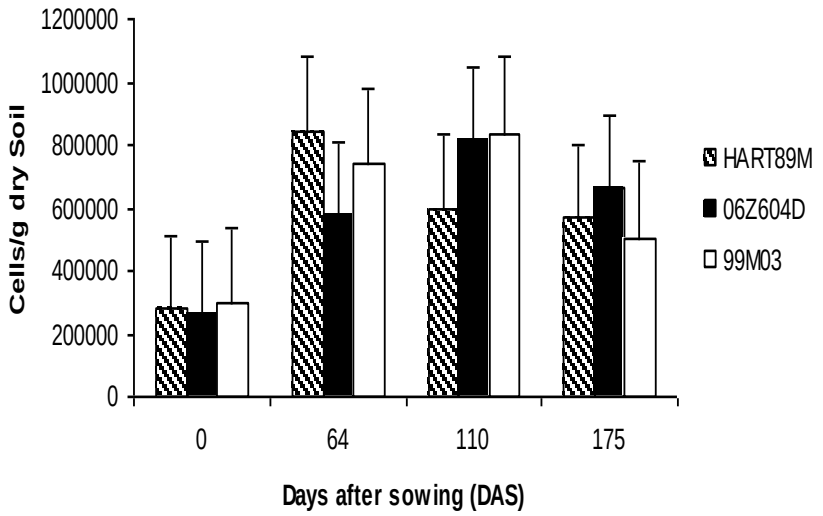

Figure 2. Actinomycetes population variation in the three crop lines with growth time.

presented in Table 1. The average population of bacteria from various plots with time are shown in Figure 1. Generally population of the two culturable bacterial groups varied considerably between treatments and among plots themselves. The overall populations between treatments arranged in decreasing order were 06Z604D > 99M03 > HART 89M. On average, HART plots had the highest population numbers ($8.799x10^5$ Cells/g dry Soil) followed by 99M03 plots ($5.908x10^5$ Cells/g dry Soil) and the least population numbers were from 06Z604D plots ($5.464x10^5$ Cells/g dry Soil). The highest bacterial population ($1.556x10^7$ Cells/g dry Soil) was measured within the 99M03 rhizosphere at 64 DAS, followed by HART 89M rhizosphere ($1.8172x10^6$ Cells/g dry Soil) at 110 DAS and the least numbers ($1.01865x10^6$ Cells/g dry Soil) was measured within 06Z604D rhizosphere at 110 DAS. Both bacterial and actinomycetes variations between plots and within the growth period were not significant different ($p>0.05$) and ($p=3249$) respectively. Generally bacterial population numbers varied considerably with time but tended to increase as growth duration increases. However there was no significant difference ($p=0.5150$) between the plots with time. Populations of rhizosphere bacteria went on increasing from 64 DAS to 154 DAS in 06Z604D, 99M03 and HART 89M plants. Reason for this trend is not clear. However it might be possible that increased total root biomass with the passage of time, might be instrumental in supporting higher bacterial population (Table 1). No significant difference was however observed in the culturable bacterial population count between 06Z604D, 99M03 and HART 89M rhizosphere. Also no potential shift in the population levels of any type of bacterium was observed between the three treatments (Figure 3). The types and shapes of colonies of the three microbial groups which grew from 06Z604D, 99M03 and HART 89M treatments were more likely similar.

Actinomycetes population

The average population of actinomycetes from various plots with time are shown in Figure 2. Generally population of the two culturable bacterial groups varied considerably between treatments and among plots themselves. The overall populations between treatments arranged in decreasing order were 06Z604D > 99M03 > HART 89M. On average, 06Z604D plots had the highest actinomycetes population numbers ($6.634x10^5$ Cells/g dry Soil) followed by 99M03 plots ($5.712x10^5$ Cells/g dry Soil) and the least population numbers were from HART plots ($5.061x10^5$ Cells/g dry Soil). The highest actinomycetes population ($1.7623x10^6$ Cells/g dry Soil) was measured within the 06Z604D rhizosphere at 110 DAS, followed by 99M03 rhizosphere ($1.7041x10^6$ Cells/g dry Soil) at 110 DAS and the least numbers ($1.434x10^6$ Cells/g dry Soil) was measured within HART 89M rhizosphere at 64 DAS. Actinomycetes variations between plots and within the growth period were not significant different ($p>0.05$) and ($p=3249$) respectively. Generally actinomycetes population numbers varied considerably with time but tended to increase as growth duration increases (Table 2 and Figure 2). However, there was no significant difference ($p=0.5150$) between the plots with time.

Fungal populations

The fungal population ranged between 1.709×10^7 cells/g dry soils and $2.8352x10^4$ cells/g dry soil and did not differ

Table 2. Effect of 06Z604D expressing both *cry1Ac* and *cry2Ac* genes on soil rhizosphere actinomycetes population at five different crop growth stages at Thika CFT site.

Treatment	Mean rhizosphere culturable actinomycetes population (Cells/g dry Soil)				
	Sampling time (DAS)				
	0	64	110	154	175
06Z604D	$2.77x10^5$	$5.74x10^5$	$8.16x10^5$	$8.91x10^5$	$7.06x10^5$
99M03	$2.98x10^5$	$7.36x10^5$	$8.38x10^5$	$9.06x10^5$	$5.71x10^5$
HART89M	$2.65x10^5$	$8.45x10^5$	$5.97x10^4$	$7.06x10^5$	$5.06x10^5$

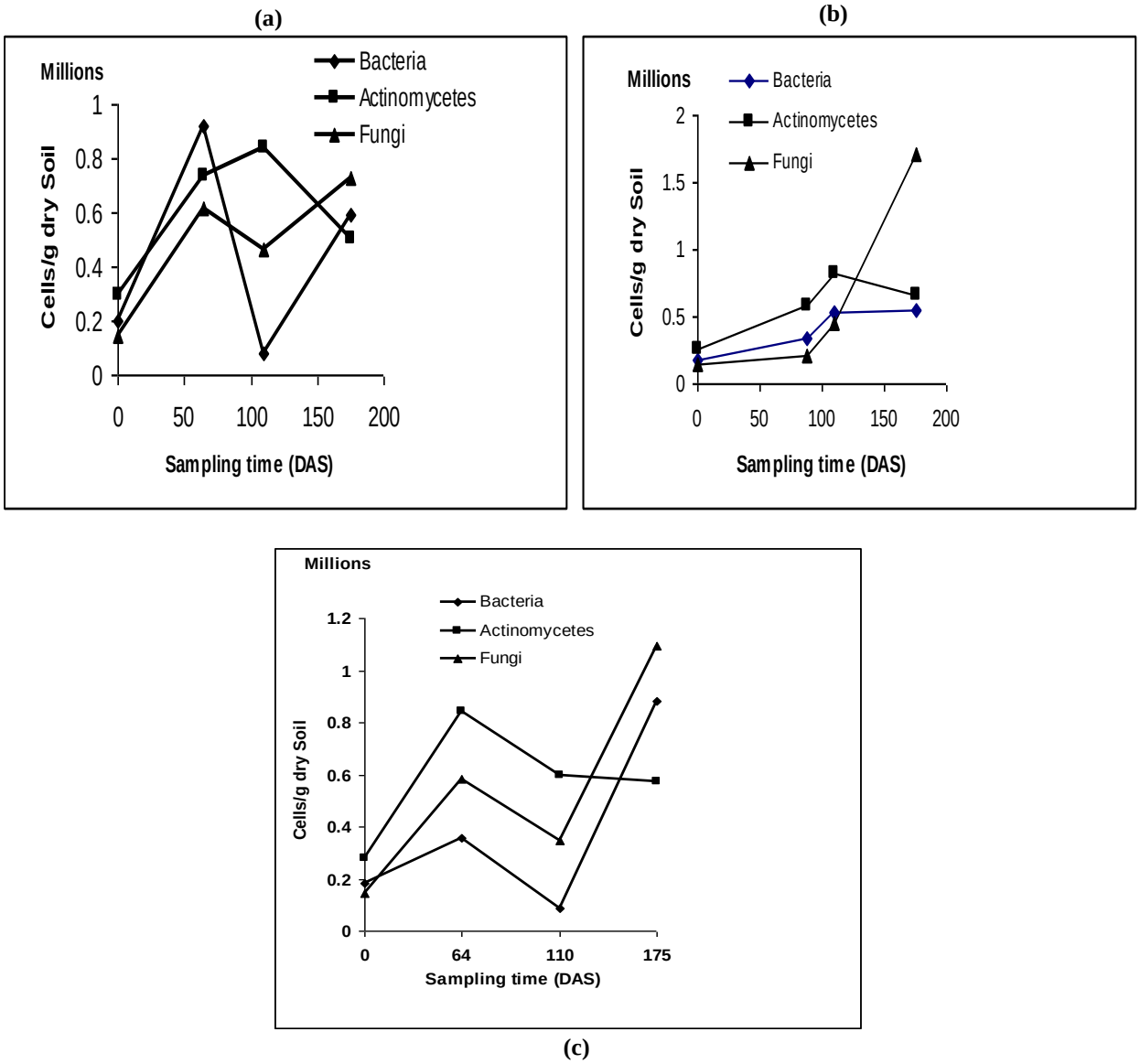

Figure 3. Mean variations of different microbial groups in 99M03 (a), 06Z604D (b) and HART89M (c) plots at different growth stages.

significantly among treatments. However, overall fungal populations were higher in 06Z604D soil and were the lowest in HART 89M soil (Table 3 and Figure 3). The overall evaluations of fungal populations between

Table 3. Effect of 06Z604D expressing both *cry1Ac* and *cry2Ab* genes on soil rhizosphere fungal population at five different crop growth stages at Thika CFT site.

Treatment	Mean rhizosphere culturable fungal population (Cells/g dry Soil)				
	Sampling time (DAS)				
	0	64	110	154	175
06Z604D	$1.46x10^5$	$2.06x10^5$	$4.56x10^5$	$7.01x10^5$	$8.02x10^5$
99M03	$1.47x10^5$	$6.17x10^5$	$4.67x10^5$	$6.84x10^5$	$1.09x10^6$
HART89M	$1.46x10^5$	$5.84x10^5$	$3.48x10^4$	$5.16x10^5$	$1.03x10^6$
CD (p=0.05)					

treatments arranged in decreasing order were 06Z604D > HART 89M > 99M03. On average, 06Z604D plots had the highest fungal population numbers ($1.709x10^6$ Cells/g dry Soil) followed by HART plots ($1.091x10^5$ Cells/g dry Soil) and the least population numbers were from 99M03 plots ($7.293x10^5$ Cells/g dry Soil). The highest fungi population ($1.709x10^7$ Cells/g dry Soil) was measured within the 06Z604D rhizosphere at 175 DAS, followed by HART 89M rhizosphere ($3.465x10^6$ Cells/g dry Soil) at 175 DAS and the least numbers ($2.053x10^6$ Cells/g dry Soil) was measured within 99M03 rhizosphere at 64 DAS. Rhizosphere fungal population declined at 88-110 DAS with the advancement of crop growth stage irrespective of the type of cotton grown (Table 3 and Figure 3). This could either be due to decline in the soil moisture content with the progress of the season or due to change in temperature regime. Fungi variations between plots and within the growth period were not significant different (p>0.05) and (p=4549) respectively. However there was no significant difference (p=0.5150) between the plots with time.

Colony forming units (CFUs)

The average CFU counts of bacteria, actinomycetes and fungi from various plots with time are shown in Table 4. Generally CFU counts of the three culturable microbial groups varied considerably between and among treatments and plots. The overall CFU counts of the three culturable groups are arranged in decreasing order were 99M03 > HART 89M > 06Z604D. On average, 06Z604D plots had the highest fungi CFU counts ($5.61x10^5$ colonies/g dry Soil), however, in contrary 99M03 plots had the highest culturable actinomycetes and bacterial CFU counts $5.98x10^5$ and $4.48x10^5$ (colonies/g dry Soil) respectively than both 06Z604D and HART89M. The highest CFU counts ($17.09x10^5$ colonies/g dry Soil) was measured within the 06Z604D rhizosphere at 175 DAS and the lowest CFU counts (1.46x105 colonies/g dry Soil) was measured at planting (0 DAS). The CFU counts between plots and within the growth period were not significant different (p>0.05) and (p=3249) respectively. Generally CFU counts varied considerably with time but tended to increase as growth duration increases. However there was no significant difference (p=0.5150) between the plots with time.

DISCUSSION

Physio chemical parameters

The total annual rainfall that occurred during the study period, November 2009- July 2010 was higher at (745.8 mm) than the annual rainfall reported in Thika in 2009 (KMD, 2010). The peak of the highest rainfall occurred in March 2010 at 209.0 mm higher than the one reported on the previous year (2009), which was 173.9 mm (KMD, 2009). The variation of rainfall affects soil temperature and percentage moisture content. The higher percentage moisture content values observed during rainy season were obviously due to increased water supply from rain. The low soil temperatures during the rainy season were undoubtedly due to the cooling effect of the rain water and low air temperatures which normally corresponds with rains. Furthermore, the finding that organic matter content of the experimental plots tended to be higher during rainy season than the dry season agrees with previous findings (Satrio et al., 2009). Satrio et al. (2009) reported values up to 97.69% higher during rainy season. Runoff, due to rains, brings organic material into the ecosystem (allochthonous), and would appear that the import of organic matter more than compensates for increased the mineralized rate (Sarkar et al., 2009). With respect to this study, (i) we are in agreement with this fact that the transient increases in the microbial populations in rhizosphere soil of the treatments are probably related to changes in root exudation and root characteristics (Figure 2 and Table 2). (ii) We are in agreement with this fact that the transient increases in the basal activity yields in rhizosphere soil of 06Z604D are related to changes in root exudation and root characteristics. Moreover, the soil microbes largely depends on the type of soil, temperature, moisture, plant growth, nutrients, pH, and many other factors which may vary between locations but also within a single plot and over very small distances (OECD, 2010).

Table 4. Comparisons of colony counts on soils from the rhizosphere of the three different cotton lines (Miles and Misra drop plate method).

Treatment	Bacteria	Actinomycetes	Fungi
06Z604D	$2.38x10^5$	$4.81x10^5$	$5.61x10^5$
99M03	$4.48x10^5$	$5.98x10^5$	$4.91x10^5$
HART 89M	$3.77x10^5$	$5.72x10^5$	$5.43x10^5$
CD (p=0.05)			

Microbial populations

The observed range of the number bacterial and fungal populations (10^4 to 10^7 Cells $gram^{-1}$ dry Soil) in Thika CFT is within the range of previous findings (Martinez et al., 2014; Jason et al., 2014). Garder et al. (2014) reported that under optimal growing conditions, total microbial abundance in background soils can exceed about 10^6 to 10^8 colony forming units per gram (dry weight) of soil (cfu/g) for bacteria, 10^6 cfu/g for actinomycetes, and 10^5 cfu/g for fungi. Garder (2014) estimated that there were approximately $4x10^3$ and $4x10^4$ species per g of soil respectively. However, due to variations on both biological and physiochemical parameters between sites, microbial populations in soils can relatively vary. In this study, the slight shift in population numbers (from 0 DAS to 175 DAS) of bacterial and fungal populations in 06Z604D plots, 99M03 and HART 89M plots of this study (Tables 1, 2 and 3) could be due to the fact that the increase of exudates supply. Previous studies revealed that qualitative and quantitative differences in root exudation could strongly affect the structure of microbial communities in the rhizosphere (Mansouri et al., 2002; Oger et al., 2000). Moreover, Bhatt et al. (2001) observed that the soil pH of the study site could affect the microbial activity of both bacteria and fungi consequently their populations through retarding organic matter decomposition rates and hence substrate availability. Though there were significant differences in numbers of the bacterial and fungal populations in the rhizosphere between 06Z604D, 99M03 and HART 89M within each sampling date from December 2009 to July 2010. But no significant differences were found in the populations and CFU numbers of the bacteria, action-mycetes and fungi among three cultivars after the growth season. Furthermore, there were no correlations between *Bt* toxin levels and numbers of the culturable bacteria and fungi. Those results were also verified by the pure *Bt* toxin fortification experiment. *Bt* toxin may not be the direct factor influencing the micro flora in the rhizosphere. The difference in the numbers of the culturable bacterial and fungal population in the rhizosphere may be due to different crop cultivars with different root exudates and root characteristics. Root exudates have a profound qualitative and quantitative effect on the rhizosphere microflora (Philippot et al., 2013). The composition of microbial communities in the rhizosphere is governed mainly by the quality and quantity of carbon sources that are released as root exudates (Philippot et al., 2013; Churchland and Grayston, 2014).

This study has shown that *Bt* protein (*Cry2Ac*) slightly stimulate the increase on populations of culturable bacterial and fungal naturally occurring in the cotton rhizosphere. Furthermore, this work fills the information gap on *Bt* cotton on East African tropical cotton soils and supplements data presented by Muchaonyerwa et al. (2014) concerning the effects and persistence of *Bt* toxin on microorganisms in some Zimbabwean soils. No statically significant ($P < 5\%$) correlation was shown between *Cry1Ac*/*Cry2Ab2* and population of other microorganisms. In 06Z604D soil and 99M03 the population of fungal was around $4.56x10^5$ cells/g dry soil to 5.6 $4.56x10^5$ cells/g dry soil and $5.56x10^5$ cells/g dry soils respectively. A change induced through genetic manipulation of the plants had produced a change in plant characteristics aside from *Bt* toxin production that could influence the growth and species composition of the soil microorganisms (Zhang et al., 2014). It had also been reported that, there is precedent for unanticipated changes in plant quality occurring from insertion of genes which resulted in changes in root exudates. Thus, an altered composition of root exudates may induce a different community of rhizosphere microorganisms. Even small modifications, as may exist between different cultivars of the same plant species, can result in the occurrence of different microbial communities in the rhizosphere (Berendsen et al., 2012). Indirect effects of *Bt* toxin, such as due to differences in invertebrate pests and their impacts on plant physiology, may also affect the rhizosphere bacteria. Although the transitory reduction of functional bacteria populations in the rhizosphere of *Bt* cotton 06Z604D, 99M03 and HART 89M may not be of environmental concern, the accompanying change in microbial species composition, with a potential to impact soil processes, may be of ecological significance and warrants further investigation.

Bt corn was reported to have no effects on numbers of culturable microorganisms (Saxena and Stotzky, 2001; Hannula et al., 2014), while transient increases in culturable microorganisms were observed with *Bt* cotton (Zhang et al., 2014) and Bt potato (Hu et al., 2013). *Bt* corn had been reported to have no impact on microbial

biomass, activity, or community structure (Turrini et al., 2015). Certain methanogenic archaeabacteria were inhibited by *Cry* proteins (Han et al., 2013), and Bt-rice straw had transient effects on microbial numbers and activity in a flooded rice paddy soil (Schmidt et al., 2015). Because the structure of the soil microbial community is an important component of soil quality and health, soil microbiological properties could be early and sensitive indicators of anthropogenic effects on soil ecology in both natural and agricultural ecosystems (Habig and Swanepoel, 2015). In the last decade many reports on potential impacts of transgenic crops on the structure and functioning of the soil microbial community have been published. Two of three transgenic *Bt* cotton lines caused a transient increase in total bacterial and fungal population levels; in contrast, neither the third transgenic *Bt* cotton line nor the purified *Bt* toxins affected the total numbers of bacteria and fungi (Zhang et al., 2014). There were no significant differences in the numbers of culturable bacteria, actinomycetes, fungi, protozoa, and nematodes in the rhizosphere of *Bt* vs non-*Bt* corn or in soil amended with biomass of Bt vs. non-Bt corn (Lu et al., 2010). Despite the detection of *Cry1Ab* protein in the rhizosphere soil of MON810 maize, the bacterial community structure was less affected by the *Cry1Ab* protein than by other environmental factors, such as plant age or field heterogeneity (Baumgarte and Tebbe 2005). However, farming practices and crop types may increase populations of beneficial microorganisms by soil amend-ments have the advantage that no improved methodology is needed to facilitate microbial growth and survival. Indigenous microorganisms, in general, have higher competence for survival in their own habitat than introduced ones. Other cultural methods, such as mulching and crop rotation, also induce microbial increases in soil (Yuliar et al., 2015).

We have found very little effect of *Cry1Ac*/*Cry2Ab2* gene expression on rhizosphere and soil microbial communities. In the Thika CFT experimental site, there was little large soil type effect. The bacterial and fungal population profiles were slightly affected by Cry gene expression in the Central Kenyan soil. Thika-Samuru soils is higher in clay content and Cry protein is known to persist longer in clay soils (Valldor et al., 2015), which may explain why this effect has also manifested in Kenyan soil. The strongest difference found so far was in the bacterial population, my results are generally similar to reports from other researchers (Hu et al., 2013; Hannula et al., 2014; Zhang et al, 2014). However, longer-term studies are needed, and newer methods may reveal effects not previously seen.

Conclusion

Our findings demonstrated that the fate of 06Z604D expressing both *cry1Ac* and *cry2Ab2* genes on culturable soil bacterial, actinomycetes, fungal populations and their CFU counts versus 99M03 and HART 89M had transient or no any adverse effect. However, knowledge of the impact of 06Z604D residues on red Kenyan soil microbial ecology is essential for understanding the long-term agronomic and environmental effects of genetically modified crops and for developing appropriate management practices for minimizing potential negative impacts.

Moreover, differences in the culturable bacterial and fungal population between rhizosphere soil of 06Z604D, 99M03 and HART 89M cotton in the same trial site were either transient or absent. The major conclusions from this study are: (1) Cultivation of 06Z604D expressing both *Cry1Ac* and *Cry2Ab2* protein did not result in significant change in the overall numbers of culturable bacterial and fungal populations; and (2) transgenic 06Z604D had no clear effect on the number of culturable bacterial and fungal populations in the rhizosphere within one growing season. These results suggest that cultivation of *Bt* crops over multiple years probably poses little ecological or environmental risk.

Overall the soils exposed to *Bt* did not show significant variation in the bacterial and fungal populations. The effect of transgenic plants on soil populations of non-target bacteria and fungi could be either transient or do not have any effect at all. Dunfield and Germida (2003) concluded that the changes in the microbial community structure associated with genetically modified plants were temporary and did not persist into the next field season. In the present study, the soil bacterial and fungal populations were comparable between the soils surrounding 06Z604D event MON 531 and event MON 15985 expressing both Cry 1Ac and Cry2Ab2 protein and the non *Bt* counterparts (99M03 and HART 89M). This observation indicates that 06Z604D, does not have adverse effect on culturable soil bacterial and fungal populations. Measurement of microbial activity is normally through the presence of culturable microbes in the soil.

The conclusion of this study is in agreement with other findings in the fact that, the insecticidal toxin released from *Bt* crops had no short-term deleterious effects on soil biological communities, but the potential long-term effects due to accumulation and persistence of the toxin on soil biodiversity have not been evaluated extensively (Donegan et al., 1995; Betz et al., 2000; Saxena and Stotzky, 2001a; Head et al., 2002; Zwahlen et al., 2003; Buiatti et al., 2013; Xiaogang and Liu, 2013; Malviya et al., 2014).

Conflict of Interests

This statement is to certify that all Authors have seen and approved the manuscript being submitted and declare no conflict of interests. We warrant that the article is the

Authors' original work. We warrant that the article has not received prior publication and is not under consideration for publication elsewhere. On behalf of all Co - Authors, the corresponding Author shall bear full responsibility for the submission.

ACKNOWLEDGEMENTS

This study was supported, by the BioSafe Train Project from the DANIDA/ENRECA in collaboration with the University of Copenhagen, Department of Terrestrial Ecology, Denmark and the University of Dar es Salaam, Department of Molecular Biology and Biotechnology, Tanzania. The opinions expressed herein are not necessarily those of the granting agencies. We thank the Monsanto Company for providing the *Bt* cotton seeds (06Z604D), the isoline (99M03) and their advices and suggestions in the beginning of this study. We also thank Dr. Waturu C.N. the Center Director KARI-THIKA for providing the experimental site, the conventional cotton seeds (HART 89M), KARI MUGUGA and KARI NARL for the laboratory facilities.

REFERENCES

Bakhshi A, Khabbazi SD, Baloch FS,. Demirel U, Çalişkan ME, Hatipoglu R, Ozcan S, Ozkan H (2015). Insect-resistant transgenic crops: retrospect and challenges. Turk. J. Agric. For. 39:531-548

Berendsen RL, Pieterse C, Bakker P (2012). The rhizosphere microbiome and plant health. Trends Plant Sci. 17(8):478-86.

Buiatti M, Christou P, Pastore G (2013). The application of GMOs in agriculture and in food production for a better nutrition: two different scientific points of view. Genes Nutr 8:255-270.

Clive J (2014). Global Status of Commercialized Biotech/GM Crops: Brief 49.

Churchland C, Grayston SJ (2014). Specificity of plant-microbe interactions in the tree mycorrhizosphere biome and consequences for soil C cycling. Front Microbiol. 5:261.

Garder JL (2014).Transport and persistence of tylosin-resistant Enterococci, *erm* Genes, and Tylosin in soil and drainage water from fields receiving swine manure. J. Environ. Qual. 43:1484-1493.

Gutierrez AP, Ponti L, Herren HR, Baumgärtner J, Kenmore PE (2015). Deconstructing Indian cotton: weather, yields, and suicides. Environ. Sci. Eur. 27:12.

Habig J. and C. Swanepoel (2015). Effects of conservation agriculture and fertilization on soil microbial diversity and activity. Environments 2(3):358-384.

Hails RS (2000). Genetically modified plants–the debate continues. Trends Ecol. Evol. 15(1):14-18.

Hannula SE, de Boer W, van Veen J A (2014). Do genetic modifications in crops affect soil fungi: a review. Biol. Fertil. Soils 50(3):433-446.

Han C, Zhong W,Shen W, Cai Z, Liu B (2013). Transgenic Bt rice has adverse impacts on CH_4 flux and rhizospheric methanogenic archaeal and methanotrophic bacterial communities. Plant Soil 369:297-316.

Hu H, M. Xie, Y. Yu, Q. Zhang (2013). Transgenic *Bt* cotton tissues have no apparent impact on soil microorganisms. Plant Soil Environ. 59(8):366-371.

Kostov K, Krogh PH, Damgaard CF, Sweet JB, Hendriksen NB (2014). Are soil microbial endpoints changed by Bt crops compared with conventional crops? A systematic review protocol. Environ. Evidence 3:11.

Lu H, Wu WX, Chen Y, Zhang X, Devare M, Thies JE (2010). Decomposition of Bt transgenic rice residues and response of soil microbial community in rapeseed-rice cropping system. Plant Soil 336(1):279-290.

Malviya N, Yadav MK, Tripathi MK, Sarangi BK, Yadav D (2014). Environmental Concerns for Transgenic Plants: An Overview. Octa. J. Biosci. 2(2):86-90.

Mapuranga R., Chapepa B. and Mudada N. (2015). Strategies for integrated management of cotton bollworm complex in Zimbabwe: A review. *Int. J. Agro. and Agri. Res.* 7(1):23-35.

Marutescu A. (2012). A brief survey regarding fate of Bt proteins synthesized by transgenic maize in soil. J. Hort. Forestry Biotechnol. 16(2):126-130.

Martinez VA, Cotton J, Gardner T, Kucera JM, Zak JC, Wester DB (2014). Predominant bacterial and fungal assemblages in agricultural soils during a record drought/heat wave and linkages to enzyme activities of biogeochemical cycling. Appl. Soil Ecol. 84:69-82.

Philippot L, Raaijmakers JM, Lemanceau P, van der Putten WH (2013). Going back to the roots: the microbial ecology of the rhizosphere. Nat. Rev. Microbiol. 11:789-790

Saxena D, Stotzky G. (2001). Insecticidal toxin from *Bacillus thuringiensis* is released from roots of transgenic Bt corn *in vitro* and in situ. FEMS Microbiol. Ecol. 33:35-39.

Saxena D., S. Pushalkar and G. Stotzky (2010). Fate and effects in soil of cry proteins from *Bacillus thuringiensis*: Influence of Physicochemical and Biological Characteristics of Soil. Open Toxinol. J. 3:133-153.

Schwember AR (2008). An update on genetically modified crops. Ciencia e investigación agraria 35(3):231-250.

Snow AA, & Palma PM (1997). Commercialization of transgenic plants: potential ecological risks. BioScience, 47(2):86-96.

Stotzky G (2010). Persistence and biological activity in soil of insecticidal proteins from *Bacillus thuringiensis* and of bacterial DNA bound on clays and humic acids. J. Environ. Qual. 29:691.

Tarafdar JC, Rathore I, Shiva V (2012). Effect of *Bt* transgenic cotton on soil biological health. Appl. Biol. Res. 14(1):15-23.

Valldor P, Miethling-Graff R,Martens R, Tebbe CC (2015).Fate of the insecticidal Cry1Ab protein of GM crops in two agricultural soils as revealed by ^{14}C-tracer studies. Appl. Microbiol. Biotechnol. 99(17):7333-7341.

Xiaogang L, Liu B (2013). A 2-Year Field Study Shows Little Evidence That the Long-Term Planting of Transgenic Insect-Resistant Cotton Affects the Community Structure of Soil Nematodes. *PLoS One* 8(4).

Yang B, Cheng H, Liu X, Ge F, Chen Q (2014). Bt cotton planting does not affect the community characteristics of rhizosphere soil nematodes. Appl. Soil Ecol. 73:156-164.

Yuliar Y, Nion A, Toyota K (2015). Recent Trends in Control Methods for Bacterial Wilt Diseases Caused by Ralstonia solanacearum. Microbes Environ. 30(1):1-11.

Zhang YJ, Xie M, Peng DL (2014). Effects of the transgenic *CrylAc* and *CpTI* insect-resistant cotton SGK321 on rhizosphere soil microorganism populations in northern China. Plant Soil Environ. 60(6): 285-289.

Zhang YJ, Xie M, Wu G, Peng D, Yu WB (2015). A 3-year field investigation of impacts of Monsanto's transgenic Bt-cotton NC 33B on rhizosphere microbial communities in northern China. Appl. Soil Ecol. 89:18-20.

academicJournals

Vol. 15(21), pp. 940-947, 25 May, 2016
DOI: 10.5897/AJB2015.15163
Article Number: 6F9C59458600
ISSN 1684-5315

http://www.academicjournals.org/AJB

African Journal of Biotechnology

Full Length Research Paper

Expression and purification of recombinant Shiga toxin 2B from *Escherichia coli* O157:H7

Marwa E. A. Aly[1], Amro S. Hanora[2]*, Tamer M. Essam[1] and Magdy A. Amin[1]

[1]Microbiology and Immunology Department and Biotechnology Centre, Faculty of Pharmacy, Cairo University, Kasr El-Aini Street, Cairo11562, Egypt.
[2]Department of Microbiology and Immunology, Faculty of Pharmacy, Suez Canal University, Ismailia, 41522, Egypt.

Received 11 December, 2015; Accepted 2 March, 2016

Enterohemorrhagic *Escherichia coli* are important human food-borne pathogens. Recently, Shiga toxin-producing *E. coli* (STEC) causes life-threatening hemolytic-uremic syndrome (HUS). In this study, Stx2B gene, a subunit of Shiga toxin, was amplified via polymerase chain reaction (PCR) from the chromosomal DNA of clinical fecal sample using appropriate primers. The PCR product was cloned to commercially available plasmid pH6HTN His6HaloTag® T7 containing two purification tags, namely, six histadine tag and Halo tag. The integrity of the constructed plasmid was confirmed using restriction enzyme mapping and sequencing. Then, Stx2B protein expressed after induction with isopropyl β-D-1-thiogalactopyranoside (IPTG) in *E. coli* JM109 (DE3) under the control of the T7 promotor. The two step purification trains were used to purify native Stx2B. First step purification was Ni-immobilized metal ion affinity chromatography (IMAC) column, followed by second step using HaloLink resin. The native Stx2B was obtained after column cleavage of halo-tag using HaloTEV protease. Maximum protein expression of Stx2B economically was obtained using 1 mM IPTG for 4 h at 37°C. Protein identity was confirmed by a band at ~11.4 kDa using 15% sodium dodecyl sulfate polyacrylamide gel electrophoresis (SDS-PAGE) and StxB2 yield was 450 µg ml^{-1} confirmed by Bradford assay. Recombinant Stx2B protein was produced in highly pure yield using HaloTag technology.

Key words: *Escherichia coli* O157:H7, StxB gene, expression, HaloTag technology, purification.

INTRODUCTION

Enterohemorrhagic *Escherichia coli* (EHEC) strains are important human food-borne pathogens (Kaper et al., 2004). The clinical manifestations of EHEC infections range from watery diarrhea or hemorrhagic colitis (HC), to the most severe outcome, the life-threatening hemolytic-uremic syndrome (HUS) (Nataro and Kaper, 1998). Currently, there are no specific protective measures or therapy against EHEC infection other than supportive therapy; as the utility of antibiotic or anti-diarrhetics treatment may be a risk factor for HUS and there is insufficient evidence to recommend antibiotic treatment for EHEC infection as reported by Nguyen and Sperandio

*Corresponding author. E-mail: ahanora@yahoo.com. Tel: +2064-3230741 or +201000323406. Fax: +2064-3230741.

(2012).

Although, the magnitude of the social and economic impacts caused by EHEC infections is high, no licensed vaccine or effective therapy is presently available for human use. So far, a number of experimental approaches are being investigated in animals. For example, Donohue-Rolfe et al. (1989) reported that a monoclonal antibody against the Stx2B subunit recognizes and neutralizes both Stx1 and Stx2 in the HeLa cell cytotoxicity assay. The immune-prophylactic potential of the Stx1B subunit has been proven in the publication from different laboratory such as Boyd et al. (1991) and Acheson et al. (1996). In recent study, the immune-modulatory potential of recombinant Shiga toxin B subunit (rStxB) protein in BALB/c mice was evaluated. Animal protection with recombinant StxB was conferred through both humoral and cellular immune responses (Gu et al., 2011). Recently, the large scale production of stx2 in *E. coli* for toxoid vaccine antigen was achieved by Hideyuki et al. (2013).

Several studies showed evidence that a closer association between Stx2 expression by Shiga toxin-producing *E. coli* (STEC) and a more severe course of illness than Stx1 as were reported in both Scotland et al. (1987) and Hashimoto et al. (1999) studies. For example, in a recent outbreak involving 131 Japanese patients infected with Stx1-producing O118:H2 STEC serotype, no case of HUS was reported, and the gastrointestinal symptoms were relatively mild (Marcato et al., 2001). In addition, it has been proposed that a cellular vaccine consisting of a nontoxic Stx2B or combined with other proteins (Dubendorff and Studier, 1991) might provide safe and effective protection against the most severe complications of EHEC infections (Hanahan, 1983). This is better than the use of holotoxin Stxs as the expression of holotoxin may lead to instability of the expression strain or mutations accumulation due to the enzymatic activity of A subunits (Hopwood, 2003). Therefore, these epidemiological findings make Stx2B a compelling candidate for vaccine development in present study.

In this research, an easy way was developed to build recombinant plasmid pH6HTN His_6HaloTag® T7-Stx2B to get high yield of recombinant Stx2B (rStx2B) that could be applied in large scale production within vaccine candidate.

MATERIALS AND METHODS

Bacterial strains, plasmid and media

One clinical isolate of *E. coli* containing stx_{1AB} and stx_{2AB} genes was collected from Abu El-Reesh Hospital, Cairo University's fecal samples. A clinical EHEC was tested for the inability to utilize sorbitol by plating on sorbitol MacConkey (SMA) agar (Oxoid, USA) at 37°C. Also, biochemical profile was performed by API 20E (BioMérieux, France) according to the manufacturer's instructions. *E. coli* DH5α (Promega, USA) (Hanahan, 1983) and *E. coli* JM109 (DE3) (Promega, USA) were used as hosts for cloning and protein expression, respectively.

The prokaryotic plasmid pH6HTN His_6HaloTag® T7 (4,014 kb, Promega, USA) was used for gene cloning and expression in *E. coli.* All *E. coli* strains were grown on Luria Bertani (LB) (Oxoid Ltd., Basingstok, Hampshire, England) liquid or agar medium at 37°C and with 100 $\mu g.ml^{-1}$ of ampicillin as a selective medium whenever necessary.

Construction of Stx2B expression plasmid

DNA cloning and further manipulations were carried out according to methods described by Hopwood (2003) and Sambrook and Russell (2001). The DNA of clinical EHEC isolate was used as template for polymerase chain reaction (PCR) amplification of Shiga toxin 2B gene after purified by wizard genomic DNA purification kit (Promega, USA) according to manufacturer's structures. PCR was performed in a programmable thermo-cycler PCR Machine (Touchgene Gradient, USA) using the specific primers (IDT DNA, USA): P1:5-cgTCTAGAATGAAGAAGATGTTTATGGCGGTT-3 and P2:5-ttGCGCCGCTCAGTCATTATTAAACTG-3. The forward primer (P1) contained an engineered *XbaI* site (underlined) and the reverse primer (P2) incorporated an engineered *NotI* site (underlined). The amplification of stx2B by PCR was performed using Flexi GoTaq DNA polymerase (Promega, USA) and primer P1 and P2 under the following conditions: one cycle of denaturation (95°C for 10 min); 30 cycles of denaturation (95°C for 30 s), annealing (54°C for 30 s), extension (72°C for 45 s); followed by a final extension (72°C for 10 min).

Both the purified amplicon of stx_{2B} gene and his6halotag t7 plasmid were double digested with FastDigest *XbaI*/*NotI* (Thermo-Scientific, USA) according to the manufacturer's specifications. Ligation took place under optimal reaction conditions using T4-DNA ligase according to New England BioLabs (NEB) manufacturer's protocol, with an insert: vector ratio of 3:1, respectively. The reaction was performed at 16°C for 18 min in thermo-cycler PCR machine at a final reaction volume of 20 µl containing 0.2 $\mu g.\mu l^{-1}$ for digested PCR fragment, 1 $\mu g.\mu l^{-1}$ for linearized vector, 2 µl for 10x ligation buffer and 1 µl for (1 unit) T4 ligase. The mixing was done gently by pipetting the solution up and down.

The cloned vector was used to transform chemically prepared competent *E. coli* DH5α and was cultured on Luria Broth (LB) medium containing 100 $\mu g.ml^{-1}$ of ampicillin. The resulted colonies were tested for further analysis for the presence of an insert into the multiple cloning sites (MCS) by using colony PCR primer for PCR amplification reaction that proceed part from MCS of pH6HTN His_6HaloTag T7 vector using the specific primers (IDT DNA, USA); P1 (forward primer): 5-GGTCTGAATCTGCTGCAAGAA-3 and P2 (reverse primer): 5-ACATGGCGATAGCTAGACTG-3. The thermal cycler protocol was performed according to the previous conditions except annealing temperature was 52.7°C for 30 s. The *E. coli* cells which carry empty vector were used as a negative control.

The positive colonies were subjected to another colony PCR analysis for identifying the correct orientation (in frame) of the gene insert (*stx2B*) in the pH6HTN His6HaloTag vector. Moreover, the positive *E. coli* DHα5 colonies harboring correct recombinant vector of *stx2B* gene were subjected to *XbaI*/*NotI* double digestion restriction analysis to ensure insertion of the desired insert.

The clone harbouring plasmid DNA from positive clone was isolated with QIAGEN® Plasmid Purification kit (Qiagen, Germany). The resulting purified plasmid pH6HTN His6HaloTag®T7–Stx2B was transformed into final host of chemically competent *E. coli* JM109 (DE3) and was cultured on LB medium containing 100 $\mu g.ml^{-1}$ of ampicillin.

Stx2B expression and purification

Expression of Stx2B in *E. coli* was carried out as described by

Studier et al. (1990). Expression was performed under the control of the T7 promotor using *E. coli* JM109 (DE3) strains. Single colony harbouring the plasmid His6HaloTag T7-Stx2B and His6HaloTag T7 (empty vector as negative control) were grown overnight in 3 ml LB medium containing 100 $\mu g.ml^{-1}$ ampicillin at 37°C on a shaker incubator 250 rpm. 200 µl of these pre-cultures were used to inoculate 20 ml fresh LB medium in 250 ml normal flasks and let them grow at 37°C on shaker incubator 120 rpm to an $OD_{600\ nm}$ of 0.5 to 0.6.

Optimization of the Stx2B expression

Five flasks of previous cultures were induced by the addition of different concentration of isopropyl β-D-1-thiogalactopyranoside (IPTG; 0.1, 0.25, 0.5, and 1 mM) and one culture was un-induced. Induction was continued for different time periods (0 h, 4 h and overnight) at incubation temperature (37°C) with shaking at 120 rpm. The above experiment was repeated at 30°C incubation temperature instead of 37°C. Then aliquots were removed at different time points for analysis. Induced cultures were transferred to falcon tube to harvest by centrifugation for 30 min at 13,000 rpm at 4°C and the pellets were washed twice with lysis buffer (ice cold 50 mM Na_2HPO_4/MOPS, 300 mM NaCl, 5 mM Imidazole, and 0.25 µg/µl (p-amidinophenyl)methanesulfonyl fluoride (APMSF), pH at 7.0) then were kept in -20°C until used.

Batch purification Stx2B protein from *E. coli* under native condition

Purification of His_6HaloTagged Stx2B proteins using IMAC by gravity-flow

The pellets were re-suspended in lysis buffer in ratio 1:10. The extent of sonication was tightly controlled: sonication in 4 cycles (each at 20 s on at 35% power, 60 s off, at 0°C) (Elma, USA). The resulting cell lysate was centrifuge at 12,000 × g for 20 min at 4°C to remove the unlysed cells and insoluble proteins. The supernatant was collected and loaded onto a profanity nickel metal charged resin (Bio-Rad, Hercules CA, USA) Econo-Pac® column that had been pre-equilibrated with 5 column volumes (CVs) buffer A (50 mM Na_2HPO_4/MOPS, 300 mM NaCl and 5 mM imidazole, pH at 7.0).

Then, the column was washed with 5 CVs of buffer A to remove unbound sample and the resulted fractures (0.5 ml/fraction) were pooled for further analysis. After that, the His_6HaloTagged Stx2B protein was eluted with buffer A containing 500 mM imidazole and then protein containing fractions (0.5 ml/fraction) were pooled and analyzed using sodium dodecyl sulfate polyacrylamide gel electrophoresis (SDS-PAGE).

Further purification of His_6HaloTagged Stx2B proteins using halo-link resin

The His_6HaloTagged Stx2B protein resulted from previous purification was subjected to further purification by HaloLink resin (Promega, USA) by batch purification. About 2 ml (0.5 ml settled) HaloLink resin was equilibrated with 10 CVs of Halotag purification buffer (50 mM MOPS and 120 mM NaCl, pH at 7.0) by inverting the tube until thoroughly mixed. Then, resin was centrifugation at 1,000 × g for 10 min at 4°C and washed twice with the same buffer followed by centrifugation. 1 ml of His_6HaloTagged Stx2B IMAC purified protein previously purified was incubated with the Halolink resin at 4°C overnight with constant mixing, and collected by centrifugation at 1,000 × g for 10 min at 4°C. The resin was washed with 10 CVs of Halotag purification buffer and mixed by inverting the tube, the resin centrifugation at 1,000 × g for 10 min at 4°C and the supernatant was discarded, and a total of two washed was performed.

Afterwards, the resin was incubated with 0.55 ml cleavage solution (50 mM MOPS and 120 mM NaCl, pH at 7.0) containing 33 µl of HaloTEV protease (Promega, USA) for 90 min at room temperature. The supernatant was separated by centrifugation at 10,000 × g for 5 min and the resin was washed with Halotag purification buffer and both supernatants were combined. The eluted purified protein was analyzed by 15% SDS-PAGE.

Protein analysis

Electrophoresis of proteins was performed using SDS-PAGE according to Laemmli (1970) where the final concentration of acrylamide in the stacking and separating gels was 4 and 15%, respectively.

The gels were scanned with a Digital Camera (Cannon, Japan) and analyzed using the software package GelCompar II, 6.5 (Applied Maths, Belgium). The pertained protein ladder" Broad Range (6.5-200 kDa) (Servea, USA) was used as internal reference of molecular weight for normalization. The concentration of resulted Stx2B protein was determined using the Bradford assay (Thermo Scientific, USA), using BSA as a protein standard (Bradford, 1976).

RESULTS

Construction of Stx2B expression plasmid

Genomic DNA from EHEC clinical isolate was used to isolate the gene coding for Stx2B. Thus, the 270 bp PCR ampilicon size carrying *XbaI/NotI* restriction sites on the 5' and 3' flanking regions, respectively (Figure 1B; Lane 1) was cloned into the pH6HTN His6HaloTag® T7 vector resulting in intermediate plasmid pH6HTN His6HaloTag® T7-Stx2B.

The digestion of double restriction the pH6HTN His6HaloTag® T7 vector and Stx2 insert with Fast Digest *XbaI/NotI* restriction enzymes resulting in the linearization of vector producing a band size ~3974 bp (Figure 1A; Lane2), while the PCR product of *stx2B* gene was observed at ~270 bp, (Figure 1B; Lane 1).

Screening for recombinant *stx2B* gene for confirmation of insert

The recombinant construct containing *stx2B* gene obtained after ligation was used for *E. coli* DH5α cells transformation. Among the colonies appeared on the LB Agar/ampicillin (100 $\mu g.mL^{-1}$), the positive clone was screened initially by colony PCR using the primers designed from MCS of vector. The 350 bp of PCR product size corresponded to negative clone, while the 595 bp ampilicon size corresponded to positive clone (Figure 1B, Lanes 3 and 4, respectively).

The positive clone was subjected to colony PCR screening for correct insert orientation resulting in 435 bp ampilicon size (Figure 1B; Lane 5). The 4.244 kb plasmid DNA of positive clone was double digested after

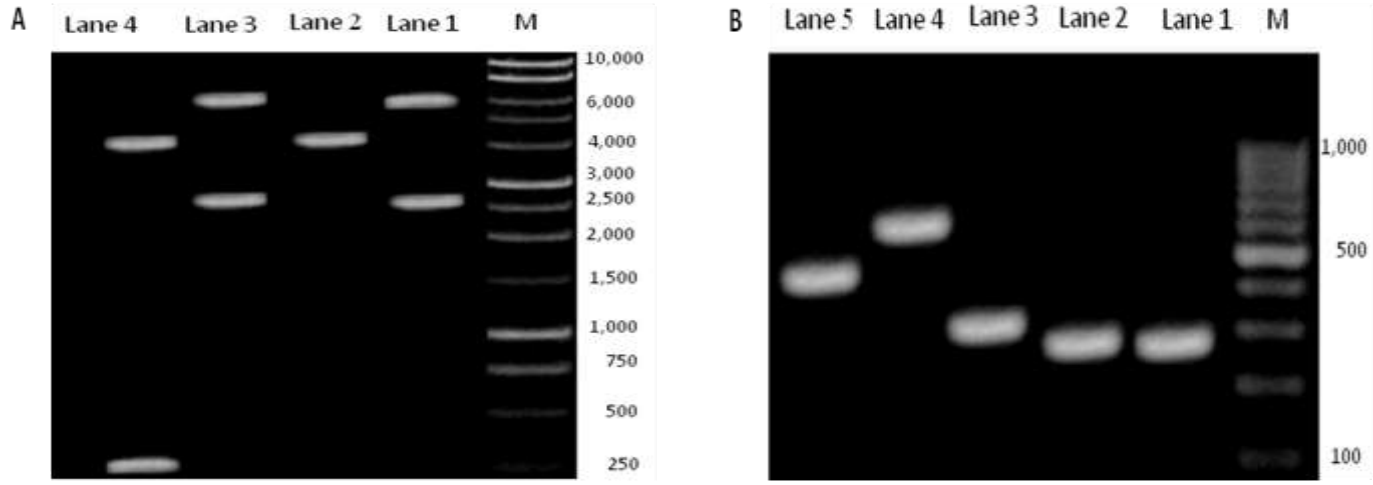

Figure 1. Gel-electrophoresis of the PCR amplification products for cloning, restriction digests, and screening for correct clone. M: 1 kb DNA Marker, Lane 1: plain super-coiled vector at 4.014 kb, Lane 2: linearized digested plasmid product at 3.974 kb by double digestion with *XbaI/NotI* for cloning, Lane 3: super-coiled positive plasmid at 4.244 kb, Lane 4: two DNA bands of *stx2B* at 0.27 kb and linearized digested plasmid at 3.974 kb after restriction analysis (A). M: 100 bp DNA Marker, Lane 1: *stx2B* gene with *XbaI/NotI* restriction sites at 270 bp, Lane 2: digested *stx2B* gene at ~270 bp, Lane 3: Negative clone at 350 bp, Lane 4: positive clone at 594 bp, Lane 5: correct *stx2B* insert orientation at 453 bp (B).

purification (Figure 1A; Lane 3) resulting in two fragments; one of larger size which correspond to linearized vector (3.974 kb) and another of smaller size, which corresponded *stx2B* gene (270 bp) (Figure 1A; Lane 4).

Stx2B protein expression and purification

The construct containing the target gene (*stx2B*) was used to transform JM109 (DE3) cell. The cell has been confirmed to be transformed in the gene (*stx2B*) in the correct orientation insertion. The transformed cells were grown to test the ability of the host cell containing construct to produce recombinant protein.

As evidenced by on GelComparII6.5 software after normalization; the expression of His_6 Halo tagged recombinant Stx2B protein increased gradually by the gradual increase in IPTG concentration (0.1, 0.2, 0.5 and 1 mM), respectively (Figure 2). Moreover, 37°C induction temperatures showed higher His_6 Halo tagged recombinant Stx2B protein expression (Figure 2B) than at 30°C induction temperature (Figure 2A). Overnight induction showed higher expression of the His_6 Halo tagged recombinant Stx2B protein when compared with the observed expression when induction was conducted for 4 h (Figure 2A and B).

Batch purification Stx2B protein from *E. coli* JM109 (DE3) under native condition

Purification of Stx2B protein using IMAC

His_6 Halo tagged recombinant Stx2B protein was obtained in a soluble form in a relatively high purity level with a band corresponding ~47.5 kDa, Lanes 5 to 9, when phosphate buffer was replaced by MOPS buffer through Profinity IMAC Ni-charged resin (Figure 3).

Further purification of His_6HaloTagged Stx2B proteins using halo-link resin

The resulted ~47 kDa His_6Halo Tagged recombinant Stx2B protein from previous purification was subjected to undergo further purification by HaloLink resin with HaloTEV protease treatment. The resulted protein band was observed at ~11.4 KDa, Lane 10 corresponded to highly pure Stx2B protein (Figure 3). The final concentration of resulted protein was 450 $\mu g.ml^{-1}$ using Bradford assay.

DISCUSSION

Several vaccine strategies have been used with variable success in a number of animal models. The strategies have involved the use of recombinant virulence proteins such as Stx, intimin and *E. coli* secreted protein A (EspA) (Gu et al., 2009) or peptides (Wan et al., 2011) or fusion proteins of A and B subunits of Stx2 and Stx1 such as Stx2Am-Stx1B (Cai et al., 2011) or avirulent host cells of EHEC O157:H7 (Cai et al., 2010). The application of live attenuated bacteria such as *Salmonella* as a carrier for vaccine proteins against mucosal pathogens including EHEC has obvious advantages (Hideyuki et al., 2013).

The choice of Stx2B in the present study as compelling candidate for vaccine development in present study was

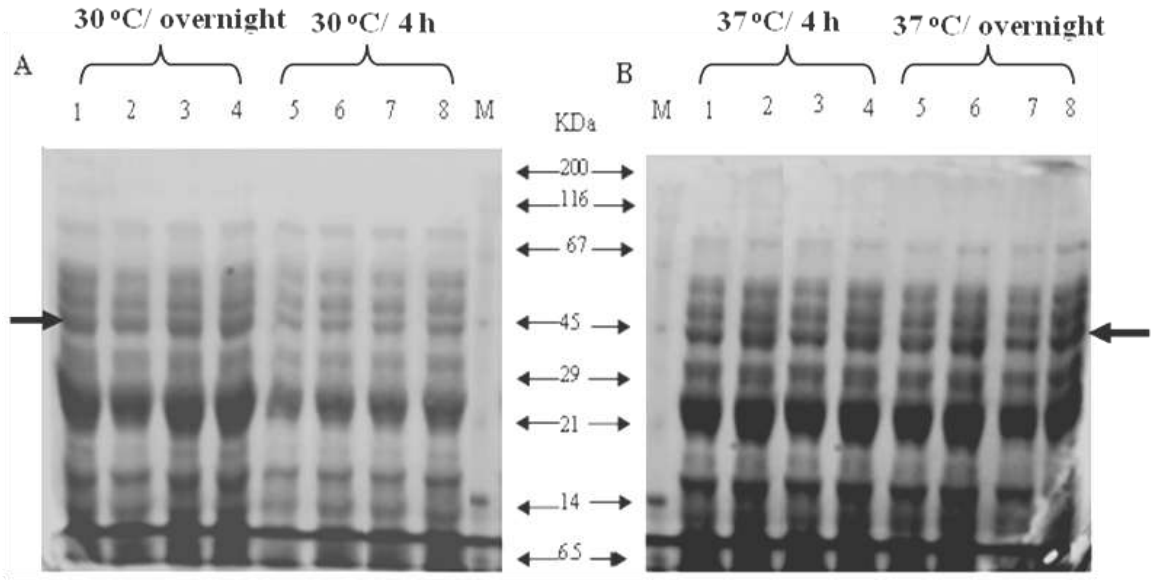

Figure 2. SDS-PAGE analysis of optimization His_6Halo tagged recombinant Stx2B protein expression in *Escherichia coli* JM 109(DE3) cells transformed with pH6HTN His6HaloTag® T7. M: protein molecular weight marker (6.5-200 kDa), Lane 1-4: culture growth under 0.1, 0.2, 0.5, 1 mM of IPTG in 30°C at overnight, Lane 5-8: culture growth under 0.1, 0.2, 0.5, 1 mM of IPTG in 30°C at 4 h) (A). M: protein molecular weight marker (6.5-200 kDa), Lane 1-4: culture growth under (0.1, 0.2, 0.5 and 1 mM of IPTG in 37°C at 4 h, Lane 5-8: culture growth under (0.1, 0.2, 0.5 and 1mM of IPTG in 37°C overnight) (B). Arrows indicated predicted protein size (~47 kDa) in supernatant fractions.

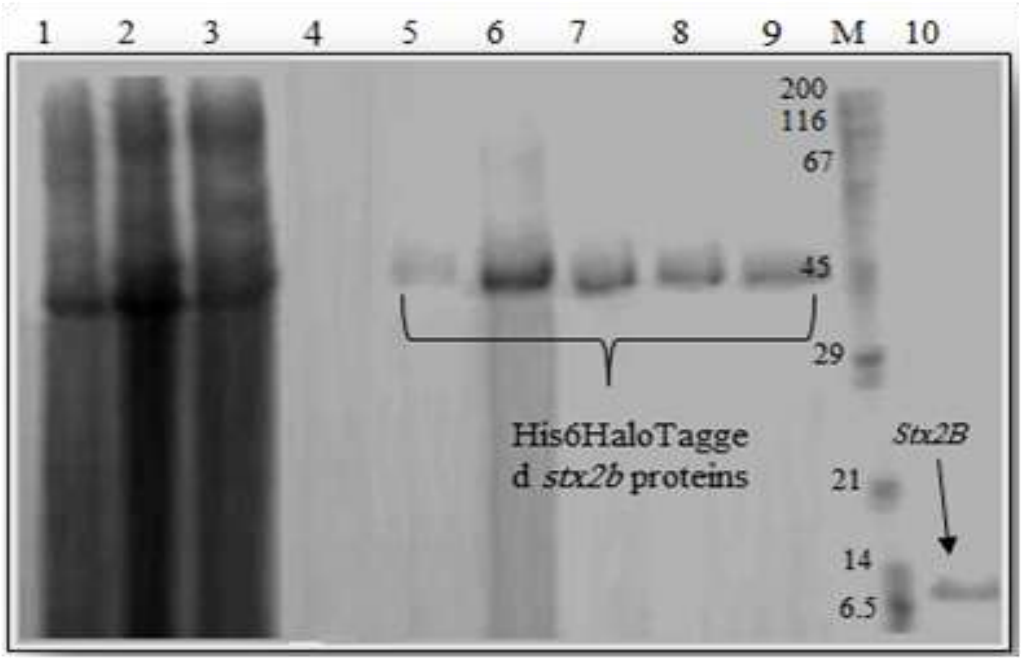

Figure 3. An image of a Coomassie blue-stained SDS-PAGE gel of cell lysates of *Escherichia coli* JM109(DE3) strain carrying the recombinant Stx2B plasmid that were either not induced with IPTG (-) in Lane 1 or induced with 1 mM IPTG for overnight (+) in Lane 2. Lane 3 contained a sample of the column flow through FT, Lane 4 contained a sample of the column wash (W), while Lanes 5-9 contain samples of the fractions eluted from the Profinity IMAC Ni-charged resin which indicates the position of the main component eluted from the column with a band size of approximately 47.5 kDa of 6xHis-Halo tagged Stx2B protein. (M) Contained protein molecular weight marker (Serva, USA) and the sizes of the respective bands were indicated. Lane 10 contained pure Stx2B ~11.4 kDa elution after removal of HaloTEV protease by Profinity IMAC Ni-charged resin. The Mops Buffer was used in all of steps of purification.

consistent with what have been reported in recent studies such as Fujii et al. (2012) and Mejias et al. (1996). However, some other studies showed contrasts, such as Liu et al. (2009) and Tu et al. (2009), where they used truncated Stx2A1 and the holotoxin Stx2 in their candidate vaccine, respectively.

In this study, different conditions for the induction of Shiga toxin expression were examined including temperature, IPTG concentration and the induction period in order to obtain the maximum level of protein production. Thus, Stx2B expression showed higher level of expression when Stx2B was induced at 37°C compared with 30°C. Similar results were obtained by Shan et al. (2010) and Madanchi et al. (2011) who reported that StxB-pQE40-DHFR and CtxB-linker-StxB-pET-28a expression systems showed a higher expression rate at 37°C. In contrast, Liu et al. (2009) and Tu et al. (2009) have reported that 30 and 16°C was considered optimal for Stx2 holotoxin pET32b and for truncated Stx2A1 pET-22b expression systems, respectively.

In the present study, the expression of Stx2B protein was gradually increased when the concentration of IPTG was gradually increased. The expression was optimal at 1 mM IPTG concentration. In contrast, Shan et al. (2010) study has employed 0.3 mM final IPTG concentration for mature StxB induction.

The overnight induction of Stx2B protein at 30°C expression, have resulted in higher yield compared to induction for 4 h also the overnight induction period at 37°C expression have little increase in yield compared to 4 h induction. The induction for 4 h at 37°C appeared more economically preferred compared to overnight induction, as it has more productivity as well as saved the energy that was consumed for shaking. These results were consistent with that of Shan et al. (2010), as they used 37°C for 3 h for induction of mature Stx protein. However, Liu et al. (2009) reported that 30°C for 14 h time of induction of truncated Stx2A1 was the optimal. Hence, the optimum condition to induce the expression of Stx2B in pH6HTN His6HaloTag vector is 4 h incubation period with 1 mM IPTG at 37°C.

The two tag system is one example of tandem affinity purification (TAP) methods which offers an effective and highly specific means to purify target protein, protein capture, quantification, and reduces contaminants significantly (Esposito and Chatterjee, 2006; Puig et al., 2011). To the best of our knowledge, this is the first report of the expression of a Halo-His6 fusion of the Stx2B protein. Despite, there were reports of purification of Stx2B as a fusion protein with glutathione S-transferase (GST) (Mukhopadhyay et al., 2013) or hexa-histidine (Madanchi et al., 2011). Block et al. (2009) has reported that protein purified using His6Tag have significantly lower purity, which might be attributed to that fact that endogenous proteins have high affinity to metal ions, which inevitably bind to the resin and co- purify with the fusion protein.

Moreover, Ohana et al. (2009) have compared the Halo tag backbone protein for expression of 23 human proteins in *E. coli* relative to GST and His6Tag revealed that 74% of the proteins were produced in soluble and pure form when fused to HaloTag compared to 39 and 22%, respectively, for the other tags.

One of the obstacles of studying protein-protein interaction is the contamination of the target protein especially with no any prior knowledge. In the present study, the His6HaloTag protein purification was affinity purified using IMAC by use of phosphate buffer. The use of phosphate buffer resulted in unstable pure protein and/or contaminated protein. In this work therefore, the pellets were incubated on ice with APMSF protease inhibitor before sonication to limit proteolytic clipping of the protein of interest. Unfortunately such treatment did not result on successful protein purification and separation. The phosphate buffer produced unstable pure protein and/or contaminated protein or non-purified protein, as all protein appeared in the flow through during purification.

In this work, an experimental purification technique was designed using MOPS buffer instead of phosphate buffer. Such procedures well separated Shiga toxin and higher protein yield was obtained. The superiority of MOPS buffer in purification and separation of Shiga toxin protein, could be explained by the fact that MOPS is a weaker metal ion ''stripping'' buffer than phosphate when used in the imidazole gradient elution (Hutchens et al., 2009). In contrast Hideyuki et al. (2013) used phosphate buffer in TALON resin for purification Stx2 holotoxin. The discrepancy between the results might be attributed to the use of different experimental design than that used in this study.

To improve the purity and yield of the target protein, further purification step by Halo tag technology coupled with proteolytic tag removal (Ohana et al., 2009) was performed. The final concentration of free tagged Stx2B reached to 450 µg/ml by using Bradford assay. This result was approximately two times higher compared to Halo tag-based purification of PKCɣ Kinase free tag protein (Ohana et al., 2011) which produced 244 µg/ml. In the present study, the final concentration of free tagged Stx2B protein suggested the large scale production of Shiga toxin by the method used in this work could by more economic and industry more feasible.

Conclusion

To the best of our knowledge, this study represents the first example of cloning, expression and purification of a Stx2B protein using HaloTag technology in highly pure form. Cloning of the Stx2B was successful in a new technology vector ''His_6 Halo dual tags'' and led to expression of soluble protein. Interestingly, due to problems that arose in all the steps of purification stage

using phosphate buffer for production contaminated unstable Stx2B protein resulted. This has been overcomed and improved by using the MOPS buffer rather than phosphate buffer in all steps of purification stage.

According to the results, Stx2B protein yields obtained in the small scale experiments described in the present study were encouraging. Determination of the immunogenicity or the sensitivity, stability, specificity, accuracy and linearity of the purified Stx2B is still required to prove the usefulness of the application of this product in both developing and developed countries against Shiga toxin type 2B enterohemorrhagic *E. coli* in future prospective.

Conflict of interests

The authors have not declared any conflict of interest.

ACKNOWLEDGEMENT

The authors gratefully thank ’Abou El-Reesh’’ Children’s Hospital, Cairo University, Egypt stuffs’ laboratory for their assistance to collect clinical specimens for our study.

REFERENCES

Acheson DW, Levine MM, Kaper JB, Keusch GT (1996). Protective immunity to Shiga-like Toxin I following oral immunization with Shiga-like Toxin I B subunit–producing *Vibrio cholerae* CVD 103-HgR. Infect. Immun. 64:355-657.

Block H, Maertens B, Spriestersbach A, Brinker N, Kubicek J, Fabis R, Labahn J, Schafer F (2009). Immobilized-metal affinity chromatography (IMAC). A review. Methods Enzymol. 463:439-473.

Boyd B, Richardson S, Gariepy J (1991). Serological responses to the B subunit of Shiga-like Toxin 1 and its peptide fragments indicate that the B subunit is a vaccine candidate to counter action of the Toxin. Infect. Immun. 59:750-757.

Bradford MM (1976). A rapid and sensitive method for the quantitation of microgram quantities of protein utilizing the principle of protein-dye binding. Anal Biochem. 72:248-254.

Cai K, Gao X, Li T, Hou X, Wang Q, Liu H, Xiao L, Tu W, Liu Y, Shi J, Wang H (2010). Intragastric immunization of mice with enterohemorrhagic *Escherichia coli* O157:H7 bacterial ghosts reduces mortality and shedding and induces a Th2-type dominated mixed immune response. Can. J. Microbiol. 56:389-398.

Cai K, Gao X, Li T, Wang Q, Hou X, Tu W, Xiao L, Tian M, Liu Y, Wang H (2011). Enhanced immunogenicity of a novel Stx2Am-Stx1B fusion protein in amice model of enterohemorrhagic *E. coli* O157:H7 infection. Vaccine 29:946-952.

Donohue-Rolfe A, Acheson DW, Kane AV, Keusch GT (1989). Purification of Shiga Toxin and Shiga-like Toxins I and II by receptor analogue affinity chromatography with immobilized P1 glycoprotein and production of cross-reactive monoclonal antibodies. Infect. Immun. 57:3888-3893.

Dubendorff JW, Studier FW (1991). Controlling basal expression in an inducible T7 expression system by blocking the target T7 promoter with lac repressor. J. Mol. Biol. 219:45-59.

Esposito D, Chatterjee DK (2006). Enhancement of soluble protein expression through the use of fusion tags. Curr. Opin. Biotechnol. 17:353-358.

Fujii J, Naito Mo, Yutsudo T, Matsumoto S, Heatherly D, Yamada T, Kobayashi H, Yoshida S, Obrig T (2012). Protection by a Recombinant Mycobacterium bovis Bacillus Calmette-Guerin Vaccine Expressing Shiga Toxin2B Subunit against Shiga Toxin-Producing *E. coli* in Mice. Clin Vaccine Immunol. 19(12):1932-1937.

Gu J, Ning Y, Wang H, Xiao D, Tang B, Luo P, Cheng Y, Jiang M, Li N, Zou Q, Mao X (2011). Vaccination of attenuated EIS-producing *Salmonella* induces protective immunity against enterohemorrhagic *E. coli* in mice. Vaccine 29:7395-7403.

Gu J, Liu Y, Yu S, Wang H, Wang Q, Yi Y, Zhu F, Yu XJ, Zou Q, Mao X (2009). Enterohemorrhagic *E. coli* trivalent recombinant vaccine containing EspA, intimin and Stx2 induces strong humoral immune response and confers protection in mice. Microbes Infect. 11:835-841.

Hanahan D (1983). Studies on transformation of *E. coli* with plasmids. J. Mol. 166:557-580.

Hashimoto H, Mizukoshi K, Nishi M , Kawakita T, Hasui S, Kato Y, Ueno Y (1999). Epidemic of Gastrointestinal Tract Infection Including Hemorrhagic Colitis Attributable to Shiga Toxin 1-producing Escherichia coli O118: H2 at a Junior High School in Japan. Pediatrics 103(1):e2-e2.

Hideyuki A, Keiko S, Takesshi S , Kentaro T, Toshiyasu S, Takao T (2013). Large scale production of Shiga Toxin 2 in *E. coli* for toxoid vaccine antigen production. J. Microb. Immunol. 57:38-45.

Hopwood DA (2003). The Streptomyces genome-be prepared Nat. Biotechnol. 21:505-506.

Kaper JB, Nataro JP, Mobley HL (2004) .Pathogenic *E. coli*. Nat. Rev. Microbiol. 2:123-140.

Hutchens TW, Yip TT (1991). Metal ligand-induced alterations in the surfaces of lactoferrin and transferring probed by interaction with immobilized Cu (II) ions. J. Chromatogr. 536:1-15.

Laemmli UK (1970). Cleavage of structural proteins during the assembly of the head of bacteriophage T4. Nature 227:680-685.

Liu L, Zeng H, Luo P, Wu J, Chen H, Shi Y, Zhang W, Mao X, Xiao B, Zou Q (2009) . Cloning a Truncated Fragment (stx2a1) of the Shiga-Like Toxin 2A1 Subunit of EHEC O157:H7: Candidate Immunogen for a Subunit Vaccine. Mol. Biotechnol. 43(1):8-14.

Madanchi H, Honari H, Sadraeian M, Hesaraki M (2011). Fusion of CtxB with StxB, Cloning and Expression of in Esherichia coli: A challenge for Improvement of Immune Response Against StxB. Iran. J. Pharm. Sci. 7(3):185-190.

Marcato P, George M, Randy J, Kathleen V, Patrick N, Glen D (2001). Immunoprophylactic Potential of Cloned Shiga Toxin 2 B Subunit. J. Infect. Dis. 183:435-43.

Mukhopadhyay S, Redler B, Linstedt AD (2013). Adam Shiga Toxin–binding site for host cell receptor GPP130 reveals unexpected divergence in Toxin-trafficking mechanisms. Mol. Biol. Cell 24(15):2311-2318.

Nataro JP, Kaper JB (1998). Diarrheagenic *E. coli* . Clin. Microbiol. Rev. 11:142-201.

Nguyen Y, Sperandio V (2012). Enterohemorrhagic *E. coli* (EHEC) pathogenesis. Front. Cell Infect. Microbiol. 12:2-90.

Ohana RF, Hurst R, Vidugiriene J, Slater MR, Urh M, Wood KV (2011). HaloTag-based purification of functional human kinases from mammalian cells. Protein Express Purif. 76:154-164.

Ohana RF, Encell LP, Zhao K, Simpson D, Slater MR, Urh M, Wood KV (2009). HaloTag7: a genetically engineered tag that enhances bacterial expression of soluble proteins and improves protein purification. Protein Express Purif. 68:110-120.

Puig O, Caspary F, Rigaut G, Rutz B, Bouveret E, Bragado-Nilsson E , Wilm M, Séraphin B (2011). The Tandem Affinity Purification (TAP) Method: A General Procedure of Protein Complex Purification. Methods 24(3):218-229.

Sambrook J, Russell DW (2001). Molecular cloning: a laboratory manual, 3rd Eds. New York: Cold Spring Harbor Laboratory Press, Cold Spring Harbor.

Scotland SM, Smith HR, Rowe B (1987). Two distinct Toxins active on Vero cells from *E. coli* O157. Lancet 2:885-886.

Shan G, Lin K, Jinglin W (2010). Expression of overlapping PCR-generated Shiga Toxin B Gene Fragment in *E. coli* and Its Ascitic Polyclonal Antibody. J Life Sci .4(1):1934-7391.

Studier FW, Rosenberg AH, Dunn JJ, Dubendorff JW (1990).Use of T7 RNA polymerase to direct expression of cloned genes. Methods Enzymol. 185:60-89.

Tu W, Cai K, Gao X, Xiao L, Chen R, Shi J (2009). Improved production of holoToxin Stx2 with biological activities by using a single-promoter vector and an auto-induction expression system. Protein Express Purif. 67:169-174.

Wan CS, Zhou Y, Yu Y, Peng LJ, Zhao W, Zheng XL (2011). B-cell epitope KT-12 of enterohemorrhagic *E. coli* O157:H7: a novel peptide vaccine candidate. Microbiol. Immunol. 55:247-253.

academicJournals

Vol. 15(21), pp. 948-959, 25 May, 2016
DOI: 10.5897/AJB2014.13990
Article Number: E9472F458602
ISSN 1684-5315

http://www.academicjournals.org/AJB

African Journal of Biotechnology

Full Length Research Paper

Genetic characterization by amplified fragment length polymorphism (AFLP) markers and morphochemical traits of *Carica papaya* L. genotypes

Mariela Vázquez Calderón[1], Javier O. Mijangos-Cortés[1], Manuel J. Zavala L.[2], L. Felipe Sánchez Teyer[1], Adriana Quiroz M.[1], Matilde Margarita Ortiz G.[1], Fernando Amilcar Contreras M.[1], Francisco Espadas G.[1], Gabriela Fuentes Ortiz[1] and Jorge M. Santamaría[1]*

[1]Unidad de Biotecnología. Centro de Investigación Científica de Yucatán A.C. Calle 43 No. 130, Chuburná de Hidalgo, CP 97200, Mérida, Yucatán, México.
[2]Instituto Nacional de Investigaciones Forestales, Agrícolas y Pecuarias. Mocochá, Yucatán, México.

Received 13 June, 2014; Accepted 20 April, 2016.

***Carica papaya* L. is a native fruit from Central America and Mexico and it is an economically important fruit. As a pre-breeding genetic study, the variability of both parents (L7 and M22) and the F1 individuals derived from their crosses (L7 × M22), was evaluated in terms of 32 morphochemical traits, and contrasted with their genetic diversity indicated by amplified fragment length polymorphism (AFLP) markers. According to morphochemical traits, L7 and M22 were grouped in two different clades. The first group included L7 and 13 genotypes from the F1, while a second group included the parent M22 and 15 other genotypes from the F1 progeny. The analysis based on morphochemical traits showed an average correlation of 0.652 among genotypes. For AFLP analysis the combination of the primers E-ACA/M-CTA had the best polymorphic index (72.73%). When they were grouped based on AFLPs markers, it was confirmed that both parents are genetically distant, and they were again grouped in two different clades. Five genotypes from the F1 population were grouped in the same clade as L7 and shared 55% similarity. Twenty six genotypes were grouped in the same clade as M22, showing 63.3% similarity. Another 12 genotypes (mainly female genotypes) were grouped in a third independent clade. This relative general agreement between the grouping based on a large number of morphochemical traits (including both plant and fruit traits) and that based on its genetic diversity using AFLPs, suggests that morphochemical characterization, together with genetic analysis by AFLPs, can be complementary and useful techniques for the identification and assessment of genetic diversity within *C. papaya* L. genotypes, that should be useful for genetic breeding programs of this important species.**

Key words: Morphological markers, AFLP markers, genetic similarity, *Carica papaya* L.

INTRODUCTION

Carica papaya L. is grown in many tropical and sub-tropical countries and it has great economic value (Jobin-Décor et al., 1997). It originated in southern Mexico and Central America (Brown et al., 2012); and several wild populations have been detected in southern of Yucatan Peninsula in Mexico (Fuentes and Santamaría, 2014). *C. papaya* was about 70% dissimilar to other *Carica* species, which has had average dissimilarities around 50% (Jobin-

Décor et al., 1997). Wild papayas shows high contrast and variation in many morphochemical characters when compared to commercial genotypes, particularly in terms of leaf traits, type of flowers, size and shape of fruit, tolerance to pest and diseases (Ocampo et al., 2006). *C. papaya* L. plants develops fast; it has wide range of variability, and is extended all over America, with high seed production (Liu et al., 2004; Yu et al., 2008). Although, there are reports of collection, conservation and documentation of different accessions of papaya (Colunga and Zizumbo, 2004), studies related to genetic variability of this species in Mexico are very limited. The determination of genetic diversity using phenotypic and molecular tools in papaya, should be useful to understand the ability of these populations to adapt to their natural environment and to develop new cultivars (Moore, 2014). Molecular markers are a useful tool and have been used in the analysis of genetic diversity to facilitate genetic improvement of many crops, including *C. papaya* L. (Eustice et al., 2008). Different molecular techniques have been applied to the analysis of genetic diversity in papaya, including markers such as isoenzymes, RAPDs, AFLPs, ISSRs and SSRs (Kim et al., 2002; Esquivel et al., 2009; Oliveira et al., 2011; Madarbokus and Ranghoo-Sanmukhiya, 2012; Sudha et al., 2013; Vegas et al., 2013).

In particular, AFLP markers do not require prior genetic information; the technique process is faster, produces a large number of markers and is highly reproducible (Vos et al., 1995; Jones et al., 1997; Rojas et al., 2007). These markers are widely used in the assessment of genetic diversity, assessing genetic distance, DNA fingerprinting, analysis of germplasm collections, construction of genetic maps or saturation in certain areas of the genome (Mueller and Wolfenbarguer, 1999). In a previous study, a preliminary analysis of phenotypic variability was performed on genotypes of *C papaya,* using only a limited number (seven) of agronomical plant traits (Vázquez et al., 2014). In the present study, a genotype collected from a native population from undisturbed areas from Yucatan (L7) were crossed with a commercial genotype (M22), the genetic variability of both parents and their F1 progeny (L7 × M22), was characterized by AFLPs, and contrasted with their grouping when using 32 different morphochemical traits, that included both plant and fruit traits.

MATERIALS AND METHODS

Plant material

All plant material was grown in the germplasm bank in the Scientific Research Center of Yucatan (CICY), Mérida, Yucatan, Mexico. A wild genotype of *C. papaya* L. (L7) collected in undisturbed areas at southern of Yucatán Peninsula (Cancún, Quintana Roo), México, and the commercial M22 (maradol tpe) were selected as parents. Both genotypes are hermaphrodites but they have contrasting plant height, fruit size and pulp color characters. M22 are shorter plants bearing large red pulp fruits, while L7 are taller plants bearing small yellow pulp fruits. The F1 progeny derived from the crosses (L7 × M22), consisted in 43 individuals, 28 hermaphrodite plants, 14 female plants and one male plant.

Morphochemical characterization

Both parents and the F1 progeny were characterized and compared morphochemically. The morphological characterization was based upon UPOV (2010). 15 morphological characters and 17 physicochemical parameters were evaluated in L7, M22 and L7 × M22 individuals (Table 1). Fruit's pulp weight was measured with a granatary balance. Fruit's diameter and length parameters were measured with a graduated vernier (cm). Plant height and height of first fruit, were measured with a ruler (cm). pH was measured with a pH meter (Oakton, Singapur). Titratable acidity was measured with a Metrohom automatized system (Thermo Fisher Scientific Inc, USA). Total soluble solids or °Brix was measured using a digital refractometer (Gardco, Florida). Lycopene and β-carotene contents from fruit shells and pulps were measured following the protocol by Nagata and Yamashita (1992), using a DU6 spectrophotometer (Beckman Coulter, USA). CIELAB color components from shell and pulp were measured with a colorimeter by reflectance (Minolta, CR-200).

Molecular characterization

A fragment of leaves from the different individuals of *C. papaya* L. were sampled and placed in liquid nitrogen. DNA extraction was performed on freeze-dried leaf tissue using the CTAB method (Doyle and Doyle, 1990) with several modifications. DNA was quantified using a spectrophotometer NanoDrop (Thermo Fisher Scientific Inc. Wilmington USA) and visualized in agarose gel 1%. A dilution was performed at a final concentration of 100 ng DNA ng μL^{-1} for AFLP analysis. AFLP analysis was performed using the method reported by Vos et al. (1995) with some modifications. Digestion was performed from 100 ng μl^{-1} DNA with combination of EcoR1 (4U) and MseI (1U) enzymes. Ligation of complementary adapters was held by 1 unit of T4 ligase. After visualization with homogeneous intensity of digestion-ligation in agarose gel 1.5%, the samples were diluted in 1:5 ratios for uses in the pre-amplification. After that, the complementary primers EcoR1 and MseI with three selective nucleotides were applied. The simple product of PCR amplification was diluted 1:5, 1:10 and 1:50, according to the band intensity displayed. Selective amplification was carried out with the combination of EcoR1 and MseI primers with the presence of three selective bases each. The primer combinations were used as follows: E-AAC/M-CTT, E-AAC/M-CAC, E-AAC/M-CTA, E-ACG/M-CTT, E-ACG/M-CGA, E-ACT/M-CGA, E-ACT/M-CTT, E-ACC/M-CTA, E-AAG/M-CGC, E-ACA/M-CTA; from those, only the combinations E-ACT/M-CGA, E-ACC/M-CTA, E-ACT/M-CTT and E-ACA/M-CTA, offered better molecular information for the samples tested. The reaction mixture for pre-amplification was 20 µL per sample and it was amplified according to the following PCR conditions: 20 cycles of denaturation; 30 s at 94°C, 60 s annealing at 56°C, and 60 s of extension at 72°C. For selective amplification,

*Corresponding author. Email: jorgesm@cicy.mx. Tel :(52) 999 942 83 30. Fax: (52) 999 981 39 00.

Table 1. 32 morphochemical traits evaluated in *Carica papaya* L. (UPOV, 2010).

Plant		**Fruit**	
Plant height (cm)	AP	Fruit weight (g)	PF
Height of first fruit (cm)	APF	Fruit length (cm)	LF
Diameter of stem (cm)	DT	Diameter of fruit (cm)	DF
Length of petiole (cm)	LP	Pulp thickness (cm)	GP
Length of leaf (cm)	LH	Proportion of fruit length:diameter	LDF
Width of leaf (cm)	AH		
Proportion of leaf length:width	LAH		
Number of flowers per node	NFL		
Number of fruits per node	NFN		
Number of fruits per plant	NFP		
Physicochemical			
pH	pH	Color component *a* in shell	a-C
Acidity	AT	Color component *b* in shell	b-C
Total soluble solids	°B	Color component *C* in shell	C-C
Lycopene in shell	Li-C	Color component *h* in shell	h-C
β-carotene in shell	βC-C	Color component *L* in shell	L-C
Lycopene in fruit pulp	Li-P	Color component *a* in fruit pulp	a-P
β-carotene in fruit pulp	βC-P	Color component *b* in fruit pulp	b-P
		Color component *C* in fruit pulp	C-P
		Color component *h* in fruit pulp	h-P
		Color component *L* in fruit pulp	L-P

20µl of reaction mixture per sample was amplified with 13 cycles "touch down" of 94°C for 30 s, 65°C for 30 s with a decrease of 0.7°C per cycle, and 72°C for 2 min; followed by 30 cycles of annealing at 56°C for 30 s. For automated detection of AFLP, a dilution of product selective amplification (amplisel) was performed. 4 µL SLS and 2 µL of PCR product derived from the amplisel were placed in a plate with 45 wells with 25 µL of the mixture of SLS and STD 400 (molecular weight marker) subsequently, one drop of mineral oil was added to avoid the formation of bubbles. The plates were placed in the automated sequencer (Prism 310, Applied Biosystem) to detect AFLP markers by capillary electrophoresis. The detected fragments are shown as spikes, and the size of the detected peaks, were denoted. These markers were recorded as presence or absence for each genotype evaluated.

Statistical analysis

Morphochemical characterization

Data from 32 morphochemical traits were analyzed with the statistical package option NTSYS v2.1p running multivariate analysis (Crisci and Lopez, 1983). The variables were used for the construction of the correlation matrix. Cluster analysis was made on the program NTSYS pc v2.1p, based on Unweighted Pair Group Method with Arithmetic Mean (UPGMA), in order to obtain the dendrogram based on the Ward method and Squared Euclidean distances.

Molecular characterization

The data generated from the detection of polymorphic fragments were analyzed. Specific amplification products were scored as present (1) or absent (0) for each DNA sample. Index of genetic similarity or distance was calculated (1-F); F values were initially calculated using Nei and Li (1979) matching coefficient method; $F = 2 \times N_{AB1}/(N_A + N_B)$, where N_A = the number of bands in accession A, N_B = the number of bands in accession B, N_{AB1} = the number of bands present in both accessions A and B (scored 1), N_{AB0} = the number of bands present upon amplification of some of the germplasm with this set of accessions, but not present in either accession A or B, and N_T = the total number of bands scored in the study. Later, F values were also calculated using the formulae: 1) $F' = N_{AB1}/(N_T - N_{AB0})$ (Jaccard's coefficient), 2) $F'' = (N_{AB1} + N_{AB0})/ N_T$ (similarity coefficient), 3) $F''' = N_{AB0}/(N_T - N_{AB1})$. An agglomerative method of clustering accessions was employed to analyze the data utilizing the UPGMA algorithm (SAS, 1985), that employs a contrasting method of classification based on a divisive clustering technique (Francisco-Ortega et al., 2000). Dendrogram was generated by UPGMA method using the similarity coefficient Dice from patterns generated by AFLPs.

RESULTS AND DISCUSSION

The F1 progeny from the cross (L7 × M22) and its parents, were evaluated both morphochemically and genetically (using AFLPs), to discriminate and identify genotypes for genetic improvement.

Morphochemical characterization

The 32 phenotypic (morphochemical traits) showed high

diversity among the evaluated papaya genotypes; these data can be used in the selection of different parents for improving this species. The Component 1, explained 33% of accumulated variance, the Component 2, explained 49% of accumulated variance and Component 3 explained 59% of the total variance from 32 morphochemical traits. The treats that show the high positive correlation for principal component (PC1) were b-P and c-P (0.89 and 0.83). For the PC2 they were Li-P and APF (both 0.56) and for the PC3 were LP (0.66), AH and LAH (both 0.61) (Table 2). The morphochemical markers formed two clear groups. A first group included L7 and 13 genotypes from the F1, and a second group included the parent M22 and 15 other genotypes from the F1 progeny (Figure 1). The F1 genotypes grouped with the parent L7, shared 55% similarity on average, being the genotype H66B, the one with the highest genetic similarity (0.688) with the parent L7. On the other hand, the genotypes grouped with the parent M22, shared on average of 63.3% similarity, and H90B genotype showed the highest genetic similarity (0.840) with M22 (Table 3). In relation to the lowest correlation of genetic similarity (0.281), the genotypes H15B, H70B and H90B had the greatest genetic distance from L7. With low genetic similarity correlation (0.130), the genotype H71B had relatively the highest genetic distance with M22.

Phenotypic similarity correlations analysis showed a 51.9% similarity, where H13B and H14B genotypes showed the highest degree of similarity (0.906), indicating that these genotypes share many of their phenotypic characters. The genotypes H66B and H12B showed the least similarity correlation (0.125) (Table 3). This indicates that among the genotypes of papaya evaluated, a contrasting morphological variability exists, which could serve as a source of genetic diversity for searching parents with desirable characteristics and it can be used in a breeding scheme to obtain new papaya varieties or genotypes adapted to the region.

Molecular characterization

The electropherograms from the four selected primer combinations of AFLP markers used to characterized papaya genotypes derived from the intraspecific crosses L7 × M22, showed a range of 22 to 74 fragments in E-ACA/M-CTA and E-ACT/M-CGA, respectively, and a total of 217 fragments with all combinations tested, with an average value of 54.48 DNA visualized fragments (Table 4 and Figure 3). The fragment sizes were in the range of 89 to 234 bp for E-ACA/M-CTA, 61 to 290 bp for E-ACT/M-CGA, 62 to 277 bp for E-ACC/M-CTA and 61 to 229 bp for E-ACT/MCTT. Monomorphic fragments showed a range from 6 to 36 fragments for E-ACA/M-CTA and E-ACT/M-CGA/E-ACT/M-CTT, respectively, with a total of 104 fragments, while polymorphic fragments showed a range from 16 to 42 fragments for E-ACA/M-CTA and E-ACC/M-CTA, respectively, with a total of 113 polymorphic fragments which represented a 54.48% polymorphism obtained with all combinations of evaluated individuals. Combinations with better percentage of polymorphic bands were E-ACA/M-CTA, E-ACC/M-CTA, E-ACT/M-CGA, with a value of 72.73, 61.74 and 51.35% of polymorphic fragments. The combination E-ACT/M-CTT, although generated one of the highest values of total fragments, had only 32.08% of polymorphic fragments (Table 4). This could be used in studies of genetic variability in other morphotypes of papaya, in order to support studies of morphological and genetic or accelerate breeding programs for the specie (Meerow, 2005; Esquivel et al., 2009).

Genetic variability among the 45 genotypes of *C. papaya* L. evaluated, was estimated by pairwise comparison of genetic similarity. The pairwise of genetic similarity showed a range of 0.35 to 0.84 (Figure 2), with an average genetic similarity of 0.639 within the population evaluated. The 81.6% of the pairwise comparison data showed a genetic similarity greater than 0.59. Cophenetic correlation values obtained from UPGMA cluster analysis and the genetic similarity matrix showed a correlation of 0.652 (Table 5). The molecular genetic similarity among all evaluated genotypes had correlation values that ranged from 0.35 to 0.84 suggesting that they are individuals with a narrow genetic similarity (Table 5). The generated dendrogram showed three groups at a distance of 0.715. The first group, was formed by six genotypes, including the parent L7. The second group was formed by 27 genotypes (20 hermaphrodite genotypes, six female and the parent M22) and the third group was formed by 12 genotypes, including 5 female genotypes and the male genotype (Figure 3). The analysis confirmed that the parents L7 and M22, that showed important phenotypical differences, also belong to a different genetic group. However, some genotypes from the F1 are genetically distant from both parents (L7 and M22). The *C. papaya* L. selection based on the progeny from complementary genetically distant parents maintains the genetic diversity, and it would allow the identification of superior progenies (“elite”) for commercial interest traits, such as pulp color and fruit size, towards pre-genetic improvement of the species. Oliveira et al. (2011), reported a value of average genetic distance of 0.735 in papaya genotypes of improved germplasm; similarly, Vegas et al. (2013) reported and classified as correlation of mean similarity of 0.899 in 28 accessions of *C. papaya* L. in Venezuelan germplasm; similar data were reported by Van-Droogenbroeck et al. (2002), who obtained a correlation of 0.873 of similarity in accessions of papaya from Ecuador. In turn, Janthasri et al. (2007) reported a correlation of 0.920 and similarity mention that these materials of papaya developed in Thailand have little genetic variability, perhaps because they were generated from the same materials of a germplasm bank. These reports support that the use of geographic provenance of plant material is important for

Table 2. Total variance in *Carica papaya* L. explained by principal component analyses. Correlations value for the different traits in the first three principal components (PC1, PC2, PC3).

Principal component	Eigen value	Explained proportion of variance (%)	
		Absolute	Accumulated
1	10.69	33	33
2	5.02	16	49
3	3.01	9	59
4	2.47	8	66
5	2.28	7	73
6	1.92	6	79
7	1.53	5	84
8	1.04	3	87
9	0.96	3	90
10	0.79	2	93
11	0.45	1	94
12	0.40	1	96
13	0.33	1	97
14	0.30	1	97
15	0.18	1	98
16	0.14	0	98
17	0.13	0	99
18	0.09	0	99
19	0.08	0	99
20	0.05	0	100

Trait	Principal components		
	PC1	PC2	PC3
AP	-0.37	0.45	0.27
APF	-0.54	0.56	0.28
DT	-0.15	-0.08	-0.20
LP	0.6	-0.17	0.66
LH	-0.21	-0.35	-0.65
AH	-0.44	-0.2	0.61
LAH	-0.66	0.3	0.61
NFL	0.40	-0.35	0.19
NFN	-0.66	0.11	-0.02
NFP	0.61	0.01	-0.25
PF	0.83	0.14	0.25
LF	-0.85	-0.13	0.12
DF	0.83	-0.04	0.23
GP	0.37	0.04	0.04
LDF	0.78	-0.05	0.29
pH	0.70	0.30	0.21
AT	-0.67	0.05	-0.02
°B	0.71	0.39	0.17
Li-C	0.92	0.12	0.08
_C-C	0.58	0.37	0.18
Li-P	-0.83	0.56	0.47
_C-P	-0.54	0.30	0.38
L-C	-0.15	-0.08	-0.20
a-C	0.79	-0.17	0.36
b-C	-0.21	-0.35	-0.15
C-C	-0.44	-0.20	0.14
h-C	-0.67	0.43	0.11

Table 2 contd.

L-P	0.40	-0.35	0.19
a-P	-0.89	0.11	-0.02
b-P	0.89	0.01	-0.25
c-P	0.83	0.14	0.25
h-P	-0.79	-0.13	0.12

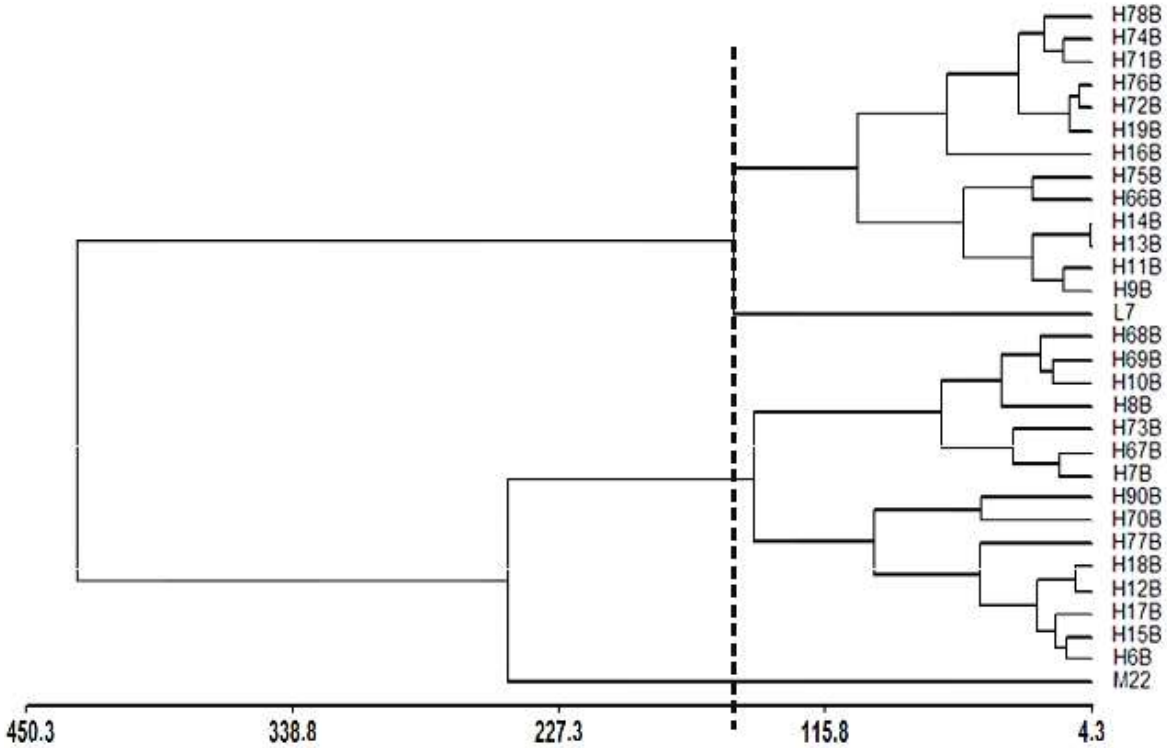

Figure 1. Dendogram of parents L7, M22 and their F1 progeny obtained from 32 morphochemical characters based on the Ward method and squared Euclidean distances.

the improvement of *C. papaya* L. Kim et al. (2002), obtained a similarity of 0.921 within Hawaiian accessions of papaya and 0.914 within Australian papayas; these exhibit little genetic diversity because they are materials that come from the same genetic pool. Brown et al. (2012), reported that the levels of genetic diversity in wild populations are higher than within cultivated (Commercial) papayas, which show heterozygote deficiency coupled with a high correlation of similarity between them. Regarding the usefulness of using AFLP, the combinations of primers of AFLP markers with better percentage of polymorphic bands were E-ACA/M-CTA, E-ACC/M-CTA and E-ACT/M-CGA, which may be employed in: 1) studies of genetic diversity in other morphotypes of papaya and 2) in studies searching for AFLP markers associated with other traits of economic interest which may in turn, accelerate breeding for the genetic improvement of this important species.

Relative agreement between the genetic and morphochemical characterization

Our data indicates that in general, the grouping of most genotypes coincides whether morphochemical or molecular markers are used. In the sense that both parents are clearly grouped in two different clades and some of the F1 genotypes from their progeny are grouped with either parent. Despite the fact that the grouping based on morphochemical traits formed two clear groups, while the grouping using AFLPs formed 3 groups, the lack of a third group when using morphochemical markers, was expected since no morphological data from the female or male individuals is available, because in the ongoing breeding

Table 3. Phenotypic similarity based on 32 morphological characters among both parents (L7 and M22) and the F1 progeny derived from intraspecific crosses (L7 × M22).

	L7	M22	H6B	H7B	H8B	H9B	H10B	H11B	H12B	H13B	H14B	H15B	H16B	H17B	H18B	H19B
L7	1.000															
M22	0.380	1.000														
H6B	0.469	0.660	1.000													
H7B	0.281	0.590	0.563	1.000												
H8B	0.563	0.480	0.594	0.531	1.000											
H9B	0.500	0.380	0.594	0.656	0.688	1.000										
H10B	0.563	0.480	0.656	0.656	0.688	0.625	1.000									
H11B	0.481	0.470	0.688	0.625	0.469	0.656	0.594	1.000								
H12B	0.375	0.750	0.656	0.594	0.500	0.375	0.438	0.406	1.000							
H13B	0.500	0.190	0.469	0.469	0.688	0.688	0.625	0.719	0.250	1.000						
H14B	0.488	0.160	0.438	0.438	0.719	0.719	0.594	0.625	0.281	0.906	1.000					
H15B	0.281	0.780	0.688	0.625	0.469	0.469	0.469	0.500	0.844	0.281	0.375	1.000				
H16B	0.688	0.310	0.406	0.469	0.563	0.563	0.500	0.406	0.438	0.563	0.656	0.406	1.000			
H17B	0.344	0.780	0.750	0.563	0.406	0.406	0.406	0.563	0.844	0.281	0.250	0.813	0.406	1.000		
H18B	0.406	0.660	0.688	0.500	0.469	0.344	0.531	0.500	0.844	0.281	0.375	0.813	0.531	0.750	1.000	
H19B	0.469	0.280	0.313	0.625	0.531	0.594	0.531	0.438	0.344	0.656	0.625	0.313	0.531	0.313	0.313	1.000
H66B	0.688	0.410	0.344	0.344	0.500	0.563	0.500	0.531	0.125	0.750	0.719	0.219	0.688	0.219	0.281	0.656
H67B	0.375	0.690	0.656	0.656	0.625	0.375	0.625	0.469	0.750	0.313	0.406	0.844	0.500	0.719	0.781	0.406
H68B	0.344	0.540	0.313	0.750	0.531	0.531	0.656	0.500	0.469	0.594	0.563	0.375	0.469	0.438	0.375	0.750
H69B	0.486	0.520	0.500	0.500	0.719	0.469	0.781	0.438	0.531	0.594	0.563	0.438	0.594	0.500	0.563	0.500
H70B	0.281	0.660	0.750	0.625	0.594	0.469	0.656	0.625	0.719	0.406	0.438	0.750	0.344	0.625	0.750	0.375
H71B	0.625	0.130	0.406	0.469	0.625	0.688	0.563	0.531	0.313	0.750	0.719	0.156	0.625	0.344	0.281	0.781
H72B	0.500	0.250	0.281	0.594	0.438	0.625	0.500	0.531	0.313	0.750	0.656	0.344	0.563	0.406	0.281	0.781
H73B	0.473	0.560	0.531	0.719	0.500	0.500	0.688	0.406	0.750	0.375	0.406	0.719	0.500	0.656	0.719	0.469
H74B	0.594	0.160	0.313	0.375	0.469	0.594	0.469	0.563	0.156	0.781	0.750	0.188	0.594	0.188	0.250	0.625
H75B	0.563	0.310	0.469	0.531	0.438	0.625	0.625	0.719	0.188	0.750	0.656	0.281	0.500	0.281	0.281	0.531
H76B	0.500	0.310	0.219	0.594	0.438	0.563	0.438	0.406	0.438	0.625	0.594	0.281	0.625	0.344	0.344	0.781
H77B	0.469	0.530	0.688	0.375	0.406	0.344	0.406	0.500	0.719	0.344	0.375	0.625	0.469	0.688	0.688	0.313
H78B	0.563	0.310	0.219	0.469	0.375	0.500	0.313	0.344	0.313	0.625	0.594	0.281	0.625	0.344	0.219	0.781
H90B	0.281	0.840	0.625	0.688	0.406	0.406	0.531	0.563	0.719	0.281	0.250	0.750	0.344	0.750	0.625	0.313
Máx.	0.688	0.840	0.750	0.750	0.719	0.719	0.781	0.719	0.844	0.906	0.750	0.844	0.688	0.750	0.781	0.781
Mín.	0.281	0.130	0.219	0.344	0.375	0.344	0.313	0.344	0.125	0.281	0.250	0.156	0.344	0.188	0.219	0.313
Prom.	0.466	0.471	0.512	0.555	0.530	0.529	0.541	0.513	0.493	0.545	0.525	0.477	0.524	0.473	0.450	0.576

Table 3. Contd.

	H66B	H67B	H68B	H69B	H70B	H71B	H72B	H73B	H74B	H75B	H76B	H77B	H78B	H90B
L7														
M22														
H6B														
H7B														
H8B														
H9B														
H10B														
H11B														
H12B														
H13B														
H14B														
H15B														
H16B														
H17B														
H18B														
H19B														
H66B	1.000													
H67B	0.250	1.000												
H68B	0.469	0.469	1.000											
H69B	0.469	0.594	0.688	1.000										
H70B	0.219	0.781	0.438	0.563	1.000									
H71B	0.688	0.250	0.719	0.594	0.281	1.000								
H72B	0.688	0.313	0.781	0.531	0.219	0.750	1.000							
H73B	0.313	0.688	0.656	0.656	0.531	0.438	0.563	1.000						
H74B	0.844	0.156	0.563	0.500	0.313	0.719	0.719	0.344	1.000					
H75B	0.813	0.250	0.594	0.469	0.344	0.625	0.688	0.438	0.844	1.000				
H76B	0.625	0.250	0.781	0.531	0.281	0.750	0.813	0.563	0.719	0.625	1.000			
H77B	0.344	0.531	0.375	0.438	0.688	0.469	0.281	0.469	0.438	0.406	0.406	1.000		
H78B	0.750	0.250	0.656	0.406	0.219	0.688	0.813	0.375	0.781	0.625	0.813	0.406	1.000	
H90B	0.156	0.719	0.500	0.500	0.750	0.219	0.344	0.594	0.188	0.344	0.406	0.625	0.281	1.000
Máx.	0.844	0.781	0.781	0.656	0.750	0.750	0.813	0.594	0.844	0.625	0.813	0.625	0.281	**Prom.**
Mín.	0.156	0.156	0.375	0.406	0.219	0.219	0.281	0.344	0.188	0.344	0.406	0.406	0.281	**gral.**
Prom.	0.510	0.438	0.614	0.519	0.403	0.582	0.603	0.464	0.594	0.500	0.542	0.516	0.281	0.512

Table 4. Combinations of primers used in obtaining DNA fingerprinting and distribution of total fragments, monomorphic and polymorphic parental and F1 progeny from *Carica papaya* L. L7 × M22.

Combination of AFLP	Number of total bands	Number of monomorphic bands	Number of polymorphic bands	Polymorphic bands (%)
E-ACA/M-CTA	22	6	16	72.73
E-ACT/M-CGA	74	36	38	51.35
E-ACC/M-CTA	68	26	42	61.74
E-ACT/M-CTT	53	36	17	32.08
Total	217	104	113	54.48

program the male or female individuals were excluded from the field trials, as commercial papaya growers preferred hermaphrodites. It can be then concluded, that the molecular tool based on AFLP was efficient to detect high degree of polymorphism in a *C. papaya* L F1 population derived from the cross (L7 × M22), through the

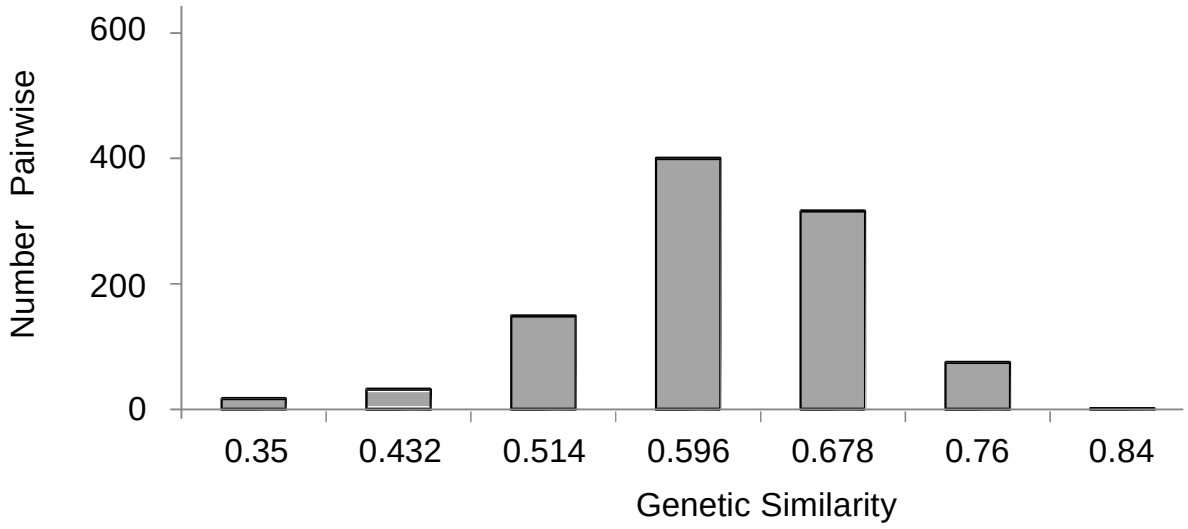

Figure 2. Distribution of data obtained by pairwise comparison of genetic similarity among 45 genotypes of *Carica papaya* L.

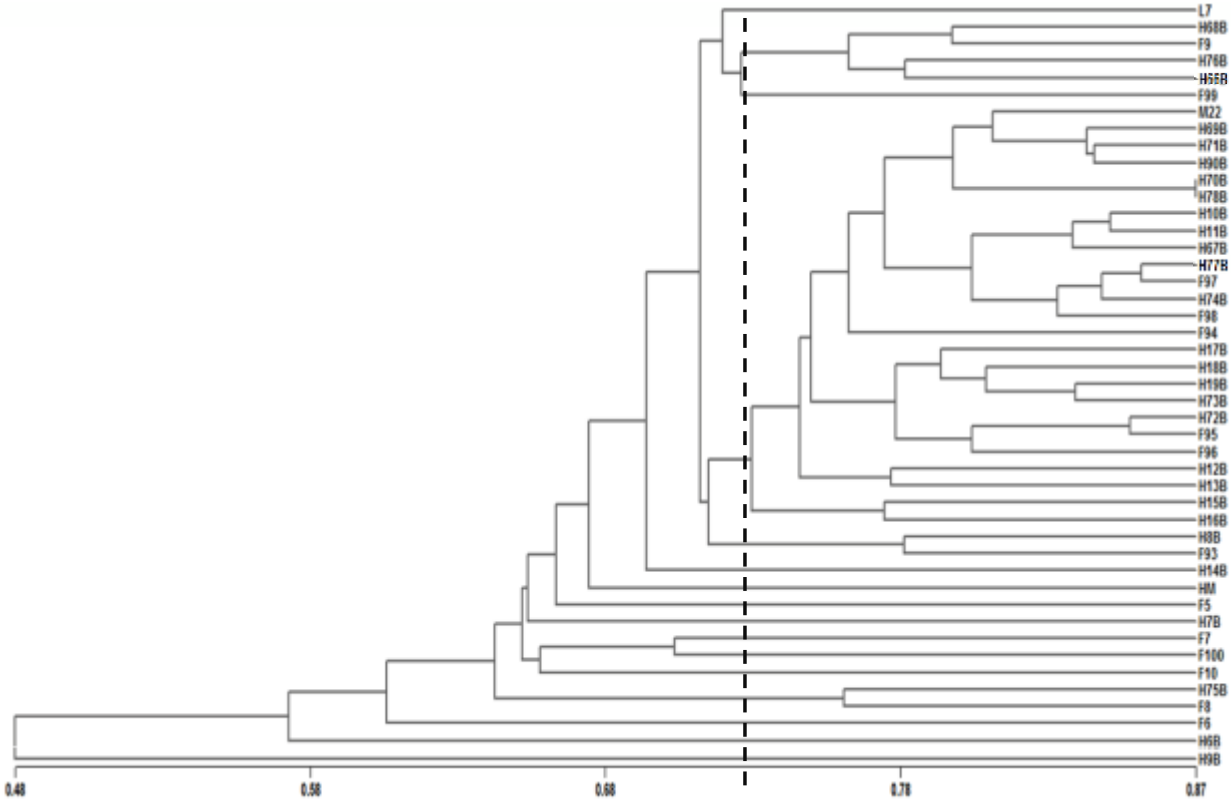

Figure 3. Dendrogram of parents L7, M22 and their F1 progeny, generated by UPGMA method using the similarity coefficient Dice from patterns generated by fragments for four combinations of AFLPs primers.

combinations E-ACA/M-CTA, E-ACC/M-CTA and E-ACT/M-CGA. The average molecular genetic similarity for L7 was 0.669 and for M22 it was 0.704.

The F1 segregated and some of them were grouped with M22, while some others were grouped with L7. A medium to high molecular genetic variation exists, associated with

Table 5. Genetic similarity of parental and F1 progeny from intraspecific crosses of *Carica papaya* L. L7 × M22 based on AFLP markers.

	L7	M22	H6B	H7B	H8B	H9B	H10B	H11B	H12B	H13B	H14B	H15B	H16B	H17B	H18B	H19B	H66B	H67B	H68B	H69B	H70B	H71B
L7	1.000																					
M22	0.620	1.000																				
H6B	0.510	0.540	1.000																			
H7B	0.600	0.620	0.620	1.000																		
H8B	0.630	0.750	0.640	0.730	1.000																	
H9B	0.540	0.510	0.460	0.480	0.580	1.000																
H10B	0.680	0.750	0.580	0.670	0.740	0.470	1.000															
H11B	0.640	0.651	0.600	0.630	0.700	0.420	0.820	1.000														
H12B	0.650	0.641	0.580	0.670	0.680	0.410	0.720	0.770	1.000													
H13B	0.670	0.680	0.590	0.580	0.660	0.460	0.740	0.730	0.770	1.000												
H14B	0.680	0.614	0.580	0.600	0.650	0.470	0.620	0.610	0.620	0.710	1.000											
H15B	0.640	0.720	0.590	0.650	0.680	0.440	0.680	0.690	0.700	0.690	0.740	1.000										
H16B	0.650	0.700	0.550	0.670	0.730	0.440	0.660	0.660	0.710	0.630	0.670	0.760	1.000									
H17B	0.660	0.670	0.550	0.680	0.630	0.360	0.740	0.720	0.760	0.690	0.660	0.750	0.730	1.000								
H18B	0.650	0.670	0.550	0.670	0.660	0.430	0.700	0.660	0.730	0.730	0.700	0.710	0.670	0.750	1.000							
H19B	0.580	0.621	0.590	0.620	0.660	0.410	0.670	0.690	0.740	0.650	0.670	0.720	0.700	0.720	0.780	1.000						
H66B	0.694	0.615	0.560	0.590	0.630	0.400	0.760	0.820	0.690	0.730	0.670	0.660	0.650	0.720	0.720	0.700	1.000					
H67B	0.660	0.670	0.610	0.640	0.720	0.460	0.830	0.800	0.730	0.740	0.660	0.660	0.670	0.720	0.690	0.660	0.760	1.000				
H68B	0.690	0.611	0.610	0.610	0.640	0.420	0.720	0.680	0.630	0.730	0.730	0.680	0.650	0.670	0.670	0.660	0.700	0.730	1.000			
H69B	0.630	0.740	0.540	0.610	0.720	0.410	0.740	0.770	0.660	0.660	0.610	0.700	0.640	0.690	0.620	0.620	0.730	0.710	0.720	1.000		
H70B	0.650	0.760	0.550	0.620	0.690	0.430	0.680	0.660	0.690	0.650	0.640	0.740	0.720	0.680	0.670	0.660	0.620	0.690	0.750	0.710	1.000	
H71B	0.660	0.740	0.560	0.600	0.680	0.420	0.750	0.780	0.700	0.700	0.650	0.750	0.700	0.760	0.680	0.660	0.770	0.740	0.690	0.790	0.710	1.000
H72B	0.640	0.700	0.520	0.620	0.660	0.350	0.740	0.750	0.770	0.740	0.650	0.710	0.690	0.800	0.730	0.750	0.770	0.730	0.670	0.700	0.670	0.770
H73B	0.620	0.660	0.530	0.640	0.660	0.390	0.700	0.710	0.770	0.700	0.660	0.740	0.720	0.780	0.800	0.820	0.740	0.700	0.690	0.650	0.680	0.750
H74B	0.660	0.720	0.540	0.620	0.690	0.380	0.780	0.780	0.700	0.680	0.630	0.680	0.670	0.730	0.700	0.740	0.820	0.750	0.730	0.750	0.660	0.750
H75B	0.670	0.610	0.590	0.600	0.640	0.520	0.640	0.590	0.630	0.640	0.580	0.580	0.570	0.560	0.590	0.610	0.550	0.640	0.620	0.560	0.590	0.570
H76B	0.710	0.616	0.580	0.630	0.670	0.480	0.710	0.640	0.630	0.740	0.690	0.660	0.640	0.660	0.640	0.590	0.680	0.690	0.760	0.730	0.660	0.640
H77B	0.610	0.710	0.580	0.690	0.750	0.550	0.690	0.660	0.660	0.680	0.650	0.670	0.670	0.650	0.650	0.600	0.660	0.680	0.720	0.710	0.680	0.670
H78B	0.650	0.770	0.560	0.650	0.740	0.440	0.750	0.740	0.670	0.630	0.610	0.730	0.750	0.740	0.630	0.600	0.700	0.750	0.720	0.800	0.830	0.780
H90B	0.640	0.750	0.550	0.570	0.640	0.370	0.740	0.750	0.700	0.700	0.650	0.770	0.670	0.790	0.680	0.690	0.750	0.720	0.720	0.780	0.700	0.810
F5	0.650	0.620	0.450	0.560	0.610	0.480	0.590	0.580	0.640	0.640	0.630	0.650	0.630	0.650	0.660	0.650	0.560	0.570	0.600	0.600	0.630	0.610
F6	0.660	0.530	0.450	0.500	0.500	0.390	0.540	0.520	0.620	0.620	0.630	0.530	0.600	0.660	0.650	0.610	0.590	0.560	0.590	0.530	0.480	0.580
F7	0.640	0.617	0.520	0.590	0.650	0.550	0.650	0.620	0.600	0.630	0.630	0.650	0.640	0.630	0.600	0.640	0.670	0.660	0.630	0.610	0.610	0.600
F8	0.630	0.610	0.590	0.590	0.680	0.530	0.630	0.610	0.610	0.680	0.680	0.620	0.550	0.570	0.630	0.650	0.610	0.680	0.660	0.580	0.590	0.570
F9	0.710	0.617	0.580	0.610	0.690	0.460	0.690	0.660	0.620	0.690	0.660	0.640	0.640	0.670	0.640	0.600	0.670	0.740	0.790	0.750	0.710	0.700
F10	0.600	0.618	0.450	0.640	0.680	0.570	0.560	0.560	0.570	0.560	0.600	0.620	0.650	0.570	0.570	0.590	0.580	0.590	0.630	0.630	0.650	0.590
F93	0.689	0.760	0.570	0.670	0.780	0.520	0.680	0.620	0.630	0.690	0.660	0.700	0.700	0.600	0.630	0.590	0.600	0.650	0.680	0.680	0.710	0.690
F94	0.670	0.690	0.540	0.560	0.670	0.390	0.720	0.750	0.680	0.730	0.620	0.670	0.630	0.730	0.640	0.660	0.710	0.710	0.690	0.720	0.670	0.740
F95	0.670	0.700	0.490	0.550	0.660	0.380	0.730	0.700	0.730	0.720	0.660	0.710	0.660	0.770	0.730	0.720	0.740	0.730	0.690	0.710	0.670	0.750
F96	0.660	0.640	0.490	0.570	0.620	0.410	0.650	0.660	0.690	0.680	0.650	0.690	0.690	0.690	0.730	0.750	0.700	0.660	0.650	0.600	0.640	0.670
F97	0.650	0.660	0.530	0.540	0.610	0.360	0.720	0.780	0.680	0.680	0.630	0.700	0.640	0.730	0.640	0.700	0.800	0.740	0.710	0.810	0.680	0.780
F98	0.680	0.720	0.590	0.620	0.700	0.440	0.770	0.750	0.700	0.740	0.660	0.650	0.650	0.720	0.680	0.660	0.790	0.790	0.740	0.710	0.700	0.740
F99	0.690	0.600	0.560	0.590	0.690	0.480	0.680	0.690	0.690	0.700	0.600	0.690	0.640	0.690	0.630	0.690	0.670	0.680	0.720	0.680	0.700	0.680
F100	0.610	0.610	0.540	0.580	0.650	0.570	0.580	0.540	0.570	0.610	0.590	0.590	0.570	0.580	0.550	0.590	0.580	0.630	0.640	0.580	0.620	0.590
HM	0.680	0.660	0.490	0.610	0.670	0.470	0.650	0.620	0.640	0.650	0.640	0.660	0.660	0.630	0.720	0.700	0.650	0.600	0.590	0.590	0.590	0.630
Max.	0.710	0.770	0.640	0.730	0.780	0.570	0.830	0.820	0.770	0.740	0.740	0.770	0.750	0.800	0.800	0.820	0.820	0.790	0.790	0.810	0.830	0.810
Min.	0.510	0.510	0.450	0.480	0.500	0.350	0.540	0.520	0.570	0.560	0.580	0.530	0.550	0.560	0.550	0.590	0.550	0.560	0.590	0.530	0.480	0.570
Prom.	0.647	0.662	0.552	0.613	0.669	0.444	0.695	0.684	0.676	0.681	0.649	0.680	0.658	0.687	0.665	0.661	0.685	0.686	0.685	0.678	0.660	0.681

Table 5. Contd.

	H72B	H73B	H74B	H75B	H76B	H77B	H78B	H90B	F5	F6	F7	F8	F9	F10	F93	F94	F95	F96	F97	F98	F99	F100	HM
L7																							
M22																							
H6B																							
H7B																							
H8B																							
H9B																							
H10B																							
H11B																							
H12B																							
H13B																							
H14B																							
H15B																							
H16B																							
H17B																							
H18B																							
H19B																							
H66B																							
H67B																							
H68B																							
H69B																							
H70B																							
H71B																							
H72B	1.000																						
H73B	0.790	1.000																					
H74B	0.760	0.730	1.000																				
H75B	0.580	0.540	0.600	1.000																			
H76B	0.640	0.600	0.670	0.650	1.000																		
H77B	0.650	0.600	0.680	0.710	0.770	1.000																	
H78B	0.680	0.660	0.770	0.560	0.700	0.740	1.000																
H90B	0.760	0.730	0.790	0.580	0.690	0.630	0.770	1.000															
F5	0.690	0.670	0.620	0.640	0.590	0.680	0.600	0.640	1.000														
F6	0.650	0.650	0.590	0.500	0.610	0.550	0.490	0.590	0.610	1.000													
F7	0.610	0.650	0.700	0.580	0.660	0.670	0.650	0.630	0.610	0.590	1.000												
F8	0.570	0.580	0.640	0.760	0.680	0.730	0.580	0.580	0.620	0.500	0.670	1.000											
F9	0.680	0.630	0.710	0.650	0.760	0.750	0.760	0.710	0.620	0.610	0.660	0.690	1.000										
F10	0.580	0.590	0.620	0.550	0.670	0.760	0.650	0.600	0.620	0.500	0.670	0.640	0.700	1.000									
F93	0.620	0.620	0.680	0.650	0.690	0.760	0.750	0.670	0.670	0.560	0.660	0.650	0.740	0.700	1.000								
F94	0.790	0.710	0.740	0.610	0.670	0.710	0.700	0.760	0.700	0.620	0.620	0.610	0.680	0.600	0.710	1.000							
F95	0.840	0.780	0.770	0.530	0.650	0.650	0.700	0.770	0.680	0.670	0.650	0.580	0.690	0.620	0.680	0.780	1.000						
F96	0.770	0.780	0.710	0.580	0.620	0.620	0.630	0.670	0.690	0.700	0.680	0.600	0.650	0.620	0.660	0.710	0.790	1.000					
F97	0.720	0.720	0.790	0.520	0.650	0.640	0.720	0.770	0.590	0.610	0.670	0.580	0.650	0.580	0.610	0.740	0.770	0.680	1.000				
F98	0.750	0.730	0.800	0.590	0.700	0.690	0.730	0.740	0.600	0.570	0.690	0.640	0.720	0.580	0.670	0.710	0.760	0.700	0.760	1.000			
F99	0.680	0.660	0.670	0.670	0.720	0.740	0.710	0.720	0.640	0.610	0.600	0.620	0.700	0.610	0.690	0.720	0.700	0.660	0.650	0.700	1.000		
F100	0.600	0.560	0.600	0.590	0.640	0.670	0.590	0.620	0.580	0.560	0.690	0.630	0.700	0.670	0.620	0.570	0.610	0.590	0.550	0.640	0.670	1.000	
HM	0.660	0.700	0.630	0.590	0.630	0.660	0.590	0.620	0.660	0.660	0.610	0.560	0.620	0.580	0.650	0.660	0.660	0.730	0.600	0.650	0.630	0.590	1.000
Max.	0.840	0.780	0.800	0.760	0.770	0.760	0.770	0.770	0.700	0.700	0.690	0.690	0.740	0.700	0.710	0.780	0.790	0.730	0.760	0.700	0.670	0.590	**Prom**
Min.	0.570	0.540	0.590	0.500	0.590	0.550	0.490	0.580	0.580	0.500	0.600	0.560	0.620	0.580	0.610	0.570	0.610	0.590	0.550	0.640	0.630	0.590	**gral.**
Prom.	0.685	0.661	0.689	0.606	0.672	0.685	0.664	0.673	0.635	0.597	0.656	0.618	0.685	0.618	0.661	0.699	0.715	0.672	0.640	0.663	0.650	0.590	0.652

an equivalent variability defined morphochemically. The existence of such correlation between the markers with the grouping based on 32 morphochemical traits, should favor the search of new QTL associated with morphological characters within F2 or backcross populations of *C. papaya* L. In addition, the detected genetic variability can be also useful in: a) the selection of distant or complementary elite genotypes that could in turn, generate F2 populations or backcrosses, to maintain variability of the species. b) as a basis to find new parents with features usable in breeding schemes, seeking new varieties with better adaptation to the regional environments.

Conflict of interests

The authors have not declared any conflict of interest.

REFERENCES

Brown JE, Bauman JM, Lawrie JF, Rocha OJ, Moore RC (2012). The structure of morphological and genetic diversity in natural population of *Carica papaya* (Caricaceae) in Costa Rica. Biotropica 44:179-188.

Colunga GMP, Zizumbo VD (2004). Domestication of plants in Maya lowlands. Econ. Bot. 58:101-110.

Crisci JV, López, MF (1983). Introducción a la teoría y práctica de la taxonomía numérica. Secretaría General de la Organización de los Estados Americanos (OEA). Washington D.C. P 132.

Doyle JJ, Doyle JL (1990). A rapid total DNA preparation procedure for fresh plant tissue. Focus 12:13-15.

Esquivel MA, Bautista AM, Ortiz GM, Quiroz A, Rohde W, Sánchez TLF (2009). Caracterización de accesiones de papaya (*Carica papaya* L.) a través de marcadores AFLP en Cuba. Rev. Colomb. Biotecnol. 2:31-39.

Francisco-Ortega JA, Santos-Guerra, Seung-Chul Kim, Crawford DJ (2000). Plant genetic diversity in the Canary Islands: a conservation perspective. Am. J. Bot. 87:909-919.

Fuentes G, Santamaría JM (2014). Chapter 1: Papaya (*Carica papaya* L.): Origin, domestication, and production. Genetics and Genomics of Papaya. Plant Genetics and Genomics: Crops Models Springer. 10:3-15.

Janthasri R, Katengam S, Khumcha U (2007). An analysis on DNA fingerprints of thirty papaya cultivars (*Carica papaya* L.) Grown in Thailand with the use of Amplified Fragments Length Polymorphisms Technique. Pakistan J. Biol. Sci. 10:3072-3072.

Jobin-Décor MP; Graham GC, Henry RJ, Drew RA (1997). RAPD and isozyme analysis of genetic relationships between *Carica papaya* and wild relatives. Genetic Resour. Crop Evol. 44:471-477.

Jones CJ, Edwards KJ, Castaglione S, Winfield MO, Sala F, Van de Wiel C, Bredemeijer G, Vosman B, Matthes M, Daly A, Brettschneider R, Bettini P, Buiatte M, Maestri E, Malcevschi A, Marmiroli N, Karp A (1997). Reproducibility testing of RAPD, AFLP and SSR markers in plants by a network of European laboratories. Mol. Breeding 3:381-390.

Kim MS, Moore PH, Zee F, Fitch MMM, Steiger DL, Manshardt RM (2002). Genetic diversity of *Carica papaya* as revealed by AFLP markers. Genome 45:503-512.

Liu Z, Moore PH, Ma H, Ackerman CM, Ragiba M, Yu Q, Pearl HM, Kim MS, Charlton JW, Stiles JL, Zee FT, Paterson AH, Ming R (2004). A primitive Y chromosome in papaya marks incipient sex chromosome evolution. Nature 427:348-52.

Madarbokus S, Ranghoo-Sanmukhiya VM (2012). Identification of genetic diversity among Papaya varieties in 12 auritius using Morphological and molecular markers. Int. J. Life Sci. Biotechnol. Pharm. Res. 1:152-164.

Meerow WA (2005). Molecular genetic characterization of Floricultural germplasm. In Vitro Int. Symp. New Floricult. Crops 683:42-63.

Moore PH (2014). Chapter 3: Phenotypic and genetic diversity of papaya. In: Moore P, Ming R. (eds). Genetics and Genomics of Papaya. Plant Genetics and Genomics: Crops Models Spinger 10:35-45.

Mueller UG, Wolfenbarger L (1999). AFLP genotyping and fingerprinting. Tree 14:389-393.

Nei M, Li WH (1979). Mathematical model for studying genetic variation in terms of restriction endonucleases. Proceed. National Acad. Sci. 76(10):5269-5273

Nagata M, Yamashita I (1992). Simple method for simultaneous determination of chlorophyll and carotenoids in tomato fruit: Nippon Shokuhin Kogyo Gakkaish 39:925-928.

Numerical Taxonomy System (NTSYS) v2.1p. (2014). Exeter Software. E. Setauket NY, USA.

Ocampo JP, d'Eeckenbrugge GC, Bruyere S, De Bellaire LL, Ollitrault P (2006). Organization of morphological and genetic diversity of Caribbean and Venezuela papaya germplasm. Fruits 61:25-37.

Oliveira EJ, Leles CJ, Ferraz DS, Moraes FC, Santos SA, Loyola DJL (2011). Molecular characterization of papaya genotypes using AFLP markers. Rev. Bras. Frutic. 333:848-858.

Rojas LE, López J, Kosky RG, Portal O (2007). Empleo de los marcadores AFLP para la caracterización molecular de dos cultivos con interés agrícola. Biotecnol Veg. 7:103-106.

SAS Institute. 1985. SAS User´s guide: statistics. Version 5 ed. Cary, NC.

Sudha R, Singh DR, Sankaran M, Damodaran V, Simachalam P (2013). Genetic diversity analysis of papaya (*Carica papaya* L.) genotypes in Andaman Islands using morphological and molecular markers. Afr. J. Biotechnol. 8:5187-5192.

Van Droogenbroeck B, Breyne P, Goetghebeur P, Romeijn PE, Kyndt T, Gheysen G (2002). AFLP analysis of genetic relationships among papaya and its wild relatives (Caricaceae) from Ecuador. Theor. Appl. Genet. 105:289-297.

Vázquez M, Zavala M, Contreras F, Espadas F, Navarrete A, Sánchez L, Santamaria JM (2014). New cultivars derived from crosses between commercial cultivar and a wild population of Papaya rescued at its center of origin. J. Bot. 2014:1-10.

Vegas GA, Miliani A, Rodríguez D, Zambrano A, Vicente VJL, Demey JR (2013). Diversidad genética de la colección Venezolana de la familia Caricáceas. Interciencia 38:171-178.

Vos PR, Hogers R, Bleeker M, Reijans, M, Van de Lee T, Hornes, M, Fijters A, Pot J, Kuiper M, Zabeau M (1995). AFLP: a new technique for DNA fingerprinting. Nucleic Acids Res. 23:4407-4414.

Yu QY, Navajas Pérez R, Tong E, Robertson J, Moore PH, Paterson AH, Ming R (2008). Recent origin of dioecious and gynodioecious Y chromosomes in papaya. Trop. Plant Biol. 1:49-57.

academicJournals

Vol. 15(21), pp. 960-973, 25 May, 2016
DOI: 10.5897/AJB2015.15185
Article Number: 5F2E9F858604
ISSN 1684-5315

http://www.academicjournals.org/AJB

African Journal of Biotechnology

Full Length Research Paper

Assessment of genetic diversity among sixty bread wheat (*Triticum aestivum*) cultivars using microsatellite markers

Vincent Mgoli Mwale[1,2]*, Xiuli Tang[2] and Eric Chilembwe[1]

[1]Lilongwe University of Agriculture and Natural Resources (LUANAR), P. O. Box 219, Lilongwe, Malawi.
[2]State Key Laboratory of Biology for Plant Diseases and Insect Pests, Institute of Plant Protection, Chinese Academy of Agricultural Sciences, Beijing 100193, China.

Received 19 December, 2015; Accepted 20 April, 2016.

Assessment of genetic diversity among wheat cultivars is important to ensure that a continuous pool of cultivars with varying desirable traits is maintained. In view of this, a molecular study was conducted to assess the genetic diversity of sixty wheat cultivars using sixty microsatellite markers. Amplified alleles from each cultivar were scored after running in 6% poly acrylamide gel electrophoresis (PAGE). A dendrogram was constructed based on the genetic similarity coefficient of un-weighted pair-wise group method with arithmetic average (UPGMA). The results showed that 276 alleles were amplified by 48 polymorphic microsatellite markers averaging 5.7 alleles per locus. A total of 12 markers did not amplify any alleles from the 60 cultivars. Polymorphism of alleles and genetic diversity measured by polymorphic information content (PIC) and Shannon index (SI) respectively, found that genome A had the highest genetic diversity followed by genome B while genome D was the lowest diverse. Cluster analysis resulted in formation of four clusters comprising of 3, 7, 9 and 41 cultivars. Genetic distance between the clusters ranged from 0.56 to 0.87 and most cultivars showed high diversity between genetic distances of 0.65 and 0.75. The four clusters and their similarities will help breeders to breed new disease resistant cultivars and make rational deployment of cultivars in production based on the established relationships.

Key words: Genetic diversity, molecular marker, microsatellite (SSR marker), *Triticum aestivum.*

INTRODUCTION

Common wheat (*Triticum aestivum* L.) is among the most important cereals currently grown in most parts of the world. The crop is among the three world's major cereal export earners with others including maize and rice (Tong et al., 2003; Abdellatif and Abouzeid, 2011). It forms more than 40% of the world's commonly consumed food and 95% of people in the developing countries eat wheat or maize in form of flour as a main food source (Akhtar et

*Corresponding author. Email: vincentmgoli@yahoo.co.uk

al., 2011; Coventry et al., 2011). The crop provides one fifth of the global required calories (Reynolds et al., 2011; Friedrich et al., 2014). Currently, wheat is grown on approximately 216 million hectares of land worldwide with an estimated production of 605 million tons (Abdellatif and Abouzeid, 2011). China is the largest wheat producer and consumer in the world (FAO, 2014). As at 2013, the crop was produced on approximately 24 million hectares of land yielding 121 million tons nationally, representing 11.2 and 17.6% of the world's total harvest area and production tonnage, respectively (FAO, 2014; Li et al., 2014). The crop is mostly produced in 30 provinces across China with 1.9 million hectares (8%) covered by spring wheat and 22.3 million hectares (92%) grown with winter wheat. Spring wheat is mainly grown in the northeastern, central northern and northwestern China including parts of Gansu, Xinjiang and Qinghai provinces, while winter wheat is mainly grown in eastern China including parts of Henan, Shandong, Anhui and Hebei provinces among others (Liu et al., 2014).

In order to sustain high levels of wheat production in China, one of the most important requirements is the maintenance of a diverse pool of wheat cultivars where 'superior' gene/alleles can be obtained for genetic improvement programs. Intensive activities aimed at improving wheat crop such as selection of cultivars with desirable attributes have led to a reduced genetic diversity over time, increased disease incidences, a decline in crop yield and compromised drought tolerance among many other biotic and abiotic challenges (Roussel et al., 2004; Fu et al., 2005; Mir et al., 2012).

Presently, it is extremely difficult to increase the land area for wheat production in China due to pressure from human population growth, urbanization and competition from other crops (Fu et al., 2001; Lu et al., 2007; Lu and Fan, 2013). By preserving the genetic diversity, growers could achieve a high improvement rate of desired attributes such as pest resistance and high yields in the available wheat cultivars while maintaining land size.

Microsatellite markers also called simple sequence repeats (SSR) or short tandem repeats (STR) (Tautz, 1989; Edwards et al., 1991; Jacob et al., 1991; Kalia et al., 2011) are among the most popular molecular markers used in genetic diversity studies. This type of markers is characterized by its high efficiency, reproducibility, co-dominant nature and high degree of polymorphism (Singh et al., 2007; Royo et al., 2010; Ruiz et al., 2012; Laido et al., 2013; Meti et al., 2013). Microsatellites are vital in cultivar identification and also offer an advantage during pedigree analysis as they are genus specific (Romero et al., 2009; Abdullah et al., 2012). Several studies conducted to identify the genetic diversity of wheat cultivars using SSRs, had shown consistent results with the polymorphism expressed being significantly more reliable than that reported using other types of markers (Corbellini et al., 2002; Ahmed et al., 2010; Khodadadi et al., 2011; Shakeel and Azam, 2012; Spanic et al., 2012).

The aim of the present study was to utilize microsatellite markers in order to assess the genetic diversity of sixty wheat cultivars collected from several parts of main wheat growing regions in China. The outcome of this research could assist breeders to set up the appropriate guidelines for proper management of the wheat cultivars, as a precursor towards the implementation of future programs.

MATERIALS AND METHODS

Selection of cultivars, DNA extraction and PCR protocol

A total of 60 wheat cultivars comprising 57 wheat cultivars collected from parts of main wheat growing regions of China and 3 cultivars collected from USA and Italy were evaluated for genetic diversity. Detailed information of cultivars is shown in Table 1.

Ten seeds of each wheat cultivar were sown on trays in greenhouse located at the Institute of Plant Protection, Chinese Academy of Agricultural Sciences, Beijing, China. About 15 days after sowing, when three to four leaves had been developed, seedling leaves were detached and their DNA was extracted following Zheng (2010) CTAB extraction method.

To test DNA purity, all extracted DNA samples were run on 2% Agarose gel of 1% TBE buffer solution and the image was captured using Gel Documentation and Image Analysis System after staining in Ethidium bromide solution for 5 min. For PCR reaction, the DNA was diluted in the range between 50 and 80 ng/µl and the mixture comprised 5 µl PCR master mix, 2 µl double distilled water, 1 µl of 10 mM Forward primer, 1 µl of 10 mM Reverse primer and 1 µl of DNA template, with a final volume of 10 µl. PCR protocol was applied using Bio-Gener Technology, Gene explorer PCR machine with the following conditions: 94°C for 3 min, 35 cycles of 94°C for 1 min, 50 to 60°C (depending on SSR primer annealing temperature) for 30 s, 72°C for 30 s and a final extension of 72°C for 10 min before soaking at 4°C. A total of sixty wheat microsatellite markers were used to estimate the genetic diversity among the sixty cultivars used herein (Table 2). SSR markers that had linkage to designated and temporarily designated wheat powdery mildew resistance genes were selected for the study. This preference was due to the fact that a subsequent study that followed the present one required the utilization of the same cultivars and markers for molecular disease resistance assessment. Marker sequences, chromosomal locations and corresponding annealing temperatures were retrieved from the graingenes website (http://wheat.pw.usda.gov/cgi-bin/graingenes/browse.cgi?class=marker).

Simple sequence repeat protocol

SSR protocol for 6% poly-acrylamide gel electrophoresis (PAGE) was used. The gel glass was stained in 1500 ml of water containing 3 g silver nitrate solution. Thereafter, the alleles were enhanced in 2000 ml of water solution containing 3 ml of 37% formaldehyde (H_2CO) and 30 g sodium hydroxide.

Data analysis

All clearly amplified alleles on the cultivars were treated as a single locus. Scoring was based on presence and absence of the alleles. Bivariate 1 and 0 data matrices obtained from the stained gel were used to construct a dendrogram based on the genetic similarity coefficient. Sahn-clustering of un-weighted pair-group method with

Table 1. Names of wheat cultivars, pedigree information and origin.

Cultivar designation	Name of cultivar	Pedigree information*	Origin
1	Lantian095	-	Gansu
2	Tian0015	-	Gansu
3	Tian01-104	93R177 / 912-2-1-2	Gansu
4	05bao1-1	Zhongliang22+ gDNA of oil sunflower	Gansu
5	Chancellor	Carina/Mediterranean//Dietz/ Carina/3/P-1068/3×Purplestraw	-
6	Tian00127	(Baidatou/C184-3-4-1)F2//85-173-4	Gansu
7	Lantian23	SXAF4-7/87-121	Gansu
8	Lantian20	CappelleDesprez/Lantian10	Gansu
9	Tian03-142	9589-8-1-2-1/Qing 95-111	Gansu
10	Tian00296	9362-13-3-4/8748-0-2-1	Gansu
11	TianTian9681	863-13/87148-1-1-2-2-2	Gansu
12	Lantian093	Lantian23/Zhou92031	Gansu
13	AvocetYrA	Avocet	USA
14	Longchun26	Yong3263/Gaoyuan448	Gansu
15	TianTian96-86	863-13/8560-2-2-1	Gansu
16	Tian02-195	Wenmai8/Tian96-1c1	Gansu
17	Tian03-160	0037-1-2/9938-2-2-1	Gansu
18	Tian02-204-1	Wenmai8/9157-3-2-2-1	Gansu
19	Longjian101	8487/85-173-12-2	Gansu
20	Longjian127	7402/Lv419//7415	Gansu
21	Tian989	9362-13-4-4/lantian1	Gansu
22	Zhongzhi2	Shan167/ Guinong22/*T. Spelta* album	Beijing
23	Longjian102	Lin87-4535/81168-4-3//Longyuan932	Gansu
24	Tian98101	9362-13-4-4/Tian94-3	Gansu
25	03bao1-1	Lantian10+ DNA of oil sunflower	Gansu
26	Zhongliang27	90293///Zhongliang12/Zhongsi// Bulgaria10/Xiannong4	Gansu
27	N. Strampelli	LIBERO//S.Pastou/C.Jrometh.lig	Italy
28	Zhongzhi4	Mianyou2/Zhongzhi1	Beijing
29	Zhongzhi1	Shan167/C591	Beijing
30	Lantian097	92R137/87-121 //Shan167	Gansu
31	Taikong06	Space-flight mutation from Yumai49	Henan
32	Kenya Kongoni	C18154/2×Fr/2/Romm/3/WIS.245-II-50-7/C8154/2/2×Fr	USA
33	Keyuan5	-	Henan
34	Xinmai19	(C5/xinxiang3577) F3d1s/Xinmai9	Henan
35	Xinyumai836	-	Henan
36	Yumai368	-	Henan
37	Zhoumai19	Neixiang185 / Zhoumai9	Henan
38	Guoan368	-	Henan
39	Zhoumai32	Zhoumai12/ Wenmai6 // Zhoumai13	Henan
40	Yangao03710	-	Henan
41	Zhou99233	-	Henan
42	Punong1	-	Henan
43	Pu02056	Zhoumai16/ Yumai24	Henan
44	Xinxuan2039	-	Henan
45	Zhengnong01059	-	Henan
46	Guomai301	G883/ Pumai9	Henan
47	Zhongxin01	-	Henan
48	Zhongyu885	-	Henan
49	04zhong70	-	Henan
50	Zheng366	-	Henan

Table 1, Contd.

51	Lankao008	-	Henan
52	Tianmin198	R81/Bainong64//Yanzhan4110	Henan
53	Zhengyumai9989	Benyumai21/Yumai2//Yumai57	Henan
54	Zhengmai9023	[Xiaoyan6/Xinong65//83(2)33/84(14)43] F3/3Shan213	Henan
55	Zhengmai366	Yumai47/PH82-2-2	Henan
56	Zhou mai16	Zhoumai9/Zhou8425B	Henan
57	Yanzhan4110	[(C39/Xibei78(6)9-2)/(FR81-3/ Aizao781-4)] /Aizao781-4	Henan
58	Bainong160	Duokang893/Wenmai6//Bainong64/ Wenmai6	Henan
59	Lantian15	Lantian10/Ibis	Gansu
60	Yujiao0338	-	Henan

*Cultivars with a dash (-) indicate that their pedigree information could not be traced.

Table 2. SSR markers (loci), sequence, location on the wheat chromosome and their annealing temperatures.

Marker (locus)	Marker sequence	Chromosomal location	Annealing temperature (°C)
Xgwm273 F	ATTGGACGGACAGATGCTTT	1B	55
Xgwm273 R	AGCAGTGAGGAAGGGGATC		
Xbarc229 F	GGCCGCTGGGGATTGCTATGAT	1D	58
Xbarc229 R	TCGGGATAAGGCAGACCACAT		
Xgwm294 F	GGATTGGAGTTAAGAGAGAACCG	2A	55
Xgwm294 R	GCAGAGTGATCAATGCCAGA		
Xwmc382 F	cATgAATggAggcAcTgAAAcA	2A	61
Xwmc382 R	ccTTccggTcgAcgcAAc		
Xgwm319 F	GGTTGCTGTACAAGTGTTCACG	2B	55
Xgwm319 R	CGGGTGCTGTGTGTAATGAC		
Xgwm210 F	TGCATCAAGAATAGTGTGGAAG	2B	60
Xgwm210 R	TGAGAGGAAGGCTCACACCT		
Xgwm257 F	AGAGTGCATGGTGGGACG	2B	61
Xgwm257 R	CCAAGACGATGCTGAAGTCA		
Xwmc356 F	gccgTTgcccAATgTAgAAg	2B	61
Xwmc356 R	ccAgAgAAAcTcgccgTgTc		
Xwmc317 F	TgcTAgcAATgcTccgggTAAc	2B	61
Xwmc317 R	TcAcgAAAccTTTTccTccTcc		
Xwmc41 F	TcccTcTTccAAgcgcggATAg	2D	61
Xwmc41 R	ggAggAAgATcTcccggAgcAg		
Xwmc445 F	AgAATAggTTcTTgggccAgTc	2D	51
Xwmc445 R	gAgATgATcTccTccATcAgcA		
Xwmc291 F	TAccAcgggAAAggAAAcATcT	3B	61
Xwmc291 R	cAcgTTgAAAcAcggTgAcTAT		
Xgwm108 F	CGACAATGGGGTCTTAGCAT	3B	60
Xgwm108 R	TGCACACTTAAATTACATCCGC		
Xgwm415 F	GATCTCCCATGTCCGCC	5A	55
Xgwm415 R	CGACAGTCGTCACTTGCCTA		
Xgwm126 F	CACACGCTCCACCATGAC	5A	60
Xgwm126 R	GTTGAGTTGATGCGGGAGG		
Xwmc75 F	gTccgccgcAcAcATcTTAcTA	5B	61
Xwmc75 R	gTTTgATccTgcgAcTcccTTg		
Xgwm408 F	TCGATTTATTTGGGCCACTG	5B	55
Xgwm408 R	GTATAATTCGTTCACAGCACGC		
Xwmc810 F	GGCACCGATGCTTCCA	5B	61

Table 2, Contd.

Xwmc810 R	GCCCCAACCACCTCCC		
Xbarc232 F	CGCATCCAACCATCCCCACCCAACA	5B	65
Xbarc232 R	CGCAGTAGATCCACCACCCCGCCAGA		
Xbarc142 F	CCGGTGAGAGGACTAAAA	5B	52
Xbarc142 R	GGCCTGTCAATTATGAGC		
Xgwm67 F	ACCACACAAACAAGGTAAGCG	5B	60
Xgwm67 R	CAACCCTCTTAATTTTGTTGGG		
Xgwm174 F	GGGTTCCTATCTGGTAAATCCC	5D	55
Xgwm174 R	GACACACATGTTCCTGCCAC		
Cfd57 F	ATCGCCGTTAACATAGGCAG	5D	60
Cfd57 R	TCACTGCTGTATTTGCTCCG		
Xgwm583 F	TTCACACCCAACCAATAGCA	5D	60
Xgwm583 R	TCTAGGCAGACACATGCCTG		
Xgwm205 F	CGACCCGGTTCACTTCAG	5D	60
Xgwm205 R	AGTCGCCGTTGTATAGTGCC		
Xgwm583 F	TTCACACCCAACCAATAGCA	5D	60
Xgwm583 R	TCTAGGCAGACACATGCCTG		
Xgwm292 F	TCACCGTGGTCACCGAC	5D	60
Xgwm292 R	CCACCGAGCCGATAATGTAC		
Xwmc553 F	cggAgcATgcAgcTAgTAA	6A	60
Xwmc553 R	cgccTgcAgAATTcAAcAc		
Xwmc684 F	CGAATCCAACGAGGCCATAGA	6A	61
Xwmc684 R	GCAATCAGGAGGCATCCACC		
Xpsp3131 F	GCTAGTCCCGACGCCCTATC	6B	61
Xpsp3131 R	GAGGAAGGAGCTTTGGTTTCTCC		
Xwmc397 F	AgTcgTgcAccTccATTTTg	6B	61
Xwmc397 R	cATTggAcATcggAgAccTg		
Xgwm325 F	TTTCTTCTGTCGTTCTCTTCCC	6D	60
Xgwm325 R	TTTTTACGCGTCAACGACG		
Xbarc183 F	CCCGGGACCACCAGTAAGT	6D	58
Xbarc183 R	GGATGGGGAATTGGAGATACAGAG		
Xcfa2240 F	TGCAGCATGCATTTTAGCTT	7A	60
Xcfa2240 R	TGCCGCACTTATTTGTTCAC		
Xcfa2019 F	GACGAGCTAACTGCAGACCC	7A	60
Xcfa2019 R	CTCAATCCTGATGCGGAGAT		
Xcfa2257 F	GATACAATAGGTGCCTCCGC	7A	60
Xcfa2257 R	CCATTATGTAAATGCTTCTGTTTGA		
Xwmc346 F	cTgAAgTTccAgccAAcAcA	7A	61
Xwmc346 R	ATTcccTcATcccgTTgc		
Xwmc525 F	gTTTgAcgTgTTTgcTgcTTAc	7A	61
Xwmc525 R	cTAcggATAATgATTgcTggcT		
Xbarc1073 F	GCGGGCACAATATTCTAATGGACAAAG	7B	55
Xbarc1073 R	GCGCAGATGCAGAGGCCAGGGGTC		
Xwmc276 F	gAcATgTgcAccAgAATAgc	7B	51
Xwmc276 R	AgAAgAAcTATTcgAcTccT		
Xcfa2040 F	TCAAATGATTTCAGGTAACCACTA	7B	60
Xcfa2040 R	TTCCTGATCCCACCAAACAT		
Xgwm611 F	CATGGAAACACCTACCGAAA	7B	55
Xgwm611 R	CGTGCAAATCATGTGGTAGG		
Xpsp3033 F	GTTGGCAGTGTAAATCGGTG	7B	61
Xpsp3033 R	GAGCCACGTATGCAATGGACG		
Xgwm46 F	GCACGTGAATGGATTGGAC	7B	60

Table 2. Contd.

Xgwm46 R	TGACCCAATAGTGGTGGTCA		
Xgwm297 F	ATCGTCACGTATTTTGCAATG	7B	55
Xgwm297 R	TGCGTAAGTCTAGCATTTTCTG		
Xpsp3029 F	CCATCGATGAGGATCTCCTCGGGCA	2A, 6A	58/61
Xpsp3029 R	GCAACAGGACCATGGTCG		
Xwmc289 F	cATATgcATgcTATgcTggcTA	5B,5D	61
Xwmc289 R	AgccTTTcAAATccATccAcTg		
Xgwm296 F	AATTCAACCTACCAATCTCTG	2D,7D	55
Xgwm296 R	GCCTAATAAACTGAAAACGAG		
Xgwm265 F	TGTTGCGGATGGTCACTATT	2A,4A	55
Xgwm265 R	GAGTACACATTTGGCCTCTGC		
Xgwm111 F	TCTGTAGGCTCTCTCCGACTG	7B, 7D	55
Xgwm111 R	ACCTGATCAGATCCCACTCG		
Xgwm344 F	CAAGGAAATAGGCGGTAACT	7A, 7B	55
Xgwm344 R	ATTTGAGTCTGAAGTTTGCA		
Xgwm159 F	GGGCCAACACTGGAACAC	5B, 5D	60
Xgwm159 R	GCAGAAGCTTGTTGGTAGGC		
Xgwm382 F	GTCAGATAACGCCGTCCAAT	2A,2B,2D	60
Xgwm382 R	CTACGTGCACCACCATTTTG		
Xpsp3003 F	GATCGACAAGGCTCTAATGC	1A,5A,7D,	63
Xpsp3003 R	CAGGAGGAGAGCCTCTTGG		
Xcfd81 F	TATCCCCAATCCCCTCTTTC	7D,5D,4D	60
Xcfd81 R	GTCAATTGTGGCTTGTCCCT		
Xcfd39 F	CCACAGCTACATCATCTTTCCTT	4B,4D,5A	60
Xcfd39 R	CAAAGTTTGAACAGCAGCCA		
Xgwm356 F	AGCGTTCTTGGGAATTAGAGA	2A,6A,7A	55
Xgwm356 R	CCAATCAGCCTGCAACAAC		
Xgdm93 F	AAAAGCTGCTGGAGCATACA	2A,2D,4B	55
Xgdm93 R	GGAGCATGGCTACATCCTTC		
Xwmc273 F	AgTTATgTATTcTcTcgAgccTg	7A,7B,7D	51
Xwmc273 R	ggTAAccAcTAgAgTATgTccTT		
Xgwm526 F	CAATAGTTCTGTGAGAGCTGCG	2A, 2B, 7A, 7B	55
Xgwm526 R	CCAACCCAAATACACATTCTCA		
Xgwm311 F	TCACGTGGAAGACGCTCC	2A, 2B, 2D, 6B	60
Xgwm311 R	CTACGTGCACCACCATTTTG		

arithmetic average (UPGMA) were applied using the software NTSYSpc 2.1 (Numerical Taxonomy and Multivariate Analysis System), version 2.1 (Rohlf, 2000). Polymorphism information content (PIC) was calculated using the following formula:

$PIC = 1 - \sum_{i=1}^{n}(fi)^2$ for *n* alleles

Where *fi* = frequency of *i*th allele for *n* alleles at a locus (Powell et al., 1996).

PIC measures the informativeness of the DNA markers over a set of genotypes during gene mapping, molecular breeding and germplasm evaluation (Peng and Lapitan, 2005; Varshney et al., 2007; Wang et al., 2007).

A molecular marker with lower PIC indicates less informativeness in expressing the polymorphism of its alleles at a locus while higher PIC value indicates the high ability of the marker to express polymorphism of alleles at a locus. Shannon-weaver index (SI) was calculated as described by Chen and Li (2007). The index estimates species diversity in a community at a particular time. The diversity index, also known as the Shannon-Wiener species diversity index or simply the Shannon index, calculates the number of different species in a community (species richness) and the proportion of individuals from a single species as compared to the number of individuals of other species in the same community. A Shannon-Weaver diversity index of zero indicates that only one species is present in the community; as diversity increases, so does the index number.

The most diverse communities have an index of seven or higher. The formula used for index calculation was:

$SI = -\sum_{i=1}^{n}(Pi \ln[Pi])$ for *n* species

Where *Pi* = number of *i*th individuals in a particular *n* species divided by the total number of individuals of all species in the community.

Table 3. Number of alleles, range of allele sizes, polymorphic information content (PIC) and Shannon-Weaver diversity index (SI) for genome A of wheat loci.

Locus	Number of alleles	Expected allele size (bp)	Range of allele sizes (bp)	Polymorphic information content	Shannon-Weaver diversity index
Xwmc382-2A	10	270	250- 450	0.882	3.290
Xgwm294-2A	7	96	90- 160	0.761	2.185
Xgwm126-5A	4	196	190- 225	0.674	1.358
Xwmc553-6A	8	395	375- 550	0.817	2.364
Xwmc684-6A	7	190	150- 290	0.833	2.234
Xcfa2240-7A	6	280	220- 300	0.675	1.474
Xcfa2257-7A	4	167	150- 220	0.503	1.006
Xcfa2019-7A	5	217	190- 260	0.728	1.638
Xwmc346-7A	6	203	180- 270	0.729	1.775
Xwmc525-7A	4	206	195- 280	0.640	1.316
Total	61		90-550	-	-
Mean	6.1		-	0.724	1.864

RESULTS

Polymorphism of SSR markers and genetic diversity

Number of amplified alleles per locus, PIC and SI values varied among wheat genomes A, B and D in the 60 cultivars analyzed. In genome A, locus Xwmc382-2A had the highest number of alleles (10) followed by Xwmc553-6A, which had 8 alleles (Table 3). Locus Xwmc382-2A also had the highest PIC value of 0.882 as well as the highest SI value of 3.290. Locus Xwmc553-6A was second with PIC of 0.817 and SI value of 2.364. The lowest number of alleles per locus (4) in genome A was recorded in the loci Xgwm126-5A, Xcfa2257-7A and Xwmc525-7A. Locus Xcfa2257-7A showed the lowest PIC and SI values of 0.503 and 1.006, respectively (Table 3). For a total of 10 polymorphic loci in the A genome, 61 alleles were recorded and their molecular sizes ranged from 90 to 550 bp. Alleles in locus Xwmc382-2A ranged from 250 to 450 bp and significant polymorphism was observed between 250 and 320 bp (Figure 1).

In genome B, locus Xbarc142-5B amplified 10 alleles, being the highest number of all polymorphic loci in the genome, with a range from 175 to 350 bp. Significant polymorphism was observed between 150 and 290 bp (Figure 2). The locus had the highest PIC and SI values of 0.834 and 2.787, respectively (Table 4). This was followed by loci Xwmc810-5B and Xgwm46-7B, having 9 alleles each. Locus Xwmc810-5B showed allele sizes ranging from 150 to 300 bp while the PIC and SI values were 0.868 and 2.533, respectively (Table 4).

The lowest number of alleles (2) in B genome was recorded in locus Xwmc276-7B with a range between 250 and 390 bp. The locus also exhibited the lowest PIC (0.132) and SI (0.378) value. Loci Xgwm108-3B and Xgwm319-2B amplified 3 alleles each and their molecular sizes ranged from 110 to 495 bp (Table 4).

In D genome, the highest number of alleles (9) was recorded in locus Xwmc445-2D (Figure 3) followed by locus Xgwm325-6D with 7 alleles. Xwmc445-2D also had the highest SI and PIC values of 2.543 and 0.815, respectively (Table 5). This was followed by locus Xgwm325-6D, which had an SI value of 1.992 and PIC of 0.776. A total of 40 alleles were recorded in the 8 polymorphic loci of the genome D, with an average of 5 alleles per locus (Table 5). Size of alleles ranged from 150 to 380 bp while average PIC and SI values were 0.613 and 1.294, respectively.

Fifteen markers amplified alleles from multiple loci of the A, B and D wheat genomes. For instance, marker Xgwm344 (Figure 4) amplified alleles from loci in genome A and B for chromosome 7 (Table 6). The marker amplified 7 alleles, as markers Xwmc273 and Xcfd39. It also had the highest PIC and SI values of the group, 0.860 and 1.810 respectively. The lowest number of alleles (4) was found in markers Xcfd81, Xgwm382, Xgwm356 and Xgwm311. These four markers had their SI values below 1.0 (Table 6).

Out of 60 markers studied herein, 48 amplified a total of 276 alleles with an average of 5.7 alleles per locus. 61 alleles were amplified in genome A, 93 in genome B and 40 in genome D. A total of 82 alleles were amplified from markers that detected multiple loci in the wheat genome. Genome A had the highest PIC mean value of 0.724, while the lowest one was recorded in genome D (0.676). Genome A also had the highest SI value of 1.864 while the lowest one of 1.312 was recorded in those markers that detected multiple loci. Sizes of the alleles ranged from 90 to 550 bp with an overall PIC and SI values of 0.703 and 1.543 respectively (Table 7).

Cluster analysis

Cluster analysis represented by a dendrogram plotted

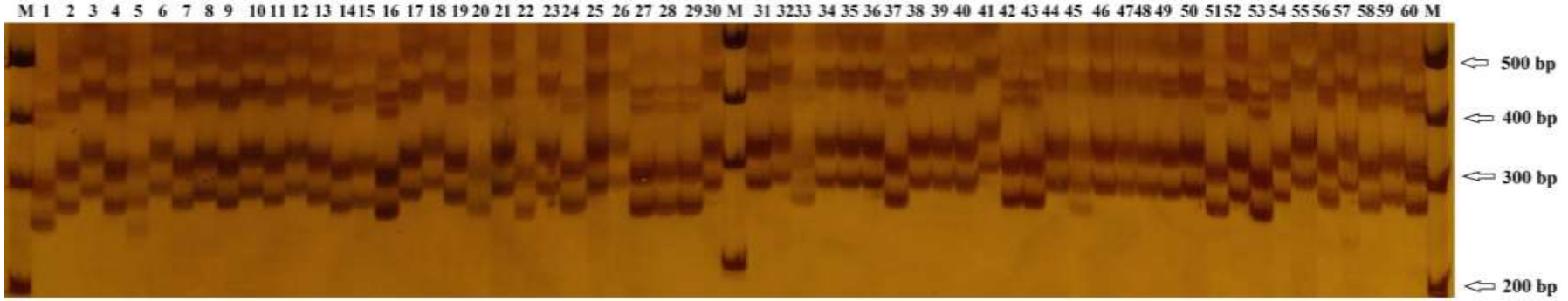

Figure 1. Amplified alleles on locus Xwmc382-2A for 60 wheat genotypes, M is 100 bp Marker.

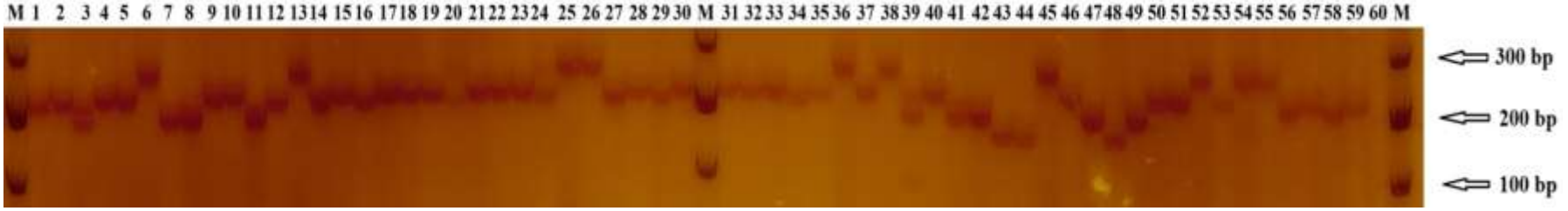

Figure 2. Amplified alleles on locus Xbarc142-5B for 60 wheat genotypes, M is 100 bp marker.

using the UPGMA method, revealed four major clusters. The genetic distance between clusters ranged from 0.56 to 0.87 and most cultivars showed a high degree of diversity within a range of 0.65 to 0.75 (Figure 5). Cluster 1 was made up of three cultivars namely, Lantian095, Tian00127 and Zhongliang27. The cultivars were spread within a distance range of 0.647 to 0.687. Cluster 2 comprised of seven cultivars, included Tian0015, 05bao1-1, Chancellor, Tian03-142, Tian96-86, Tian01-104 and Longchun26 spread on a distance range of 0.642 to 0.752. Cluster 3 was the largest and most diverse cluster consisting of 41 cultivars. It contained several sub-clusters within a genetic distance range of 0.642 to 0.87. The fourth cluster was composed of 9 cultivars namely Lantian23, Lantian093, Tian9681, Longjian101, Tian989, Lantian20, Tian00296, Zhongxin01 and Zheng366. Its genetic distance ranged between 0.643 and 0.832 (Figure 5).

DISCUSSION

Polymorphism of SSR markers in wheat genomes

SSR markers have been used widely in genetic studies due to their high polymorphism in the genomes (Gupta and Varshney, 2000; Kalia et al., 2011; Jamalirad et al., 2012). In this study, a total of 276 alleles were identified by 48 polymorphic markers with an average of 5.7 alleles per locus. The results are comparable to findings reported elsewhere. In assessing genetic diversity of 62 Sichuan wheat landraces using 114 SSR markers, Li et al. (2013) reported an average of 4.76 alleles per locus, which is slightly lower as compared to the findings herein. Wang et al. (2007) also reported a mean of 3.3 alleles per locus when 60 durum wheat accessions were analyzed using 26 SSR markers. Hazen et al. (2002) found 4.7 and 6.8 alleles per locus in two assays using 24 wheat accessions obtained from Shaanxi province.

Table 4. Number of alleles, range of allele size, polymorphic information content and Shannon-Weaver diversity index for genome B of wheat loci.

Locus	Number of alleles	Expected allele size (bp)	Range of allele sizes (bp)	Polymorphic information content	Shannon-weaver diversity index
Xbarc142-5B	10	208	175- 350	0.834	2.787
Xwmc810-5B	9	196	150- 300	0.868	2.533
Xgwm46-7B	9	187	160- 490	0.853	2.363
Xgwm273-1B	8	171	170- 490	0.875	2.179
Xwmc397-6B	8	160	155- 300	0.822	1.877
Xgwm210-2B	6	303	160- 550	0.760	1.645
Xgwm257-2B	7	190	180- 350	0.794	1.999
Xwmc317-2B	8	139	115- 290	0.804	2.059
Xgwm319-2B	3	170	110- 495	0.461	0.383
Xwmc291-3B	6	233	210- 350	0.806	1.480
Xgwm108-3B	3	135	110- 150	0.374	0.521
Xbarc232-5B	4	368	160- 390	0.689	1.056
Xgwm408-5B	4	182	175- 210	0.636	1.025
Xwmc75-5B	6	206	195- 500	0.787	1.830
Xwmc276-7B	2	292	250- 390	0.132	0.378
Total	93		110- 550	-	-
Mean	6.2		-	0.700	1.608

However, Spanic et al. (2012) reported a higher mean value of 8.44 alleles per locus following an assessment of 30 wheat genotypes using 24 SSR markers, while Jamalirad et al. (2012) found a mean value of 9.26 allelesper locus when 70 wheat genotypes were evaluated with 50 SSR markers. In some cases, the average number of alleles per locus as 12.06 (Abdellatif and Abouzeid, 2011) and 16.8 (Laido et al., 2013).

Genome A had the highest PIC value followed by genome B while the lowest PIC value was recorded in genome D. The highest PIC value in genome A was recorded for locus Xwmc382-2A (0.882). Kitavi et al. (2014) found a highest PIC of 0.86 in marker Xtxp 265 and a mean PIC value of 0.54, when 30 sorghum accessions were analyzed using 22 markers. Fu et al. (2006) reported a highest PIC value of 0.98 when 37 eSSR markers were tested on 75 Canadian hard red spring wheat. Salem et al. (2008) also obtained a highest PIC value of 0.816 for locus Xgwm437 when 15 SSR markers were analyzed in 9 wheat varieties. In another study, the highest PIC value of 0.93 was found with 45 markers on sixteen bread wheat samples (Cifci and Yagdi, 2012). The results herein are, therefore, consistent with previously reported findings.

Genetic diversity of wheat cultivars

Genetic diversity as measured by Shannon Weaver Index revealed that genome A was the most diverse followed by genome B and then genome D was the least (genome A>genome B>genome D). Similar results were reported by Li et al. (2013). Schuster et al. (2009) also found that genome A had the higher genetic diversity followed by genomes B and D, when analyzing 23 SSRs in 36 Brazilian cultivars. Furthermore, Zhang et al. (2011) reported a low level of polymorphism in D genome when testing DarT markers in 111 common wheat cultivars from northern China. Studies on molecular markers and many other agronomic traits have shown the genetic base of cultivated wheat (Parker et al., 2002; Prasad et al., 2000). The low genetic diversity of genome D has caused a delicate genetic basis for modern cultivated wheat (Jia et al., 2001; Zhang et al., 2002; Chen and Li, 2007).

However, the donor of genome D, *Aegilops squarrosa* was more diverse than cultivated wheat (Dudnikov, 2000; Pestsova et al., 2000; Gianibelli et al., 2001). It is believed that the low diversity of genome D emanated from evolution of hexaploid wheat. During evolution of hexaploid wheat, genomes A and B produced more tetraploid wheat including *Triticum turgidum*, *Triticum turani-cum*, *Triticum dicoccoides*, *Triticum dicoccum*, *Triticum polonicum*, *Triticum carthlicum* and *Triticum durum*. These tetraploid wheat species were able to cross with hexaploid wheat thereby enriching the genetic diversity of A and B genome species. The crossing was carried out with *Aegilops tauschii*, resulting in production of more hexaploid wheat. On the other hand, D genome species did not produce any tetraploid wheat species. This resulted in minor genes exchange in genome D and, consequently, led to the reduction of genetic diversity in this genome benefiting genomes A and B (Perugini, 2007; Wang et al., 2007).

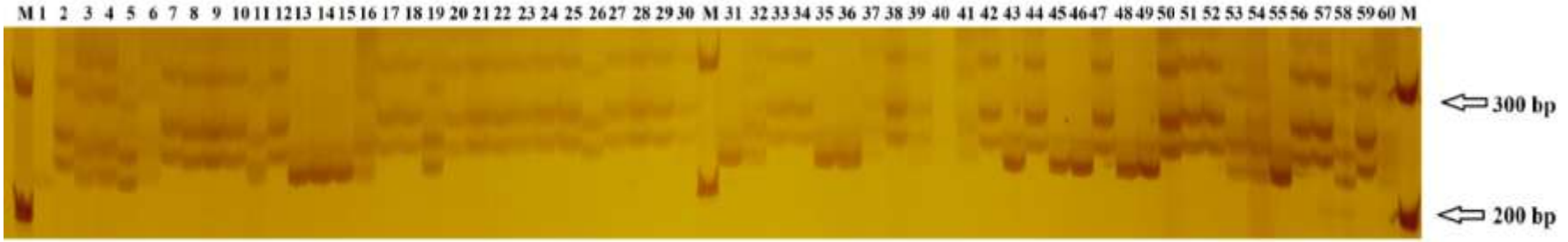

Figure 3. Amplified alleles of locus Xwmc445-2D for 60 wheat genotypes, M is 100 bp marker.

Table 5. Number of alleles, range of allele size, polymorphic information content (PIC) and Shannon-weaver diversity index (SI) for genome D of wheat loci.

Locus	Number of alleles	Expected allele size (bp)	Range of allele sizes (bp)	Polymorphic information content	Shannon-weaver diversity index
Xwmc445-2D	9	229	220- 380	0.815	2.543
Xwmc41-2D	3	163	150- 310	0.571	0.798
Xgwm174-5D	5	233	195- 300	0.746	1.241
Xgwm292-5D	6	214	205- 300	0.753	1.688
Xgwm583-5D	3	265	210- 380	0.317	0.744
Cfd57-5D	3	291	280- 300	0.228	0.429
Xbarc183-6D	4	179	175- 310	0.701	0.917
Xgwm325-6D	7	183	150- 250	0.776	1.992
Total	40		150- 380	-	
Mean	5.0		-	0.613	1.294

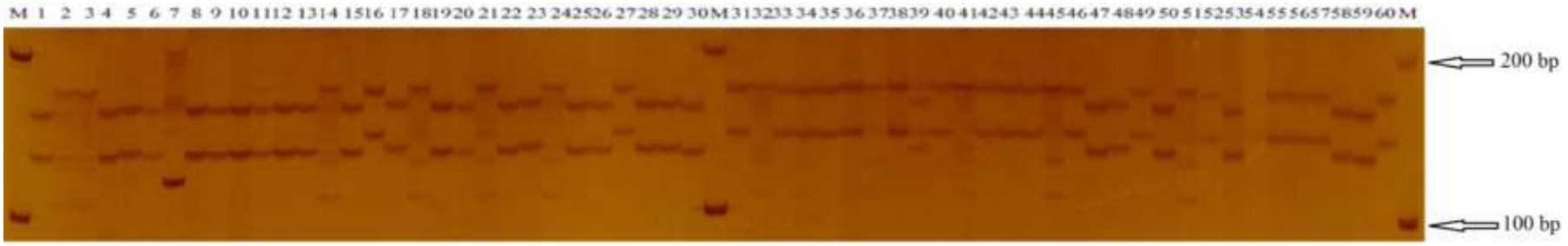

Figure 4. Amplified alleles on locus Xgwm344 for 60 wheat genotypes, M is 100 bp marker.

Table 6. Number of alleles, expected allele size, range of allele size, polymorphic information content (PIC) and Shannon-Weaver Diversity index (SI) for multiple loci in wheat genomes.

Marker	Chromosome	Number of alleles	Expected allele size (bp)	Range of allele sizes (bp)	Polymorphic Information Content	Shannon-Weaver Diversity Index
Xgwm344	7A, 7B	7	141	120-190	0.860	1.810
Xgwm526	2A, 2B, 7A, 7B	6	184	150-250	0.622	1.774
Xpsp3029	2A, 6A	6	180	160-450	0.638	1.319
Xgdm93	2A,2D,4B	6	135	125-175	0.653	1.548
Xwmc273	7A,7B,7D	7	279	190-400	0.787	1.795
Xpsp3003	1A,5A,7D	6	210	195-450	0.760	1.260
Xgwm111	7B, 7D	6	206	150-290	0.752	1.729
Xcfd39	4B,4D,5A	7	175	150-210	0.771	1.798
Xwmc289	5B,5D	5	200	175-490	0.767	1.217
Xcfd81	7D,5D,4D	4	283	170-310	0.710	0.742
Xgwm265	2A,4A	5	179	125-295	0.676	1.414
Xgwm296	2D,7D	5	182	150-220	0.681	1.129
Xgwm311	2A, 2B, 2D, 6B	4	120	120-225	0.629	0.416
Xgwm382	2A,2B,2D	4	86	80-190	0.645	0.726
Xgwm356	2A,6A,7A	4	216	195-290	0.588	0.999
Total		82		120-490	-	-
Mean		5.5		-	0.703	1.312

Table 7. Total number of alleles, range of allele size, polymorphic information content and Shannon-Weaver Diversity index for A, B and D genomes of wheat loci.

Genome	Number of alleles	Mean of alleles per genome	Range of allele sizes (bp)	Average polymorphic information content	Shannon-Weaver diversity index
A	61	6.1	90- 550	0.724	1.864
B	93	6.2	110- 550	0.700	1.608
D	40	5.0	150- 380	0.613	1.294
Multiple A, B, D	82	5.5	120- 490	0.703	1.312
Grand total	276	-	90- 550	-	-
Grand mean	5.7	5.7	-	0.685	1.520

Clustering of wheat cultivars

Cluster analysis using UPGMA method delineated the 60 cultivars into four clusters comprising of 3, 7, 9 and 41 cultivars. Within the major cluster consisting of 41 cultivars, several sub-clusters were formed, showing the effectiveness of microsatellite markers in genetic diversity assays. Several studies using SSR have resulted in successful clustering of wheat cultivars. This type of markers is very effective in delineating diversity based on parental source by grouping cultivars with similar pedigree information (Plaschke et al., 1995; Kitavi et al., 2014) as well as grouping based on agronomic characteristics and geographical origin (Naceur et al., 2012). Depending on the degree of diversity, two (Tahir, 2008; El-Bakatoushi, 2010) or three clusters (Hazen et al., 2002; Wang et al., 2007) can be formed following the UPGMA analysis. In addition, as high as 9 (Naceur et al., 2012) and 13 clusters (Schuster et al., 2009) have been reported in genetic diversity studies. Grouping into four clusters herein is, therefore, within the expected ranges as compared to previously reported results. The 41 cultivars grouped in cluster 3 should be of significant attention to breeders as this may offer a useful guide when doing rational deployment in the field. Most of the cultivars studied herein have not been fully utilized in breeding programs. As such, by belonging to one cluster, it shows that these 41 cultivars share genetic similarities from their parental source, which could make them easily compatible when transferring desirable traits.

Conclusion

The present study contributes further to developing suitable science-based approaches for molecular

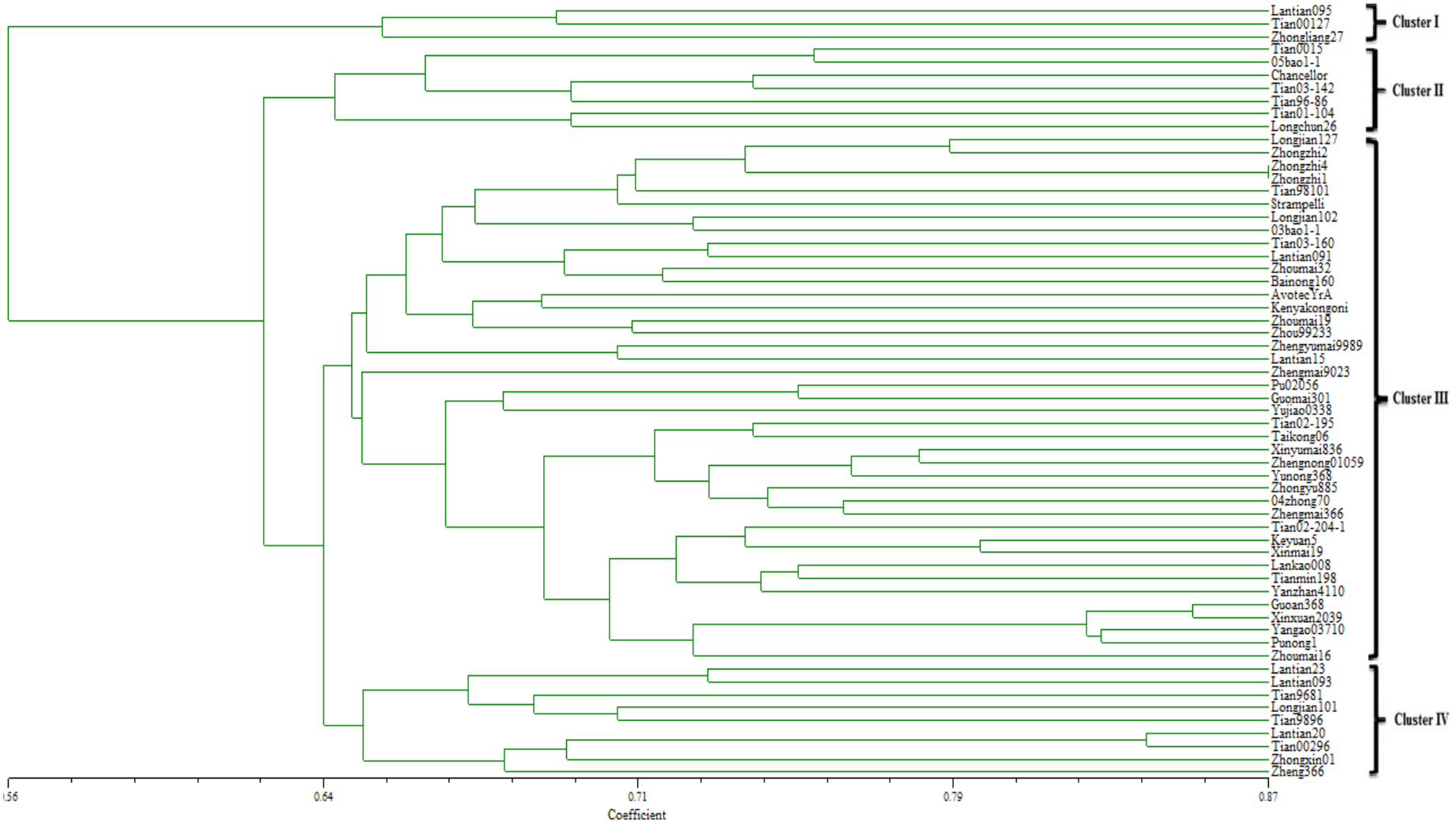

Figure 5. A dendrogram indicating genetic diversity of 60 wheat cultivars.

techniques in wheat. It offers an effective and reliable monitoring of wheat genetic diversity, which should be the starting point for future selection programs. Genome A was the most diverse and having most polymorphic loci as shown by SI and PIC values. Genome B was second, followed by genome D. Cluster analysis using UPGMA method delineated the 60 cultivars into four main clusters and several sub-clusters. Furthermore, it

was verified that microsatellite markers are effective in conducting genetic diversity studies as a total of 276 alleles were identified by using 48 wheat SSR markers with an average of 5.7 alleles per locus.

The present molecular genetic assay managed to shed more light on the genetic relatedness of wheat cultivars. This might assist breeders to set up the appropriate guidelines for successful breeding of wheat cultivars based on the established relationships.

Conflict of Interests

The authors have not declared any conflict of interests.

ACKNOWLEDGEMENT

The authors thank the Chinese Government through the Chinese Scholarship Council (CSC) for provision of funds to carry out this work.

REFERENCES

Abdellatif KF, Abouzeid HM (2011). Assessment of genetic diversity of Mediterranean bread wheat using Randomly Amplified Polymorphic DNA (RAPD) markers. J. Genet. Eng. Biotechnol. 9:157-163.

Abdullah NAP, Saleh GB, Putra ETS, Wahab ZB (2012). Genetic relationship among *Musa* genotypes revealed by microsatellite markers. Afr. J. Biol. 11(26):6769-6776.

Ahmed MF, Igbal M, Masood MS, Rabbani MA, Munir M (2010). Assessment of genetic diversity among Pakistani wheat (*Triticum aestivum* L.) advanced breeding lines using RAPD and SDS-PAGE. J. Biotechnol. 13:3.

Akhtar S, Anjum FM, Anjum MA (2011). Micronutrient fortification of wheat flour: Recent development and strategies. F. Res. Int. 44:652-659.

Chen G, Li L (2007). Detection of Genetic Diversity in Synthetic Hexaploid Wheats Using Microsatellite Markers. Agric. Sci. Cn. 6(12):1403-1410.

Cifci EA, Yagdi K (2012). Study of genetic diversity in wheat (*triticum aestivum*) varities using Random Amplified Polymorphic DNA (RAPD) analysis. Turkish J. Field Crops 17(1):91-95.

Corbellini M, Perenzin M, Accerbi M, Vaccino P, Borghi B (2002). Genetic diversity in bread wheat, as revealed by coefficient of parentage and molecular markers, and its relationship to hybrid performance. Euphytica 123:273-285.

Coventry DR, Gupta RK, Yadav A, Poswal RS, Chhokar RS, Sharma RK, Yadav VK, Gill SC, Kumar A, Mehta A, Kleemann SGL, Bonamano A, Cummins JA (2011). Wheat quality and productivity as affected by varieties and sowing time in Haryana, India. Field Crop Res. 123:214-225.

Dudnikov AJ (2000). Multivariate analysis of genetic variation in *Aegilops tauschii* from the world germplasm collection. Genet. Res. Crop Evol. 47:185-190.

Edwards A, Civitello A, Hammond HA, Caskey CT (1991). DNA typing and genetic mapping with trimeric and tetrameric tandem repeats. Am. J. Hum. Genet. 49:746-756.

El-Bakatoushi R (2010). Genetic diversity of winter wheat (*Triticum aestivum* L.) growing near a high voltage transmission line. Rom. J. Biol. Plant Biol. 55 (2):71-87.

FAO (2014). Food and Agricultural Organization of the United State(FAOSTAT) FAO, http://faostat3.fao.org/browse/Q/QC/E (Accessed 21 November 2014).

Friedrich C, Longin H, Reif CJ (2014). Redesigning the exploitation of wheat genetic resources. Trends Plant Sci. 19 (10):631-636.

Fu Y, Peterson GW, Gao JUL, Jia J, Richards KW (2006). Impact of plant breeding on genetic diversity of the Canadian hard red spring wheat germplasm as revealed by EST-derived SSR markers. Theor. Appl. Genet. 112:1239-1247.

Fu YB, Peterson GW, Richards KW, Somers D, DePauw RM, Clarke JM (2005). Allelic reduction and genetic shift in the Canadian hard red spring wheat germplasm released from 1845 to 2004. Theor. Appl. Genet. 110:1505-1516.

Fu ZQ, Cai YL, Yang YX (2001). Research on the relationship of cultivated land change and food security in China. J. Nat. Resour. 16: 313-319.

Gianibelli MC, Gupta RB, Lafiandra D, Margiottaa B, MacRitchie F (2001). Polymorphism of high M, glutenin subunits in *Triticum tauschii*: Characterization by chromatography and electrophoretic methods. J. Cereal Sci. 33:39-52.

Gupta PK, Varshney RK (2000). The development and use of microsatellite markers for genetics and plant breeding with emphasis on bread wheat. Euphytica 113:163-185.

Hazen SP, Zhu L, Kim H, Tang G, Ward RW (2002). Genetic diversity of winter wheat in Shaanxi province, China, and other common wheat germplasm pools. Genet. Res. Crop Evol. 49:437-445.

Jacob HJ, Lindpaintnesr K, Kusumir EL, Bunkery K, Mao IP, Gantenv D, Dzau J, Lander ES (1991). Genetic mapping of a gene causing hypertension in the stroke-prone spontaneously hypertensive rat. Cell 67:213-224.

Jamalirad S, Mohammadi SA, Toorchi M (2012). Assessing genetic diversity in a set of wheat (*Triticum aestivum*) genotypes using microsatellite markers to improve the yellow rust resistant breeding programs. Afr. J. Agric. Res. 7(48):6447-6455.

Jia JZ, Zhang ZB, Devos K, Gale MD (2001). RFLP map based genetic diversity in wheat *(Tritivum aestivum* L). Sci. Cn. 31:13-21.

Kalia RK, Rai MK, Kalia S, Singh R, Dhawan AK (2011). Microsatellite markers: an overview of the recent progress in plants. Euphytica 177:309-334.

Khodadadi M, Fotokian MH, Miransari M (2011). Genetic diversity of wheat (*Triticum aestivum* L.) genotypes based on cluster and principal component analyses for breeding strategies. Aust. J. Crop Sci. 5(1):17-24.

Kitavi MN, Kiambi DK, Haussman B, Semagn K, Muluvu G, Kairichi M, Machuka J (2014). Assessment of genetic diversity and pattern of relationship of West African sorghum accessions using microsatellite markers. Afr. J. Biol. 13(14):1503-1514.

Laido G, Mangini G, Taranto F, Gadaleta A, Blanco A, Cattivelli L, Marone D, Mastrangelo AM, Papa R, De Vita P (2013). Genetic Diversity and Population Structure of Tetraploid Wheats (*Triticum turgidum* L.) Estimated by SSR, DArT and Pedigree Data. Plos One 8(6):1-17.

Li W, Bian C, Wei Y, Liu A, Chen G, Pu Z, Liu Y, Zheng Y (2013). Evaluation of genetic diversity of Sichuan common wheat landraces in China by SSR markers. J. Integr. Agric. 12(9):1501-1511.

Li K, Yanga X, Liu Z, Zhang T, Lua S, Liu Y (2014). Low yield gap of winter wheat in the North China Plain. Europ. J. Agron. 59:1-12.

Liu H, Wanga ZH, Li F, Li K, Yang N, Yang Y, Huang D, Liang D, Zhao H, Mao H, Liub J, Qiu W (2014). Grain iron and zinc concentrations of wheat and their relationships to yield in major wheat production areas in China. Field Crops Res. 156:151-160.

Lu C, Fan L (2013). Winter wheat yield potentials and yield gaps in the North China Plain. Field Crops Res. 143:98-105.

Lu CH, Li XB, Tan MH (2007). China's farmland use: A scenario analysis of changes and trends. In: Spoor, M., Heerink, N., Qu, F. (Eds.), Dragons with Clay Feet? Transition, Sustainable Rural Resource Use, and Rural Environment in China and Vietnam. Rowman & Littlefield, Lexington Books, Lanham and Boston, USA. pp. 309-326.

Meti M, Samal KC, Bastia DN, Rout GR (2013). Genetic diversity analysis in aromatic rice genotypes using microsatellite based simple sequence repeats (SSR) marker. Afr. J. Biol. 12:4238-4250.

Mir RR, Kumar J, Balyan HS, Gupta PK (2012). A study of genetic diversity among Indian bread wheat (*Triticum aestivum* L.) cultivars released during last 100 years. Genet. Resour. Crop. Evol. 59:717-726.

Naceur AB, Chaabane R, El-Faleh M, Abdelly C, Ramla D, Nada A,

Sakr M, Naceur MB (2012). Genetic diversity analysis of North Africa's barley using SSR markers. J. Genet. Eng. Biotechnol. 10:13-21.
Parker GD, Fox PN, Langridge P, Chalmers K, Whan B, Canter PF (2002). Genetic diversity within Australian wheat breeding programs based on molecular and pedigree data. Euphytica 124:293-306.
Peng JH, Lapitan NLV (2005). Characterization of EST-derived microsatellites in the wheat genome and development of eSSR markers. Funct. Inter. Genom. 5:80-96.
Perugini LD (2007). Genetic Characterization of Wheat Germplasm with Resistance to Fusarium Head Blight (FHB) and Powdery Mildew. A dissertation submitted to the Graduate Faculty of North Carolina State University in partial fulfillment of the requirements for the degree of Doctor of Philosophy. pp. 2-123.
Pestsova EG, BBrner A, Roder MS (2000). Development of a set of *Triticum aestivum-Aegilops tauschii* introgression lines. Hereditas 135:2-3.
Plaschke J, Ganal MW, Roder MS (1995). Detection of genetic diversity in closely related bread wheat using microsatellite markers. Theor. Appl. Genet. 91:1001-1007.
Powell W, Morgante M, Andre C, Hanafey M, Vogel J, Tingey S, Rafalski A (1996). The comparison of RFLP, RAPD, AFLP and SSR (microsatellite) markers for germplasm analysis. Mol. Breed. 2:225-238.
Prasad M, Varshney RK, Kumar A (2000). A microsatellite marker associated with QTL for grain protein content on chromosome arm 2DL of bread wheat. Theor. Appl. Genet. 100:341-345.
Reynolds M, Bonnett D, Chapman SC, Furbank RT, Manes Y, Mather DE, Parry MAJ, 2011. Raising yield potential of wheat. I. Overview of a consortium approach and breeding strategies. J. Exp. Bot. 62:439-452.
Rohlf FJ (2000). NTSYS-pc. Numerical Taxonomy and Multivariate Analysis System: Version 2.1. Appl. Biostat. New York.
Romero G, Adeva C, Battad Z (2009). Genetic fingerprinting: Advancing the frontiers of crop biology research. Philipp. Sci. Lett. 2:8-13.
Roussel V, Koenig J, Beckert M, Balfourier F (2004). Molecular diversity in French bread wheat accessions related to temporal trends and breeding programmes. Theor. Appl. Genet. 108:920-930.
Royo C, Maccaferri M, A lvaro F, Moragues M, Sanguineti MC, et al. (2010). Understanding the relationships between genetic and phenotypic structures of a collection of elite durum wheat accessions. Field Crops Res. 119:91-105.
Ruiz M, Giraldo P, Royo C, Villegas D, Aranzana MJ (2012). Diversity and genetic structure of a collection of Spanish durum wheat landraces. Crop Sci. 52: 2262-2275.
Salem KFM, El-Zanaty AM, Esmail RM (2008). Assessing wheat (*Triticum aestivum* L.) genetic diversity using morphological characters and microsatallite markers. World J. Agric. Sci. 4(5):538-544.
Schuster I, Vieira ESN, da Silva GJ, Franco FDA, Marchioro VS (2009). Genetic variability in Brazilian wheat cultivars assessed by microsatellite markers. Genet. Mol. Biol. 32(3):557-563.
Shakeel M, Azam S (2012). Microsatellite based investigation of genetic diversity in 24 synthetic wheat cultivars. Afr. J. Biol. 11(72):13627-13632.
Singh R, Nagappan J, Tan S, Panandam JM, Cheah S (2007). Development of simple sequence repeat (SSR) markers for oil palm and their application in genetic mapping and fingerprinting of tissue culture clones. Asia Pac. J. Mol. Biol. Biotechnol. 15(3):121-131.
Spanic V, Buerstmayr H, Drezner G (2012). Assessment of genetic diversity of wheat genotypes using microsatellite markers. Period. Biol. 114(1):37-42.
Tahir NA (2008). Assessment of Genetic Diversity Among Wheat Varieties in Sulaimanyah using Random Amplified Polymorphic DNA (RAPD) Analysis. Jordan J. Biol. Sci. 1(4):159-164.
Tautz D (1989). Hypervariability of simple sequences as a general source for polymorphic DNA markers. Nucl. Acid Res. 17:6463-6471.
Tong C, Hall CAS, Wang H (2003). Land use change in rice, wheat and maize production in China (1961–1998). Agric. Ecosyst. Environ. 95:523-536.
Varshney RK, Marcel TC, Ramsay L, Russell J, Roder MS, Stein N, Waugh R, Langridge P, Niks RE, Graner A (2007). A high density barley microsatellite consensus map with 775 SSR loci. Theor. Appl. Genet. 114:1091-1103.
Wang H, Wang X, Chen P, Liu D (2007). Assessment of Genetic Diversity of Yunnan, Tibetan, and Xinjiang Wheat Using SSR Markers. J. Genet. Genom. 34(7):623-633.
Wang H, Wei Y, Yan Z, Zheng Y (2007). EST-SSR DNA polymorphism in durum wheat (*Triticum durum* L.) collections. J. Appl. Genet. 48(1): 35-42.
Zhang L, Liu D, Guo X, Yang W, Sun J, Wang D, Sourdille P, Zhang A (2011). Investigation of genetic diversity and population structure of common wheat cultivars in northern China using DArT markers. Bio-Med. Center Genet. 12(42):1471-2156.
Zhang XY, Li CW, Wang LF, Wang HM, You GX, Dong YS (2002). An estimation of the minimum number of SSR alleles needed to reveal genetic relationships in wheat varieties. Information from large-scale planted varieties and cornerstone breeding parents in Chinese wheat improvement and production. Theor. Appl. Genet. 106:112-117.
Zheng Y (2010). Detection of latent infection of wheat leaves caused by *Blumeria graminis* f. sp. *tritici* using Real-time PCR. MSc thesis. Chin. Acad. Agric. Sci. pp. 9-34.

academicJournals

Vol. 15(21), pp. 974-979, 25 May, 2016
DOI: 10.5897/AJB2015.14755
Article Number: 5DBCFD158606
ISSN 1684-5315

http://www.academicjournals.org/AJB

African Journal of Biotechnology

Full Length Research Paper

Fermentative intensity of L-lactic acid production using self-immobilized pelletized *Rhizopus oryzae*

Shuizhong Luo, Xuefeng Wu, Yu Zhu, Xingjiang Li, Shaotong Jiang and Zhi Zheng*

Key Laboratory for Agricultural Products Processing of Anhui Province, College of Food Science and Engineering, Institute of Agricultural Products Processing Technology, Hefei University of Technology, Hefei, Anhui, 230009, China.

Received 25 May, 2015; Accepted 28 April, 2016

L-Lactic acid is a promising three-carbon building-block chemical, widely used in the food, pharmaceutical, leather and textile industries and *Rhizopus oryzae* is an important filamentous fungus for the production of L-lactic acid with high optical purity. This study investigated the medium compositions for the maximum biomass cultivation of *R. oryzae* L-lactic acid fermentation, and optimized the operation parameters for semi-continuous repeated fermentation in a stirred tank fermentor using response surface method (RSM) analysis. The results indicated that a higher biomass cultivation of 3.750±0.05 g/L was achieved when the medium was composed of 12% (w/v) glucose, 0.4% (w/v) ammonium sulfate and 0.045% (w/v) monopotassium phosphate. The optimal fermentation conditions for the initial batch were as follows: the aeration was 0.75 L/(L·min), inoculation of germs was 11% and agitation speed was 560 rpm. The fermentative intensity of the initial batch and the sequentially repeated batches with self-immobilized pelletized *R. oryzae* were 2.162 g/(L·h) and 3.704 g/(L·h), respectively.

Key words: Self-immobilized, *Rhizopus oryzae*, pellet, lactic acid, response surface method (RSM).

INTRODUCTION

L-Lactic acid is a natural chemical, widely used as acidulant, flavor and preservative in the food, pharmaceutical and leather industries (Efremenko et al., 2006; Rojan et al., 2007; Gullon et al., 2008). It can further be polymerized into polylactic acid, which is applied in biodegrable plastics and textile fiber production. Currently, this environmental friendly polymer attracts the interest of the researchers all over the world (Zhang et al., 2007; Sauer et al., 2008; Maneeboon et al., 2010).

Rhizopus oryzae belongs to the family of filamentous fungus and possess excellent fermentation capability in producing optically pure L-(+)-lactic acid from biomass. The morphology of *R. oryzae* vary from dispersed filamentous clumps to pellet mycelia during the fermentative process to produce L-lactic acid when produced by submerged fermentation technology. Physical forms of fungal growth are influenced by the strain of fungi, nutrient compositions, spore concentrations, pH of medium, agitation and aeration (Yang et

*Corresponding author. E-mail: zhengzhi@hfut.edu.cn. Tel: 86-551-62901507. Fax: 86-551-62901507.

al., 1995; Zhou et al., 2000; Bai et al., 2003; Buyukkileci et al., 2006; Liu et al., 2008; Zhao et al., 2010; Mohamed et al., 2013). The relationship between morphology of *R. oryzae* and lactate productivity was investigated for the purpose of enhancing the conversion rate of glucose.

R. oryzae mycelia having floc and pellet forms are biologically active at the end of the submerged batch fermentation and these two forms have been demonstrated to be the feasible morphologies to achieve a more efficient conversion of lactate (Kosakai et al., 1997; Liu et al., 2006; Yu et al., 2007). Therefore, *R. oryzae* mycelia with floc and pellet forms have been utilized to produce L-lactic acid in the semi-continuous fermentation. In order to obtain *R. oryzae* mycelia with floc and pellet forms, an initial fermentation was performed, in which at the end, the liquid broth was drained and the mycelia were separated and kept in the fermentor for reuse. The fresh medium was then supplied into the fermentor, and the next cycle of fermentation started. This semi-continuous fermentation had some merits such as immobilization carrier-independence, lower viscosity of the suspension in favor of mass transfer, shorter fermentation cycles and good production stability (Yang et al., 1995; Yin et al., 1998; Yu et al., 2007). Pellet was an appropriate form for recycling use of *R. oryzae* mycelia (Liu et al., 2006, 2008; Liao et al., 2007).

In the semi-continuous fermentation, the biomass cultivation is another important factor besides the optimal medium compositions and operation parameters. Since more mycelia are formed in the initial batch fermentation, the fermentation period for the following repeated batches would be shortened and the productivity of lactate would be enhanced (Du et al., 1998; Yin et al., 1998; Martak et al., 2003; Yu et al., 2007; Liu et al., 2008; Wang et al., 2013).

In the present study, the medium constituents were optimized to form more biomass cultivation and the initial batch fermentation parameters in a 4 L fermentor were established by using response surface methodology. Moreover, the fermentative intensity of the initial and the repeated production of L-lactic acid were also comparatively investigated.

MATERIALS AND METHODS

Microorganism and media

R. oryzae As 3.819, a highly optical purity L-(+)-lactic acid producing strain was provided by China General Microbiological Culture Collection Center. The strain was maintained on potato dextrose agar (PDA) slants.

Seed culture

Spores of *R. oryzae* were grown on a PDA slant at 32°C for 3 days. They were collected with a platinum loop and suspended in sterilized distilled water. 1 mL (2% (v/v) of the sterile seed medium broth) of the fungi spore suspension (the concentrations were adjusted to be $5\times l0^6$ spores/mL) were inoculated into 50 mL sterile seed medium in a 250 mL flask with the composition of 12% (w/v) glucose, 0.4% (w/v) ammonium sulfate, 0.045% (w/v) monopotassium phosphate, 0.044% (w/v) heptahydrate and 0.025% (w/v) magnesium sulfate. The culture was incubated in a rotary shaker for 12 or 24 h (12 h for stirred tank fermentor, 24 h for flask) at 32°C, with the agitation speed of 200 rpm. 0.1% (w/v) sterilized calcium carbonate was added to the seed medium at the beginning of the culture in order to prevent a decrease in pH.

Biomass culture in the flask

5 mL (10% (v/v) of the sterile production medium broth) seed culture of *R. oryzae* As 3.819 was inoculated in 50 ml production medium in a 250 mL flask with the composition of 12% (w/v) glucose, 0.3% (w/v) ammonium nitrite, 0.0214% (w/v) dihydrogen phosphate ions with 1:1 of the concentration ratio of K^+/Na^+, 0.022% (w/v) heptahydrate, 0.025% (w/v) magnesium sulfate. The rotary shaker ran at the speed of 200 rpm under 32°C for 60 h, and the broth was taken out for the analysis of biomass content. 0.6% (w/v) sterilized calcium carbonate was added to the production medium at the beginning of the culture in order to prevent a decrease in pH.

Biomass culture in the fermentor

A 4 L stirred tank (Zhenjiang East Biotech Equipment and Technology Co., Ltd, P.R.C.) was used in this study. Culture was performed in a working volume of 2.5 L production medium at 32°C, 250 mL seed culture were inoculated. The fermentation was incubated at 32°C for 60 h, with the aeration rate of 1.0 L/(L·min) and agitation speed of 300 rpm. 0.6 % (w/v) sterilized calcium carbonate was added to the culture medium at the beginning of the fermentation in order to prevent a decrease in pH.

The repeated fermentation in the fermentor

In the end of each batch, the agitation and aeration were stopped, five sixth volume of broth was flowed out through a given outlet due to inner pressure from sterilized air and the vegetative mycelia were kept in the fermentor. Then, the sterile repeated fermentation medium was added into the tank to the volume of the initial batch with the composition of 8% (w/v) glucose, 0.3% (w/v) ammonium nitrite, 0.0075% (w/v) monopotassium phosphate, 0.022% (w/v) heptahydrate, 0.025% (w/v) magnesium sulfate and 0.4% (w/v) calcium carbonate. The operation parameters of the fermentor for the repeated batches were the same as the biomass culture in the fermentor.

Effect of glucose, ammonium sulfate and monopotassium phosphate on the fungal biomass cultivation

To optimize the medium compositions of glucose, ammonium sulfate and monopotassium phosphate (Wu et al., 2011) and obtain higher biomass cultivation, an orthogonal test of L_9 (3^4) with 3 replicates was designed. The factors and their levels of the orthogonal test were designed according to the single-factor experiments results in advance and listed in Table 1. The results were treated with the variance analysis of Pan and Chen (2008).

Effect of operation parameters on the fermentative intensity of initial batch in stirred tank

In order to study the productivity in the initial batch of fermentation

Table 1. Factors and levels for orthogonal test.

Factors	Levels of each factor		
	1	2	3
A: Glucose (%(w/v))	9	12	15
B: Ammonium sulfate (%(w/v))	0.25	0.4	0.55
C: Monopotassium phosphate (%(w/v))	0.015	0.030	0.045

Table 2. Factors and levels of the fermentation for the principle of central composite design of Box-Behnken.

Factor	Coding	Value of factor	Level
(A) aeration (L/(L·min))	X_1[a]	+1	1.0
		0	0.6
		-1	0.2
(B) inoculation (%(w/v))	X_2[b]	+1	15
		0	10
		-1	5
(C) agitation (rpm)	X_3[c]	+1	700
		0	500
		-1	300

[a] X_1 = (A-0.6)/(0.6-0.2), [b] X_2 = (B-10)/(10-5), [c] X_3 = (C-500)/(500-300).

in fermentor, an experiment based on the principle of central composite design Box-Behnken with three factors of aeration, inoculation and agitation speed, each in three levels was designed (Table 2) (Thana et al., 2008; Wei et al., 2009). The response surface and contour plots were generated to understand the interaction of various variables and then used to find the optimum operation parameters mainly affecting the response.

Analytical methods

L-lactic acid was extracted from the fermented medium with 0.5 M H_2SO_4, diluted with distilled-water and filtered through a 0.22 μm membrane. L-lactic acid concentration was analyzed by HPLC equipped with Purospher STAR C18 (Merck, USA) 250×4.6(5 μm) column and UV detector at 210 nm. The eluent was 5 mM H_2SO_4 with a flow rate of 0.8 mL/min. The residual glucose concentration was determined by the 3,5-dinitrosalicylate method. Dry biomass was monitored by harvesting culture samples, filtering and washing the mycelia with 0.01 M HCl to remove potential calcium carbonate, then washed with distilled water to pH 6. The washed mycelia were dried at 80°C until constant weight was achieved, then weighed (Zheng et al., 2009; Wu et al., 2011). The formula of calculating the productivity was:

$$I_F = \frac{D_L}{T}$$

Where I_F is the productivity (g/(L·h), D_L is the concentration of lactic acid (g/L) and T is the time of fermentation (h).

Statistical analysis

All the determinations reported in this work were carried out in triplicate and experiments were executed at least in duplicate; the results are given as the mean values. In the experiment design of Box-Behnken, the software package SAS9.0 (SAS Institute, USA) was used for experimental design, data analysis and the quadratic model building.

RESULTS AND DISCUSSION

Optimization of the culture medium for fungal biomass cultivation

Previous study showed that the concentrations of glucose, ammonium sulfate and monopotassium phosphate in medium showed significant impact on the biomass cultivation and formation of pellet. High biomass cultivation in initial batch fermentation and the pelletized mycelia are beneficial to the enhancement of lactic acid productivity (Liao et al., 2007). The effects of glucose, ammonium sulfate and monopotassium phosphate in the production medium on biomass were investigated by using orthogonal experiment $L_9(3^4)$ in Table 3.

With the computational analysis in Table 4, it was not difficult to show that the optimal combination was $A_2B_2C_3$ from the values of K_1, K_2 and K_3 (the sum of the results with each level) of each factor in Table 3, which was the same for the result of the directly analysis, and it means that when the glucose was 12% (w/v), ammonium sulfate was 0.4% (w/v) and monopotassium phosphate was 0.045% (w/v), the achieved L-lactic acid concentration reached the highest level. The results of verification tests with the optimum conditions from direct analysis and computational analysis (test results were not shown) suggested that the biomass was 3.750±0.05 g/L in triplicate experiments, and the optimized results were tested to be consistent with a further independent experiment.

Optimization of operation parameters of initial batch in stirred tank

The initial batch fermentation played an important role in the total process with self-immobilized *R. oryzae*. Under the feasible fermentation conditions, mycelia can flocculate into proper size of compact pellets together

Table 3. The optimization of the culture medium by orthogonal experimental design.

Number	Factor				Biomass
	A (%)	B (%)	C (%)	D	(g/L)
1	1 (9)	1 (0.25)	1 (0.015)	1	1.530
2	1	2 (0.4)	2 (0.030)	2	1.964
3	1	3 (0.55)	3 (0.045)	3	2.096
4	2 (12)	1	2	3	2.610
5	2	2	3	1	3.790
6	2	3	1	2	2.306
7	3 (15)	1	3	2	1.924
8	3	2	1	3	1.824
9	3	3	2	1	1.564
K_1	5.590	6.064	5.660	6.884	
K_2	8.706	7.578	6.138	6.194	
K_3	5.312	5.966	7.810	6.530	
$K_1/3$	1.863	2.021	1.887	2.295	T=19.604
$K_2/3$	2.902	2.526	2.046	2.065	
$K_3/3$	1.771	1.989	2.603	2.177	
SS	2.367	0.544	0.850	0.079	

Table 4. Analysis of variance for the orthogonal design.

Source of variance	SS	f	MS	F	Significant
A	2.367	2	1.184	29.827	**
B	0.544	2	0.272	6.860	*
C	0.850	2	0.425	10.705	*
E	0.079	2	0.040		
sum	3.840	8			

$F_{0.01}(2,8) = 8.65$, **, $F_{0.05}(2,8) = 4.46$,*, $F_{0.1}(2,8) = 3.11$, $F_{0.25}(2,8) = 1.66$. SS, sum of square for each factor; f, freedom; MS, mean of sum of square for each factor; F, F-ratios, e, total of error; sum, total of sum of square.

with the production terminal arrival and is promising for further fed-batch fermentation. The impacts of operation parameters of initial batch in stirred tank on lactic acid productivity are shown in Table 5. The following mathematical regression model in terms of coded factors was built to analyze the data by the SAS9.0 software.

$$Y=2.09+0.25X_1+0.13X_2+0.069X_3-0.31X_1^2-0.042X_1X_2-0.02X_1X_3-0.24X_2^2+0.028X_2X_3-0.11X_3^2$$

And the best optimal regression equation was as follows.

$$Y=2.09+0.25X_1+0.13X_2+0.069X_3-0.31X_1^2-0.042X_1X_2-0.24X_2^2-0.11X_3^2$$

Where *Y* is the response, productivity of the lactic acid, X_1, X_2 and X_3 are the factors of aeration, inoculation and agitation speed, respectively.

The analysis results showed that there was a highly significant relationship of multiple regression between the dependent variable and the independent variable (R^2=0.9877). This indicated that the experiment was designed reliably. The pictures of response surface was drawn based on the analysis data of RSM, which visually showed the effects of aeration and inoculation of germs (Figure 1). An order partial derivative of the nonlinear regression model was based on the optimum of each independent variable, and then let the result to be zero, to obtain the maximum of the surface,

$$0.25-0.62X_1-0.042X_2=0$$

$$0.13-0.042X_1-0.48X_2=0$$

$$0.069-0.22X_3=0$$

The results calculated from the equations are: X_1=0.387, X_2=0.237 and X_3=0.314. These numerical values

Table 5. Arrangements and results of the fermentative strength by the principle of central composite design of Box-Behnken.

Number	X_1	X_2	X_3	Y (productivity) (g/(L·h))
1	-1	-1	0	1.15
2	-1	1	0	1.51
3	1	-1	0	1.66
4	1	1	0	1.85
5	0	-1	-1	1.58
6	0	-1	1	1.64
7	0	1	-1	1.79
8	0	1	1	1.96
9	-1	0	-1	1.29
10	1	0	-1	1.89
11	-1	0	1	1.49
12	1	0	1	2.01
13	0	0	0	2.10
14	0	0	0	2.08
15	0	0	0	2.08

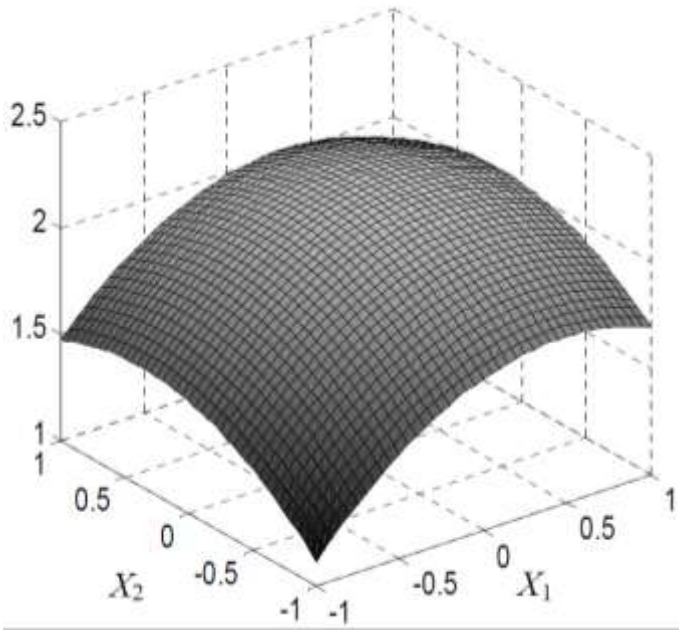

Figure 1. 3D graph of response surface for fermentative intensity (Y) of L-lactic acid between the aeration (X_1) and inoculation of germs (X_2) at agitation speed (X_3=0).

corresponded to the fermentation conditions of aeration of 0.755 L/(L·min), inoculation of 11.18%, and agitation speed of 562.8 rpm. The estimated productivity (Y) upon these solutions was (2.16±0.12) g/(L·h). Based on the feasible of operation, the aeration was 0.75 L/(L·min), the inoculation was 11%, and agitation speed of 560 rpm. The productivity of testing experiment was 2.10±0.05) g/(L·h), which was about 5% of relative error when g/(L·h), which was about 5% of relative error when compared with model predicted values. This showed that using RSM to realize better fermentation parameters was feasible.

Productivity of repeated batches fermentation

During the semi-continuous fermentation by self-immobilized *R. oryzae*, five sixth volume of the fermented broth was drained, the pellets remained and fresh medium was supplied to reach the former volume. The semi-continuous fermentation conditions were kept as those of the initial batch: aeration 0.75 L/(L·min), inoculation 11% and agitation speed off 560 rpm. Under these conditions, the mycelia morphology was maintained as pellet form with diameter of about 1.5 mm, except for a small portion adsorbed to the baffle and impellers. The L-lactic acid productivity was stable at 3.704 g/(L·h).

The fermentative intensity is an important index for the evaluation of fermentation technology and product cost. As for L-lactic acid production by *R. oryzae*, the fermentative intensity of batch submerged fermentation varied from 0.70 g/(L·h) (Liu et al., 2006), 1.80 g/(L·h) (Park et al., 1998) to 2.73 g/(L·h) (Yu et al., 2007). The combination of immobilization technology and semi-continuous fermentation is a good way to enhance the fermentative intensity. Production of lactic acid from glucose with loofa sponge immobilized *R. oryzae* RBU2-10 showed that repeated batch fermentation could be carried out for 10 cycles and the maximum productivity (1.84 g/(L·h)) was obtained at the third cycle of fermentation (Ganguly et al., 2007). The average calculated productivity of L-Lactic acid production from glucose with a semi-batch process using poly(vinyl alcohol)-cryogel-entrapped *R. oryzae* was 2.8±0.4 g/(L·h) (Efremenko et al., 2006). The fungal mycelia of *R. oryzae* NRRL 395 was immobilized on cotton cloth in a rotating fibrous-bed bioreactor to produce L-lactic acid from glucose and a high productivity of 2.50 g/(L·h) was obtained in fed-batch fermentation (Tay and Yang, 2002). In this study, L-lactic acid production using self-immobilized pelletized *R. oryzae* and fed-batch fermentation can reach a higher productivity of 3.704 g/(L·h).

Conclusion

The biomass was achieved (3.75±0.05 g/L) in flask with the optimum medium by self-immobilized *R. oryzae*. Combination theoretical analysis with the actual test, the best fermentation parameters of stirred tank fermentations by self-immobilized *R. oryzae* was: aeration 0.75 L/(L·min), inoculation 11%, agitation speed 560 rpm. Under these conditions, the L-lactic acid productivity of the initial patch was 2.10±0.05 g/(L·h). In the repeated semi-continuous fermentation with the same fermentation conditions as the initial batch, the mycelia morphology was kept in proper pellet size, and the L- lactic acid

productivity was sustained at 3.704 g/(L·h), which is higher than that of other reports.

Conflict of interests

The authors have not declared any conflict of interests.

ACKNOWLEDGEMENTS

Financial support from National Natural Science Foundation of China (31171741, 31371728, 31101352, 31470002), Anhui Provincial Natural Science Foundation (1408085MKL17), Young Teachers Innovative Project of Hefei University of Technology (2014HGQC0008) and the Key Laboratory for Agricultural Products Processing of Anhui Province, the Institute of Agricultural Products Processing Technology, the School of Biotechnology and Food Engineering, Hefei University of Technology are gratefully acknowledged.

REFERENCES

Bai DM, Jia MZ, Zhao XM, Ban R, Shen F, Li XG, Xu SM (2003). L(+)-lactic acid production by pellet-form *Rhizopus oryzae* R1021 in a stirred tank fermentor. Chem. Eng. Sci. 58:785-791.

Buyukkileci AO, Hamamci H, Yucel M (2006). Lactate and ethanol productions by *Rhizopus oryzae* ATCC 9363 and activities of related pyruvate branch point enzymes. J. Biosci. Bioeng. 102:464-466.

Du JX, Cao NJ, Gong CS, Tsao GT (1998). Production of L-lactic acid by *Rhizopus oryzae* in a bubble column fermentor. Appl. Biochem. Biotechnol. 70-72:323-329.

Efremenko EN, Spiricheva OV, Veremeenko DV, Baibak AV, Lozinsky VI (2006). L(+)-lactic acid production using poly(vinyl alcohol)-cryogel-entrapped *Rhizopus oryzae* fungal cells. J. Chem. Technol. Biotechnol. 81:519-522.

Ganguly R, Dwivedi P, Singh RP (2007). Production of lactic acid with loofa sponge immobilized *Rhizopus oryzae* RBU2-10. Bioresour. Technol. 98:1246-1251.

Gullon B, Yanez R, Alonso JL, Parajo JC (2008) L-lactic acid. production from apple pomace by sequential hydrolysis and fermentation. Bioresour. Technol. 99:308-319

Kosakai Y, Park YS, Okabe M (1997). Enhancement of L(+)-lactic acid production using mycelial flocs of *Rhizopus oryzae*. Biotechnol. Bioeng. 55:461-470.

Liao W, Liu Y, Frear C, Chen SL (2007). A new approach of pellet formation of a filamentous fungus-*Rhizopus oryzae*. Bioresour. Technol. 98:3415-3423.

Liu Y, Liao W, Chen SL (2008). Co-production of lactic acid and chitin using a pelletized filamentous fungus *Rhizopus oryzae* cultured on cull potatoes and glucose. J. Appl. Microbiol. 105:1521-1528.

Liu Y, Liao W, Liu CB, Chen SL (2006). Optimization of L-(+)-lactic acid production using pelletized filamentous *Rhizopus oryzae* NRRL 395. Appl. Biochem. Biotechol. 131:844-853.

Maneeboon T, Vanichsriratana W, Pomchaitaward C, Kitpreechavanich V (2010). Optimization of lactic acid production by pellet-form *Rhizopus Oryzae* in 3-L airlift bioreactor using response surface methodology. Appl. Biochem. Biotechnol. 161:137-146.

Martak J, Schlosser S, Sabolova E, Kristofikova L, Rosenberg M (2003). Fermentation of lactic acid with *Rhizopus arrhizus* in a stirred tank reactor with a periodical bleed and feed operation. Process. Biochem. 38:1573-1583.

Mohamed AA, Tashiro Y, Sonomoto K (2013). Recent advances in lactic acid production by microbial fermentation processes. Biotechnol. Adv. 31:877-902.

Pan LJ, Chen JQ (2008). Design of experiment and data processing. Southeast University Press, Nanjing. pp. 56-63, 100-173.

Park EY, Kosakai Y, Okabe M (1998). Efficient production of L-(+)-lactic acid using mycelial cotton-like flocs of *Rhizopus oryzae* in an air-lift bioreactor. Biotechnol. Progr. 14:699-704.

Rojan PJ, Nampoothiri KM, Pandey A (2007). Fermentative production of lactic acid from biomass: an overview on process developments and future perspectives. Appl. Microbiol. Biotechnol. 74:524-534.

Sauer M, Porro D, Mattanovich D, Branduardi P (2008). Microbial production of organic acids: expanding the markets. Trends Biotechnol. 26:100-108.

Tay A, Yang ST (2002). Production of L(+)-lactic acid from glucose and starch by immobilized cells of *Rhizopus oryzae* in a rotating fibrous bed bioreactor. Biotechnol. Bioeng. 80:1-12.

Thana P, Machmudah S, Goto M, Sasaki M, Pavasant P, Shotipruk A (2008). Response surface methodology to supercritical carbon dioxide extraction of astaxanthin from *Haematococcus pluvialis*. Bioresour. Technol. 99:3110-3115.

Wang P, Chen Z, Li J, Wang L, Gong G, Zhao G, Liu H, Zheng Z (2013). Immobilization of *Rhizopus oryzae* in a modified polyvinyl alcohol gel for L(+)-lactic acid production. Ann. Microbiol. 63:957-964.

Wei ZJ, Liao AM, Zhang HX, Liu J, Jiang ST (2009). Optimization of supercritical carbon dioxide extraction of silkworm pupal oil applying the response surface methodology. Bioresour. Technol. 100:4214-4219.

Wu XF, Jiang ST, Liu M, Pan LJ, Zheng Z, Luo SZ (2011). Production of L-lactic acid by *Rhizopus oryzae* using semi-continuous fermentation in bioreactor. J. Ind. Microbiol. Biotechnol. 38:565-571.

Yang CW, Lu ZJ, Tsao GT (1995). Lactic acid production by pellet-form *Rhizopus oryzae* in a submerged system. Appl. Biochem. Biotechnol. 51:57-71.

Yin PM, Yahiro K, Ishigaki T, Park Y, Okabe M (1998). L(+)-lactic acid production by repeated batch culture of *Rhizopus oryzae* in air-lift bioreactor. J. Ferment. Bioeng. 85:96-100.

Yu MC, Wang RC, Wang CY, Duan KJ, Sheu DC (2007). Enhanced production of L(+)-lactic acid by floc-form culture of *Rhizopus oryzae*. J. Chin. Inst. Chem. Eng. 38:223-228.

Zhang ZY, Jin B, Joan MK (2007). Production of lactic acid from renewable materials by *Rhizopus* fungi. Biochem. Eng. J. 35:251-263.

Zhao B, Wang LM, Li FS, Hua D, Ma C,Ma Y, Xu P (2010). Kinetics of D-lactic acid production by *Sporolactobacillus* sp. strain CASD using repeated batch fermentation. Bioresour. Technol. 101:6499-6505.

Zheng Z, Luo SZ, Li XJ, Wu XF, Pan LJ, Jiang ST (2009). Screening of allyl alcohol resistant mutant of *Rhizopus oryzae* and its fermentation characterization. Afr. J. Biotechnol. 8:280-284.

Zhou Y, Du JX, Tsao GT (2000). Mycelial pellet formation by *Rhizopus oryzae* ATCC 20344. Appl. Biochem. Biotechnol. 84:779-789.

academicJournals

Vol. 15(21), pp. 980-988, 25 May, 2016
DOI: 10.5897/AJB2015.14886
Article Number: 2CB7CE558608
ISSN 1684-5315

http://www.academicjournals.org/AJB

African Journal of Biotechnology

Full Length Research Paper

Effect of pH, various divalent metal ion and different substrates on glucoamylase activity obtained from *Aspergillus niger* using amylopectin from tiger nut starch as carbon source

Ezugwu A. L.*, Ottah, V. E., Eze, S. O. O. and Chilaka F. C.

Department of Biochemistry, University of Nigeria Nsukka, Enugu State, Nigeria.

Received 24 July, 2015, Accepted 9 November, 2015.

Glucoamylases were obtained from *Aspergillus niger* using amylopectin from tiger nut starch as carbon source on the 5th (GluAgTN5) and 12th day (GluAgTN12) of fermentation. The optimal pH for GluAgTN5 at 55°C were 6.5, 7.0, 6.0 while that for GluAgTN12 were 8.5, 6.0, 7.5 at 50°C using cassava, guinea corn and tiger nut starch as substrates, respectively. The enzyme activity in GluAgTN5 was enhanced by Ca^{2+} and Fe^{2+} while Zn^{2+} and Co^{2+} had inhibitory effects on the enzyme activity. $Mn^{2+}$and Pb^{2+}, however completely inactivated the enzyme. Enzyme activity in GluAgTN12 was enhanced by Ca^{2+} while $Co^{2+}$and Zn^{2+} had inhibitory effects, Fe^{2+}, Mn^{2+} and Pb^{2+} completely inactivated the enzyme. The Michealis-Menten constant, K_m and maximum velocity, V_{max} obtained from Line-Weaver-Burk plot of initial velocity data at different substrate concentrations were 222 mg/ml and 500 µmol/min, 291 mg/ml and 1000 µmol/min, 137.5 mg/ml and 500 µmol/min using cassava, guinea corn and tiger nut starch as substrate, respectively for GluAgTN5. While that for GluAgTN12 were 176.6 mg/ml and 100 µmol/min, 491 mg/ml and 1000 µmol/min, 131.5 mg/ml and 500 µmol/min using cassava, guinea corn and tiger nut starch as substrate, respectively.

Key words: Glucoamylase, pH, metal ions, *Aspergillus niger*, tiger nut starch, amylopectin.

INTRODUCTION

Glucoamylase (α-1, 4-glucan-glucohydrolases, EC 3.2.1.3) is an exoenzyme that hydrolyzes 1,4-alpha-glycosidic bonds from the non-reducing ends of starch and 1,6-alpha-glucsidic linkages in polysaccharides yielding glucose as the end-product, which serves as a feedstock for biological fermentations (Kumari et al., 2013). Glucoamylase from *Aspergillus niger* has been shown to be an acidic enzyme that shows highest activity within a pH range of 2.0 to 4.0 (Imran et al., 2012), whereas glucoamylase from *Aspergillus candidus* and *Rhizopus* lost their activities and conformation at this pH range (Shenoy et al., 1985). Glucoamylase from *Aspergillus oryzae* showed maximum activity at pH 5.0 (Parbat and Singhal, 2011), unlike α-amylase which

*Corresponding author. Email: arinzelinus.ezugwu@gmail.com. Tel: +2348063743436.

exhibited maximum activity at neutral pH (pH 7.0) (Acharya et al., 2014). The pH value at which an enzyme exhibits highest activity is called “optimum pH” (Devasena, 2010). Changes in pH can result in the protonation or deprotonation of a specific side groups at the enzyme’s active site thereby changing its chemical features. For instance, the deprotonation of carboxyl termini could result in a potential loss of interaction with an adjacent subunit, changing the enzyme conformation which could cause a decrease in substrate affinity, or a complete loss of activity. Changes in pH can however, be utilized by enzymes for regulation or protein function. Variations in pH can influence the following characteristics of an enzyme; the binding of the substrate to the enzyme, the ionization states of the amino acid residues at the catalytic site of the enzyme, the ionization state of the substrate and variation in protein structure or complete denaturation of the enzyme (which occurs at extreme pH values) (Berg, 2007).

Glucoamylase obtained from *A. niger* in solid state fermentation was reported to be metalloenzyme and its activity has been shown to be increased by Mn^{2+} and Fe^{2+} (Selvakumar et al., 1996). Yusaku and Hiroshi (1996) reported that Ca^{2+} and Zn^{2+} ions increased glucoamylase activity from *Rhizopus sp*. Glucoamylase from *Aspergillus flavus* was activated by Mn^{2+}, Co^{2+} and Ba^{2+} and was inhibited by Hg^{2+}, Fe^{3+}, Zn^{2+} and Cu^{2+} (Koç, and Metin, 2010). Mn^{2+} and Mg^{2+} were shown to increase the activity of glucoamylase from *Rhizopus nigricans* while Fe^{2+}, Zn^{2+} and Cu^{2+} reduced glucoamylase activity (Jambhulkar, 2012). Metal ions affect enzyme catalysis by the formation of a nucleophilic hydroxide ion at neutral pH by activating a bound water molecule, thus stabilizing the negative charges that are formed which are highly susceptible to neucleophilic attack (Fersht, 1985). This study is aimed at establishing the effect of metal ion concentrations in relation to pH changes and different substrate concentrations on the activity ofglucoamylases obtained from *A. niger* using amylopectin from tiger not starch as carbon source.

MATERIALS AND METHODS

Collection of plant materials

Plant materials were obtained from Ogige main market in Nsukka Local Government Area of Enugu State, Nigeria.

Processing of tiger nut and guinea corn starch

The tiger nut and guinea corn starch were processed using the method described by Agboola et al. (1990) with the following modifications. The seeds were sun dried and ground to fine flour. 300 g of the flours were suspended in 3 L of distilled water for 24 h. The suspended flour was sieved using muslin cloth. The extracted starch was allowed to sediment for 4 h at room temperature. The supernatant was decanted off and the starch washed with 3 L of distilled water twice and finally allowed to stand for 4 h. The supernatant was then decanted and the resulting wet starch was sun dried and then packaged in an air tight container and stored at room temperature.

Processing of cassava starch

Cassava starch was processed using the method described by Corbishley and Miller (1984) with the following modifications. Freshly harvested cassava tubers were peeled, washed clean and grated. The grated cassava (1.2 kg) was soaked in 4 L of distilled water for 1 h after which it was sieved (3 times) with muslin cloth. This was allowed to stand for 4 h and the supernatant decanted. The isolated wet starch was sun dried and packaged in plastic air tight container, labelled and kept in a cool, dry place.

Fractionation of tiger nut starch into amylose and amylopectin

Fractionation of amylose and amylopectin was carried out by following the general procedure of Sobukola and Aboderin (2012). This consists of heating and stirring starch dispersion (0.8%, w/v in water) in water bath at 100°C until starch is gelatinized. Starch solutions were filtered using filter paper to remove insoluble residues, and the pH adjusted to 6.3 using phosphate buffer. The solution was stirred in a boiling water bath for 2 h to disperse the starch molecules. Thereafter, n-Butyl alcohol was added (20%, v/v), and the solution was stirred at 100°C for 1 h, followed by cooling to room temperature over a period of 24 to 36 h. Amylose butyl alcohol complex crystals was formed and precipitated during cooling, and was separated by filtration. The amylopectin remaining in the supernatant was recovered by adding excess methyl alcohol.The percentage yield of amylopectin was calculated using:

$$\%\ \text{amylopecting} = \frac{\text{Amount of amylopectin}}{\text{ammount of starch}} \text{x}100$$

Isolation of glucoamylase producing fungi

Glucoamylase producing fungi were isolated by adopting the method of Martin et al. (2004) as modified by Okoye et al. (2013). Tiger nut starch was fractionated into amylose and amylopectin. The wet amylopectin was left open on shelve to allow micro-organisms to grow on it. A loop of each organism was streaked onto potato dextrose agar PDA under the flame of Bunsen burner. Streaks were made from each side of the plate, marking an initial point, with sterilization of the wire loop after each side has been completed. The plates were thereafter incubated at 35°C till visible colonies were observed. All morphological contrasting colonies were purified by repeated streaking and sub-culturing on separate plates. This process was continued till pure fungal culture was obtained. Pure fungal isolates were maintained on potato dextrose agar (PDA) slopes or slants as stock cultures. PDA media were prepared according to the manufacture’s description. In the description, 3.9 g of PDA powder was weighed and added in small volume of distilled water and made up to 100 ml. The medium was autoclaved at 121°C, 15 psi for 15 min. It was allowed to cool to about 45°C and then poured into Petri dishes and allowed to gel. The plates were then incubated in a B and T Trimline incubator at 37°C for 24 h to check for sterility. Three days old pure cultures were examined. The colour, texture, nature of mycelia or spores and growth patterns were also observed. The three day old pure cultures were used in preparing microscopic slides. A little bit of the mycelia was dropped on the slide and a drop of lactophenol blue was added to it. A cover slip was placed over it and examination was performed under the light microscope at X400 magnification.

Identification was carried out by relating features and the micro-graphs to “Atlas of mycology” by Barnett and Hunter (1972).

Glucoamylase production

Glucoamylase was produced by adopting the method described by Bagheri et al. (2014) with the following modifications. The 250 ml Erlenmeyer flask contained 100 ml of sterile cultivation medium optimized for glucoamylase with 0.3% ammonium sulphate $(NH4)_2SO_4$, potassium dihydrogen phosphate (0.6% KH_2PO_4), magnesium sulphate hepta hydrate0.1% ($MgSO_4.7H_2O$), 0.01% ferrous sulphate hepta hydrate ($FeSO_4.7H_2O$), 0.1 %calcium chloride ($CaCl_2$) and 1% amylopectin from tiger nut starch. The flask was stoppered with aluminum foil and autoclaved at 121°C, 15 psi for 15 min. From the PDA slants, fresh plates were prepared and three day old cultures were used to inoculate the flasks. In every sterile flask, two discs of the respective fungal isolates were added using a cork borer of diameter 10 mm and then plugged properly. The culture was incubated for 14 days on MK V orbital shaker (150 rpm) at room temperature (30°C). At each day of harvest, flasks were selected from the respective groups and mycelia biomass separated by filtration using filter paper. Each day, the filtrate was analyzed for glucoamylase activity and extracellular protein concentration till the 14^{th} day of fermentation. After the 14 days pilot SmF studies, 5^{th} and 12^{th} day of fermentation were chosen for mass production of enzymes coded GluAgTN5 and GluAgTN12, respectively.

Glucoamylase assay

Glucoamylase activity was assayed by the method of Parbat and Singhal (2011) with the following modifications. 0.5 ml of the enzyme was added into a clean test tube followed by 0.5 ml 1% soluble starch solution in 50 mM acetate buffer (pH 5.5) at 50°C and was allowed to stand for 20 min. 1 ml of 3, 5-dinitrosalicyclic acid (DNSA) reagent was added and boiled for 10 min to stop the reaction. 1 ml of sodium potassium tartarate was added to stabilize the red colour produced. The mixture was then allowed to cool and the glucose released was measured using a JENWAY 6405 UV/VIS spectrophotometer (Beckman/Instruments, Inc., Huston Texas) at 540 nm. Absorbance values were converted to glucose concentrations by extrapolation from the glucose standard curve. Glucoamylase activity unit (U) was expressed as the amount of enzyme releasing one µ mole of glucose equivalent per minute per ml.

α-amylase assay

The α-amylase activity was assayed by adopting the method of Bernfield (1955). The reaction mixture contained 0.5 ml of the enzyme preparation and 0.5 ml of 1% w/v starch solution in 20 mM sodium phosphate buffer (pH 7.0). The reaction mixture was incubated at 55°C for 60 min after which the reaction was stopped by addition of 1 ml of 3, 5-dinitrosalicyclic acid (DNSA) reagent and boiling for 10 min. 1 ml of sodium potassium tartarate was added to stabilize the red colour produced. The mixture was then allowed to cool and the glucose released was measured using a JENWAY 6405 UV/VIS spectrophotometer (Beckman/Instruments, Inc., Huston Texas) at 600 nm. α-Amylase activity unit (U) was expressed as the amount of enzyme releasing 1 µ mole of reducing end groups (maltose) per minute under assay conditions.

Protein determination

Protein content of the enzyme was determined by the method of Lowry et al. (1951), using Bovine Serum Albumin as standard.

Purification of crude glucoamylase

Ammonium sulphate saturations of 20 and 70% were found suitable to precipitate protein with highest glucoamylase activity in GluAgTN5 and GluAgTN12, respectively.The crude enzyme preparation was made up to 20 and 70% ammonium sulphate saturation with solid $(NH_4)_2SO_4$ for GluAgTN5 and GluAgTN12, respectively. This was kept at 4°C for 30 h, thereafter it was centrifuged with Cole-palmer VS-13000 micro centrifuge at 4000 rpm for 30 min. The precipitate was collected and redisolved in 20 mM acetate buffer pH 5.5. The glucoamylase activity and protein were determined as described above.

Gel filtration

A volume (20 ml) of the precipitated enzyme was introduced into a (50 × 2.5 cm) gel chromatographic column and subjected to gel filtration using sephadex G-100 pre-equilibrated with 0.02 M sodium acetate buffer pH 5.5. Fractions were collected at a flow rate of 5 ml/20 min. The protein concentration of each fraction was monitored using a JENWAY 6405 UV/VIS spectrophotometer (Beckman/Instruments, Inc. Huston Texas) at 280 nm. The glucoamylase activity of each fraction was assayed with the active fractions pooled together and stored at -10˚C.

Effect of pH

The optimum pH for enzyme activity was determined using 0.02 M sodium acetate buffer (pH 3.5 - 5.5), phosphate buffer (pH 6.0 - 7.5) and Tris-HCl buffer (pH 8.0 - 10.0) at intervals of 0.5. The reaction mixture contains 0.5 ml of starch solution (1%) and 0.5 ml of enzyme solution and the enzyme activity was assayed as described above.

Effect metal ions concentration

The concentrations, 20, 30, 40 and 50 mM of metal salts ($ZnCl_2$, $CoCl_2$, $MnCl_2$, $FeCl_2$, $PbCl_2$ and $CaCl_2$) were prepared in 20 mM sodium acetate. Each of the reaction mixtures contains 0.5 ml of enzyme solution, 0.5 ml of starch solution (1%) and 1 ml of metal ion solutions (Ca^{2+}, Mg^{2+}, Mn^{2+}, Fe^{2+}, $Co^{2+}$and Zn^{2+}). The mixtures were incubated for 20 min at the predetermined optimal pH and temperatures. To study the effect of metal ionson glucoamylase activity/stability, the reaction was carried out with and without metal ions. In all the above experiments, the enzyme activity was calculated as the average of three independent sets of experiments and the standard deviation in all cases was negligible.

Determination of kinetic parameters

The effect of substrate concentration on glucoamylase activity was determined by incubating 0.5 ml of enzyme with 10, 20, 30, 40, 50, 60, 70, 80, 90, and 100 mg/ml of starch solution for 20 min at the respective predetermined optimal pHs and temperatures. The glucoamylase activity was assayed as described above using starch from cassava, guinea corn and tiger nut starch as substrate. The V_{max} and K_m values of the enzyme were determined using the Line-Weaver-Burk plot of initial velocity data.

RESULTS AND DISCUSSION

The percentage yield of amylopectin fractionated from

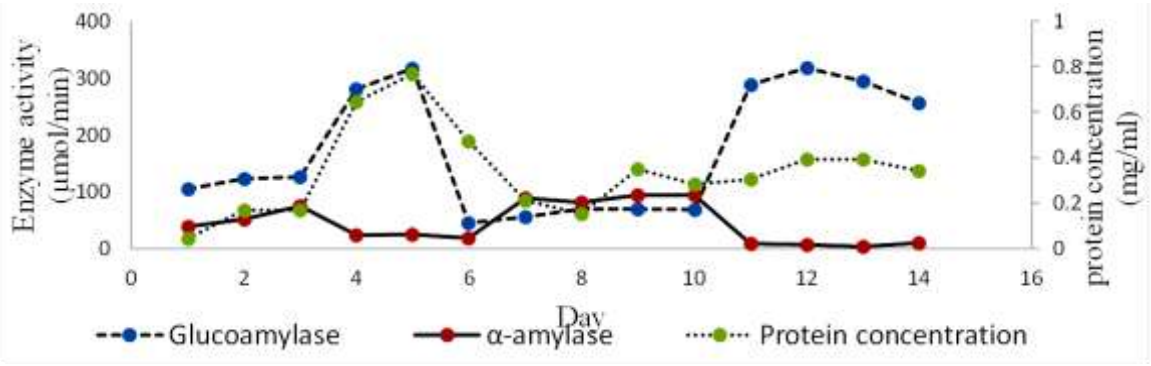

Figure 1. Monitoring the day of highest glucoamylase production in liquid broth using amylopectin from tiger nut starch as the only carbon source (using cassava starch was used as substrate).

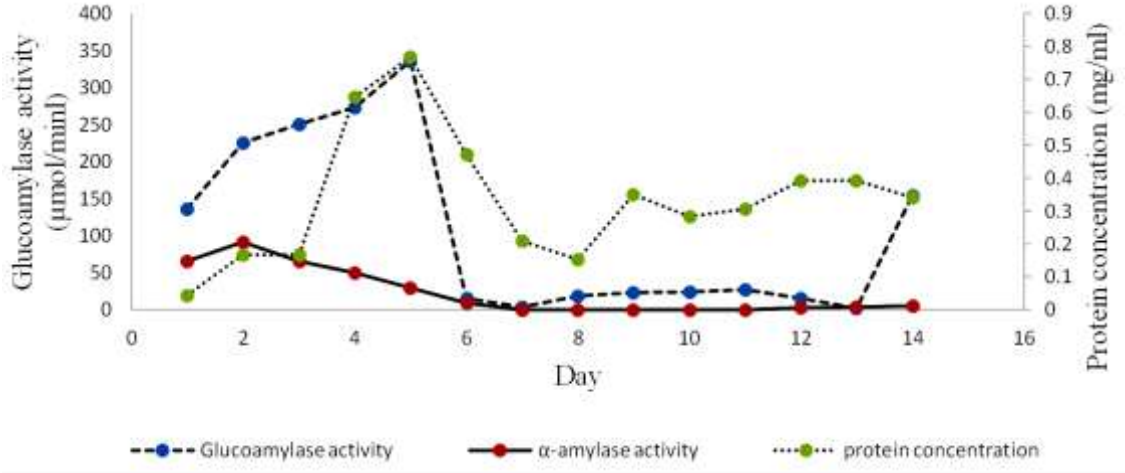

Figure 2. Monitoring the day of highest glucoamylase production in liquid broth using amylopectin from tiger nut starch as the only carbon source (using guinea corn starch as substrate).

tiger nut starch was 60%. A fourteen day pilot study was carried out to determine the day of highest protein production, α-amylase activity and glucoamylase activity in submerged fermentation using amylopectin obtained from tiger nut starch as carbon source. Enzyme activities were assayed using cassava, guinea corn and tiger nut starch as substrate (Figures 1 to 3). Two major peaks were obtained on day 5 and 12 with activities 316.51 and 318.15 µmol/min, respectively using cassava starch as substrate. When guinea corn starch was used as substrate, a major peak was obtained on day 5 with glucoamylase activity of 336.00 µmol/min. More so, the major peaks were observed on the 5th and 12th day with glucoamylase activities of 242.16 and 158.53 µmol/min using tiger nut starch as substrate. Therefore, day 5 and 12 were chosen for mass production of the enzyme. The steady increase in glucoamylase activity observed between days 1 and 5 may have occurred due to multiple branched points in amylopectin from tiger nut. Since glucoamylase is an inducible enzyme produced by the organism in high amounts in the presence of highly branched amylopectin, at the initial stage of fermentation, the organism is prompted to express increasing amounts of glucoamylase to enable the utilization of the amylopectin in the medium for glucose primarily needed for production of energy and other biomolecules required by the organism for growth and replication. When the amylose and glucose level of the broth increase as a consequence of the debranching activity of glucoamylase, the mechanism for the production of glucoamylase is turned off and later turned on when the amylose content in the fermentation broth decreases. This result correlates with the findings of Nahid et al. (2012) and Imran et al. (2012) that reported maximum glucoamylase activity on day 4 of fermentation from *Aspergillus niger* using different carbon sources. Lin et al. (2013) reported maximum glucoamylase production on day 10 of fermentation from *Aspergillus awamori* using pastry wastes as carbon source. The decrease in glucoamylase activity could be due to depletion in the level of branch

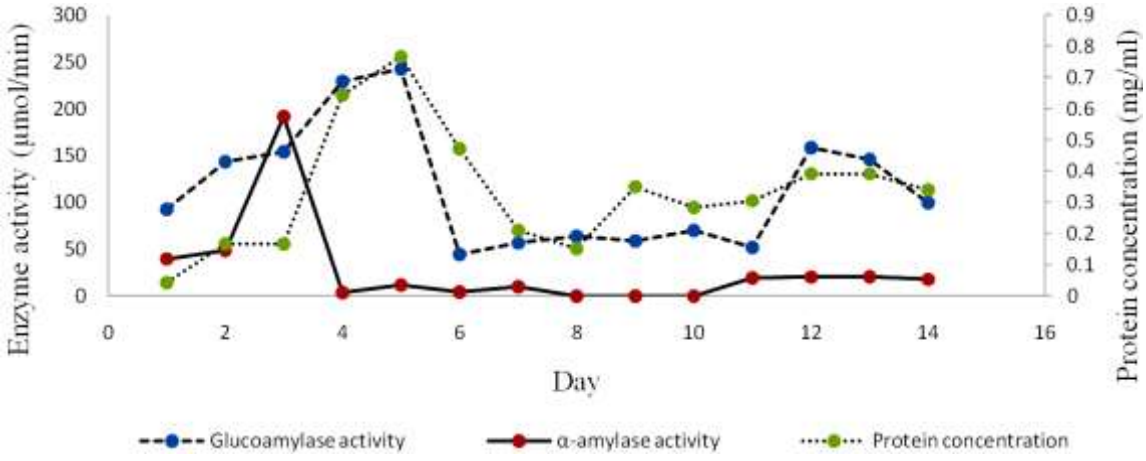

Figure 3. Monitoring the day of highest glucoamylase production in liquid broth using amylopectin from tiger nut starch as the only carbon source (using tiger nut starch as substrate)

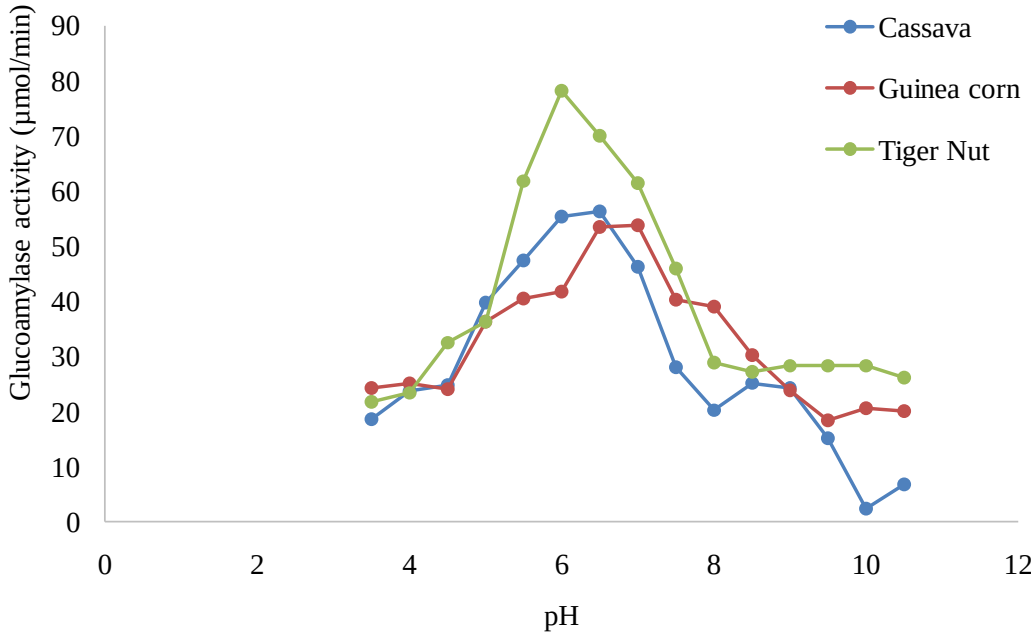

Figure 4. Effect of pH on glucoamylase activity obtained on the 5th day of fermentation (GluAgTN5).

points in the carbon sources, product inhibition as well as depletion in growth supplement in the broth (Nahar et al., 2008).

The optimum pH required for maximum activity of the glucoamylase harvested on days 5 and 12 varied when the activities were assayed using cassava, guinea corn and tiger nut starch as substrates. Glucoamylase harvested on the 5th day was found to have optimum activity at a slightly acidic pH range of 6.0 to 7.0, while glucoamylase harvested on the 12th day was found to have an optimum pH within a basic range of 7.5 to 8.5 when cassava and tiger nut starch were used as substrates, respectively (Figures 4 and 5). Differences in optimum pH obtained may be attributed to the ionic state of the amino acid residues as well as that of substrate due to protonation or deprotonation of specific side groups at the active site of the enzyme thereby changing its chemical conformation (Lee and Paetzel, 2011). At the active site of glucoamylase, deprotonation of carboxyl termini of glutamate or aspartate could result in a potential loss of interaction with an adjacent subunit, changing the enzyme conformation leading to a decrease or complete loss of activity with a change in pH (Berg, 2007). Imran et al. (2012) reported an optimum pH between the range of 4.5 to 6.0, while Lin et al. (2013) reported an optimum pH of 5.5.

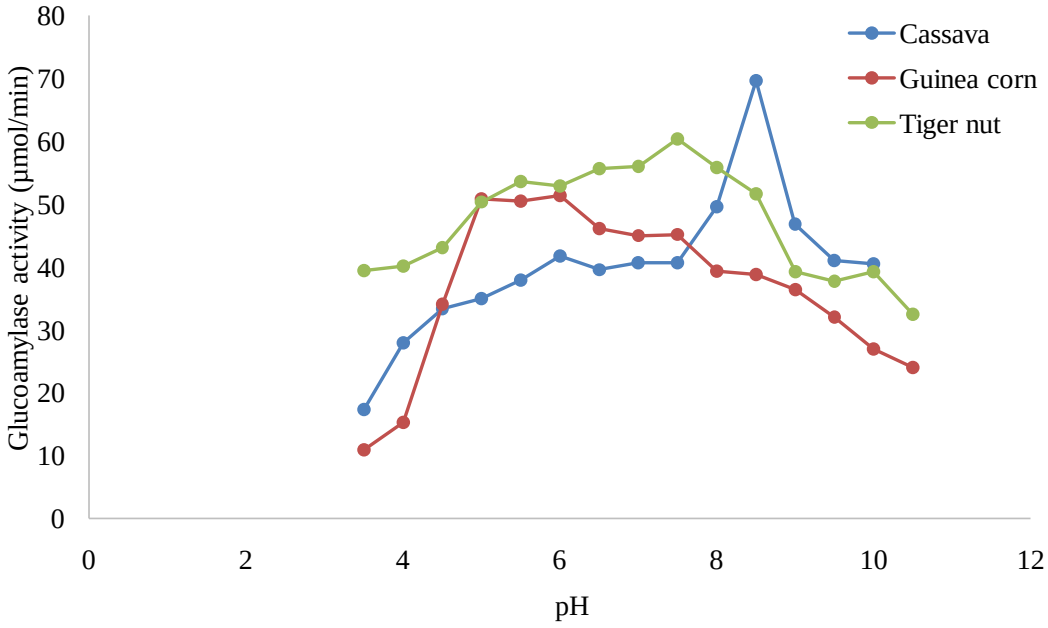

Figure 5. Effect of pH on glucoamylase activityobtained on the 12th day of fermentation (GluAgTN12).

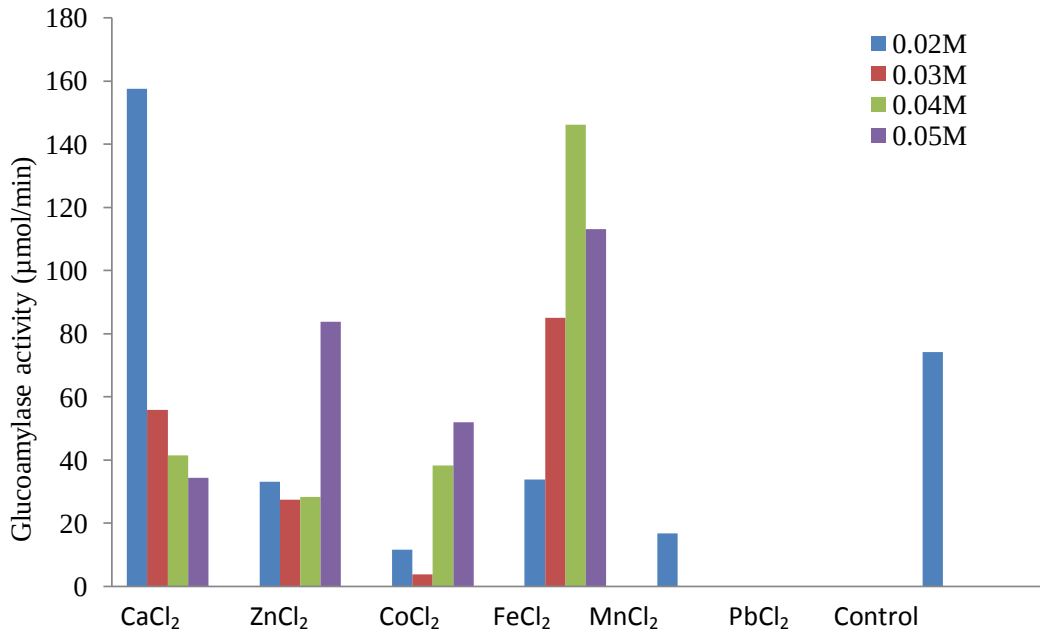

Figure 6. Effect of metal ion concentrations on the activity of glucoamylase harvested on day 5 of fermentation (GluAgTN5).

The effect of several metal ion concentrations on the activity of glucoamylase was monitored and it was observed that low concentration of Ca^{2+}increased the activity of GluAgTN5 and GluAgTN12. Whereas Zn^{2+} and Fe^{2+}caused a slight increase in the activity of gluco-amylase (GluAgTN5). Co^{2+} and Mn^{2+} were observed to have inhibitory effect on glucoamylase activity while Pb^{2+} totally inhibited the enzyme. Zn^{2+} and Co^{2+} had inhibitory effect on GluAgTN12) while Mn^{2+}, Fe^{2+} and Pb^{2+} completely inactivated the enzyme (Figures 6 and 7). This result is in accordance with the report of Jambhulkar (2012) which reported a complete inactivation of glucoamylase produced from *R. nigricans* by Pb^{2+}. Since the glucoamylase harvested on day 5 (GluAgTN5) was stable at neutral pH 7.0, it is more likely to readily form neucleophilichydroxide ions with metals by activating a

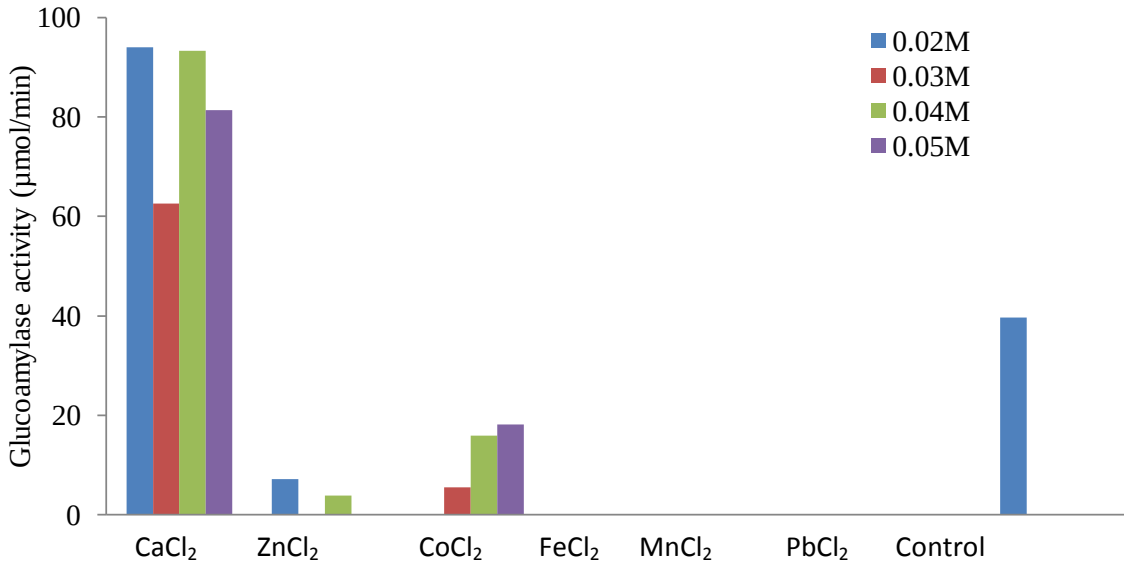

Figure 7. Effect of metal ion concentrations on the activity of glucoamylase harvested on day 12 of fermentation (GluAgTN12).

bound water molecule (Fersht, 1985); this stabilizes the negative charges that are formed at the active sites allowing more weak interactions to hold the substrates in proper orientation at the active site of the enzyme. Thus, the presence of Fe^{2+} and Ca^{2+} will be needed by GluAgTN5 to hold the substrates in close proximity for proper binding by the weak interactions involving the nucleophilic hydroxide ions created by the metal ions at the active site. Since glucoamylase harvested on the day 12 was not stable at neutral pH 7, it could be suggested that less neucleophilic hydroxide ions were formed by metal ions at the active site of GluAgTN12. Hence, low concentration of metal ions will be required at the active site for stability to enable substrate binding to improve catalytic activity. Enhancement of glucoamylase activity such as the ones observed with Ca^{2+}, Zn^{2+} and Fe^{2+} ions could be based on its ability to interact with negatively charged amino acid residues, such as aspartic and glutamic acid by stabilizing the negative charges established at the enzyme active site. This could be observed in other starch degrading enzymes (Carvalho et al., 2014).

High level of hydrogen ions may compete with the cations at the ion binding site of the enzyme. Thus an increase in hydrogen ion concentration as a result of acidic pH will lead to a simultaneous decrease in the concentration of bound metal ions. On the other hand, decreasing the hydrogen ion concentration by increasing the pH may lead to an increase in hydroxyl ion concentration. This may compete with the enzymes for divalent cations, leading to formation of hydroxides.

The Michaelis constant (K_m) and maximum velocity (V_{max}) obtained from the Lineweaver-Burk plot of initial velocity data at different substrate concentration were 222 mg/ml and 500 µmol/min, 291 mg/ml and 1000 µmol/min, 137.5 mg/ml and 500 µmol/min using cassava, guinea corn and tiger nut starch as substrates, respectively for GluAgTN5 while 176.6 mg/ml and 100 µmol/min, 491 mg/ml and 1000 µmol/min, 131.5 mg/ml and 500 µmol/min, were obtained for GluAgTN12 using cassava, guinea corn and tiger nut starch substrate, respectively (Figure 8 and 9). Thus the enzymes, GluAgTN5 and GluAgTN12, had high affinity for cassava and tiger nut starch and low affinity for guinea corn starch. This results suggests that a small amount of the enzyme should be efficient in hydrolyzing large amount of starch especially that from tiger nut and cassava. The charge distribution on the substrates is also affected by changes in the pH of the medium. This can lead to a reduction or an increase in affinity of the substrate and glucoamylase since enzyme-substrate interaction at the enzyme active site occurs through non-covalent interactions of the side chains of amino acids with charged groups on the substrate. Hence, changes in the pH in the medium influences the substrate binding to the enzyme, reducing the catalytic activity of glucoamylase.

Conclusion

Glucoamylase harvested on the 5th day was found to operate at acidic pH range of 6.0 to 7.0, 55°C while glucoamylase harvested on the 12th day was found to operate at basic pHrange of 7.5 and 8.5, 55°C. The addition of divalent metal ions showed significant increase in enzyme activity suggesting its suitability for industrial application especially in starch processing, high glucose syrup production and other biotechnological applications.

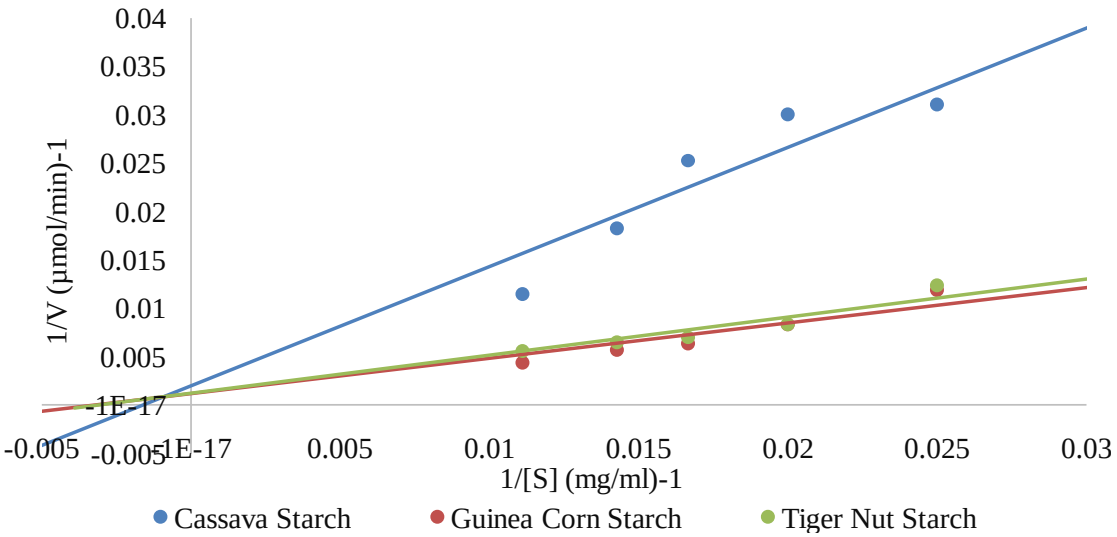

Figure 8. Line-Weaver-Burk plot of initial velocity data at different substrate concentration for glucoamylase harvested after five days of fermentation monitored using different substrates.

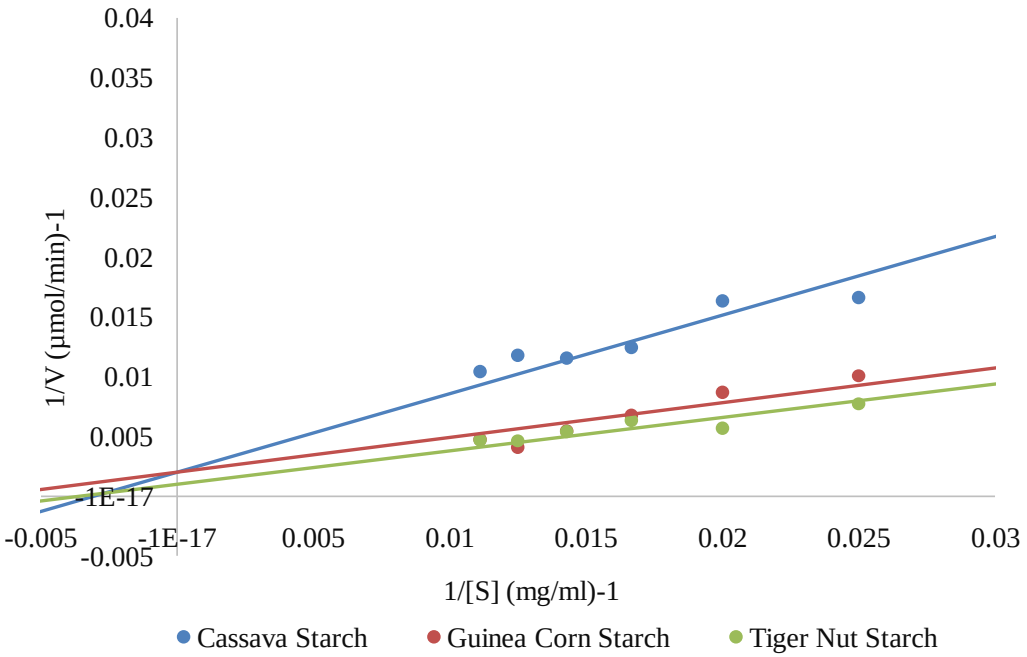

Figure 9. Line-Weaver-Burk plot of initial velocity data at different substrate concentration for glucoamylase harvested after 12 days of fermentation monitored using different substrates.

The results suggest that the affinity of the enzyme for substrate is affected by the pH and divalent metal ion concentration which could be the reason while optimum pH varied with different substrates used.

Conflict of Interests

The authors have not declared any conflict of interest.

REFERENCES

Acharya DK, Shah IJ, Gami PN, Shukla RM (2014). Optimization for α-amylase production by *Aspergillus oryzae*using submerged fermentation technology. Basic Res. J. Microbiol. 1(4):1-10.

Agboola SO, Akingbala JO, Oguntimi GB (1990). Processing of cassava starch for adhesives production. Starch/Starke 42(1):12-15.

Berg J (2007). Biochemistry. 6th Ed. Macmillian, New York pp. 193-194.

Carvalho CC, Ziotti LS, Pereira GM, Furquim da Cruz A, Jorge JA, Polizeli MTM (2014). Production and Functional Properties of Free and Immobilized Glucoamylases of *Penicilliumcitrinum.* Jacobs J.

Biotechnol. Bioeng. 1(2):1-10.
Corbishley DA Miller W (1984). Tapioca, Arrow Root and Sago Starches: Production. In: Starch Chemistry and Technology, Whistler, R.L., BeMiller, J.W. and Paschal, E.F. (Editors). Academic Press, New York. pp. 469-476.
Devasena T (2010). Enzymology. 1st Edn. Oxford University Press, New Delhi. pp. 9-12.
Fersht A (1985). Enzyme Structure and Mechanism. 1stEd. WH Freeman and Company, New York. pp. 47-77.
Imran M, Asad JM, Gulfraz M, Qureshi R, Gul H, Manzoor N, Choudhary AN (2012). Glucoamylase production from *Aspergillus niger*by using solid state fermentation process. Pakistan J. Bot. 44(6):2103-2110.
Jambhulkar V (2012). Effect of various metal ions on glucoamylase and citrate lyase activities of *Rhizopusnigricans* in production of lipids. Asiatic J. Biotechnol. Resour. 3(9):1134-1139.
Koç O, Metin K (2010). Purification and characterization of a thermostable glucoamylase produced by *Aspergillus flavus*HBF34. Afr. J. Biotechnol. 9(23):3414-3424.
Kumari MS, Lakshmi MVNC, Sridevi V (2013). Production and optimization of Glucoamylase from wheat bran by *Aspergillus oryzae*NCIM 1212 under Solid State Fermentation. Int. J. Appl. Innov. . Eng. Manag. 2(10):318-323.
Lee J Paetzel M (2011). Structure of the catalytic domain of glucoamylase from *Aspergillus niger*. *ActaCrystallographica*, 67:188-192.
Lin CS, Lam WC, Pleissner D (2013). Production of fungal glucoamylase for glucose production from food waste. Biomolecules, 3:651-661.
Lowry OH, Rosebrough NJ, Farr AL Randall RJ (1951). Protein measurement with the Folin Phenol reagent. J. Biol. Chem. 193(1):265-275.
Martin N, de Souza SR, da Silva R, Gomes E (2004). Pectinase production of fungal strains in solid-state fermentation using agro-industrial bioproduct. Braz. Arch. Biol. Technol. 47:813-819.
Nahar S, Hossain F, Ferosa B, Hallm MA (2008). .Production of glucoamylase by *Rhizopus*in liquid culture. Pak. J. Bot. 40(4):1693-1698.
Nahid P, Vossoughi M, Roostaazad R, Ahmadi M (2012). Production of glucoamylase by *Aspergillus niger*under solid state fermentation. Int. J. Epidemiol. 25(1):1-7.
Okoye IG, Ezugwu AL, Udenwobele DI, Eze S OO, Anyawu CU, Chilaka FC (2013). Production and Partial Characterization of Cellulases from *Apergillusfumigatus*Using Two Distinct Parts of Corn Cob as Carbon Sources. Nigerian. J. Biotechnol. 26:50-59.
Parbat R, Singhal B (2011). Production of Glucoamylase by *Aspergillus oryzae*UnderSolid State Fermentation Using Agro Industrial Products. Int. J. Microbiol. Res. 2(3):204-207
Selvakumar P, Asherhumari L, Helen A, Pandey A (1996). Purification and characterization of glucoamylase produced by *A. niger* in solid state fermentation. Letters Appl. Microbiol. 23(6):403-406.
Shenoy BC, Katwa LC, Rao AG, Rao MR (1985). Fungal glucoamylases. J. Biosci. 7:399-419.
Sobukola OP, Aboderin AP (2012). Studies on some properties of starches from three *Mucuna* species. Int. Food Res. J. 19(3):913-921.
Yusaku F, Hiroshi M (1996). Improved glucoamylase production by *Rhizopus sp.* A-11 using metal ion supplementated medium. J. Ferment. Bioeng. 82(6):554-557.

academicJournals

Vol. 15(21), pp. 989-994, 25 May, 2016
DOI: 10.5897/AJB2015.15155
Article Number: 1612E7A58610
ISSN 1684-5315

http://www.academicjournals.org/AJB

African Journal of Biotechnology

Full Length Research Paper

Trials to improve the response of *Orechromis niloticus* to *Aeromonas hydrophila* vaccine using immunostimulants (garlic, Echinacea) and probiotics (Organic Green™ and Vet-Yeast™)

Salah Mesalhy Aly[1]*, Mohamed A. Al Zohairy[2], Arshad H. Rahmani[2], Mohamed Fathi[3] and Nashwa M. Abdel Atti[4]

[1]Department of Pathology, Faculty of Veterinary Medicine/Fish Farming and Technology Institute, Suez Canal University, Ismailia, Egypt.
[2]Department of Medical Laboratory, Faculty of Applied Medical Sciences, Qassim University, KSA.
[3]National Institute of Oceanography and Fisheries, Suez, Egypt/Post-Doctoral Fellow, Aquaculture and Genetic Improvement WorldFish, Egypt.
[4]Animal Health Research Institute, Ismailia Lab, Dokki Giza, Egypt.

Received 8 December, 2015; Accepted 19 April, 2016

This work aimed to investigate the role of some immunostimulants and probiotics in improving the response of overwintered tilapia to *Aeromonas hydrophila* vaccine. In this study, 15000 Nile tilapia fry (*Orechromis niloticus)* were collected and divided into five groups. Group 1 was the control, groups 2 to 5 were fed diet supplemented with garlic, Echinacea, Organic Green™ and Vet-Yeast™ respectively for 5 months. Vaccination with *A. hydrophila* bacteria was done by the end of the feeding experiment. The antibody titer of the vaccinated overwintered tilapia of all groups showed no significant changes during the same sampling time. A significant high value in the antibody titer was recognized in vaccinated overwintered tilapia at the end of 6th-8th week post-vaccination (PV) in the control group and between the 4th – 8th week PV in the immunostimulant supplemented groups (Groups 2-3), and between the 2nd – 10th week PV in probiotic supplemented groups (Groups 4 and 5). The challenge infection of the vaccinated tilapia showed the highest mortality in Group 1 while the lowest mortality was seen in Group 5. However, maximum protection after challenge was seen at 6th week PV in other treated groups. The immunostimulants and probiotics under test proved efficient in improving the immune response to vaccination which will improve the resistance of tilapia fry against infection during the winter. The overall results are promising to implement overwintering fry culture program to economically maximize and efficiently use the available aquaculture facilities throughout the year.

Key words: Tilapia, overwintering, immunostimulants, probiotics, vaccines, pathogens.

INTRODUCTION

Aquaculture is a promising sector of fish industry in the world with about 80 million tones being produced annually (Kolkovski and Kolkovski, 2011). The development of aquaculture faced several constraints; among these are

diseases constituting the most limiting factors. Bacterial infections, pose one of the most significant threat to successful fish production throughout the world (Rahman et al., 2009). In Egypt, bacterial diseases induce heavy mortality in farm fish (Aly, 2013). Moreover, winter season in Egypt stress tilapia causing low survival and render hatcheries unable to produce fry to stock in the ponds during winter which limit the length of the production season until June with a huge economic loss for the inability to use the fish farm during that period. Recently, the control of bacterial infection in fish is managed through the use of vaccines or via biological control using safe microorganisms (Aly et al., 2015; Aly and Mohamed, 2010).

Overwintering of tilapia fry may provide sufficient fingerlings for the following season and is carried out using heated facilities, underground warm water and in green houses (Cruz and Ridha, 1994; Jiazhao, 1991). But these resources are generally not available in Egypt. Overwintering late-season fingerlings in deep hapas (3.0 m) suspended in deep ponds (3.5 m) has also been constructed (Nguyen and Little, 2000).

Aeromonas hydrophila is one of the most common bacterial pathogens in the Egyptian aquaculture. It causes septicemia with mortalities among tilapia and other fish species reared under the hatchery and farm environment in Egypt (Aly, 2013; Aly et al., 1998). The intestinal microbiota of fry plays a role in the defense against opportunistic pathogens. The application of immunostimulants and probiotics in improving fish health was tested previously (Aly et al., 2007, 2008a, b). Garlic and Echinacea improved the body gain, survival and resistance to infection in Nile tilapia (Aly and Mohamed, 2010). Garlic plays a role in the control of bacteria and fungi (Corzo-Martinez et al., 2007). The allium enhances the immune activities through promotion of lymphocyte-synthesis, cytokine release, phagocytosis and activation of natural killer cell (Kyo et al., 2001). Few data on the use of garlic extract as immune stimulant in fish in Egypt are available (Aly et al., 2008). Echinacea, also, seems to activate the macrophages and other immunological functions in laboratory animals and humans. The evidences on the role of the polysaccharidic fraction of Echinacea on immunity are reported (Bauer, 1999). On the other hand, *Bacillus* spp., lactic acid bacteria (LAB) and other Gram-negative bacteria have been tested as fish probiotics (Irianto and Austin, 2002; VaŁ zquez et al., 2005). Moreover, the usage of *Saccharomyces cerevisae* in fish is a good enhancer of fish immune system, it also improves the survival and growth rate of supplemented fish (Abd El-Tawab et al., 2008). Previous study showed the effect of some immunostimulants and probiotics on the survival rate and final weight of overwintered tilapia fry where no significant differences was recognized in the growth while significant improvement in the survival was seen in diets containing immunostimulents or probiotics (Aly et al., 2010). The current work was designed to investigate the role of selected immunostimulants (garlic and Echinacea) and probiotics (Organic Green^{TM} and Vet-Yeast^{TM}) on improving the response of overwintered tilapia fry to vaccination with *A. hydrophila* vaccine.

MATERIALS AND METHODS

Fish

Nile tilapia fry, *Orechromis niloticus* (Fifteen thousand, initial weight 0.02 g) were divided into five equal groups, each of three equal replicates that are reared in 15 cement ponds (5 x 2.5 x 1 m). Ponds were filled with tap water and partially renewed during the experiment. The water quality was optimal throughout the period of experiment, except temperature which was lower than optimal range for tilapia culture because of winter season (November-March). The water was exchanged 20% daily to maintain its quality within an acceptable range for the survival of tilapia {NO_3 (0.20 mg/L,), total ammonia nitrogen (0.2 mg/L), Chl *a* (42.27 mg/L), and orthophosphate (0.02 mg/L)}. Water temperatures during the experiment ranged from 10 to 20°C.

Preparation of diets

Dietary ingredients of 35% protein were prepared in the World Fish Center as pellets [21]. Ingredients were prepared by grinding the corn to granules (0.5 mm mesh size) (Thomes-Willey Laboratory Mill Model 4, Swedesboro, NJ 08085 U.S.A). Ingredients were mixed by mixer (Hobart model D300T, U.S.A.) at a low speed for 30 min. Oil (vegetable and cod liver) was added gradually to ensure the homogeneity of the ingredients.

The immunostimulants {Garlic (*Allium sativum* L), Echinacea (*Echinacea purpurea*)} and probiotics {Organic Green^{TM} and Vet-Yeast^{TM}) were procured from the local market of Egypt. Echinacea (*E. purpurea*) extract contains 1.5% chicoric acid grade. Organic Green^{TM} contains 1 x 10^{11} bacterial cells each from *Lactobacillus acidophilus, Bacillus subtilis, Saccharomyces cervisiae* and *Aspergillus oryzae*. One gram (1 g) of Vet-Yeast^{TM} product contains 1 x 10^{9} *Saccharomyces cervisiae* dried cells according to the manufacturers.

The tested immunostimulants and probiotics prepared and mixed with formulated balanced diet where garlic (*A. sativum* L) used at a rate of 40 g of garlic kg^{-1} feed, Echinacea (*E. purpurea*) extract at 4 g of Echinacea kg^{-1} feed, Organic Green^{TM} at 4 g Organic Green^{TM} kg^{-1} feed while Vet-Yeast^{TM} at 4 g Vet-Yeast^{TM} kg^{-1} feed. The feed were prepared each two weeks and the pellets were left for 24 h to air dry, and stored in a refrigerator (4°C).

Bacterial pathogen

A pathogenic *A. hydrophila* was obtained as a reference strain from

*Corresponding author. E mail: salahaly@hotmail.com. Tel: 00201212789838.

Table 1. Design of the vaccination experiment of overwintering tilapia and challenge following vaccination.

Groups		Treatment	Total number of fish	Number of tilapia (I/P injection)		Challenge infection in weeks		
				Saline	*Aeromonas* vaccine	6th	8th	10th
1	a	Control negative	150	150	0	30	30	30
	b	Control Positive	150	0	150	30	30	30
2		Garlic	150	0	150	30	30	30
3		Echinacea	150	0	150	30	30	30
4		Organic green	150	0	150	30	30	30
5		Vet-Yeast	150	0	150	30	30	30

Fish Health Management Division of the WorldFish Center, which was isolated from infected tilapia species and was identified by polymerase chain reaction (PCR). The isolate was used in the vaccination trial to test response of the overwintered vaccinated-fry.

Vaccine preparation

Formalin-killed *A. hydrophila* bacterin was prepared by addition of formalin (0.3%) to the bacterial culture, which had been previously incubated at 35°C for 48 h (Baba et al., 1988). The formalized bacterial culture was held at room temperature overnight, and then subjected to sterility and safety tests according to earlier study (Cardella et al., 1990). The sterility test was performed by culturing washed bacterin on TS agar. Plates were incubated at 37°C for 24 h and examined for bacterial growth. The safety test was performed by the intraperitoneal (IP) inoculation of 20 susceptible tilapia (20 ± 4 g) with the prepared bacterin cells (0.1 ml). The fish were reared for 2 weeks post-injection and then morbid fish were subjected to necropsy for re-isolation of *A. hydrophila* using RS media. The prepared and tested vaccine was stored in the refrigerator at 4°C. Immediately before use, formalin killed bacterial cells were washed twice with sterile saline solution and prepared to a concentration of 3 mg wet-weight/ml saline.

Experiment

Fish of group 1 (control) was fed a balanced ration without other additives. Groups 2-5 were fed on a balanced diet supplemented with 4% garlic (group 2), 4 ppt Echinacea (group 3), 4 ppt Organic Green™ culture (group 4) or 4 ppt Vet-Yeast™ (group 5); respectively. Fish were fed three times daily in a plastic feeder for five months (November – March). At the end of feeding experiment, the overwintered *O. niloticus* (n = 900) were collected; 300 fish from the control group 1 (150 for control negative and 150 for control positive subgroups a and b) and 150 fish each from the 4 treated overwintered tilapia groups were also collected. Fish were collected equally from the three replicates of the 1st stage experiment in a random way and subdivided into 3 equal replicates groups (each of 50 fish). Fish were vaccinated following the schedule shown in Table 1. Fish were anaesthetized with 100 mg/L MS_{222} (Tricain methane sulfonate; Argent Chemical Laboratories, Fisheries Division). The negative control fish of group 1 were intraperitoneally (IP) injected by 0.1 ml sterile saline solution. Fish of other treated groups (2-5) and control positive subgroup were inoculated with 0.1 ml formalin-killed *A. hydrophila* diluted in 0.1 ml sterile saline (Badran et al., 1993)

Laboratory evaluation

Antibody determination

By the end of 1st, 2nd, 3rd, 4th, 6th, 8th and 10th week post-vaccination (PV), fish were anesthetized by immersion in water containing 0.1 ppm MS-222 and blood samples were collected. Whole blood (0.5 ml) was obtained from caudal vein of fish of experiment 2, (n = 30/group, 10/replicate), using syringes (1-ml) and 27-gauge needles and transferred to blood Eppendorf tubes without anticoagulant. The blood samples were centrifuged at 3000 x g for 15 min and the supernatant serum was collected and stored at -20°C in screw-capped glass vials until used. Specific antibody titers, in collected sera, were determined using the bacterial agglutination test (Baba et al., 1988).

Challenge after vaccination

Fish (n = 90), with average weight of 6 ± 0.3 g, were randomly obtained from the three replicates of each treatment of experiment 2, and were used for challenge test at the end of the 6th, 8th and 10th weeks post-vaccination (30 fish/challenge group). Fish were splitted into 3 equal groups (each of 3 equal replicate (10 fish) being reared in a separate glass aquarium (50 x 60 x 70 cm). Fish was IP inoculated with 0.5 ml (10^8 bacteria cells ml^{-1}) of culture suspension of the reference pathogenic strains of *A. hydrophila* (Aly et al., 2008a). Mortality was recorded and the dead fish was subjected to necropsy for bacterial re-isolation. The relative level of protection (RLP) among the vaccinated and challenged fish was determined using the following equation (Ruangroupan et al., 1986):

RLP% = 100 - (percent stimulated mortality ÷ percent mortality in thecontrol group) x 100

Statistical analysis

One-way and two-way analyses of variance (ANOVA) were carried. Also, Duncan's multiple range test (Duncan, 1955) was used to determine differences among treatments (mean at significance level of $P<0.05$). Standard errors were also estimated. Analysis was carried out using the SAS package (Duncan, 1955).

RESULTS

The antibody titer was not different among all the

Table 2. Antibody titer of overwintered tilapia from the 1st till the end of the 10th week PV (Mean ± SE).

Group	Antibody titer/ week					
	1st	2nd	4th	6th	8th	10th
(1) Control	$4^{Ac} \pm 0.32$	$4.8^{Abc} \pm 0.37$	$5^{Abc} \pm 0.32$	$6.6^{Aa} \pm 0.51$	$6.2^{Aa} \pm 0.37$	$5.8^{Aab} \pm 0.37$
(2) Garlic (4%)	$4.6^{Ac} \pm 0.51$	$5.6^{Ac} \pm 0.40$	$5.8^{Aab} \pm 0.37$	$7^{Aa} \pm 0.45$	$6.6^{Aa} \pm 0.24$	$6.4^{Aab} \pm 0.24$
(3) Echinacea (4 g/kg feed)	$4.6^{Ab} \pm 0.40$	$5.6^{Aab} \pm 0.58$	$5.8^{Aa} \pm 0.51$	$6.8^{Aa} \pm 0.37$	$6.4^{Aa} \pm 0.40$	$5.8^{Aab} \pm 0.58$
(4) Organic green (4 g/kg feed)	$4.4^{Ab} \pm 0.51$	$5.2^{Aa} \pm 0.49$	$5.2^{Aa} \pm 0.37$	$6.6^{Aa} \pm 0.51$	$6.2^{Aa} \pm 0.37$	$6^{Aa} \pm 0.32$
(5) Vet-yeast (4 g/kg feed)	$4.8^{Ab} \pm 0.37$	$5.8^{Aa} \pm 0.55$	$6^{Aa} \pm 0.37$	$7^{Aa} \pm 0.32$	$6.6^{Aa} \pm 24$	$6.2^{Aa} \pm 0.37$

Capital letters compare between columns and small letters compare between rows. Columns with the same letter are not significant different.

Table 3. Relative level of protection of overwintered vaccinated tilapia after challenge infection of all the groups at the end of the 6th, 8th and 10th week PV.

Group	RLP (%)		
	6th	8th	10th
Negative control	0	0	0
(1) Positive Control	$35.5^{Ca} \pm 0.61$	$35.3^{Ca} \pm 0.36$	$35.2^{Ca} \pm 0.55$
(2) Garlic (4%)	$45.1^{Ba} \pm 1.67$	$40.4^{Bb} \pm 1.16$	$40.7^{Bb} \pm 1.35$
(3) Echinacea (4 g/kg feed)	$50.7^{Aa} \pm 1.77$	$45.4^{Ab} \pm 1.22$	$40.7^{Ac} \pm 1.67$
(4) Organic green (4 g/kg feed)	$50.8^{Aa} \pm 1.67$	$40.5^{Ab} \pm 2.11$	$40.1^{Ab} \pm 2.07$
(5) Vet-yeast (4 g/kg feed)	$50.9^{Aa} \pm 0.67$	$50.4^{Aa} \pm 0.55$	$45.8^{Ab} \pm 1.49$

Capital letters compare between columns and small letters compare between rows. Columns with the same letter are not significant different.

treatment groups (Table 2). The antibody titer of the vaccinated overwintered tilapia of the control group initially did not significantly differ but later started to increase at the 6th - 8th week PV. In the garlic and Echinacea supplemented group, a statistically significant increase began during the 4th - 8th week PV, while in the organic green and Vet-yeast supplemented groups, a significant increase was seen earlier than in the other groups (2nd – 10th week PV). *A. hydrophila* challenge infection of the overwintered-vaccinated tilapia induced the highest mortality in the non-vaccinated control group, followed by the vaccinated control. Lowest mortality was seen in the Vet-yeast supplemented group at the three challenge periods (6th, 8th and 10th week PV). The other groups showed variable results for the three periods of challenge (Table 3).

DISCUSSION

Two important challenges face fish culture in Egypt: first making fry available throughout the year, especially during and immediately after the winter season, which retard tilapia growth and production as well as fry survival. The second challenge is to recover the time (winter and early spring) lost, when there is no investment in fish production due to shortages of fry. This study aimed to improve the survival and resistance of tilapia fry stressed during the winter season to infection through the use of immunostimulants and probiotics together with vaccination.

According to Aly et al. (2010), an improved survival among tilapia fed on diets containing immunostimulents or probiotics was recorded where garlic-supplemented diet resulted to a higher total harvest weight. It was previously stated that, immunostimulants improve the protection of fish against diseases by enhancing non-specific and humoral defense mechanisms (Sakai, 1999). Garlic has been effect against many bacteria (Ress et al., 1993), fungi (Adetumbi et al., 1986) and viruses (Weber et al., 1992).

These findings show the effect of immunostimulants on non-specific immunity by increasing the number of phagocytes or improving phagocytosis (Shoemaker et al., 1997). Garlic and other immunostimulants enhance the bactericidal activity of the fish's phagocytic cells (Sahu et al., 2007). Moreover, garlic shows positive action against several bacteria (Ress et al., 1993). Previous studies revealed that, yeast, b-1,3 glucan enhances resistance against several major bacterial pathogens (*Vibrio anguillarum, Vibrio salmonicida, Yersinia ruckeri, Edwardsiella tarda* and *A. hydrophila*) in fish species such as carp, *Cyprinus carpio* (Yano et al., 1991), Atlantic salmon*, Salmo salar* Robertsen et al., (1990) and African catfish, *Clarias gariepinus* (Yoshida et al., 1995). Several researchers reported the effect of β-(1,3) D-glucan on the

nonspecific cellular and humoral defense mechanisms, including the function of phagocytes, bacterial killing activity of macrophages in rainbow trout, Atlantic salmon and catfish (Nikl et al., 1991). β-(1, 3) D-glucan induces the production of superoxide anion by macrophages (Dalmo and Seljelid, 1995) and accelerates the synthesis of cytokine-like molecules (Yoshida et al., 1995). The protective effect of echinacea preparations may be due to the activation of lymphocytes (Wagner et al., 1986). However, the immunomodulatory effects of echinacea are considered to be via non-specific activation of the immune system (Maass et al., 2005).

In the present study, although the antibody titer showed no significant difference among supplemented groups at the same time post-vaccination, they were significantly increased in the vaccinated overwintered tilapia at the end of the 6^{th} - 8^{th} week PV in the control group, at 4^{th}- 8^{th} week PV in garlic and echinacea supplemented groups and at 2^{nd} – 10^{th} week PV in organic green and Vet-yeast supplemented groups. Previous studies revealed that, glucan treatment in fish enhanced the expression of interleukin 1 (Fujiki et al., 2000) and complement activity (Engstad et al., 1992). Moreover, glucan accelerated the specific immune response in catfish and Atlantic salmon against vaccines for *E. ictaluri* and *A. salmonicida*, respectively (Chen and Ainsworth, 1992; Baulny et al., 1996). Earlier finding reported that, oral administration of *Lactobacillus delbreckii* sp. *lactis* and *B. subtilis*, alone or combined increased phagocytic activity in gilthead seabream (*Sparus aurata* L.) after 2 weeks of feeding (Salinas et al., 2005).

The challenge infection of the overwintered-vaccinated tilapia using *A. hydrophila* showed lowest mortality in the Vet-yeast supplemented group at three challenging periods (6^{th}, 8^{th} and 10^{th} week PV). Yeast glucans revealed increase in the macrophage-chemotactic and phagocytic activities, the lysozyme and complement activities and also stimulated cytokines (IL-1, tumor necrosis factor) release and leukocyte migration (Secombes and Fletcher, 1992). Thereby, it significantly reduces fish mortality after challenge with various pathogens (Aly et al., 2015; Abel and Czop, 1992; Verlhac et al., 1996, 1998).

It may be concluded that, immunostimulants and probiotics can improve the response of overwintering tilapia fry to vaccination and resistance to diseases. Its use is recommended together with a vaccination program in order to improve the economic outcomes and to avoid environmental contamination through the widespread application of drugs and antibiotics.

Conflict of interests

The authors declare that there is no conflict of interests regarding the publication of this paper.

ACKNOWLEDGEMENT

The authors express their deep thanks and appreciation to World Fish Center, CGIAR, Abbsaa, Egypt for supporting the research idea and providing Nile tilapia fish and facilities for this experiment.

REFERENCES

Abd El-Tawab M, Mousa A, Maaly M (2008). Effect of yeast suplimentation on the growth performance and resistance of galilee tilapia, Sarotherodon galilaeus (L.) to environmental copper toxicity. The 8th international Symposium on tilapia in Aquaculture, Cairo, pp.1015-1031.

Abel G, Czop K (1992). Stimulation of human monocyte b-glucan receptors by glucan particles induces production of TNF-a and IL-1b. Int. J. Immunopharmacol. 14:1363-1373.

Adetumbi M, Javor T, Lau H (1986). Allium sativum Garlic) inhibits lipid synthesis by Candida albicans. Antimicrob. Agents Chemother. 30:499-501.

Aly S (2009). Probiotics and aquaculture. CAB Reviews: Perspectives in Agriculture, Veterinary Science, Nutrition and Natural Resources 4(074):1-16.

Aly S (2013). A Review of Fish Diseases in the Egyptian Aquaculture Sector. Working Report, Research Program in Livestock and Fish.

Aly S, Abdel Atti M, Fathi M (2008b). Effect of garlic on the survival, growth, resistance and quality of *Oreochromis niloticus*. 8^{th} International Symposium on Tilapia in Aquaculture, Cairo, Egypt.

Aly S, Albutti S, Rahmani A, Abdel Atti N (2015). The response of New-season Nile tilapia to *Aeromonas hydrophila* vaccine. Int. J. Clin. Exp. Med. 8(3):4508-4514.

Aly S, El-Meleigy A, Ellzey J, Mayberry L (1998). Pathological and electron microscopic studies on aeromonaisis among carp. Suez Canal Vet. Med J. 12:259- 266.

Aly S, Elnaggaar G, Mohamed F, Mohamed W (2010). Effect of Garlic, Echinacea, Organic Green and Vet-Yeast on Survival, Weight Gain, and Bacterial Challenge of Overwintered Nile Tilapia Fry (*Orechromis niloticus*). J. Appl. Aquac. 22:210-215.

Aly S, Fathi M, John G (2008a). Echinaceaa as immunostimulatory agent in Nile Tilapia *Oreochromis niloticus*) via earthen pond experiment. 8^{Th} International Symposium on Tilapia in Aquaculture, Cairo, Egypt, pp.1033-1042.

Aly S, John G, El-Naggar G, Fathi M (2007). Effect of Echinacea on body gain, survival and some hematological and immunological parameters of Oreochrmis niloticus and their response to challenge infection. Egypt. J. Fish. Aquatic Biol. 11(3):435-445.

Aly S, Mohamed F (2010). Echinacea purpurea and Allium sativum as immunostimulants in fish culture using Nile tilapia (*Oreochromis niloticus*). J. Anim. Physiol. Anim. Nutr. 94:e31-e39.

Aly SM, Ahmed YA, Ghareeb AA, Mohamed MT (2008). Studies on Bacillus subtillis and lactobacillus acidophilus, as potential probiotics, on the immune response and resistance of Tilapia nilotica (*Oreochromis niloticus*) to challenge infections. Fish Shellfish Immunol. 25:128-136.

Baba T, Imamura J, Izawa K (1988). Immune protection in carp, *Cyprinus carpio* L., after immunization with *Aeromonas hydrophila* crude lipopolysaccharida. J. Fish Dis. 11:237-244.

Badran A, Eissa A, Essa E (1993). Studies on the role of lymphoid organs in the antibody production and protection of Nile tilapia against infection with *Aeromonas hydrophila*. Zagazig Vet. J. 21(2):153-160.

Bauer R (1999). Chemistry, analysis and immunological investigations of Echinacea phytopharmaceuticals. In: Wagner H, editor. Immunomodulatory agents from plants. Base l7 Birkauser Verlag; 41

Baulny D, Quentel C, Fournier V, Lamour F, Gouvello L (1996). Effect of long-term oral administration of b glucan as an immunostimulant or an adjuvant on some non-specific parameters of the immune

response of turbot Scophthalmus maximus. Dis. Aquatic Org. 26:139-47.
Cardella A, Eimers E (1990). Safety and potency testing of federal licensed fish bacterins. J. Aquatic Anim. Health 2:49- 55.
Chen D, Ainsworth J (1992). Glucan administration potentiates immune defence mechanisms of channel catfish, Ictalurus punctatus Rafinesque. J. Fish. Dis. 15:295-304.
Corzo-Martinez M, Corzo N, Villamiel M (2007). Biological properties of onions and garlic. Trends Food Sci.Technol. 18:609-625.
Cruz E, Ridha M (1994). Overwintering tilapia *Oreochromis spilurus* Gunther) Fingerlings using warm underground seawater. Aquac. Fish.Manag. 25:865-871.
Dalmo A, Seljelid R (1995). The immunomodulatory effect of LPS, laminaran and sulphated laminaran b 1,3)-D-glucan) on Atlantic salmon, Salmo salar L., macrophages in vitro. J. Fish. Dis.18:175-185.
Duncan B (1955). Multiple Range and Multiple F tests. Biom. 11:1-2.
Engstad E, Robertsen B, Frivold E (1992). Yeast glucan induces increase in activity of lysozyme and complement e mediated haemolytic activity in Atlantic salmon blood. Fish Shellfish Immunol. 2:287-297.
Fujiki K, Shin H, Nakao M, Yano T (2000). Molecular cloning and expression analysis of carp (*Cyprinus carpio*) interleukin-1b, high affinity immunoglobulin E FC receptor g subunit and serum amyloid A. Fish Shellfish Immunol. 10:229-242.
Irianto A, Austin B (2002). Probiotics in aquaculture: review. J. Fish Dis. 25:633-642.
Jiazhao L (1991). Tilapia. *In: Pond Fisheries in China* ed. by Z Lin). International Academic Publisher. Beijing. China. pp. 161-166.
Kolkovski S, Kolkovski J (2011). Herbal medicine in aquaculture. International Aqua Feed 14(2):28-31.
Kyo E, Uda N, Kasuga S, Itakura Y (2001). Immunomodulatory effects of aged garlic extract. J. Nutr. 131:1075S-1079S.
Maass N, Bauer J, Paulicks R, Böhmer M, Roth-Maier A (2005). Efficiency of Echinacea purpurea on performance and immune status in pigs. J. Anim. Physiol. Anim. Nutr. 89(7-8):244-252.
Nguyen CD, Little DC (2000). The culture performance of monosex and mixed-sex new-season and overwintered fry in three strains of Nile tilapia_Oreochromis niloticus/in northern Vietnam. Aquac. 184:221-231.
Nikl L, Albright J, Evelyn T (1991). Influence of seven immunostimulants on the immune response of coho salmon to Aeromonas salmonicida. Dis. Aquatic Org.12:712.
Rahman T, Akanda M., Rahman M, Chowdhury M (2009). Evaluation of the effiecies of selected antibiotics and medicinal plants on common bacterial pathogens. J Bangladesh Agric. Univ. 7(1):163-168.
Ress P, Minney F, Plummer J, Slater H, Skyrme A (1993). A quantitative assessment of the antimicrobial activity of garlic (Allium sativum). World. J. Microbiol. Biotechnol. 9:303-307.
Robertsen B, Rorstad G, Engstad E, Raa J (1990). Enhancement of non-specific disease resistance in Atlantic salmon Salmo salar L., by a glucan from Saccharomyces cerevisiae cell wall. J. Fish. Dis. 13:391-400.
Ruangroupan L, Kitao T, Yoshida T (1986). Protective efficacy of *Aeromonas hydrophila* vaccines in Nile tilapia. Vet. Immunol. . Immunopathol. 12(1-4):345-350.
Sahu S, Das K, Mishra K, Pradhan J, Sarangi N (2007). Effect of Allium sativum on the immunity and survival of Labeo rohita infected with *Aeromonas hydrophila*. J. Appl. Ichthyol. 23:80-86.
Salinas I, Cuesta A, Esteban MA, Meseguer J (2005). Dietary administration of Lactobacillus delbrueckii and Bacillus subtilis, single or combined, on gilthead seabream cellular innate immune. Fish Shellfish Immunol. 19:67-77.
SAS (2005). Statistical Analysis System. User`s Guide: *SAS Institute Cary, North Carolina. 27.* Sakai M., (1999): Current research status of fish immunostimulants. Aquac.172:63-92.
Secombes J, Fletcher C (1992). The role of phagocytes in protective mechanism of fish. Ann. Rev. Fish Dis. 2:53-71.
Shoemaker A, Klesius H, Plumb A (1997). Killing of Edawrdsiella ictaluri by macrophages from Channel catfish immune and susceptible to enteric septicemia catfish. Immunol. Immunopathol. 58:190-181.
VaŁ zquez A, GonzaŁ lez P, Murado A (2005). Effects of lactic acid bacteria cultures on pathogenic microbiota from fish. Aquaculture 245:149-161.
Verlhac V, Gabaudan J, Obach A, Schuep W, Hole R (1996). Influence of dietary glucan and vitamin C on non-specific and specific immune responses of rainbow trout (*Oncorhynchus mykiss*). Aquac. 143:123-133.
Verlhac V, Obach A, Gabaudan J, Schueep W, Hole R (1998). Immunomodulation by dietary vitamin C and glucan in rainbow trout (*Oncorhynchus mykiss*). Fish Shellfish Immunol. 8:409-424.
Wagner H, Jurcic K, Doenicke A, Rosenhuber E, Behrens N (1986). Die Beeinflussung der Phagozytosefähigkeit von Granulozyten durch homöopathische Arzneipräparate: *in vitro*-Tests und kontrollierte Einfachblindstudien. Arzneimittel-Forschung, 36(9):1421-1425.
Weber N, Anderson O, North A, Murray K, Lawson D, Hughes G (1992). In vitro virucidal effects of Allium sativum (garlic) extract and compounds. Planta Med. 58:417-423.
Yano T, Matsuyama H, Mangindaan P (1991). Polysaccharide induced protection of carp Cyprinus carpio L., against bacterial infection. J. Fish. Dis. 14:577-582.
Yoshida T, Kruger R, Inglis V (1995). Augmentation of non-specific protection in African catfish, Clarias gariepinus (Burchell) by the long-term oral administration of immunostimulants. J. Fish. Dis. 18:195-198.

African Journal of Biotechnology

Related Journals Published by Academic Journals

- *Biotechnology and Molecular Biology Reviews*
- *African Journal of Microbiology Research*
- *African Journal of Biochemistry Research*
- *African Journal of Environmental Science and Technology*
- *African Journal of Food Science*
- *African Journal of Plant Science*
- *Journal of Bioinformatics and Sequence Analysis*
- *International Journal of Biodiversity and Conservation*

academicJournals